UNIVERSITÀ DEGLI STUDI DI PADOVA

Facoltà di Ingegneria
Dipartimento di Ingegneria Meccanica – Settore Materiali

Tesi sperimentale di laurea

CARATTERIZZAZIONE METALLURGICA DELL'ACCIAIO INOX 15-5 PH FABBRICATO CON PROCESSO DI RIFUSIONE VAR ED ESR

Relatore: Prof. Ing. Gian Mario PAOLUCCI
Tutor: Ing. Roberto BERTIN

Laureando: Alberto SPALIVIERO
Matricola: 601754 - IR

Anno Accademico 2010 – 2011

Chapter 1

Introduction

1.1 Solidification of stainless steel

The solidification of steel is governed, as is the solidification of all metals, by the laws of the phase diagram. However, the kinetics of the solidification process determine the microstructure that actually is formed. When solidification occurs, solvent-lean alloy forms first and then grows, usually by dendritic solidification, in the directions of heat and alloy gradients. Thus, for most special stainless steel it is necessary that they be solidified under controlled conditions. When solidification rates are too slow, the solute rejected from the first dendrites formed (primary dendrites) may form continuous channels of very high solute content. When these channels solidify (as "freckles"), they are too concentrated in solute to be dissolved by subsequent heat treatment, and thus form continuous hard defects. Figure 1.1 shows a transverse slice through a freckle structure and the analysis associated with the freckles. Laves phases and carbides are hard particles, which form in these heavy solute concentration regions and are highly detrimental to fatigue life. Freckled structure must be avoided in special steel that is intended for service where fatigue life is an important design criterion.

The primary dendrites reject solute into the interdendritic liquid and, as seen in the niobium trace, the niobium content in the liquid may reach about 9%. The low niobium primary dendrites grow into the solidifying metal in a direction perpendicular to the solidification front.

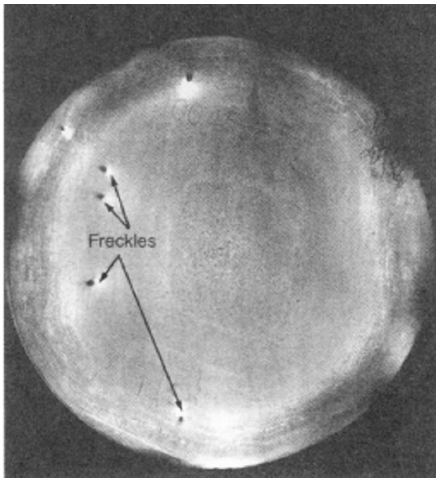

Fig. 1.1 Freckles in steel billet forged from vacuum arc remelted ingot in which control of melt conditions was lost.

This region of solid dendrites and liquid interdendritic regions has a temperature gradient defined by the width of this "mushy" zone and the liquidus and solidus temperatures. The size of the dendrites in the mushy zone is related to the local solidification time (LST).

Local solidification time is defined as:

$LST=T_L-T_S/G\cdot R$

where T_L is the liquidus temperature (°C), T_S is the solidus temperature (°C), G is the temperature gradient (°C/cm), and R is the solidification rate (cm/min).

Increasing heat extraction or decreasing heat input (rate of molten metal introduction to the ingot) increases both G and R. This decreases LST, and, as is intuitively obvious, increasing heat extraction or decreasing heat input thus decreases dendrite size. When the solidification conditions become sufficiently slow (high LST) that the dendrites and the separation between them becomes large, the interdendritic regions may combine into a continuous channel of liquid. The channel remelts some of the primary dendrites and becomes several dendrites in diameter. This makes the feature visible at 1X magnification; that is, it becomes a macroscopic feature, while the normal interdendritic segregation is a microscopic feature. A critical characteristic of the large channel is that it becomes self-perpetuating.

Several theories have been proposed to explain the self-perpetuating nature of a freckle. They may be divided into two classes: those that assume that the interdendritic liquid is of lower density than the density of the liquid found in the region just above the liquidus (presumably alloys strengthened primarily with titanium and aluminum), and those that assume that the interdendritic liquid is of greater density than the liquid in the region just above the liquidus (presumably alloys strengthened with niobium). Low-density freckle formation tends to take the form of vertical channels at slight angles to the longitudinal axis of the ingot. High-density freckle formation favours the formation of radial freckles, which follow the shape of the boundary between the liquid plus solid/solid zone (but do not necessarily form on the boundary). Alloys forming high-density interdendritic liquids also may form vertical freckles.

1.1.1 Conditions for defects formation

Freckles occur in regions with high LSTs, that is, in large ingots, solidifying slowly and thus with large mushy zones (low G·R). In general, the more highly alloyed the material, the thinner the mushy zone must be to avoid the formation of freckles. The mushy zone thickness is affected by both melt rate and ingot diameter. It is seen that, for a

given ingot diameter, increasing melt rate increases mushy zone thickness and thus favours freckle formation.

The use of LST measurement and mushy zone thickness calculation cannot yet be used to predict freckle formation. It can be used to evaluate the qualitative effect of changing solidification conditions. With regard to changes in alloy content, it may be generalized that those elements (titanium and niobium) that contribute greatly to effective precipitate formation. Furthermore, the segregated regions are different in density from the matrix; thus, increasing hardener content in a steel increases the tendency to freckle.

The channellike nature of the freckle is seen when viewed in the longitudinal direction. When viewed from the transverse direction, the channels are seen as dark, etching round spots, thus the common name of freckles. For most commercially useful wrought steel, the solidification conditions of static casting will produce freckles. Thus, these alloys are normally static cast as electrodes, which are consumably remelted under controlled conditions.

The consumable remelt processes, vacuum arc remelting (VAR) and electroslag remelting (ESR), can greatly reduce LST by enhanced cooling and by limiting the amount of alloy that is molten at a given time (melt rate). Unfortunately, the electric currents used in consumable remelting processes generate magnetic fields. These magnetic fields affect the flow of the interdendritic liquid, further complicating prediction and control of freckle generation. Additionally, while the formation of features related to positive segregation may be suppressed, the nature of the remelting process is such that features that are solute-lean may be introduced into the final ingot. These features are discussed in the sections on consumable remelting. As is discussed in the subsequent sections of this chapter, melting methods for specific alloys are selected primarily on three criteria: economics, melt segregation requirements, and degree of chemistry control required.

1.2 Alloy composition and charge assembly

First, if the product is to be used in the AOD-cast condition, then alloy selection is driven by the composition of the steel and the solidification characteristics of this composition. The product from an AOD vessel is generally static cast. The segregation structures of the product must be acceptable in the final form of the product. This means

that the solute content of the steel must be low or not segregate strongly. Exceptions to this would be for alloys that segregate moderately but that have applications where the presence of the segregate is not detrimental to the performance of the steel.

Second, if the product does not require the extremely low gas contents or chemical control that are typical of vacuum primary melt processes, then the steel may be EAF/ AOD melted, cast as electrode, and consumably remelted. The foremost reasons for using EAF/AOD in preference to vacuum processes are the inherently lower cost of the raw materials used in the charge and the reduced melting times. The refining of chromium is difficult. With the cost increasing as both iron and carbon are removed. The ability of the EAF/AOD process to reduce carbon levels while recovering most of the chromium addition allows high-carbon ferrochrome to be used in place of low-carbon ferrochrome or even elemental chromium. Excess carbon is simply consumed as fuel for the process. Similarly, scrap alloy to be used in the melt does not have to be degreased or otherwise specially prepared, because carbonaceous contamination is removed during the process.

The elimination of costs for scrap preparation is again a cost saving. The recycling of scrap is a significant feature of the steel industry. Internal scrap losses/recycling may range between 25 to 50% in producing mill products. Many major components are machined into their final shapes from these mill products, with large losses of material to machining chips. The ability of EAF/AOD to forego the removal of oil and grease from these chips is a major saving. Additionally, as EAF/AOD removes elements with high free energies of formation for oxides, alloy scrap of compatible but not necessarily identical alloys may be used, thus increasing the supply of scrap while reducing the overall inventory of scrap that needs to be maintained. The down-side of this process is that steels containing high levels of elements with high free energy of formation of oxides are generally difficult to control in EAF/AOD for both tight composition ranges and freedom from oxide inclusions. Just as raw materials that are high in carbon may be used for EAF/AOD, so may materials that are high in sulphur. Sulphur is another element that is costly to remove from ores. Thus, high-sulphur charge material is less costly than low-sulphur material. The ability of the EAF/AOD process to intimately mix sulphur-reducing compounds (such as lime) into the liquid ensures that reduction of the sulphur into the slag will occur.

Chapter 2

Stainless Steel AL 15-5™ Precipitation Hardening Alloy (UNS Designation S15500, ASTM Type XM-12)

2.1 General properties

Allegheny Ludlum's AL 15-5™ Precipitation Hardening Alloy (S15500 or X5CrNiCuNb15-5) is a variant of the older AL 17-4™ (S17400) chromium-nickel-copper precipitation hardening stainless steel. Both alloys exhibit high strength and moderate corrosion resistance. High strength is maintained to approximately 316°C. The AL 15-5 alloy was designed to have greater toughness than S17400, especially in the through-thickness (short transverse) direction. This improved toughness is achieved by reduced delta ferrite content and control of inclusion size and shape. The composition and processing of AL 15-5 alloy is carefully controlled to minimize its content of delta ferrite, which is present in the S17400 material. Inclusion control is done by consumable electrode remelting using the electro-slag remelting (ESR) process.

The S15500 alloy is martensitic in structure in the annealed condition and is further strengthened by a relatively low temperature heat treatment which precipitates a copper containing phase (Ni_3Cu) in the alloy. Like the S17400 alloy, the S15500 alloy requires only a simple heat treatment; a one step process conducted at a temperature in the range 482°C to 621°C depending on the combination of strength and toughness desired. A wide range of properties can be produced by this one step heat treatment. Heat treatment in the 482°C range produces highest strength, although slightly less than those of semi-austenitic alloy like S17700 or S15700. The latter precipitation hardening alloys generally require more steps to complete heat treatment. The AL 15-5 alloy is generally better-suited for plate applications than are the semiaustenitic alloys.

2.1.1 Forms and conditions

The Allegheny Ludlum AL 15-5 Precipitation Hardening Alloy is furnished as plate. Long products are produced by Allvac, an Allegheny Technologies Company.
In all forms, the material typically is furnished in the annealed condition.

Element	Composition (Weight percent)
Carbon	0.05
Manganese	0.4

Phosphorus	0.02
Sulphur	0.005
Silicon	0.5
Chromium	15.0
Nickel	5.0
Niobium + Tantalum	0.3
Copper	4.0
Iron	74.73

Tab. 2.1 Composition (weight percent) of 15-5PH stainless steel.

2.2 Specifications

The Al 15-5 Precipitation Hardening Alloy (S15500) is covered by the following wrought product specifications.

Specification	**Product Form**
AMS 5862	Sheet, strip and plate
AMS 5659	Bars, forging, tubing and rings
AMS 5826	Welding wire
ASTM A 564 ASTM SA 564	Bars, wire and shapes
ASTM A 693 ASME SA 693	Sheet, plate and strip
ASTM A 705 ASME SA 705	Forgings

Tab. 2.2 15-5PH stainless steel product specifications.

2.3 Corrosion and oxidation resistance

Tests have shown that the corrosion resistance of AL 15-5 Precipitation Hardening Alloy is comparable to that of Type 304 stainless steel in most media. In general, the corrosion resistance of AL 15-5 alloy is superior to that of the hardenable 400 series stainless steels. As with other precipitation hardening alloys, AL 15-5 Precipitation Hardening Alloy is more susceptible to stress corrosion cracking at peak strength. Consequently, in applications in which chloride stress corrosion cracking is a possibility, the material should be precipitation hardened to produce the lowest hardness compatible

with the intended end use. This is done by heat treating at the highest temperature which will produce suitable minimum properties. Material in the annealed condition should not generally be put into service. In this condition, the material has an untempered martensite structure and is less ductile than aged material. The untempered martensite may be subject to unpredictable brittle fractures. In corrosive environments, the untempered martensite is more sensitive to embrittling phenomena such as hydrogen embrittlement than material which has had one of the precipitation hardening heat treatments. Similarly, untempered martensite is more sensitive to chloride stress corrosion cracking than material in which the martensite has been tempered. The oxidation resistance of the AL 15-5 alloy is superior to that of 12 percent chromium alloys like Type 410, but slightly inferior to that of Type 430. Precipitation hardening can produce surface oxidation.

2.4 Physical properties

The 15-5 PH steel's physical properties vary with the condition of the treatment of precipitation hardening.

The density increases with increasing of the treatment temperature as well as the linear coefficient of thermal expansion, that increases from 11.3 to 13.0 10.6 ° C, and showing direct proportionality.

The electrical resistivity proportionality to the precipitation hardening temperature is not known. In fact, it decrease with increasing temperature from the beginning, but it increase again in condition H1150.

15-5 PH	**Condition**			
	A	**H900**	**H1075**	**H1150**
Density (g/cm^3)	7.75	7.81	7.83	7.86
Linear coefficient of thermal expansion (10^{-6}/°C) Temperature range				
-73°C to 21°C	-	10.4	10.8	11.0
21°C to 427°C	11.3	11.7	12.2	13.0

Magnetic permeability	Strongly ferromagnetic in all condition			
Thermal conductivity (W/m·K) 21°C to 100°C 21°C to 500°C	 18.3 22.7	 17.8 22.7	 - -	 - -
Electrical resistivity (μΩ·cm)	98	77	80	86

Tab. 2.3 15-5PH stainless steel physical properties.

2.5 Mechanical properties

Room temperature tensile properties can vary substantially with heat treatment in the 482°C to 621°C range. Values shown below are typical room temperature properties which could be expected for various precipitation hardening heat treatments as well as the 1038°C solution heat treatment.

15-5 PH		**Condition**			
		A	**H900**	**H1075**	**H1150**
0.2% Offset Yield Strength	MPa	760	1200	930	860
Ultimate Tensile Strength	MPa	1030	1340	1070	1000
Modulus of Elasticity	GPa	196	196	196	196
Modulus of Rigidity	GPa	77.2	77.2	77.2	77.2
Elongation	%	8	15	15	15
Hardness HRc	-	33	43	31	28

Tab. 2.4 15-5PH stainless steel mechanical properties.

2.6 Heat treatment

Commonly produces the AL 15-5 Precipitation Hardening Alloy in the annealed condition. This is also called the solution heat treated condition, or Condition A. Annealing is conducted by heat treating at approximately 1040°C to 1065°C and cooling to room temperature. In this condition, the material possesses a martensitic structure. As a

martensitic material, the AL 15-5 alloy possesses a relatively high strength and hardness in the annealed condition. The strength and hardness of the material is generally somewhat lower in the H 1150 overaged condition.

Minimum Properties Specified for Products up to 4.762 mm thick in Aerospace Material Specification (AMS) 5862				
Heat Treat to Produce Martensitic Structure	**Precipitation Heat Treatment to Produce Desired Strength**			
	Precipitation Hardening Heat Treatment	**Yield Strength** MPa	**Tensile Strength** MPa	**Hardness** HRc
Solution Heat Treatment at 1066 °C **Condition A**	482 °C 60 minutes Condition H 900	1170	1310	40
	496 °C 4 Hours Condition H 925	1070	1170	38
	552 °C 4 Hours Condition H 1015	1000	1070	33
	579 °C 4 Hours Condition H 1075	860	1000	29
	593 °C 4 Hours Condition H 1100	790	965	29
	621 °C 4 Hours Condition H 1150	725	930	26
	760 °C 2 Hours + 621 °C 4 Hours Condition H 1150-M from SA 693	515	790	26 to 36

Heat Treating Parameters for AL 15-5™ alloy		
Condition	Temperature	Time
H 900	482 °C ± 5	60 min. ± 5 min.
H 925	496 °C ± 5	4 hrs. ± 0.25 hr.
H 1025	552 °C ± 5	4 hrs. ± 0.25 hr.
H 1075	579 °C ± 5	4 hrs. ± 0.25 hr.
H 1100	593 °C ± 5	4 hrs. ± 0.25 hr.

H 1150	621 °C ± 5	4 hrs. ± 0.25 hr.

Tab. 2.5 15-5PH stainless steel mechanical properties versus precipitation-hardening procedures.

To develop further increase in strength, the annealed material is precipitation hardened by heat treatments at 482°C. Heat treatments above 579°C generally result in material softer than material in the annealed condition. However, the precipitation hardening reaction can be driven past peak strength by heat treating at an excessively high temperature or by extended time at the precipitation temperature.

2.7 Welding and brazing

The AL 15-5 Precipitation Hardening Alloy is readily welded using conventional inert gas methods used for stainless grades. Preheating is not usually required. Postweld heat treating is needed to produce the various precipitation hardened heat treatment properties. If matching filler material is used, properties comparable to those of the parent metal can be produced in the weld by postweld precipitation hardening heat treatment. When a number of welding passes are made, a substantial thermal cycling has been conducted on the material. More uniform mechanical properties can be obtained by solution annealing the material before conducting precipitation hardening heat treatments.

The solution anneal has the effect of minimizing the effects of the thermal cycling. In the case of welding with non-matching filler, an austenitic stainless steel such as 308L or other ductile austenitic should be used. This filler will not produce the precipitation hardening response, however.

2.8 Forming

The tensile data for the AL 15-5 Precipitation Hardening Alloy indicate that the alloy does not possess the high tensile elongation characteristic of the austenitic stainless steels. The material is capable of being mildly formed but is not capable of being severely formed.

Forming is more easily accomplished in the overaged condition (such as H 1150), as opposed to the annealed condition. The table on page 3 shows the effect of higher temperature heat treatment. A less dramatic downward shift in strength results from excessively long precipitation hardening times. For maximum softness to provide best machinability and formability, a two-step “1400 + 1150” heat treatment may be used. This treatment, as described in ASTM A-693, involves a 2-hour exposure at 760 ± 8°C (1400 ± 15°F), air cooling, and a subsequent 4-hour exposure at 621 ± 8°C (1150 ± 15°F), and final air cooling. Properties in this condition are shown in the table on Page 3.

Chapter 3
Electric arc furnace processes

Small electric arc furnaces were in use in about 1900 lo manufacture tool steels and these small door charged Heroult designed units were installed to replace crucible

steelmaking. By the l920s top charging through swing aside roofs had been introduced on furnaces of up to 30 tonne capacity. These furnaces were powered with 7.5 MVA transformers Lo produce alloy steels in competition with open hearth furnaces. By the 1950s 90 tonne furnaces with 20 MVA transformers were making mild and plain carbon steels and the electric arc furnace became a modern steelmaking unit able to produce a wide range of steel grades. Such a unit had tap to tap times of about 4.5 hours and a corresponding production rate of about 20 tonnes/hour. Currently, with ultra high power (UHP), oxy-fuel assisted melting, and oxygen lancing, 140 tonne furnaces melting mild and low alloy steel have Lap to tap Limes of about 1.5 hours and production rates approaching 100 tonnes/hour. Straightforward arc furnaces are seldom used nowadays to make bulk stainless steels as these can be more efficiency made by associating arc furnace melting with secondary refining as discussed in Chapter 5. This chapter will, therefore, be concerned with the arc furnace as a high production unit for quality carbon and low alloy steels. The arc furnace is shown diagrammatically in figure 3.1a & b.

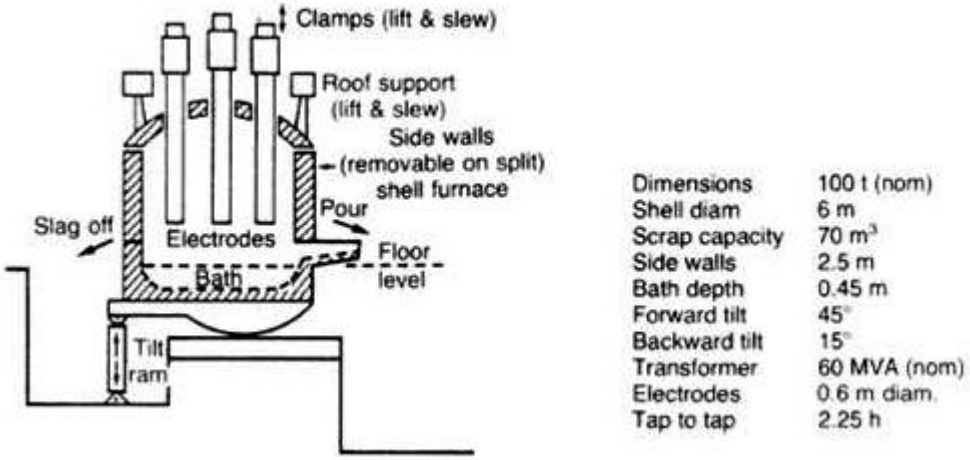

Fig. 3.1a The Electric Arc Furnace Processes

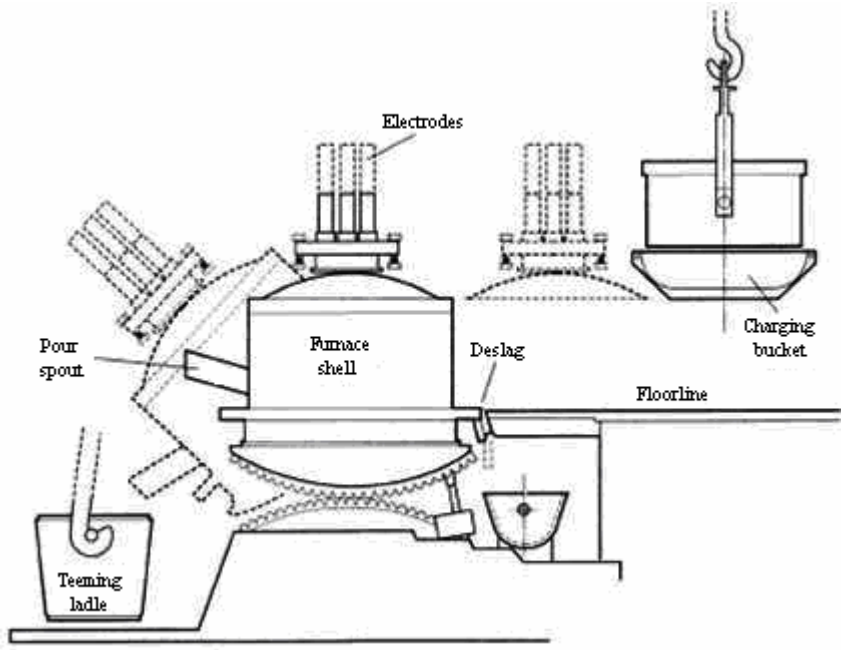

Fig. 3.1b Schematic of electric arc furnace

The furnace is a round, steel, water-cooled shell lined with refractory brick. The choice of brick is dictated by the alloys being melted and the furnace design. The economics of melting are that a furnace lining for a medium-sized arc furnace (18000 kg, capacity) may cost in the order of $10,000.

The bottom of the furnace is fixed, but the top may be swung in the horizontal plane entirely clear of the furnace shell so that the charge may be added. The furnace top has three carbon electrodes that protrude through the roof and may be extended or retracted. The front of the furnace has a pour spout, while 180° away there is an opening in the shell wall through which slag may be removed during the melt. The furnace is generally located in a pit, so that the pour lip and the slag removal openings are at floor level for the furnace crew. The pit allows the placement of transfer vessels and deslagging vessels next to the pour lip and the deslag opening, but at levels so that the tops of these vessels are slightly below the openings from which they will be receiving metal or slag from the furnace. The entire furnace is mounted on trunions so that the furnace may be tilted up to 90° forward to empty the molten metal charge into the teeming vessel.

The backward tilt for deslagging is normally less than 20°. Initially, because of the low apparent densities of charge material, not all the charge may be added to the furnace. After that portion of the charge that is feasible is added to the furnace, the cover is relocated on the furnace, the electrodes are lowered into the charge, and the arcs are struck between the charge and the electrodes. Initially, the arc is maintained at lower voltages. As melting begins and the electrodes move lower into the charge (bore in), the voltage is gradually increased to attain longer arc length and more efficient melting. Melting continues until the entire charge is molten. At this point, the initial charge volume is reduced to that of the molten metal, and the furnace may be opened and the remaining portions of the charge added (the recharge). This additional charge is melted by the arcs until the entire bath is molten. Further heating of the melt may now be done by blowing the heat with an oxygen/ argon mix injected through a hand-held lance. The oxides generated may be very aggressive in attacking the refractory lining of the furnace. In fact, general erosion of the refractory occurs in every melt. However, to protect against severe localized attack at the melt line, lime is usually added to the charge. As slag is formed in the arc furnace, it is removed manually.

The furnace is tilted backward and the slag is raked off the top of the melt, drawn through the slag removal opening, and falls into the vessel placed there to receive it. This process may be repeated as necessary, depending on the charge. After the major portion of the slag has been formed and removed, a ladle sample is taken to determine the chemistry of the melt. Based on that chemistry, further blowing may be conducted, or small levels of alloying addition may be made to attain the chemistry desired prior to transfer to the AOD vessel. Typical melt times for the EAF portion of the EAF/AOD process are in the order of 3 h.

When the arc furnace charge has been melted, adjusted to the desired temperature, and deslagged, it is poured into a transfer vessel. Generally, a transfer ladle (a refractory-lined vessel with a pour lip) is positioned in front of the arc furnace, and the furnace is rotated to pour the contents of the furnace into the vessel. The vessel may be lined with MgO so as to modify the nature of the lime-based slag. Unless the composition of the slag is properly maintained, it may become liquid and mix with the molten metal rather than

remain solid and float to the top of the melt. To avoid temperature loss during transfer, the vessel is usually preheated. The transfer ladle is moved to the AOD vessel and its contents poured into that vessel.

As may be deduced by the dual nature of the process name, there are two pieces of equipment involved in the process: an electric arc furnace and an argon oxygen decarburizing vessel.

The assembled charge is placed into the EAF. The arc furnace power is provided through large carbon electrodes, which protrude into the furnace through the furnace roof and may be extended into or withdrawn from the charge. To begin the melt, the electrodes are extended into the charge, and a current is passed from the electrodes through the charge to the base of the furnace. As the electrodes are gradually withdrawn. an arc is established between the charge and the electrode. This arc provides the power for the initial melt-in of the charge.

After melt-in of the charge, lime (CaO) is introduced to provide a slag that will reduce the sulfur level of the melt. Additionally oxygen is introduced into the melt by insertion of a pressurized oxygen lance underneath the liquid surface. The reaction of oxygen with carbon, silicon, and aluminum removes most of these elements into the slag. while the heat of the exothermic reaction maintains the desired melt temperature. This process of removing the undesired elements from the melt is known as the reduction phase of the melt. It is a notable feature of the EAF/AOD process that after the initial melt-down, temperatures are maintained in both pieces of equipment by the oxidation of reactive elements in the melt, not by use of external power. When necessary, cooling is accomplished by the addition of solid scrap to the melt. This process generates large amounts of slag, both from oxidation and desulfurization.

The slag is removed manually from the melt by scraping the metal surface so as to draw the slag through an opening at the back of the arc furnace and collect it in a ladle below the opening. After deslagging, a chemistry sample is obtained for the heat. Adjustments to the heat chemistry will be made on the basis of the sample analysis. To maintain temperature during this period, aluminium may be added to the heat and then removed completely by an oxygen "blow."

When the desired chemistry is obtained, the charge in the arc furnace is poured from the front of the furnace into a transfer ladle.

The transfer ladle is brought to the second piece of equipment involved in this process, the AOD vessel.

3.1 The metallurgy of arc furnace steel production

Precise temperature control and clean melting in a sulphur free atmosphere made the electric arc furnace an attractive proposition for the melting of quality alloy steels. Arc furnaces are charged with clean scrap, steel and pig iron, limestone and possibly anthracite or broken electrodes as a source of carbon and melted as quickly as possible. Nickel and molybdenum, when required, are added with the scrap as these elements are not- oxidised out during refining. At melt out, the bath is sampled for analysis and temperature determined. Bath temperature would be raised to I530°C-1550°C whilst the analysis is being obtained and studied to decide on the metallurgical actions required to complete the heat. Since there is an inherent, random variation in composition of the scrap, there is a similar variation at melt-out. With good practice the melt-out carbon should be at least 0.2 to 0.1% above the specification; sulphur and phosphorus are generally low and below 0.01%. If alloy steels are being made scrap is selected to ensure that the bath contains some of the alloys required, eg nickel, molybdenum and chromium. Such practice reduces the amounts of expensive ferroalloys needed to bring the steel into specification. Silicon and manganese are always present in steel scrap and plate iron and the quantity at melt -out will depend on the nature of the scrap and the relative amounts of plate iron and scrap charges. Plate iron is usually 75mm thick and can be contaminated by blast furnace slag and the plating bed sand. Oxygen lancing follows melting.

3.1.1 Refining

Carbon is the principal element removed by the oxygen blow but other elements in minor quantities are also removed. These are silicon, manganese, phosphorus and chromium and each can be treated as an equivalent amount of carbon. The carbon equivalent for these elements is given below in Table 3.1

Element	Carbon equivalent % of 1% of element
Silicon	0.85
Manganese	0.22
Phosphorus	0.97
Chromium	0.35

Tab. 3.1 Carbon equivalents for oxidation

Oxidation occurs in the manner already discussed in previous chapters and once again carbon removal and carbon monoxide evolution produces the "carbon boil" which is an essential feature of all steemaking process. The boil promotes stirring which results in good slag/metal mixing, elimination of temperature and concentration gradients, and the reduction of dissolved hydrogen and some nitrogen in the melt. For these reactions, it is possible to calculate the theoretical amount of oxygen needed to remove 0.01% of each element and the resulting temperature rise. The data so calculated is given below in table 3.2.

Element	O_2 needed m^3/0.01%/t	Temperature rise °C/0.01% element oxidised
Iron	0.021	0.5
Carbon	0.099	1.3
Silicon	0.083	3.1
Manganese	0.021	0.8
Phosphorus	0.096	2.0
Chromium	0.035	1.2
Sulphur	0.075	0.8

Tab. 3.2 Theoretical amount of oxygen needed and temperature rise resulting from oxidation of 0.01% of elements

This data is useful in showing relative amounts of oxygen needed together with the corresponding temperature rise resulting. In practice, the amount of oxygen needed depends on the initial carbon content and temperature of the bath. The temperature rise is dependent mainly on furnace size and rate of oxygen input. Oxygen injection also increases the iron oxide content of the slag. Whilst this is not significant above about 0.2%C, below this level of carbon in the bath, the oxygen requirement for decarburising

increases significantly. This is shown in figure 3.2 where the specific oxygen consumption in m^3/0.01 %/tonne is given for bath carbons between 0.05% and 0.6%. Above 0.25%, the oxygen required is approximately 0.12m^3/0.01 % C/tonne. The theoretical amount to convert C to CO is 0.093m^3/0.01%C/t. Further oxygen oxidises iron, manganese and to a lesser extent silicon, chromium and phosphorus into the slag. Injection at too high a rate reduces the efficiency of oxidation and increases the oxygen requirement.

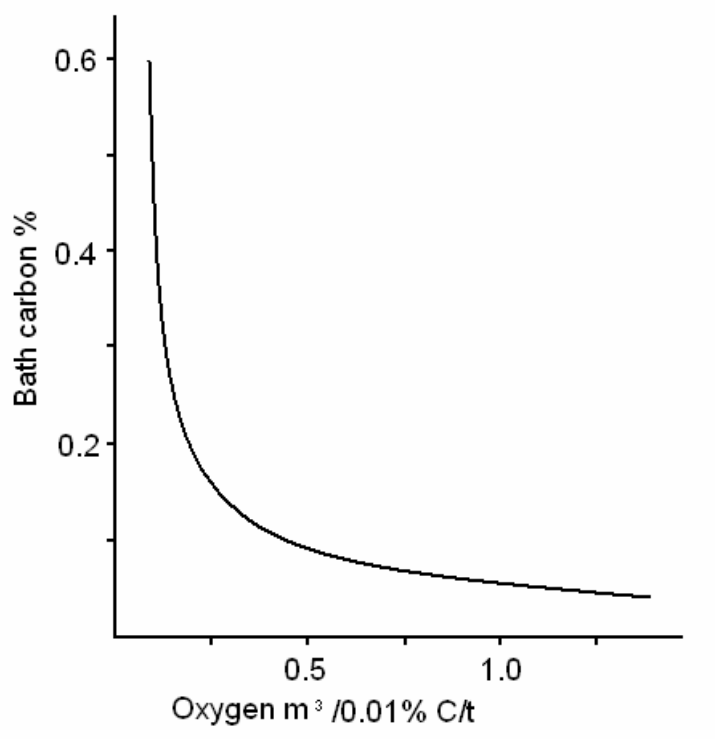

Fig. 3.2 Practical oxygen requirements for decarburisation as a function of bath carbon

For a finishing carbon in the range 0.1 -0.2% having removed 0.25% C, the typical quantity of oxygen used would be 5.5-7.0 m^3/tonne. It would be usual to remove this amount of carbon in l0-15 min depending Lo some extent on the furnace size. For a given furnace, the oxygen needed to remove the carbon would be known more precisely than the range quoted above. Similarly, the probable temperature rise would be known. For furnaces above about 50 tonne capacity, 0.05 m^3/t/min will increase bath temperature by about 1°C.

For a 100 tonne furnace where 0.25% has to be removed in 15min, the oxygen required, its blowing rate and probable temperature rise are given below in Table 3.3.

Criteria	Magnitude
Furnace	100 tonnes
Carbon removal	0.25%
Specific oxygen	0.25 m^3/0.1/C/t
Total oxygen	625 m^3
Time	15 min
Oxygen flow rate	41 m^3/min
Specific temp rise	1°C/0.05m^3/min
Temperature rise	82°C

Tab. 3.3 Criteria for 100t arc furnace 0.25%C removal in 15min.

3.1.2 Desulphurisation

Sulphur can enter the arc furnace bath only from the charge, hence by good scrap management, the sulphur burden can be limited. Sulphur is, however, always present, to some extent, in scrap steel and this is best removed after the oxygen blow which removes carbon and other oxidisable elements. The highly oxidised CaO-FeO "first slag" is removed and a new slag is made by adding calcined lime, fluorspar and carbon to the bath. This is the reducing slag which promotes desulphurisation of the bath. The sulphur, present in the steel as iron sulphide, reaches equilibrium with iron sulphide in the slag. The iron sulphide in the slag reacts with the lime to form calcium sulphide thus removing iron sulphide from the equilibrium with sulphide in the metal. These reactions are shown below:

$$FeS_{(\text{in metal})} = FeS_{(\text{in slag})}$$

$$FeS_{(\text{in slag})} + CaO_{(\text{in slag})} = FeO_{(\text{in salg})} + CaS_{(\text{in slag})}$$

With excess lime (CaO) in the slag, the free iron oxide FeO, which is the oxidising unit in the slag, can be reduced to less than 2%. Such a slag would be very reducing and promote rapid sulphur removal. The small amount of carbon added will reduce the dissolved oxygen content in the metal to the equilibrium level required by bath carbon.

This reduction in the metal will influence the oxygen (ie Fe) content of the slag and promote the reducing conditions conducive to sulphur removal.
These can be expressed as:

FeO (in slag) = FeO (in iron)
FeO (in iron) + C → Fe + CO

The small evolution of carbon monoxide prompts gentle stirring which brings unreacted metal into contact with the slag. The fluorspar may contain appreciable quantities of sulphur itself and may affect the slag basicity but physically fluxes and increases the fluidity of the slag which allows the slag reactions to proceed more rapidly and uniformly than would be possible in a viscous slag. Some sulphur is oxidised from the slag into the furnace atmosphere.

It is estimated that reducing slags can remove about 40% of the sulphur in the bath. (Some sulphur is removed by partition into the first oxidising slag) at rates of about 0.006/7%/hour. Such rates are low and 30 to 60 minutes would be needed for desulphurisation under one reducing slag. If sufficient sulphur is removed a second reducing slag would be made after removal of the first sulphur saturated slag. Since such a procedure would add a further 50-60 min to cycle time and hence significantly decrease productivity, it is important to avoid high sulphur charges.

The gentle stirring caused by the carbon monoxide boil can be enhanced to increase the desulphurisation rate. This was originally done .by mechanical rabbling with greenwood poles which also burned to increase gas evolution in the bath still further. Induction stirring and argon gas bubbling also increase stirring and slag/metal contact and desulphurisation rates of up to 0.009/0.010%/h have been achieved to reach final sulphurs of 0.008-0.010%.

More recently, techniques have been developed to inject desulphurising powders with argon or nitrogen into the ladle. Using these methods, which are discussed in Chapter 4, desulphurisation can be completed in about l5 min.

3.1.3 Hydrogen

Hydrogen is introduced into the steel bath by rusted and damp charge materials and additions of lime and fluorspar. Drying of fluxes can be particularly beneficial in reducing the hydrogen load. Some hydrogen is, however, absorbed from the water vapour in the atmosphere. From charging to commencement of the carbon boil at about l5l0°C, the hydrogen content of the steel could be in the range 6-8 ml/100q. Oxidising conditions favour reduction of hydrogen and the carbon boil with the evolution of carbon monoxide rapidly reduces the hydrogen content. The violence of the boil directly affects hydrogen removal and this is illustrated in figure 3.3. After the oxygen blow outlined in table 3.3, ie 1.0%C/h, the hydrogen content could be in the range 1-2 ml/ 100g.

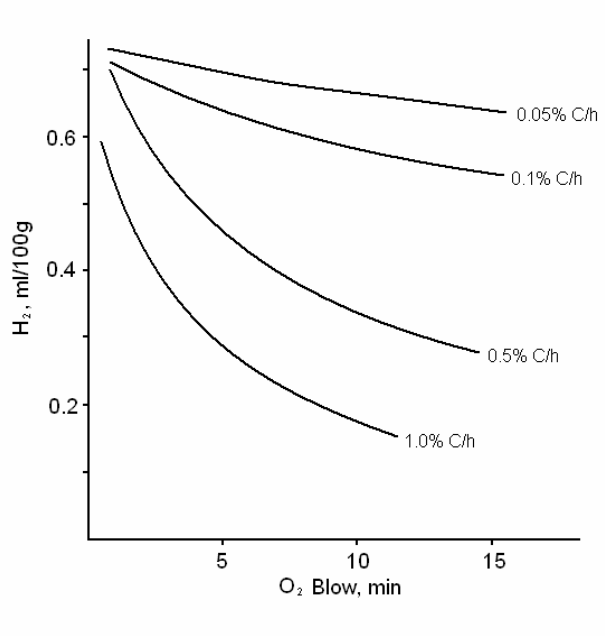

Fig. 3.3. The effect of carbon removal rate on H_2 removal

The danger period for hydrogen pickup comes at the end of the carbon boil when the reducing slag is being employed for sulphur removal. Although the partial pressure of hydrogen is low in the arc furnace atmosphere the arc itself readily dissociates water vapour to molecular and atomic hydrogen. The latter form of hydrogen diffuses readily into liquid steel where it tends to remain because of the absence of a purging evolution of carbon monoxide during the reducing cycle. High quality low alloy steels are frequently

made in the arc furnace and these steels are particularly susceptible to "hair-line" crack formation caused by hydrogen. For this reason it is usually necessary to vacuum degas these steels lo avoid prolonged and expensive hydrogen removal by heat treatment.

3.1.4 Nitrogen

Nitrogen is added to the arc furnace bath in the charge but most is absorbed directly from the atmosphere. The higher the temperature, the greater is the rate of absorption.
Nitrogen is reduced by gas evolution during the carbon boil and if desulphurisation were not necessary (ie single slag practice) then the steel would finish at about 70 ppm nitrogen. Double slag practice (ie one oxidising slag and one reducing slag) produces steels with nitrogen in the range 80-110 ppm.

3.1.5 Deoxidation and final additions

This step would be brought about as for the open hearth by additions of mixed deoxidisers such as ferromanganese, ferro silicon and aluminium. Other ferroalloys to bring the steel into specification would be added and the bath temperature increased to the desired tapping temperature. Trim additions would be made in the ladle.

3.1.6 Residual element control by charge selection

Residual elements cause the greatest problems during reheating and subsequent rolling operations, particularly tin and copper. These elements are enriched at the surface during reheating for rolling by the preferential oxidation of iron, and form low melting point phases with iron. (Nickel, chromium and molybdenum are essential components in alloy steel production, but in many plain carbon steels, these elements are deleterious to properties, for example weldability). The important feature about residuals such as copper, tin, nickel, molybdenum (and to some extent chromium) is that they are not removed during steelmaking.

The majority of the charge to the arc furnace is merchant scrap bought from out-side the steel works. Such scrap has, even within grades, unpredictable variations in physical size, shape and composition. Crushing and baling to increase bulk density to assist

charging will retain any non-ferrous scrap and increase copper, tin and aluminium in the steel. Size reduction and magnetic separation will reduce such physical scrap contamination. However, scrap processing is only now becoming accepted and increasing contamination from copper, tin and aluminium significantly affects steel quality.

Such processing cannot segregate different steel qualities. Hence alloy scrap for plain carbon steel charges increases nickel, chromium and molybdenum which will affect end use properties. Free cutting steel (with up to 0.1% sulphur) and cast iron (with up to 0.3% phosphorus) significantly increases the sulphur and phosphorus burden. While these two elements can be reduced during steelmaking, such operations need time and power to bring the steel within specification and the costs of production are thus increased.

At some stage, a high grade of furnace charge, ie one containing less residuals has to be introduced into the charge mix so that the final steel remains within specification. Such iron sources are of higher cost than scrap and are hence kept to a minimum.

One source of high quality scrap of known and consistent composition is virgin scrap directly from a blast furnace - LD steelmaking operation. Such scrap is not usually available on the open market and therefore only available in large steel.

Another source of predictable consistent qualify iron units is blast furnace iron. It is available in broken plate or granulated. Such iron contains at least 4% C whereas most steels from arc furnaces generally contain less than 0.6% C. Clearly there is a limit d the amount of such iron units that can be charged. (The carbon could, of course, be removed by oxygen blowing but this would add time and cost to the operation.) The growth of the arc furnace as a steelmaking unit using all scrap began to affect the availability of scrap in the mid 1960s. The scrap quality was deteriorating, and its cost to the steelmaker was increasing.

There was, therefore, a need for another source of iron units. Direct reduction of iron ores to metallic iron (not involving the liquid iron stage as in blast furnace operation) had been used on a very limited scale for many years. During the late 1950s and early 1970s several processes using static reactors, vertical shafter kilns or horizontal rotating kilns were developed using gas, oil or coal as the reductant. The product., usually pelletted for ease of handling has predictable and low residual elements and controllable carbon making

an ideal charge iron source for arc furnaces. The residual contents of the iron units discussed is given below in table 3.4.

Source	Cu %	Ni %	Sn %	S %	P %
Pressed & sheared scrap	0.42	0.24	0.02	0.08	0.04
Old baled scrap	0.45	0.1	0.1	0.11	0.04
Mech fragmented scrap	0.13	0.08	0.01	0.03	0.01
Cryogenically fragmented scrap	0.16	0.1	0.01	0.03	0.02
New detinned scrap	0.05	0.01	0.15	0.02	0.01
Turning (loose)	0.29	0.34	0.02	0.08	0.03
Turnings (briquettes)	0.26	0.29	0.02	0.15	0.03
BOF scrap	0.03-0.06	0.02-0.06	0.01-0.02	0.01-0.02	0.02-0.04
Blast furnace iron	0.01-0.02	0.01-0.03	0.01	0.03-0.05	0.01-0.03
Directly reduced iron	0.005	0.01	0.005	0.01	0.01
Specification	0.3 max	0.3 max	0.05 max	0.06 0.03	0.06[1] 0.03[2]

Tab. 3.4 Residual contents of various iron units ([1] bulk steel; [2] alloy steel)

It must be stressed that the data given in Table 3.4 for scrap gives only a general indication of residual elements for the class of scrap to which the analysis is ascribed. Scrap sampling is notoriously difficult as is its "quality control". The analyses do highlight the problem of the arc furnace steelmaker who has to charge large tonnages for different grades of scrap with large variations of analyses within grades. The scrap grades are diluted with known composition iron sources to ensure an adequate safety margin below specification for the steel being made. This is usually 0.1% for copper and nickel, 0.02% for tin and phosphorus. A greater latitude exists for sulphur (probably 0.03%) since this can be removed by furnace or ladle treatment. Pressed and sheared (not a UK classification) or baled scrap is widely available. Further upgraded scrap is not. Some mechanical fragmentisers are in operation but there is only one cryofragmentiser in Europe and no hot briquetting plant.

3.2 The engineering of the arc furnace system

The engineering system will be examined in relation to the metallurgical stages of operation which are given below in Table 3.5. This Table has been constructed for the previously used example of a 100 tonne furnace tapping in 4 hours.

Stage	Operation	Duration (min)
1	Charging	20
2	Melt down	120
3	Refining	15
4	Desulphurisation	45
5	Alloying	10
6	Heating to tapping temperature	10
7	Tapping	5
8	Fettling	15
Total	Tap to tap	240

Tab. 3.5 Stages in arc furnace melting

This table identifies the stages where engineering changes will have most effect on the overall cycle time. These are melt down and desulphurisation but small reductions in other stages, cumulatively, can also have an effect.

3.2.1 Initial capacity

For a new arc shop, the installation of the largest capacity furnace, suitable for production plans, is the first step to take. Since the 1950s, the maximum arc furnace size has increased from about 100 tonnes to about 400 tonnes. For existing furnaces, productivity can be increased by several methods: charge preparation, increase in power input, assisted melting and reduction in metallurgical load.

3.2.2 Charge preparation and handling

Scrap A significant portion of scrap for arc furnaces comes from the "consumer durable" sector, ie scrap cars, refrigerators etc, which has a low bulk density. The furnace had a finite volume and increasing bulk scrap density could decrease the number of baskets typically used from 3 to 2.

Generally, yield of iron from the scrap also increases with increase in density. This is due to the removal of non metallic material and decrease of oxidation during melting. Table 3.6 gives typical bulk densities and yields on melting the range of scrap available.

Scrap type	**Bulk density**	**Melting yield**
	Kg/m^3	%
Pressed and sheared	600	65 – 70
Turnings	600 - 1200	70 – 75
N°5 bales	1300 – 2000	70
Mech fragmented n°5 bales	1000	90 - 92
Bale fragmented	2000 – 2500	90 - 92
Cryogenically fragmented n°5	2000 – 2500	90 – 95
Cold pressed turnings	4000	90 - 95
Hot pressed turnings	6000	95 - 98

Tab. 3.6 Bulk density and metallic yields of scrap grades

Computer programs are generally used to select the initial charge materials from the available inventory. The form of material and the nature of the arc furnace into which it will be charged dictates a specific loading order for charging the selected material. Generally, the charge is loaded into several bottom-opening containers. Each container may, in its turn, be located over the arc furnace, the bottom opened. and the contents dropped into the furnace.

The impact of large scrap pieces on the refractory bottom of the arc furnace may severely damage that refractory and reduce furnace lining life. Thus, lighter scrap pieces, such as machining chips, are generally added to the arc furnace first, so as to provide a cushion upon which subsequent larger pieces may be charged. The last material added to the top of the charge is also of lighter form. This is done so that when the carbon electrodes are driven into the charge to initiate melting, they will be submerged in the charge material. This allows the arc to be drawn through the charge metal and not to the lining or roof of the arc furnace. Again, the purpose is protection of the refractory lining.

3.2.3 Directly reduced iron

Because the reduction process is a gas-solid reaction the degree of reduction of the iron ore and the carbon content can be controlled. The iron ore, although pretreated, still contains other oxides, eg, alumina, silica and lime which persist to a limited extent in the pellet. The acceptable range of parameters for DRI for arc furnace is given below in Table 3.7

Parameter	Range %	Aim
Metallisation	90 – 96	as high as possible
Total iron	88 – 94	not more than 2% below metallisation
Metallic iron	83 – 91	not more than 5% below total iron
Gauge	4 – 10	as low as possible
Sulphur and Phosphorus	0.03 – 0.05	as low as possible
Carbon	0.8 – 1.5	dependent on arc furnace practice
Size	>5mm	reduce dust burden on fume cleaner

Tab. 3.7 Direct reduced iron for arc furnace

The ranges given are to cover most arc furnaces, operation. For a given furnace, the actual specification required from the DRI plant would depend on furnace size, steels to be made, quality of available scrap and method of operation, the overall aim being Lo reduce total production costs. The effect of the variations of the parameters on other aspects of furnace operation (and hence costs) are discussed below.

3.2.4 Degree of metallization

All reduced materials contain oxides of iron which, on melting, will enter the slag phase. Yield losses may be higher due to increased slag bulk but since some pellets have lower gangue content than some scrap, this may not occur. There is no evidence to suggest any difference in slag chemistry between pellet and scrap charge, but any higher oxide contents can be reduced.

FeO, Fe_3O_4, Fe_2O_3 + carbon + heat → Fe + CO

In the first case for wustite (FeO) it has been shown for an 85 tonne furnace that the energy requirements increase by l0 kWh/tonne per 1% decrease in the degree of

metallization. For the magnetite (Fe_3O_4) and ematite (Fe_2O_3) reactions, the energy increase is likely to be 20 kWh/tonne/l% decrease in metallization. It is obvious that the metallic content of the pellet should be as high as possible.

3.2.5 Gangue content

The gangue, usually silica (Si0z), can alter steelmaking by changing both slag weight and chemistry. For an increase of 100 kg of slag weight per tonne of steel, there is an increase in energy needs of between 85 and 150 kWh/tonne. It follows that gangue content should be kept to a minimum.

Composition is also important since, if all the gangue content is acidic, ie, silica, then lime will have to be added separately to the furnace to give the desired lime/silica balance. The gauge composition can be modified in the reduction unit lo produce a self fluxing pellet. The gangue of such a pellet would have a lime/silica ratio of between 2:1 and 3:1. No additions other than the pellets would be needed. Generally an all scrap melt will produce between 50 and 75 kg slag/tonne of steel. The gangue content of pellets would have to be as low as 2% Lo give a similar slag bulk for 100% pellet charge. The desired range of 4-6% for 100% charge would give slag bulks of about 100-l50kg. The more usual practice is Lo mix charge thus reducing the effect of the gangue content on slag bulk.

3.2.6 Charging Practice - baskets

Most arc furnaces have swing-aside roofs so that the full cross section is available for charging. Scrap from the arc furnace stockyard is packed in baskets or buckets with a clam shell base closure. For the first basket into an empty furnace, light scrap is placed in the base (to act as a cushion) with heavier scrap above and light scrap above again to allow the arcs to penetrate quickly and save roof refractories. The basket is lowered into the furnace and the rope, which holds the base closed, burns through and discharges the scrap into the furnace. The roof is swung back and power switched on to melt the charge.

For a 100 tonne furnace, it would be usual to use no more than three baskets, probably 40, 40 and 20 tonne to complete the furnace charge. Time would be saved and production increased by two basket charging with higher bulk density scrap.

3.2.7 Charging practice - continuous

Processed scrap, ie mechanically or cryogenically fragmentised and pellets, all have a consistency of size and shape which make these forms of iron units suitable for bunkering and conveying and hence continuous charging into an arc furnace. Continuous charging can be used to supplement batch charging or used as the only method of charging. In the developing countries continuous charging of pellets is a major production route.

Where continuous charging is required, the iron is fed into a molten heel of metal. This practice has the advantage of decreasing power fluctuation associated with all scrap melting during the melt-down period. The stable melt conditions can reduce power consumption by up to l0% and decrease charging time.

3.3 Refractory linines for electric arc furnace

There has been a downward trend in refractory consumption over the past few years. As is evident, a considerable improvement has been achieved in refractory costs, despite a significant rise in installed electrical power. The consumption figures for sidewall and roof bricks, gunning material, and dolomite and magnesite masses are already so low that no further significant improvements can be expected in the near future. Consumption of sidewall bricks is currently 0.1 kg/t, roof bricks 0.15 kg/t, gunning material 0.5 kg/t and dolomite and magnesite 5 kg/t.

During the last ten years the application of water cooled panels for the roof and walls of the electric arc furnace has spread rapidly. For this reason this update will not deal with the refractory lining techniques for fully refractory lined furnaces.

The practice of eccentric bottom tapping (EBT) is now widely adopted. Higher quality refractory materials have come to be employed for this purpose recently though other tapping systems, such as the slide gate type, are now being tried.

At the same time there have been changes in the internal profile of the EAF, an example of this being given in Figure 3.5.

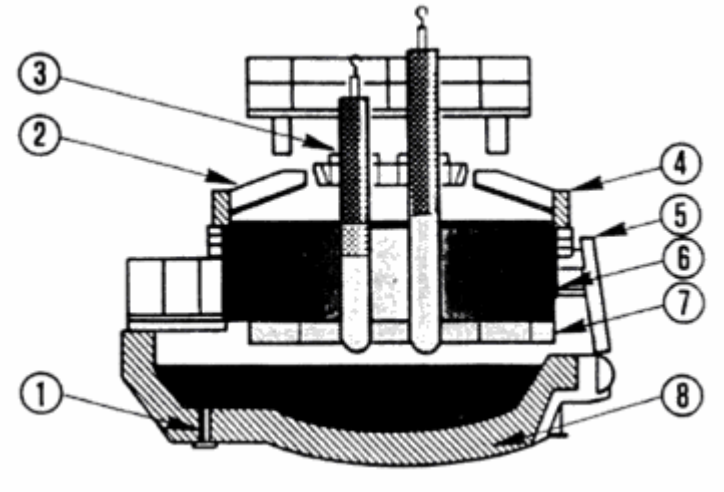

Fig. 3.5 Internal profile of an EAF

3.3.1 Hearth area

Several chemical, thermal and mechanical factors act continuously on the hearth, i.e. corrosion, steel and slag infiltration, level and fluctuation of temperature, erosion and scrap impact. So far, the materials most commonly used for the working hearth continue to be dolomite and magnesite in the form of monoliths or bricks.

In Japan and the USA, magnesite hearths are still the most frequently employed. In Europe the use of magnesite rather than dolomite is on the increase. In particular, the last layer generally consists of a magnesite ramming mix which is much simpler and faster to install than bricks.

To reduce costs the hearth area can be constructed in two layers where the sole casing is lined with two layers of magnesite bricks for safety, topped by a layer of dolomite bricks and rammed with a layer of magnesite mass. The tapping area is equipped with a perforated brick which encloses the cylindrical tapping bricks.

Hearth repairs are made either with masses of the same kind or with special hearth repair mixes. To achieve a satisfactory life, the repair layer should be at least 150 mm

thick. Repairs are possible in hot and cold furnaces alike, but it goes without saying that prior to repair the hearth has to be cleaned thoroughly.

3.3.2 Taphole systems

The EBT system has found increased application in recent years. However, some recent applications of a taphole slide gate system are also giving good results.

The lower slope of the EAF necessary for tapping (less than 10°) compared with conventional furnaces (35°) has permitted extension of the panelled zones to cover some 90% of the side walls, it has also allowed reduction in the distance between the slag line and panels by installing copper panels (for safety reasons) to replace some of the refractory. In order to reduce heat losses in the lower part of some plants, shorter magnesite carbon bricks (15% carbon) have been built in front of the copper panels Taphole tubes have an average life of 150 to 250 heats, depending to a large extent on the refractory material chosen. Very good thermal shock resistance and sufficient erosion resistance at high temperatures are required for achieving satisfactory lifetimes. Due to their high structural flexibility, synthetic resin bonded MgO-C qualities have given good results. Their residual carbon content is between 14 and 20%. Taphole tubes are laid absolutely dry, without mortar.

The end brick must also be highly resistant to mechanical damage, which can be caused during clearing. The danger of decarbonisation is also particularly great during cleaning. Depending on operating conditions, end bricks have a life of between 90 and 160 heats.

A quality of refractory that has provided very good results recently is synthetic resin bonded MgO-C brick containing antioxidants. These are characterised not only by good structural flexibility but also by very high structural strength and oxidation resistance with a residual carbon content of around 14%.

A plugging compound mixture of MgO-SiO_2 with 10% F_2O_3, grain size 0.5 to 0.6 mm is generally used to fill the taphole at the end of the heat.

3.3.3 Taphole slide gate

A new system has been developed recently. This involves a taphole slide gate set up in place of the spout on the furnace shell. The installation utilises a fixing flange on the external channel.

The centreline of the internal refractory channel slopes 10° to the horizontal. It is closed by means of lime chippings. Zirconium inserts are used to increase the life of the outlet nozzles. The great advantage of this closure system is that it allows almost complete retention of the slag in the EAF, permitting not more than 200 kg to pass into the ladle. The average life of the refractory channel is about 68 heats, while that of the box nozzle is about 28.

3.3.4 Side wall lining

Under normal conditions the safety lining of the sub wall never comes into contact with the steel bath. Fired magnesite bricks made from high iron sinter magnesia are frequently utilised in this zone.

The safety lining usually extends up to the sill, whereas in the eccentric extension of the furnace it is often installed along the full wall height, since even the top rows of bricks in this area can come into contact with the steel bath when the furnace is tilted too quickly. A further advantage of this practice is the reduction of energy losses in the extension area. Magnesite carbon bricks are still used for lining the slag zone, owing to their very good characteristics. For severe conditions, these bricks may now also contain fused magnesite.

Compared with fired, pitch impregnated magnesite bricks, pitch bonded magnesite qualities have a higher residual carbon content and therefore exhibit better resistance to slag attack. Fused magnesite has the advantage of having higher density and lower chemical reactivity than sintered magnesite, thus offering greater resistance to reduction of carbon in the brick.

Product	Dim.	Pitch bonded magnesia bricks	Pitch bonded magnesia bricks	Pitch bonded magnesia bricks
Description	-	Tempered, low iron, slag repellent, excellent high temperature strength	Tempered, made from low iron synthetic sinter magnesia, excellent resistance against slag, excellent high temperature strength	Tempered, made from very pure synthetic sinter magnesia, extremely low Fe_2O_3, SiO_2 and B_2O_3 contents, slag resistant
MgO	%	-	95	96.5 – 99
Cr_2O_3	%	-	-	-
Fe_2O_3	%	1.5	0.3	0.2
Al_2O_3	%	0.4	0.3	0.1
CaO	%	2.3	2.2	0.7
SiO_2	%	0.6	0.3	0.1
Residual carbon	%	5	5	5
Bulk density	g/cm^3	3.09	3.11	3.11
Open porosity	%	<7	<7	<7
Cold crushing strength resistance	N/mm^2	>40	>40	>40
Pitch impregnated on request	-	*	*	*
Special after treatment on request	-		*	*

Tab. 3.8 Characteristic of some types of pitch bonded magnesia carbon bricks

It is customary to leave a safety gap of 300 to 350 mm between the bottoms of the water cooled steel panels and the slag in order to avoid explosion. This safety gap can be reduced to 200 mm by the insertion of copper panels beneath the steel water cooled panels. These copper panels can, in fact, withstand an occasional surge of slag.

In order to reduce slag line refractory wear, they have developed moulded copper blocks with wings (Figure 3.6) which are intended to be inserted at slag level. These wings collect slag (Figure 3.7) and the energy losses are slight, while the consumption of patching refractories is reduced by 70 to 80%. Any danger can be averted by following the heating up of the copper by means of thermocouples.

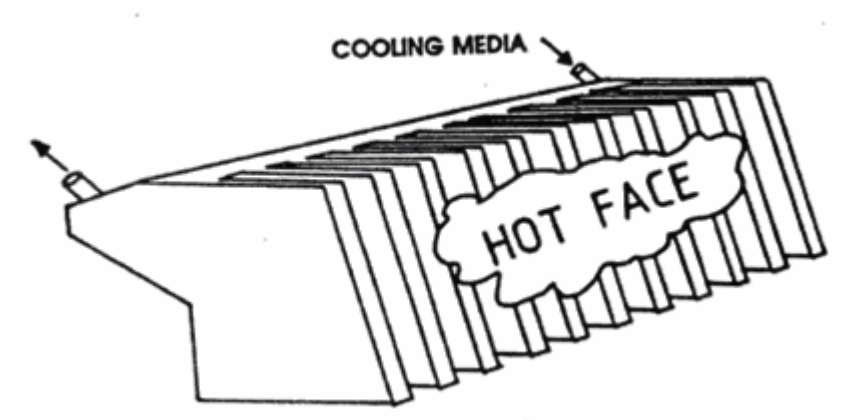

Fig. 3.6 Copper moulded blocks which can help to reduce slagline refractory wear

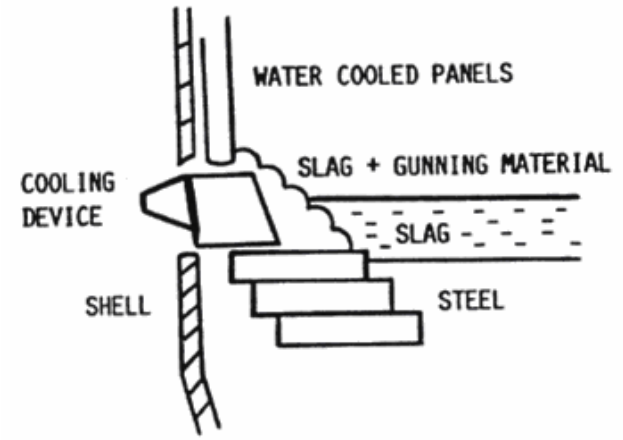

Fig. 3.7 Device for cooling of the safety zone in EAF.

Where hot spots are concerned, owing to the particular stresses generally encountered in that area, synthetic resin bonded MgO-C types from top quality sinter magnesia having a residual carbon content of more than l0% are suitable.

The qualities frequently contain varying amounts of fused magnesite, as well as antioxidant additives.

The recent introduction of the latter has markedly improved the performance of magnesite carbon refractories. Metals being used are aluminium, silicon and magnesium. One reason for adding these metals is to improve oxidation resistance, since the metals consume oxygen that would otherwise oxidise carbon. Another reason for adding metals is to improve the hot strength of the magnesite carbon brick.

Low cost magnesia carbon bricks or pitch bonded magnesite bricks are installed in the interphase areas which are less subject to wear. The qualities should be chosen in view of achieving a balanced lining. For better stability, metal cased bricks are often used for the two or three courses.

Pitch bonded magnesite bricks are mainly used for lining the eccentric furnace extension. In most cases the quality is identical with that installed in the slag zone. For heat balance reasons, however, the bricks installed there should have low thermal conductivity. Metal cased bricks, if any, are used in the extension area in the top courses only.

3.4 Energy input

The prime source of energy is electrical which is transmitted to the steel via the three carbon electrodes.

Power is needed not only to melt down the steel scrap and superheat the molten metal, but also to compensate for heal losses to the furnace structure and waste gas system. Melt down time can be reduced by increasing the power available and by supplementary firing with gas or oil burners with or without oxygen.

Oxygen alone burning both the carbon monoxide generated from the charge and electrodes and the light scrap will also reduce melt down time.
These latter techniques are generally known as assisted melting.

3.4.1 Electric power

The power from the electricity supply company is routed to the furnace through step down, regulating and furnace transformers. The furnace power is available on modern units at l50V to 600V in 25V steps. In the 1950s it was usual to have installed power of 150-250kVa/tonne and this has risen to 400-600kVA/tonne in the 1970s.

Such furnaces are known as ultra high power furnaces or UHP. The effect of such increases in power on melt-down time is shown in Table 3.9.

Class	Power transformer		Melt down time
	MVA	kVA/t	h
RP	20	200	3.0
HP	45	450	1.5
UHP	60	600	1.0

Tab. 3.9 Effect of power increase on melt down time for a 100t nominal furnace

With the higher power, electrode consumption increases and for a UHP would be in the 5.0-5.5 kg/tonne range while in an RP it would be 4.0-4.5 kg/tonne. Because of the significant decrease in melting time, even at a high power input, il is possible to reduce specific Power consumption from 580-600kgVh/tonne to 500-520 kWh/tonne.

3.4.2 Assisted melting

Air-fuel burners have been used to preheat scrap in the scrap baskets. This technique will remove water from scrap and prevent explosions in the furnace front trapped water and reduce hydrogen pick-up. It is usual to heat the scrap to between 200 and 500°C. At the higher temperatures, the efficiency of heat transfer falls and heal losses increase so the process becomes less economical. At high preheat temperatures, welding and bridging of scrap near the burner can lead to problems in discharging the basket into the furnace.

The most advanced use of air fuel burner techniques is in the SKF MR process which uses a double shell furnace. Scrap is charged to one shell and preheated by an oil burner. The burner and roof are exchanged for an electrode roof so that melting can be completed. The use of two shells and interchangeable roof also permits two melting cycles suitably out of phase to be carried out at the same time. Residual heat in the furnace after tapping helps to preheat the scrap and since the scrap is already in the melting unit, high preheat temperatures are possible. There are three basic techniques used in assisted melting which are in the order of supplementary energy added:

1. Oxygen infiltration without a hydrocarbon fuel.
2. Oxy-fuel burners with burner fired substoichiometrically.
3. Oxy -fuel burners with burners fired super stoichiometrically.

3.4.3 Oxvgen infiltration

The waste gases from the arc furnace contain between l5 and 10% of carbon monoxide and hydrogen. These gases are not normally burned in the furnace but by gentle lancing of oxygen into the scrap above the liquid bath, these gases can be burned and the heat of the reaction released in the furnace. Carbon can be added to the charge and light scrap will also be oxidised to release heal. The reactions involved are:

$2CO + O_2 = 2CO_2 + heat$
$2H_2 + O_2 = 2H_2O + heat$
$C + O_2 = CO_2 + heat$
$2Fe + O_2 = 2FeO + heat$

Typically $10m^3$ of O_2/t would be used with 5-10kg carbon/t saving 10-15% of tap to tap time and 50kWh/t of electric power.

3.4.4 Oxy-fuel burners (substoichiometric firing)

Using burners, the rate and amount of supplementary energy can be controlled provided that the waste gas system can deal with the increase in volume and temperature of the extra gases produced. To distribute the energy release, up to 3 burners would be used especially on furnaces exceeding about 60 tonnes capacity. The burners would be individually mounted to fire through special ports in the side wall so that direct impingement of flame on the electrodes and side walls is avoided. The burners used are controllable both in total heat release and the ratio of oxygen to fuel so that desired stoichiometric requirements are used. The stoichiometric ratio controls both flame temperature and free oxygen in the waste gases. The relationship is shown in figure 3.5.

For practical purposes, flames with only I % free oxygen are neutral and at this level oxidation of the charge due to the burner would be negligible. Maximum flame temperature occurs at about 85% oxygen wh6re there would be about 7% free oxygen in the flame. This level would be the maximum with some oxidation of the charge. The actual

operation condition would normally be set for a particular furnace operation and for plain carbon steels this would be 75%.

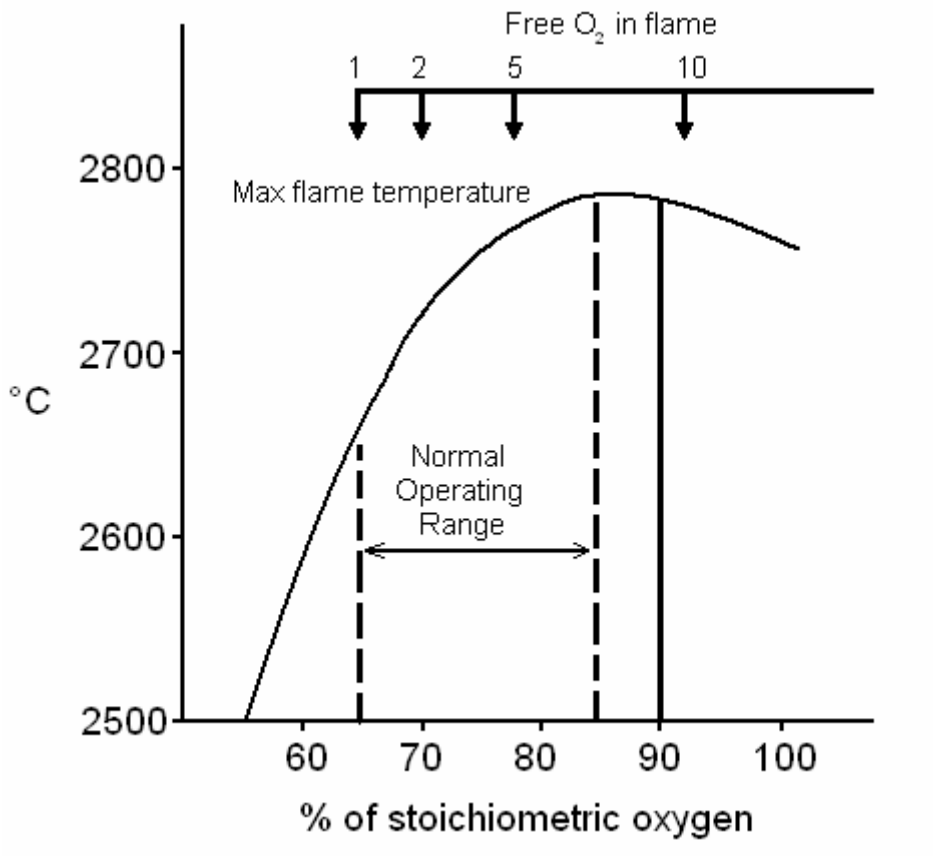

Fig. 3.8 Relationship between stoichiometric ratio, flame temperature and free O_2 for O_2 and natural gas

It is usual to fire the burners only while solid scrap remains so that there is an adequate heal sink for the thermal energy released. The burners are therefore turned off when 50% 60% of scrap has been melted. This mode of practice would use no more than $28m^3$ of oxygen/tonne on a small furnace and $15m^3$ of oxygen/tonne on a large furnace. The corresponding fuel input rates would be about 220kWh/t (20 l oil/t) and 110 kWh/t (10 l oil/t).

This method of substoichiometric firing can be used for almost any grade of steel including low and medium alloy steels because the level of oxidation of the charge is controlled and minimised. The supplementary thermal energy can be used to reduce electrical power without increasing melting rate by operating at lower transformer settings

thereby reducing maximum demand charges. Such operation is aimed at reducing melting costs and depends on the relative costs of electric power, oxygen and fuel.

It is more common to use the technique to reduce melt down time and increase output. The additional cost of fuel and oxygen is then compared with alternative means of increasing output and the extra profit from the higher sales. The time and power savings possible for a range of furnaces is given below in Table 3.9.

Furnace size	**MVA rating**	**Fuel**	**Oxygen**	**Time saved**	**Power saved**
t	-	kWh/t	M^3/t	min	kWh/t
5 – 10	2 – 3.5	220	28	40	120
20 – 25	8 – 10	150	21	30	120
70 – 80	15 – 20	140	17	30	100
100 – 120	40 – 60	100	15	20	60

Tab. 3.10 Saving with oxy-fuel assisted melting

Electrical energy is saved by using heat energy from the oxy-fuel burner and time savings of 25% are typical. with the reduced operation time, total heat losses and hence energy are also decreased.

3.4.5 Oxy - fuel burners (Superstochiometric Firing)

Aimed at maximising arc furnace output for bulk and low alloy steels, this technique was developed at the Toshin Steel Co in Japan. The technique was developed on a 50 tonne furnace and applied on a 140 tonne furnace and is used by many other operators throughout the world. Three oxy-oil burners capable of being fired at 200% stoichiometric ratio are used for about 70% of the melt down time with the furnace at full electrical power. The oil contributes about 60kWh/t but the excess oxygen by burning scrap, carbon and metalloids from ferroalloy additions contributes a further 145kWh/t. The burners are supplemented by oxygen lances which not only cut the scrap down into the bath but also infiltrate oxygen into the furnace to burn carbon monoxide and hydrogen. With correct metallurgical control, the 50 tonne furnace had a tap to tap time of 1h 8min and the 140 tonne, 1h 27min giving a production rate of 100 t/h.

The increase in output from one 50t furnace as the technique was developed is shown in Fig 3.6, showing the increasing world steel production.

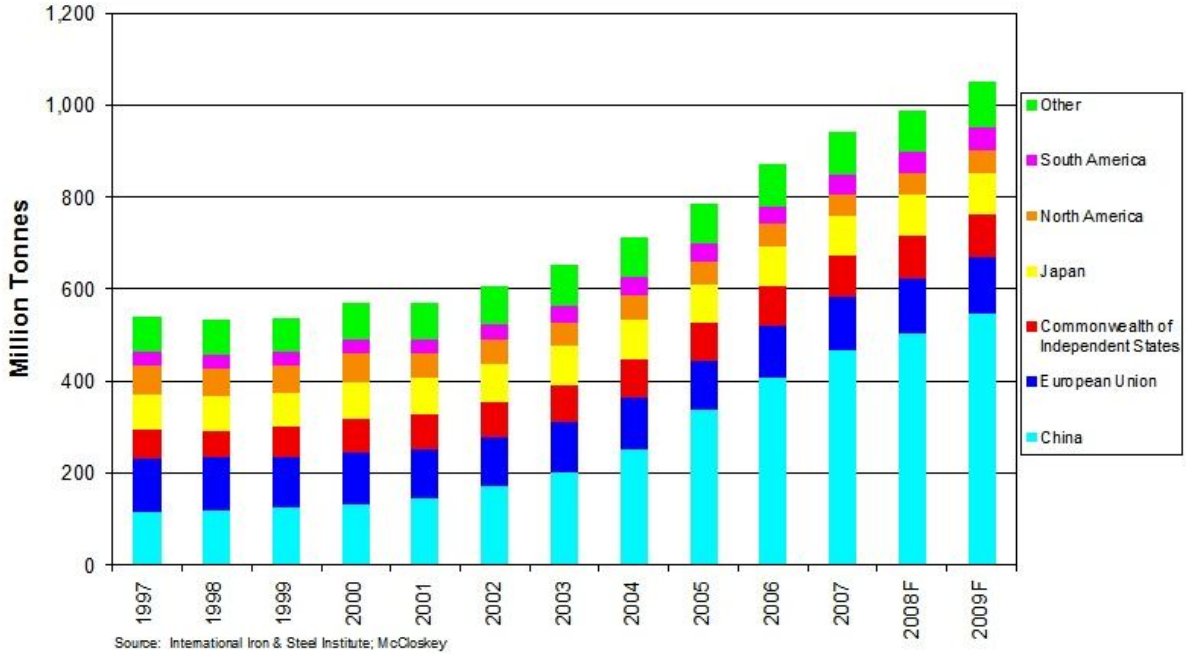

Fig. 3.9 Increase in output of steel production.

The details of one cycle are given below in Table 3.10 and the use of consumables and production rates achieved are given in Table 3.11

Operation	Action	Duration (min)
Repair and charge	1st basket in	6
Melt down	2nd and 3rd baskets in Burners on – 35 min Lances on – 44 min Carbon 0.1-0.25% Slag of at 1540°C	48
Refining	Decarburising, dephosphurising Increase temperature to 1620°C Lances on for 6min Slag off	11
Finishing	Desulphurising to 0.04% max Killing and final additions	3
Heat time	Tap to tap	68

Tab. 3.11 Details of furnace operations (Toshin System)

These very high production rates which the oxy-fuel techniques make possible can only be achieved when the engineering of the system can contain the energy release involved. The two most significant changes are the split shell to enable the side walls to be removed completely from the furnace at sill level to permit relining of the furnace. This means that one shell can be removed and a relined shell repositioned with a minimum of delay. The second innovation is the introduction of water cooled carbonaceous brick panels in the side walls. With these and mechanised relining equipment, well maintained high speed ancillary equipment such as cranes, improvement in electrode quality, balancing of gas output and fume extraction to minimise air in leakage and training of skilled operators makes such short tap to tap times possible.

	Quantity	Dimensions	Value
	Liquid metal yield	%	91.1
	Tap to tap time	min	68.0
	Productivity	t/h	41.8
Consumables	Power	kWh/t	333.0
	Oxygen	Nm^3/t	42.3
	Oil	litres/t	6.1
	Electrodes	kg/t	4.4
	Wall refractory	kg/t	2.1
	Roof refractory	kg/t	3.4
	Ferro alloys	kg/t	18.8

Tab. 3.12 Operational results from sequence given in table 5.10

3.4.6 Materials handling

The yearly amounts to be handled depend on the arc furnace practice used. The lowest quantities are required by an alloy steelmaking furnace using oxygen for decarburising only, followed by substoichiometric oxy-fuel firing with the highest output from a Toshin type practice. The amounts required for 18 shift per week operation for 45 weeks per year is given in Table 3.12 for a 100t arc furnace.

Quantity		Oxygen for decarburisation	Sub-stochiometric assisted melting	Super-stochiometric assisted melting
Production rate	t/h tpy	25 162000	33 214000	66 428000
Tap to tap	min	240	180	90
Liquid metal yield	%	95 - 96	95 - 96	91 - 92
Scrap	-	170000	225000	465000
Electrical power	kWh/t	600	540	333
Oxygen	m^3/t	6	20	42
Oil	l/t	-	9	6

Tab. 3.13 Products and consumables for 100t arc furnace

3.5 Future developments

Already being applied on a small number of arc furnaces, is the use of coal as a supplementary fuel. Electric power consumptions for electric melting alone are in the range 450-520kWh/1. Power use as low as 300kWh/b when injecting 25-30 Kg of coal/L and combusting. This with oxygen are probable. Oxygen use increases to about $35m^3/t$ for the coal combustion. Gas injection through annular tuyeres in the base of the unit is also being tried. The tuyeres are similar to those used in AOD vessels, ie there is a methane or an inert gas in the outer annulus with inert gases and or oxygen in the centre pipe. The gases injected provide bath agitation and are intended to promote rapid reactions and reduce melt time. The geometry of the arc furnace, does not, however, help in the uniform promotion of reactions and this development is less likely to succeed than coal injection with oxygen.

Chapter 4

Secondary steelmaking for stainless steel AOD

4.1 Introduction

This chapter therefore concentrates on the AOD (argon oxygen decarburisation) process. Processes for The manufacture of stainless steel will be described. In both cases the metal has been melted in an arc furnace, as described in chapter 5 and then transferred to the secondary refining vessel, ie both vessels are converters.

To explain the AOD processes it will be necessary to outline stainless steel production from an arc furnace alone so as to emphasize the importance of the vessel and explain the metallurgical reactions.

The molten charge is transferred to the AOD vessel. The AOD vessel has no independent power supply. It is, however, set up with tuyeres in the bottom of the vessel to bottom-inject selected mixtures of oxygen and argon into the charge. The degree of oxidation is decreased by increasing argon content (reduced partial pressure of oxygen) until, thermodynamically, chromium metal becomes more stable than chromium oxide, and oxidized chromium is recovered from the slag. Similarly to the blown arc furnace, aluminium may be added to the melt and preferentially oxidized so that the aluminum reduction increases the temperature of the melt. When the recovery process has neared completion, final chemistry trim additions are made, based on the results of a chemistry sample, and the heat is manually deslagged and poured into a teeming vessel. The teeming vessel, most commonly equipped with a moveable stopper plug in the vessel bottom, is used to introduce the metal into molds.

Molds may be direct poured through the top of the mold, or more commonly, the melt ispoured into a central sprue that feeds a number of molds that are filled from the bottom up. Round electrodes and rectangular slab molds are most commonly used in steel production. The product may be hot-worked directly or, depending on the alloy solidification characteristics, consumably remelted to obtain a less segregated structure than that obtainable through direct casting.

4.2 Stainless steel production from the arc furnace alone

In the arc furnace, decarburisation is brought about by lancing the bath with pure oxygen. The product of decarburisation is CO essentially at 1atm pressure and the stainless steel is in equilibrium with that gas at the temperature of the bath. These conditions determine the maximum amount of Cr that can remain in the bath at a given carbon content and temperature. The equilibrium curves are shown in figure 4.1.

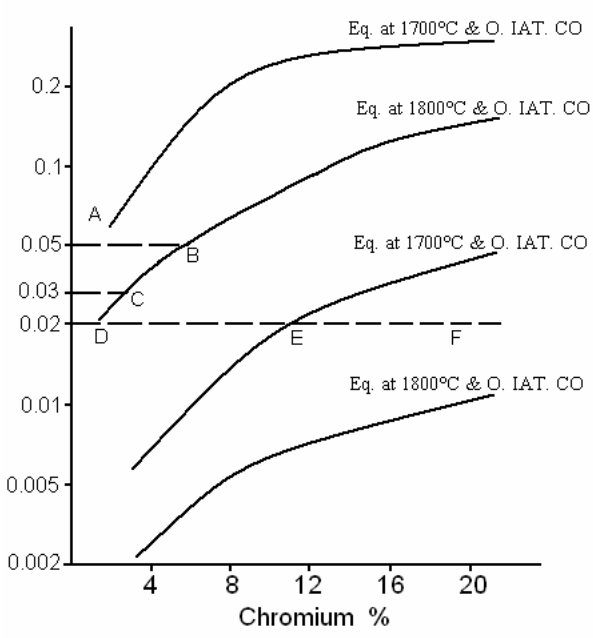

Fig. 4.1 Carbon-chromium equilibrium curves

The curves clearly show that, as the carbon is removed from the bath, the equilibrium chromium content is also lowered and any chromium in excess of equilibrium is very rapidly oxidised out. If the temperature is raised, then the amount of chromium that can remain in the bath is also raised. For example, at 0.05% C and 1700"C (point A figure 4.1) the equilibrium chromium content is approximately 2%. At l800°C (point B) the equilibrium chromium is approximately 7.5%.

Most stainless steel production requires carbon at or below 0.03% at which the equilibrium chromium level, even at 1800°C is only 4% (point C). Since carbon is contained in small amounts in all ferro-alloys, for a specification of 0.03%C it would be necessary to finish at 0.02%C to allow for added carbon even where low carbon ferroalloys

were used. At this level of carbon the equilibrium chromium is about 3% (point D). In conventional arc practice, for the manufacture of an 18% Cr, 8% Ni, 0.04%C steel, it was only possible to use a charge mix with 4% Cr in it. The molten charge would be blown down with pure oxygen to about 0.02% C giving a temperature of about 1800°C. During the blow about 2% of the charge chromium would be oxidised into the slag. About 1% would be reduced back into the metal by using ferrosilicon giving a bath analysis of 3% Cr, 0.02%C for a specification of 18% Cr and 0.04% C. (The nickel content is largely unaffected by the decarburisation reaction).

Large amounts of ferrochromium of the very low carbon type were added to bring the bath analysis to 18% Cr and still remain under 0.03% C. These large amounts of alloys also cooled the bath to the required tapping temperature.

The natural penalties of the arc only process are summarised below:

1. Low charge chromium only possible. This meant that only small amounts of stainless steel scrap could be used.
2. Very high temperatures 1900°C in the furnace requiring high cost refractories.
3. Large additions of high cost, low carbon ferrochrome.
4. A lower limit on carbon of about 0.025%.

4.3 The AOD process

The AOD process was developed from a laboratory study of methods of producing the data given in figure 4.1. When blowing small melts with oxygen, it was not possible to maintain isothermal conditions because of the very exothermic reaction of chromium oxidation. It was to control this reaction that argon was used to dilute the oxygen and so reduce the rate of chromium oxidation and the attendant heat release. The technique worked and it was observed that for a given temperature and carbon level, the chromium that could remain in equilibrium was significantly increased. It was concluded that the partial pressure of CO in the decarburisation reaction had been reduced and the data obtained, produced the two lower curves in figure 6.1 for a partial pressure of CO of 0.1atm.

Using the 0.02% obtained at 1800°C (point D) where only 3% Cr could be retained in the bath, it is now possible to retain 11% Cr at l700°C (point E) and 18% Cr at about l750°C (point F). The research work was started in I954 and progressed through larger laboratory trials to a l5 tonne pilot industrial scale in 1968. In 1978, the installed AOD vessels had a production capacity approaching 5 Mt/year.

The AOD technique is to melt the charge in the arc furnace with all the elements added in the lowest cost form, ie stainless steel scrap and high carbon ferroalloys. At melt out, the chromium is up to 0.5% above the minimum in the specification to be made with carbon in the range 0.25% - 0.2% and silicon 0.2% to 1.5%. The particular levels of carbon and silicon depend on the specification, practice and vessel size as does the temperature of transfer which is about 1500°C. A simplified sequence is given in Table 4.1.

	Action	**Cr**	**Ni**	**C**	**Si**	**S**	**Temp (°C)**	**Ar/O_2**	**Time (min)**
1	Aim at	18,0	10,0	0,025	0,5	0,015	1550	-	-
2	Charge AOD	18,5	9,8	1,5	0,3	0,035	1500	-	2
3	Blow 1	17,8	10,0	0,4	0,1	0,03	1700	1:3	25
4	Blow 2	17,8	10,1	0,15	-	0,03	1720	1:2	15
5	Blow 3	16,5	10,1	0,018	-	0,03	1740	2:1	15
6	Reduce	18,2	9,9	0,02	0,5	0,02	1650	Ar*	5
7	Desulphurise	18,2	9,9	0,02	0,5	0,01	1625	Ar*	10[T]
8	Trim	18,2	10,1	0,02	0,5	0,01	1550	Ar*	1

* Ar stirring of bath
[T] Includes slag off

Tab. 4.1 AOD sequence and composition changes.

The main features to note are the progressive dilution of the oxygen with argon to control both temperature rise and partial pressure of carbon monoxide in the bath. The consequence of that control is the retention in the bath of almost all the charge chromium. Return to the melt from the slag of oxidised chromium is achieved by ferrochromium silicon and desulphurisation by lime.

4.4 The metallurgy of the AOD process

4.4.1 Carbon and chromium

The heart of the process is the control of the partial pressure of carbon monoxide to control the rate of the oxidation of carbon and chromium so that chromium is retained in the bath while carbon is removed to low levels. To show the interaction of chromium and carbon during AOD operation, the chemical changes given in the AOD operation of Table 4.1 have been combined with the theoretical equilibrium data from Figure 4.1. The combined data is given in figure 4.2 where both AOD and arc only changes are shown.

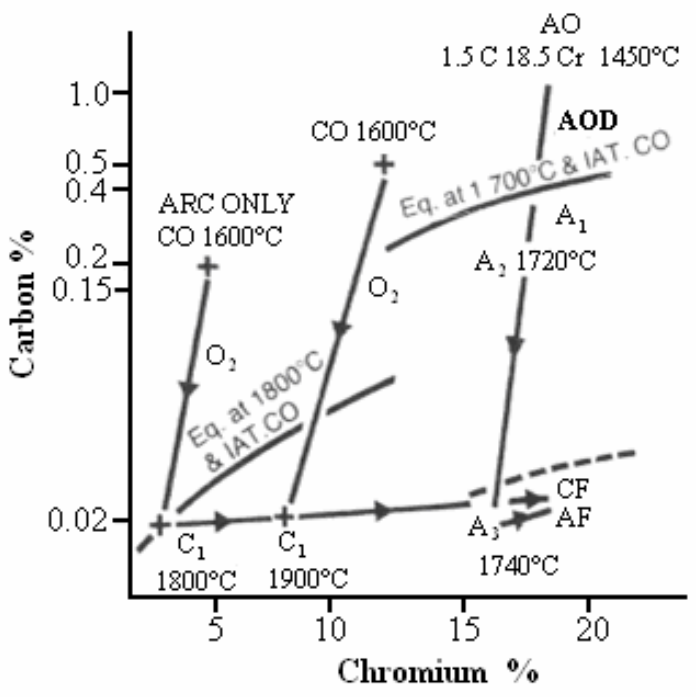

Fig. 4.2 Composition changes in stainless steel making

The vessel is charged at 1500°C with 1.5% C and 18.5% Cr. The initial blowing gas is 75% O_2 and 25% Ar. Such a mixture promotes rapid oxidation of carbon but at the low temperature and high C of the bath only a small dilution effect is required. Towards the end of the blow as the carbon content falls below 0.5% then the dilution effect of the argon on the partial pressure of the carbon monoxide is beginning to have an effect. Blow 1 is stopped at 0.4% C, 17.8% Cr and a temperature of I700°C which is approximately at the equilibrium point for a 1atm pressure of CO (A1). If the temperature had been higher than

1700°C then scrap coolant would have been added to reduce the temperature to about this level prior to beginning Blow 2. For Blow 2 higher Ar dilution of the oxygen is needed to reduce the partial pressure of CO to promote carbon removal without significant temperature increases or Cr loss. This blow is stopped at l7% Cr 0.15% C at a temperature of l720°C (A2).

The final blow is 65% Ar 35% O_2 so that the partial pressure of the carbon monoxide is approaching 0.1atm. Carbon removal continues with a small temperature rise to give bath conditions of 16.5% Cr, 0.0l8% C at 1740°C (A3). 2% Cr has been oxidised into the slag so ferrosilicon and lime are added and gently stirred with argon alone. About 1.7% Cr is reduced back from the slag to bring the steel into specification with regard to chromium (AF).

In contrast, two arc furnace only practices have been outlined on the same diagram. The starting point of oxygen only blowing is designated CO and the end of oxygen blowing C1. The right hand C0-C1 curve represents a high charge chromium melt (14% Cr and 0.5% C) which has to be blown to about 1900°C to achieve 0.02% C losing 7% Cr to the slag in the process. This practice represents lower charge costs but high refractory costs in the arc. The left hand curve shows a low charge chrome practice (4% Cr 0.2% C) which reaches I800°C to achieve 0.018% C. There is less wear on arc refractories but a high cost penalty for low carbon ferrochrome to bring the steel up to the 18% chromium required (CF).

In both cases, unit costs would be higher than the AOD and the final carbon would be about 0.025%. It is difficult and expensive to achieve lower carbons than this with arc only practice. Steels with carbon of less than 0.01% have been made in AOD units.

4.4.2 Sulphur

In arc furnace practice, desulphuring by rabbling with a time slag is time consuming. One or more treatments requiring more than one deslagging operation can be needed to get the sulphur down to levels below 0.02% (depending of course on the sulphur load in the charge). In the converter, even with high charge sulphurs of 0.04% -0.06%, sulphur contents down to 0.005% have been achieved in a short desulphurising step after the

chromium reduction (step which also removed some sulphur) by adding desulphurisers and stirring with argon.

4.4.3 Lead

From some grades of scrap the lead content in the bath can reach 0.01% at which level there are serious problems during the rolling of the product leading to low yields of saleable product. The use of use AOD with normal control of leaded scrap probably giving melt out lead contents of about 0.007% can reduce the lead to the 0.001 – 0.002% range where no problems are experienced in rolling.

4.4.4 Oxygen

When oxygen alone is used to decarburise, oxygen can reach 0.35% requiring significant amounts of deoxidant to reduce the oxygen content to an acceptable level in the range 0.005-0.01% (50-100 ppm). This reduction produces oxides which may not be completely removed from the system. In the AOD, oxygen contents at the end of the third blow can be in the range 0.15-25% reducing to 50-100 ppm during the argon only stirring for reduction. The reduced amount of deoxidant needed to remove the oxygen in the AOD steel produces a lower volume of oxides and hence cleaner steel. Oxygen contents in the semi finished product were reported as being 20% lower than when made by the AOD route compared with arc only production.

4.4.5 Nitrogen

In the simplified sequence given in Table 4.1, the gases used were oxygen and argon. Nitrogen can be used as a replacement for argon depending on the stainless steel being made. For low nitrogen melts, nitrogen will be used as a process gas up to the end of Blow 2 but thereafler argon must be used. The purging effect of the argon reduces the nitrogen picked up during the earlier blows down to the 100-350 ppm range. Where high nitrogen contents are required, then nitrogen can be used as a process gas in stage 3. In these cases, nitrogen contents in the range 1000 - 2500 ppm can be achieved. These levels are usually

required for high proof stress alloys where the alternative method of increasing the nitrogen content is to add high cost nitrided ferroalloys.

4.4.6 Hydrogen

Hydrogen contents in the range 3-5 ml/100g are typical of AOD practice. Levels down to 1ml/100g have been observed as have contents up to 7ml/100g. The high contents (5-7ml/100g) usually result from partially hydrated lime used in the reduction of desulphurisation steps. These levels can be reduced to the normal range by argon blowing for 1 -2 minutes prior to tapping.

4.5 The engineering of the AOD system

With every AOD vessel there is the associated arc furnace of comparable capacity to provide the hot metal charge. The arc will not be considered in this section, only the blowing vessel itself. To show the magnitude of the engineering problem, the materials to be handled for a 50 tonne capacity vessel are given in Table 4.2.

4.5.1 The Vessel

A typical vessel is shown in figure 4.3. Capacities range from 5-100 tonnes with 2-6 tuyeres on the back wall so that when the vessel tilts to tap or deslag, the tuyeres are lifted clear of the metal. The tuyeres can have an upward tilt up to 5° and are generally within an angle of 120° symmetrically along the back wall, and about 20 cm from the floor of the vessel. The tuyere height is approximately constant because metal depths are no greater than l.5m and usually between 1 and 1.5m. Specific volume, ie vessel volume to steel volume is in the range 0.7 -0.9 m^3 per ton. It is interesting to note this is the same range for the BOF vessel shown in figure 4.6. Both vessels are gas-steel reaction vessels but with different injection techniques which change bath depth needs but do not change the reaction volume. The refractory lining of the vessel has to contain a very aggressive metallurgical reaction and thicknesses from 0.3-0.4m are needed. Even so the lining life is generally about 40-50 heals with some vessels reaching 80. The severity of the wear can be

highlighted by comparing the life of an LD vessel lining which has a typical range of 300-500 heals and over 1000 heats possible.

Since wear is severe, there are large variations from any average figure which is about 25 kg/tonne of steel. Lining wear adds to the slag volume but has no effect on refining chemistry which is a gas-metal reaction.

Hot metal from arc	93000 tpy	
Scrap	5000 tpy	
Ferro alloys	4000 tpy	
Lime etc	9000 tpy	
Refractories	2500 tpy	
Oxygen	3000000 m^3/year	30 m^3/t
Argon	2000000 m^3/year	20 m^3/t
Nitrogen	500000 m^3/year	5 m^3/t
Stainless steel	100000 tpy	
Slag	13500 tpy	
Gas	6000000 m^3/year	

Tab. 4.2 Consumable and products of a 50t AOD vessel

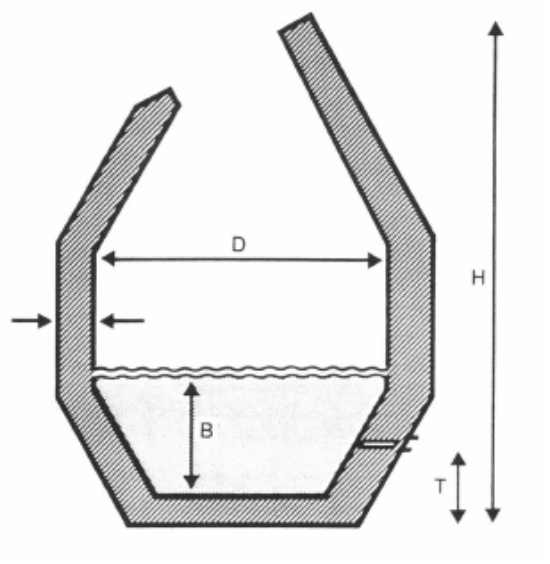

Paramater		**Symbol**	**Ratio**	**Example**
Capacity	t	C		50
Volume	m^3	V	V/C (0,7)	28
Height	m	H	H/D	5.1
Diam	m	D	H/D (2)	2.7
Bath	m	B	H/B (3,5)	1.5
Tuyere	m	T	B/T	0.2
Lining	m	t		0.35

Fig. 4.3 The AOD vessel

Figure 4.4 illustrates, schematically, an AOD vessel. The vessel, like the EAF, is steel walled and refractory lined. The general shape is that of a concrete mixer, that is, a container with a generally rounded bottom, a conical top, and mounted on trunions so that it may be tipped in the vertical plane. The size, of course, is matched to the arc furnace and may hold upward of 36,000 kg of molten metal. The essential feature of the AOD vessel is that in the bottom of the vessel are several tuyeres for the injection of an argon-oxygen gas mix. The tuyeres consist of concentric tubes, the center of which injects the argon-oxygen mix into the vessel. The outer tube carries inert gas only (usually additional argon) to cool the reaction occurring at the end of the center tube. The refractory lining of the AOD vessel is similar in composition to that of the EAF furnace and also erodes during the processing, contributing oxides to the slag formed during the process. Control of the basicity of the slag formed is, again, a key item in ensuring that selective attack of the refractory by the slag does not occur. In the AOD vessel, the first operation is to decarburize the melt. If the melt were blown through the tuyeres with pure oxygen, the result would be not only decarburization but a conversion of much of the chromium alloy content into chromium oxide. The economic feasibility of the decarburization reaction is related to the discovery that reduction of the oxygen partial pressure over the melt by inert argon greatly decreased the amount of chromium oxidized. When carbon levels are high, a typical ratio used of argon to oxygen is 3 to 1. As the carbon content is reduced, the proportion of argon may be increased. By the time that decarburization is complete, the ratio of argon to oxygen may be as high as 6 to 1. The decarburization reaction heats the bath, as does the small amount of chromium oxidation that occurs. Silicon also will be removed, but the heat of reaction is low, so there is little contribution to heating the charge.

It is important to remember that the AOD vessel contains no external heating sources. The temperature is raised by the exothermic reactions. Should the charge need to be cooled, this is accomplished by adding solid scrap to the charge. It is economically important that the charge temperature be kept uniform, because the percentage of valuable alloying elements (principally chromium but also niobium) that becomes slag is affected by the charge temperature. Overheating the charge, followed by cooling. and then followed by heating again is time-consuming and detrimental to the full recovery of the elements

that have partitioned to the slag. During the decarburization cycle, lime is added to the charge. The lime is very thoroughly mixed into the liquid charge during blowing, leading to a high degree of desulphurization of the charge. The CaS formed in this reaction becomes part of the slag. When a chemistry control sample shows that the desired degree of decarburization has been obtained, the melting operation enters the recovery phase. In this phase, the slag is reacted with cheap elements (principally silicon and/or aluminum mired with lime) that will preferentially form oxides compared to chromium and niobium. This causes the reduction these expensive elements in the charge and their return into the melt. Very sophisticated programs exist to use the known composition from the sample taken from the transfer ladle plus the amount of oxygen blown through the charge to predict the amount of oxidized chromium and niobium to be recovered. The correct amount of reduction mix may be added accordingly. When reduction is complete (often confirmed by yet another chemistry sample), the charge is deslagged manually, by scraping the slag from the surface of the molten charge and out the tilted top of the cone. Final trim additions are made to bring the charge to its desired composition, and the AOD vessel is rotated to decant the molten charge into a teeming ladle.

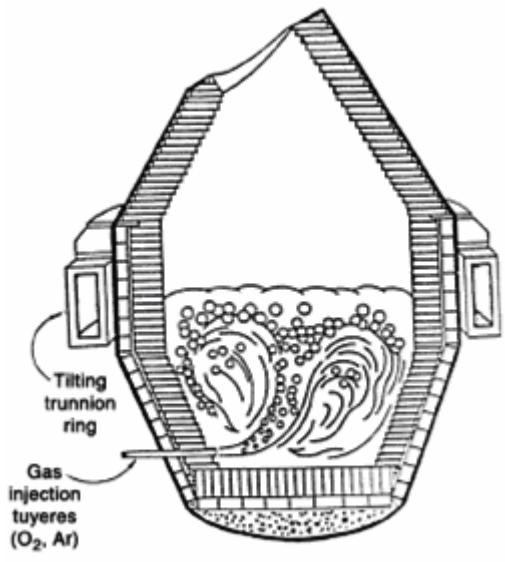

Fig. 4.4 Schematic of argon oxygen decarburizing vessel

The teeming ladle and charge are transferred to the area where the heat is to be tapped. Figure 4.5 shows a schematic for a bottom-pour mold setup. The heat is tapped by the opening of a bottom plug in the teeming ladle. As the heat enters the central pouring sprue or "trumpet," a stream of argon may be flowed alongside it to provide shrouding against oxygen and nitrogen pickup from the atmosphere. The trumpet feeds a number of runners located radially around it. The runners feed the molten metal into the bottom of the molds. Mold powders or fluxes are added to the advancing metal front to improve surface quality by providing thermal insulation from the mold surface. At the end of the pour, exothermic compounds may be added to the top of the mold to insulate the top of the solidifying electrode and provide a degree of hot topping, where the molten metal will fill the shrinkage occurring upon solidification lower in the electrode. Argon oxygen decarburized electrodes also may be top poured, but the need to continually close the teeming ladle tap, transfer the ladle, and reinitiate argon shrouding produces variable conditions from electrode to electrode. Should difficulty in closing the nozzle be experienced during top pour, then a safety problem arises. Thus, bottom pouring is the more generally used process.

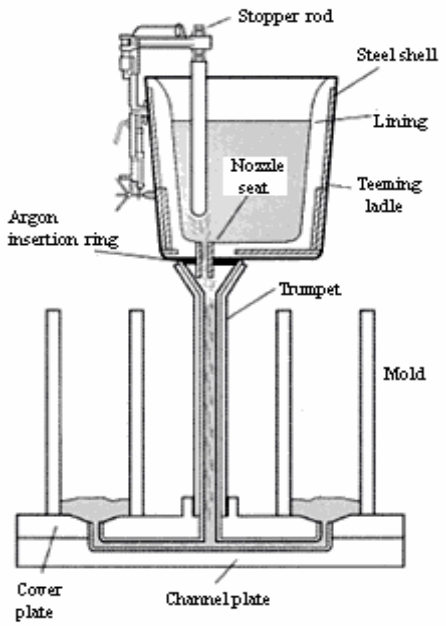

Fig. 4.5 Schematic of bottom-pour teeming EAF/AOD melting

4.5.2 Refractory linings for AOD

The AOD process was first introduced in the 1970s and rapidly gained acceptance for the production of stainless steels in association with the electric arc furnace as the primary melting unit.

From the refractory lining aspect, the walls of the converter are subject to the very highest stresses, the refractories being exposed mainly to two types, mechanical and chemical, the former due particularly to the marked turbulence of the liquid steel especially near the tuyeres through which the treatment gases are introduced, and the latter to the slag, the composition of which varies from treatment to treatment.

It is thus necessary to employ refractories that have good mechanical resistance at high temperatures and which are compatible with the slag whose basicity can be very high. Specific refractory consumption in the AOD process can sometimes be in excess of 10 kg/t and is, in fact, the highest of the various treatments comprising the steelmaking process. Refractories are thus an extremely important item in the overall cost of refining and producing stainless steel.

An AOD converter typically has a dolomite or magnesite chromite refractory lining, the former being more commonly adopted in Europe, and the latter in Japan and North America. Regarding the use of these refractories, it should be observed that while those belonging to the magnesite chromite family may have the desired qualities of good hot strength and chemical inertness to basic slags, they suffer from the drawback of poor resistance to thermal shock and call for particular care in the removal of demolition residues, owing to the danger of hexavalent chromium contamination.

Figure 4.6 shows an example of refractory arrangements for an AOD converter with a magnesite chromite lining and Table 4.3 indicates the typical refractory compositions.

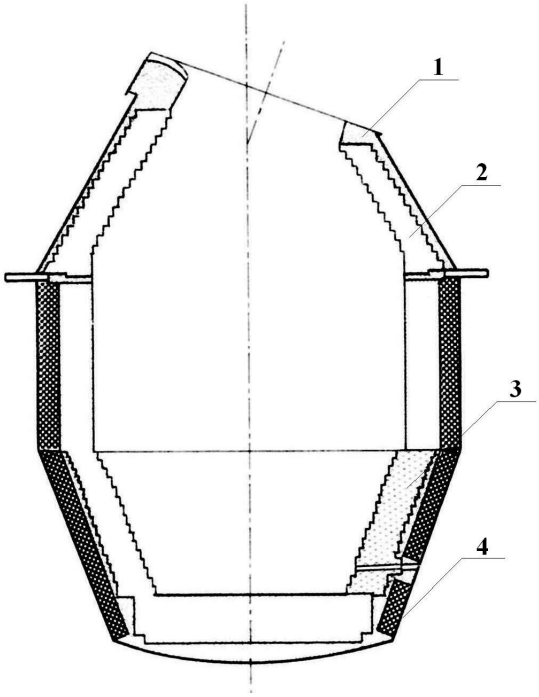

1 - Ramming course (refractory type 4)

2 - Working lining (refractory types 1 - 2)

3 - Tuyere zone (refractory type 2)

4 - Permanent lining (refractory type 3)

Fig. 4.6 Typical arrangement of magnesite chromite refractory lining for AOD converters.

	Refractory type		**1 - 2**	**2**	**3**	**4**
	MgO	%	57	55	58	93
	Cr_2O_3	%	21	-	19	-
	Fe_2O_3	%	13	1.5	14	0.5
	Al_2O_3	%	6.5	0.3	6	0.2
	CaO	%	1.2	42	2	2
	SiO_2	%	0.2	0.5	0.4	4
	Bulk density	g/cm^3	3.27	2.91	3.24	-
	Open porosity	%	<18	<18	<10	-
	Cold crushing strength resistance	N/mm^2	>30	>40	>30	-
	Termal expansion	$10^{-6}K^{-1}$	11	15	12	-
Thermal conductivity	at 600°C	W/mK	2.2	5.2	2.2	-
	at 1200°C	W/mK	2.2	3	2.2	-

Tab. 4.3 Typical refractory composition for AOD converters shown in Fig. 5.1

Dolomite is employed mainly in sintered form which has better mechanical strength than the tar bonded type. MgO-C bricks, which guarantee better resistance to this kind of stress, are sometimes used in the zones subject to the highest thermal stresses and those in contact with slag.

4.6 Process Gas System

Total gas blowing rates are in the range 0.7- 1.0 m^3/t to give adequate stirring of the bath without ejection of metal from the vessel. The gas system has lo supply this rate which for a 50 tonne vessel would be 3000 m^3/h. The mixture changes through the process as detailed in table 4.4.

Condition	Composition %			Flow rate	Duration
	O_2	Ar	N_2	m^3/min	min
Blow 1	75	-	25	50	25
Blow 2	34	66	-	50	15
Blow 3	66	34	-	40	15
Reduction	-	100	-	15	5
Tuyere shroud	-	100	-	4	60

Tab. 4.4 Gas changes in AOD operation

Supply pressure of all gases is up to 16 bar and the control system changes the composition of the mixture as the operator requires. The tuyeres are made from concentric tubes and down the outer annulus flows pure argon to cool and protect the inner tube down which the oxidising mixture passes.

Average use of the gases is : follows:

Oxygen	30 m^3/t
Argon	20 m^3/t
Nitrogen	5 m^3/t

The O_2 needs for a given steel can be derived from:

$$O_2 = 2 + 9.3C + 8Si + 1.4Mn + \frac{17.2}{1 + 50C_1}$$

O_2 = m^3/t

C = initial carbon in melt %

C_1 = required final carbon %

Si = initial Si + Si for reduction

Mn = initial Mn + Mn from reduction

Nitrogen and argon depend on the nitrogen specification in the steel and the amount of oxygen to be blown. Generally the total inert gas is somewhat less than the total oxygen.

4.7 Output and cost

Since the AOD vessel is a secondary refining vessel linked to an arc furnace of the same capacity, output from the original plant can be doubled. One heat can be processed in the AOD whilst the next charge is being prepared in the arc. With a slightly shorter tap to tap time in the AOD, the process can be easily integrated and synchronised to achieve double output. Standing charges can therefore be carried by the higher output.

However, another vessel requires added capital but the charges for a refining vessel are lower than charges for another arc furnace.

Operationally, the costs in arc furnaces have been reduced since the arc acts as a melting unit at lower temperatures than required for refining. The costs at this stage are reduced by lower consumption of electrodes, power, refractories, labour and oxygen. High carbon ferrochrome is used instead of expensive low carbon qualities.

With the added vessel, costs are incurred for argon, nitrogen, oxygen, refractories and labour. The overall balance is in favour of the arc-AOD system which also produces a higher quality product than the arc alone.

4.8 The CLU process

In this process, the main diluents of the oxygen is steam to control the carbon removal while maintaining high chromium levels in the stainless steel. As for the AOD, the charge is melted in an arc furnace and transferred to the CLU vessel. Transfer carbon up to 3% and silicon up to 1.2% with all the

arc furnace slag has been practised but carbon up to 1.2%, silicon up to 0.5% with some furnace slag is more usual. This practice results in less refractory wear and a lining life of about 85 heats. The vessel is shown in figure 4.7 showing that the process gases are injected from the base.

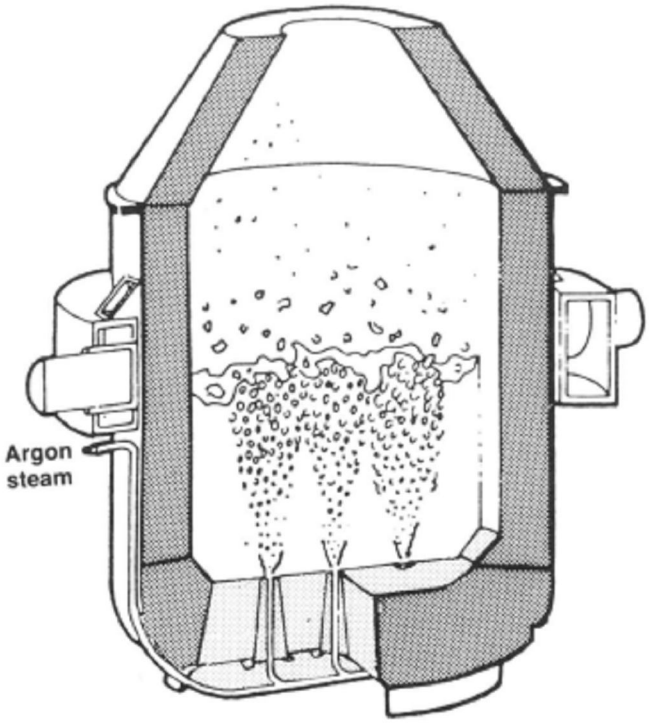

Fig. 4.7 The CLU vessel

The process has a 1-1.5 hour blowing time in which control of the steam oxygen and nitrogen in the blowing gas holds the temperature to less than 1680°C, reduces carbon and retains chromium. The use of steam however increases the hydrogen content and from 1.5 to 5 m^3/tonne of argon are needed to purge the hydrogen to less than 1 ppm. The process consumables are given in Table 4.5. The specific use depends on the grade of stainless being produced.

Consumable	**Use per tonne**
Steam	10 – 25 m^3
Nitrogen	10 – 25 m^3
Argon	1.5 – 4 m^3
Lime	50 – 80 kg
Silicon	2 – 20 kg
Oxygen	10 – 40 m^3

Tab. 4.5 Process consumables in the CLU process

Chapter 5

Consumable remelt overview

5.1 Introduction

Static casting is the process of pouring a large volume of molten metal into a mold and controlling its solidification by mold design and metal feed so as to eliminate porosity. However, for large castings, the solidification rate is generally so slow that for steels, positive segregation defects will be formed (as discussed in the section on solidification).

Thus, the production of steels by EAF/AOD or by VIM is generally by static casting the alloy into electrodes for subsequent remelting under controlled conditions. There are two commonly used remelting processes, VAR and ESR. In both processes, the electrode is located in a water-cooled crucible. The working face of the electrode is heated to the melting point, so that drops of liquid metal fall from the face and are collected in the crucible and rapidly solidified. As the electrode is consumed by the advance of the melting face, it is fed into the crucible to maintain a uniform distance between the melting face and the solidifying pool of molten metal.

While having these broad characteristics in common, the methods by which the electrode face is melted are drastically different. The different melting methods have implications regarding the magnitude of cooling rates obtained and the nature of defects created by the remelting process itself.

5.2 Electrode quality

5.2.1 Composition

A common factor affecting consumable remelt quality for both ESR and VAR is the quality of the electrode. Electrode quality is affected by composition, cleanliness (low oxide and nitride content), an soundness (freedom from porosity and cracks). The most important characteristic of an electrode is composition. With the exception of reductions in volatile elements, VAR does not change the composition of the electrode. (For high-nitrogen electrodes, some reduction of nitrogen is accomplished by flotation of nitrides. As

the solubility levels of TiN in the alloy are approached, this mechanism is no longer effective.) Electroslag remelting reduces sulfur content but may also cause minor changes in composition through reaction of titanium, aluminum, zirconium, and silicon with components of the slag.

These changes are predictable in a mature process. Thus, there is no practical way to achieve composition modification once the master heat has been cast, but departure from normal practice in ESR may change titanium, aluminum, zirconium, or silicon content.

5.2.2 Cleanliness

The cleanliness of the cast electrode with regard to entrained oxide and nitride is an important characteristic for VAR electrodes. The introduction of a high volume of oxide or nitride onto the molten pool in VAR may degrade the efficiency of melting of the arc as well as disturb the electrical characteristics measured to maintain control of the arc gap. This is not a problem in electrodes to be melted by ESR.

5.2.3 Porosity

The porosity (secondary shrinkage) of an electrode may be of some concern in VAR. Vacuum arc remelting of electrodes with centerline porosity results in the preferred melting of the face in the porosity area. Thus, the melt face is no longer flat. The effect of this with regard to gap control during melting has not been quantified.

A secondary problem connected with centerline porosity is the concern that projecting dendrites in this region may become detached from the electrode and fall, unmelted, into the molten pool. Then they may be incorporated into the structure without being remelted.

The composition of such a region thus will be that of a primary dendrite (alloy-lean) rather than representative of the bulk composition.

Theoretically, these concerns might also apply to ESR processes, but the necessity for melted or unmelted material to pass through the slag makes ESR products inherently less sensitive to electrode porosity.

5.2.4 Cracking

The final electrode characteristic affecting remelt quality is the freedom of the electrode from transverse cracking. In highly alloyed steels, the thermal stresses generated upon cooling of electrodes or upon heating in the remelt process may be sufficient to form transverse cracks. When the melt front of either VAR or ESR approaches such a crack, the heat transfer up the electrode is diminished, because of the thermal barrier presented by the crack. Thus, the material in front of the crack becomes hotter than would occur under equilibrium conditions and will tend to melt at a faster rate. After the melt front has gone through the crack, it encounters cold material, and the melt rate will tend to drop. In both VAR and ESR, the result is that the controls respond with changes in applied power to try to keep the melt rate constant. This, however, is seldom accomplished without some discernable disruption to the continuous nature of the growth of the solidification front. The only defense against these melt rate excursions (MREs, also called "events") is to produce an electrode free of cracks. In the future, it is hoped that more sophisticated melting controls will be able to detect the melt rate changes earlier and thus compensate for them more efficiently.

5.3 Vacuum Arc Remelting (VAR)

The vacuum arc remelting process was the first commercial remelting process for superalloys. It was used in the late 1950s to manufacture materials for the aircraft industry. The primary feature of vacuum arc remelting is the continuous melting of a consumable electrode by means of a dc arc under vacuum. The molten material solidifies in a water-cooled copper mold.

The basic design of the VAR furnace has remained largely unchanged over the years; however, significant advances have been made in the fields of control and regulation of the process with the object of achieving a fully automatic melting procedure. This in turn has had a decisive positive influence on the metallurgical properties of the products. The manufacture of homogeneous ingots with minimal segregation requires careful control

of remelting parameters. Of these, the melting current density has the largest influence on the melting bath geometry and conditions of solidification.

5.3.1 Process advantages

The primary benefits of melting a consumable electrode under vacuum are:

- Removal of dissolved gases, such as hydrogen and nitrogen
- Minimizing the content of undesirable trace elements having high vapour pressures
- Improvement of cleanliness by removal of oxides
- Achievement of directional solidification of the ingot from bottom to top in order to avoid macrosegregation and to minimize microsegregation

Oxide inclusion removal is optimized because of the relatively short reaction paths during melting of the hot electrode end and because of a good drop dispersion in the plasma arc. Oxide removal is achieved by chemical and physical processes. Less stable oxides or nitrides are thermally dissociated or are reduced by carbon present in the alloy and are removed by conversion into the gas phase. However, in high-alloy steels and in superalloys, the nonmetallic inclusions (for example, alumina and titanium carbonitride) are very stable. The removal of these inclusions during remelting takes place by flotation.

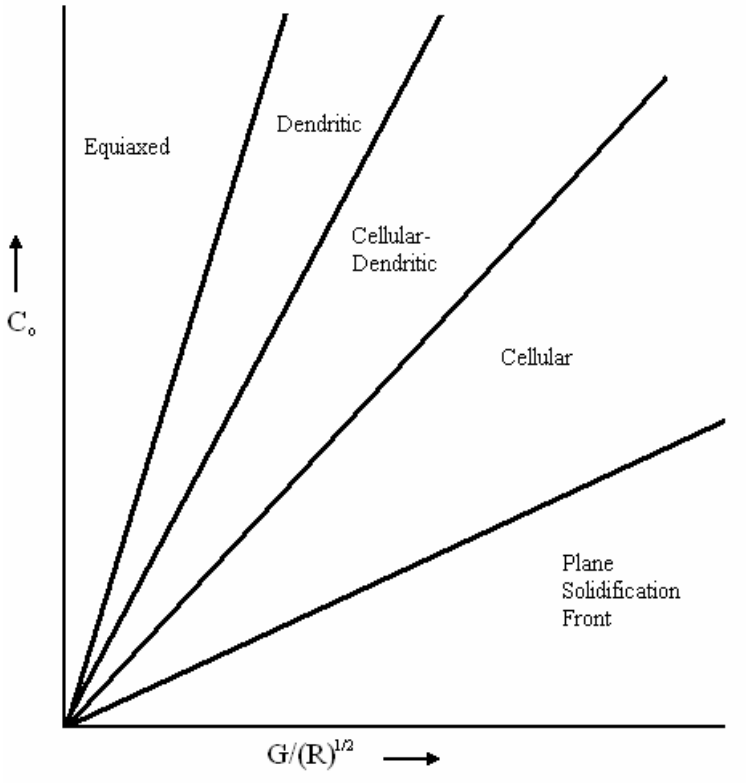

Fig. 5.1 Primary structure of a VAR ingot as a function of temperature gradient in the melt G, solidification rate R, and chemical analysis of the melt Co.

The remaining inclusions in the solidified ingot are small and are evenly distributed in the cross section. The solidification structure of an ingot of a given composition is a function of the local solidification time and the temperature gradient at the liquid/solid interface, as shown schematically in Fig. 5.1.

To achieve a directed dendritic primary structure, a relatively high temperature gradient at the solidification front must be maintained during the entire remelting period. The growth direction of the cellular dendrites corresponds to the direction of the temperature gradient or the direction of the heat flow at the moment of solidification at the solidification front. The direction of heat flow is always perpendicular to the solidification front or, in the case of a curved interface, perpendicular to the tangent. The growth direction of the dendrites is a function of the metal pool profile during solidification. For remelting processes in water-cooled copper molds, the pool profile has a rotationally symmetric paraboloidal shape in the first approximation. The pool depth increases with melting rate.

The gradient of the dendrites, with respect to the ingot axis, increases with melting rate. In extreme cases, the growth of the directed dendrites can come to a stop. The ingot core then solidifies nondirectionally in equiaxed grains, which leads to segregation and micro-shrinkage. Even in the case of directional dendritic solidification, the microsegregation increases with dendrite arm spacing. A solidification structure with dendrites parallel to the ingot axis yields optimal results.

However, this is not always possible. A good ingot macrostructure requires a minimum energy input and, accordingly, a minimum melting rate. Optimal melt rates and energy inputs depend on ingot diameter. This means that the necessary melting rate for large-diameter ingots cannot be maintained for axis-parallel crystallization.

Figure 5.2 shows melting rates for various steels and alloys as a function of ingot diameter. These are empirical values that were obtained from experience in operation. These melting rates gave low microsegregation while achieving acceptable surface quality. The importance of pool depth was also investigated by numerous researchers.

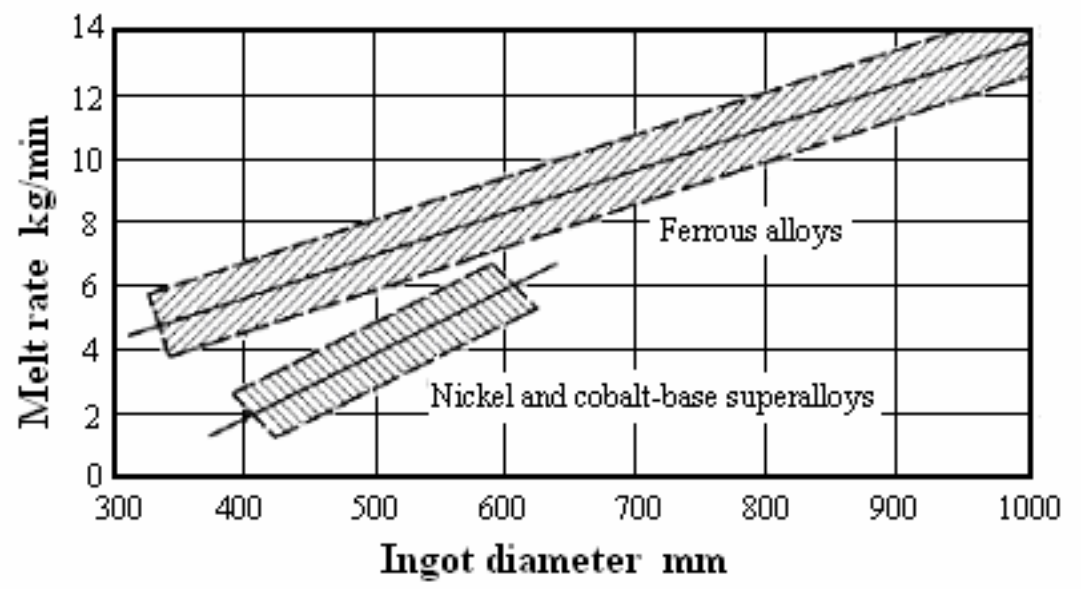

Fig. 5.2 Typical VAR melting rates for various steels and nickel and cobalt-base superalloys.

5.3.2 Vacuum arc remelting process description.

In VAR, the electrode is remelted in a vacuum chamber, of which the water-cooled crucible is an integral part. A direct electric current (dc) is passed through the electrode to the bottom of the crucible (the stool) and the electrode withdrawn, so that an arc is formed between the stool and the electrode face. The heat generated by this arc melts the face of the electrode, and metal transfer onto the stool begins as the molten metal drips onto the stool and is solidified. As the volume of metal on the stool (the ingot) builds up, an equilibrium state is reached in which there is a solid ingot, a mushy zone of both liquid and solid above that. and then a zone that is totally liquid. Because the heat extraction in the steady-state condition of melting is fastest through the sidewalls and slower down the ingot and through the stool. the mushy zones and liquid zones are shallower near the sidewalls and deeper in the ingot center. As noted in the section on solidification the thickness and growth angles of the mushy zone determine if the interdendritic liquid regions will coalesce to form positive segregation channel defects. The thickness of the mushy zone at the center of a VAR ingot is controlled by the efficiency of heat extraction. the size (diameter) of the crucible. and the melt rate of the electrode face. The melt rate is controlled by the magnitude of current passed through the electrode. Other factors that are

controlled so as to positively affect the solidifying structure are the distance of the melting face above the molten pool (arc gap) and the clearance of the sides of the electrode from the crucible (annulus).

It should be recognized that. when the electrode face becomes molten. the metal droplets are immediately transformed by gravity into the molten pool. Thus. VAR is a process in which it is inherently impossible to superheat the metal. This, coupled with the very high heat-extractive capability of the process, makes VAR the choice for economic manufacture of the largest-diameter ingots of segregation-prone. Additionally. the exposure of small volumes of molten metal to high vacuum is capable of removing detrimental high-vapor-pressure elements, such as lead and bismuth. Unfortunately, beneficial high-vapor-pressure elements such as magnesium are also reduced greatly in concentration.

Vacuurn arc remelting ingots, however, Are not guaranteed to be defect-free. The nature of the arc that provides the heat for the process is such that a different type of defect becomes inherent in the product. These defects, which are solute-lean (negative segregation), are not inherently as detrimental to the properties of a component as are defects resulting from positive segregation. For the most part, these defects also occur in discrete regions, as opposed to continuous channel defects, and their presence may be considered and accommodated in component design.

5.3.3 Vacuum arc remelting operation: the VAR furnace

Figure 5.3 illustrates, schematically, the construction of a VAR furnace. The VAR crucible is immersed in a tank of cooling water. Often. a tube is used to further enclose the crucible and limit the thickness of the water stream moving past the crucible surface. This increases the water velocity and thus increases heat removal from the crucible surface.

Such tubes are called water guides. The crucible base (stool) has provision for the inlet of a gas (usually helium). When an ingot is solidifying in the crucible, it pulls away from the crucible wall as it cools. This reduces heat conduction to the crucible wall. To maintain the highest possible heat removal from the solidifying ingot, a high-heat-capacity gas such as helium is introduced into the gap that is formed by the ingot shrinkage.

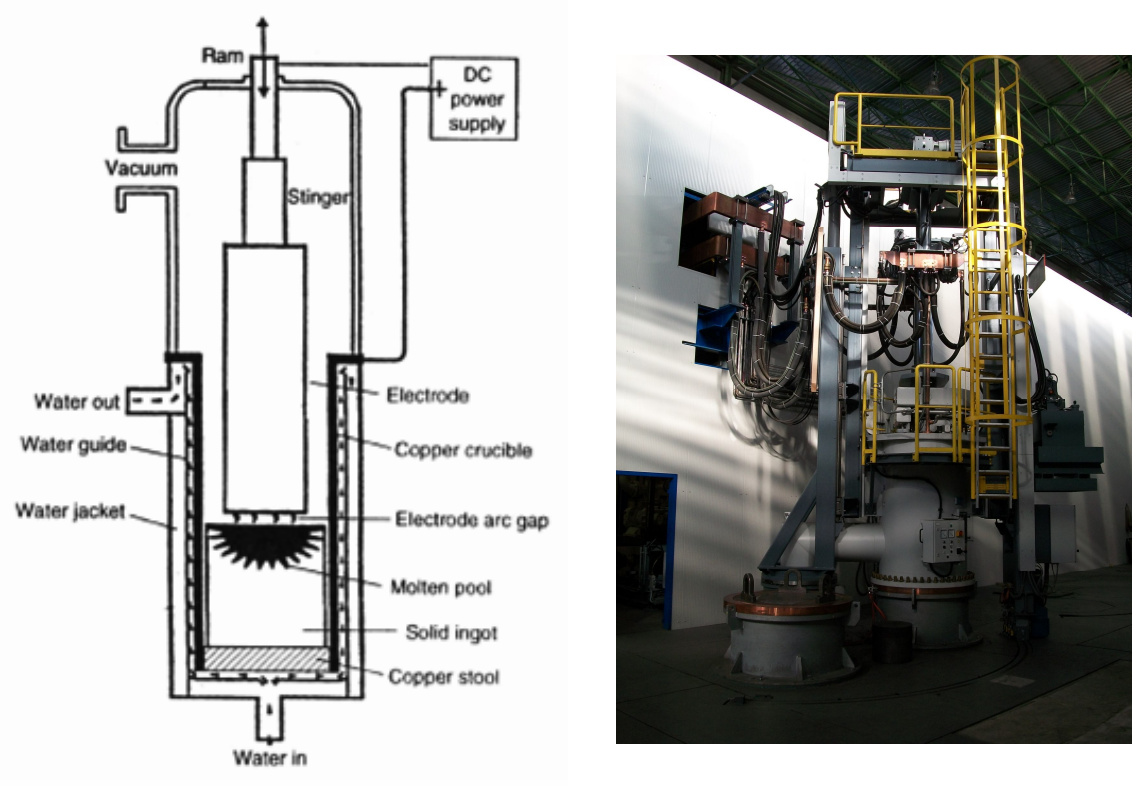

Fig. 5.3 Schematic of VAR furnace

The top of the crucible mates with the VAR head. The head contains the vacuum ports and the ram, which drives the electrode into the crucible as it is consumed. The power supply is dc. Most VAR furnaces have two melting stations (crucible setups). While an electrode is melting in one station, the next station is prepared for melting. When one melt is finished, the VAR head is rotated in the horizontal plane to be located over the second crucible/electrode setup. The electrode is attached to the ram through a stinger, which is welded to the electrode. The ram in newer designs is capable of X-Y movement.

In VAR, this is not movement in the horizontal plane, which would allow centering of stinger/electrode assembly in the crucible. It is actually angulation of the ram from the vertical, so that if the stinger is not perfectly parallel with the electrode, then the ram may be angled to make the electrode parallel to the crucible sides. The VAR head mates to the crucible flange through an O-ring seal.

5.3.4 Vacuum arc remelting furnace operation

Electrode preparation is an important part of high-quality VAR operation. Oxides are not desired on a VAR electrode, because they add a source of oxide particles to the system, and many oxides are unstable at high temperatures in vacuum. Ionized volatile components from oxides create conditions under which the arc becomes unstable and causes a lack of control over the consistency of the remelt process. Thus, it is common practice to grind all electrode surfaces free of oxide. In general, the stinger is welded to the electrode externally from the furnace. Preference for electrode orientation (stinger welded to electrode top or to electrode bottom) varies from producer to producer, with the choice being made primarily for operational reasons, rather than for quality effects. The furnace is pumped down and leak checked (leak-up rate measurement). Vacuum levels vary from producer to producer but are in the range of 0.1 to 10 μm.

The only known effect of higher vacuum is to improve resistance of the arc to occurrences of instability. The arc is struck between the electrode and the stool, and melt power (current) is stepped up to either the desired steady-state level or beyond (high-amp start-up). High-amp startups are often used to develop the steady-state pool shape as rapidly as possible. Pool shape in the start-up region is drastically different from regions higher in the ingot because of the additional heat-extractive contribution of the stool.

5.3.5 Vacuum arc remelting control

The three major parameters defining the melt process are ingot and electrode diameter, arc gap, and melt rate. The choice of ingot and electrode diameter defines the clearance (annulus) between the crucible and the electrode. Insufficient clearance, either through a poor choice of annulus or through an off-center set-up, will lead to excessive current loss from the electrode to the crucible wall, rather than through the arc to the ingot.

The choice of ingot diameter controls the amount of possible heat extraction and dictates the choice of melt rate so as to avoid positive segregation defects in the ingot. These choices, of course, are long-term choices dictated in the purchase of VIM molds and VAR crucibles. They are not controllable (except for alignment) in the day-to-day melting

process. The arc gap is the nominal distance of the melting electrode surface above the molten pool at the top of the solidifying ingot. While often shown in schematics as a large distance, the commercially useful gaps range from a minimum of about 2.5 to a maximum of 12.5 mm. When one considers that the nominal diameter of a molten metal drip from the electrode melt surface is 18.8 to 25.4 mm, then it is obvious that the arc gap is not the precise clearance implied by schematics. Vacuum arc remelting is a dc system, and the arc gap may be considered as the resistance in this circuit. As the melt current is held constant, any increase or decrease in the resistance of the circuit (change in arc gap) is seen as a change in voltage. Early VAR controls actually did measure these changes in voltage as a means for maintaining a uniform arc gap throughout the melt. Modern systems control the arc gap by measurement of drip short frequency (DSF). When a drip (drop) of molten metal is formed on the melting electrode surface, there is a point in time at which it is in contact with both the electrode and the molten pool. This causes a sudden decrease in voltage (an electrical short) across the arc gap. The duration of the short is measured in milliseconds. Control systems measure the number of drips of a given duration. It has been demonstrated that the frequency of drip shorts (usually in drips/min) is related to the width of the arc gap. The relationship is not linear over the whole range of melt conditions that may be experienced but does allow useful measurement and control of the arc gap in the ranges that are currently used commercially. The higher the DSF, the smaller the arc gap.

Making the gap smaller increases the duration of a short and thus increases the number of shorts counted. The relationship between arc gap and DSF also changes with changes in the melt current. At higher currents (higher melt rate), the drips are larger but less frequent. Thus, as illustrated in Fig. 5.4, raising the current requires a reduction in DSF to maintain equivalent arc gap. Drip short frequency is measured over a period of time, usually fractions of a minute. Individual DSF values vary widely. Thus, control signals for the ram drive (electrode feed speed) are fluctuating. Normally, the ram is in continuous motion. The response to changes in DSF is to increase or to decrease the ram speed.

Monitoring of the consistency of the ARC gap may be accomplished by computing a rolling average or by simple observation of the width of the band generated in recording each individual DSF measurement. The electrode melt rate is the other important

parameter to be controlled. The melt rate is dependent on the melt current. Many producers choose to select a given melt amperage and hold it constant. Other producers use load cells built into the VAR furnace to measure electrode weight and thus, the change in weight.

The change in weight is used to calculate a melt rate, and the applied current is varied to attempt to maintain uniform melt rate. Similarly to DSF measurement, individual melt rate measurements will vary widely depending on the time frame chosen for the measurement. Melt rates are generally calculated using rolling averages. A common averaging time is 20 minutes.

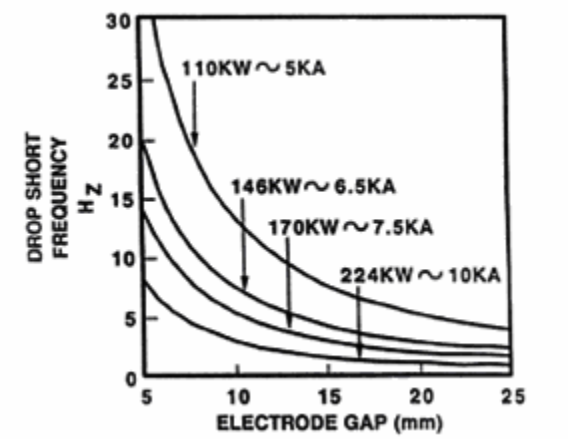

Fig. 5.4 Drip short frequency vs. arc gap a function of melt current

Load cells are subject to the generation of false signals. Load cell design and maintenance are important factors in maintaining the quality of material melted in melt rate control. In addition to attention to detail in the design and maintenance of the load cells, it is possible to restrict the response of the system to perceived rapid changes in melt rate, so that false load cell signals do not generate an unnecessary change in the melt current, which would cause a real change in the equilibrium size and shape of the melt pool. Figure 5.5 shows a nominal representation, for a hypothetical melt, of some of the major control parameters measured during VAR. The melt begins with a high-amperage start-up (in amperage control) and, at the completion of the start-up, is placed into melt rate control.

Note that the changes in voltage and DSF are not independent changes but are the result of the deliberate change in amperage. The voltage and amperage traces show a large

number of spikes. This is a normal VAR characteristic. Much-larger spikes, either in magnitude or duration, might indicate a departure of the melt from the intended conditions.

At the end of the melt, if the electrode were completely consumed or the power was just abruptly shut off, the large molten pool would solidify, with the formation of shrinkage cavity several hundred pounds deep into the ingot. This cavity would have to be removed during subsequent processing. To minimize the amount of material that must be cropped because of the end of melt shrinkage, it is common to step down the melt current as the end of melt approaches and to leave a small amount of electrode (a nominal 25.4 mm, of electrode length) unmelted. This "biscuit" allows continued heat to be put into the solidifying ingot at levels that are below those that would melt the biscuit but that serve to shrink the molten pool before final solidification and formation of the shrinkage cavity. Because the shrinkage cavity is always removed by cropping, this process is an economic issue, not a quality issue.

5.3.6 Vacuum arc remelting control anomalies

Variations in the traces of VAR parameters may indicate changes in melt conditions that will be detrimental to the quality of the solidification structure. Two of the more easily recognized problems are dead shorts and MREs. Dead shorts occur when the electrode is driven into the top of the molten pool, causing direct transfer of the melt current to the solidifying ingot. Such a problem might be caused by an unusually shaped primary shrinkage cavity in the electrode.

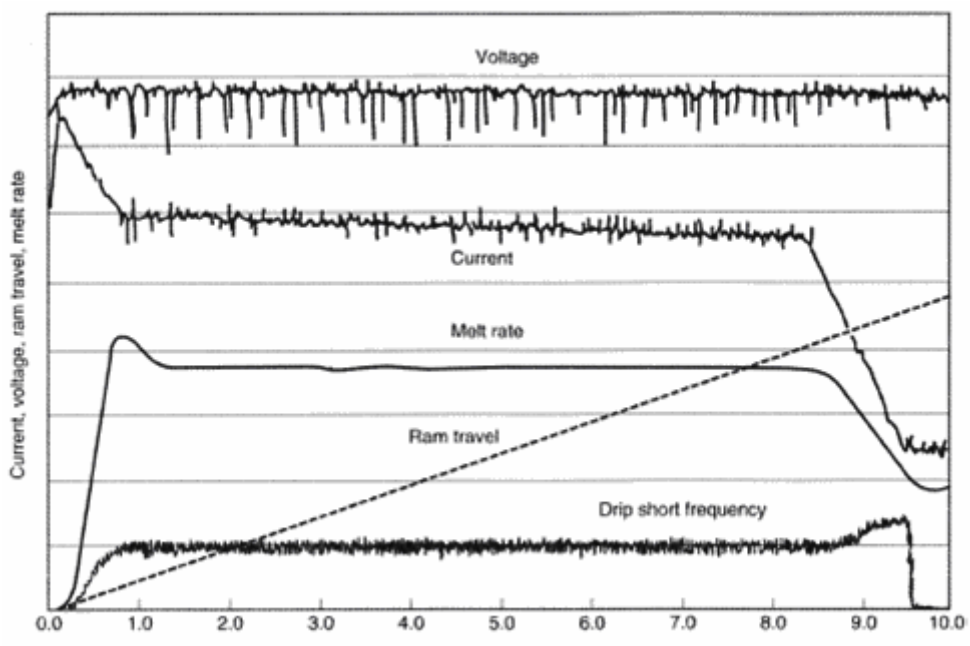

Fig. 5.5 Melt trace for VAR process showing variation in drip short frequency, melt current, melt rate, ram travel, and voltage during the melt

If the normal ram drive programming cannot accommodate the unusual shape, the electrode may be driven into the pool. This will show on the recorded parameters as a sudden reduction of voltage to zero and an immediate ram back-out from the dead short situation. Drip short frequency, of course, would also go to zero while the electrode face was in contact with the pool. (This would not show as zero DSF, because DSF is measured over a time period.) Dead shorts will cause a major change in solidification characteristics in the molten pool in that region. Another cause of multiple dead shorts is the presence of high volumes of oxides and nitrides in the VAR electrode. If the oxidenitride volume being melted onto the molten pool surface exceeds the capability of the process to sweep the "dirt" to the side and incorporate it into the ingot surface, then the ability to sustain an arc will be deteriorated.

Melt rate will drop, and the ram travel, unable to react rapidly to sudden changes in arc gap, will drive the electrode into the pool, causing a short. This may happen repetitively as the ram backs out of the pool and then advances into it again. Transverse cracks in the electrode cause MREs, the most readily definable VAR chart anomaly.

Electrodes may develop transverse internal cracks due to thermal stresses. This may happen in the cooling of the electrode, or, often, due to the thermal stresses generated as the VAR melt front moves up the electrode. When the melt front approaches a transverse crack, heat transfer across the crack is diminished, and the material below the crack becomes hotter than normal. Thus, the melt rate begins to increase. The ram speed, which responds to a decreasing DSF, does not respond fast enough to maintain arc gap, thus the arc gap increases. This decrease may be observed on the chart. Similarly, the voltage responds to the larger gap, and the voltage on the VAR chart is seen to increase. Because the melt rate is increasing. the melt current drops rapidly to attempt to bring the melt rate back into control. Thus. the first part of an MRE may be seen as an increase in melt rate, increase in ram speed, decrease in DSF, an increase in voltage, and a decrease in amperage. When the melt front progresses through the crack, the process reverses. The metal behind the crack is relatively cold. and melt current is low. The melt rate thus begins to drop rap idly, the arc gap begins to close, and thus voltage decreases and DSF increases.

Ram speed also slows, and the melt current increases. This region of an MRE is generally larger than the region of increased melt rate, and the structures generated are those that are typical of the cessation or drastic reduction of melting.

5.3.7 Process variables

5.3.7.1 Atmosphere

The heat generated by melting of the metal in vacuum arc remelting results from the electric arc between the consumable electrode and the liquid pool on the top of the ingot.

The pressure in the remelting vessel is usually of the order of 0.1 to 1 Pa (10-3 to 10-2 mbar, or 7.5 × 10-4 to 0.0075 torr). In some exceptional cases, the melting is also carried out under inert gas with a pressure up to 10 kPa (100 mbar, or 75 torr). Evaporation losses of volatile alloying elements are minimized at this pressure.

5.3.7.2 Melt rate

As mentioned earlier, the melt rate is an important factor in the quality of the ingot macrostructure. A modern VAR furnace is therefore equipped with a load cell system to

measure the weight of the electrode at a particular interval of time. The actual values of the melt rate are compared by computer with the desired set values. Any difference between the measured melt rate and the desired value is eliminated by the proper accommodation of the power input. Figure 5.6 shows the melt rate and the melting current at start-up, during steady-state melting, and during hot topping.

Start up and hot topping are usually controlled based on time. The melting phase is controlled based on weight.

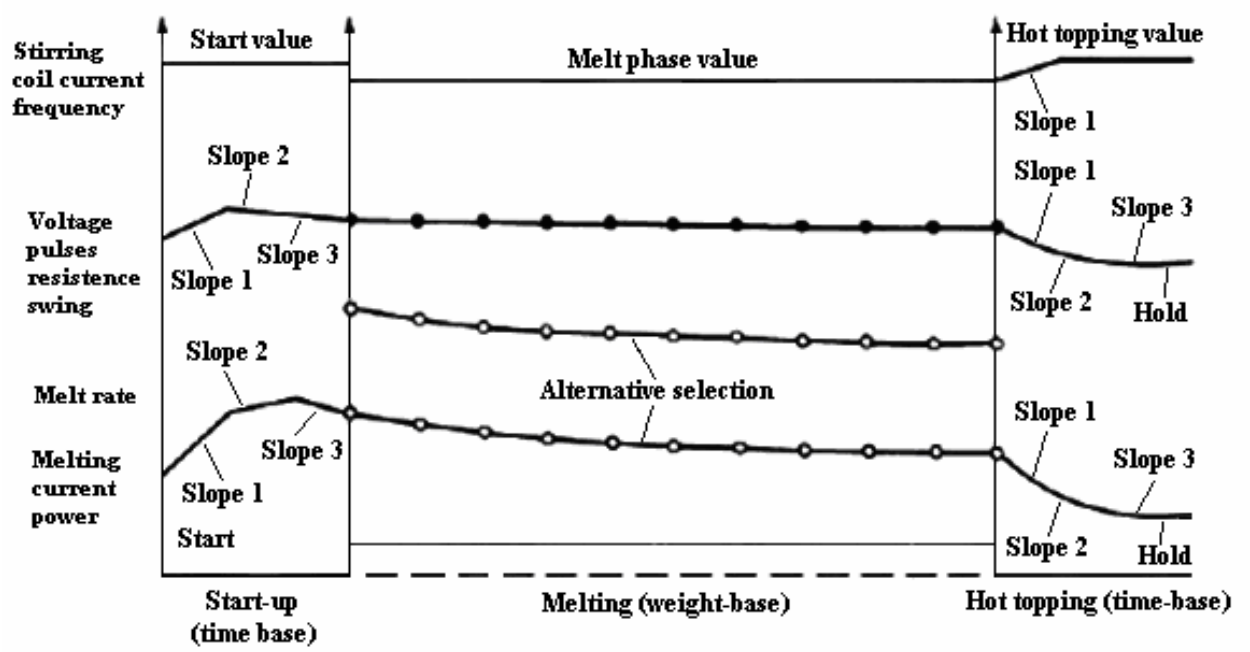

Fig. 5.6 Process control parameters and set point functions in vacuum arc remelting.

Hot topping begins when a preselected residual electrode weight is reached. A computer controls the melting parameters, which are stored in the form of up to 250 different recipes in the computer. Figure 5.7 shows a simplified version of the computer furnace control. With this, melting rate can be controlled with a precision of better than ±2%. The computer also provides documentation in the form of tables and graphs for the relevant process parameters.

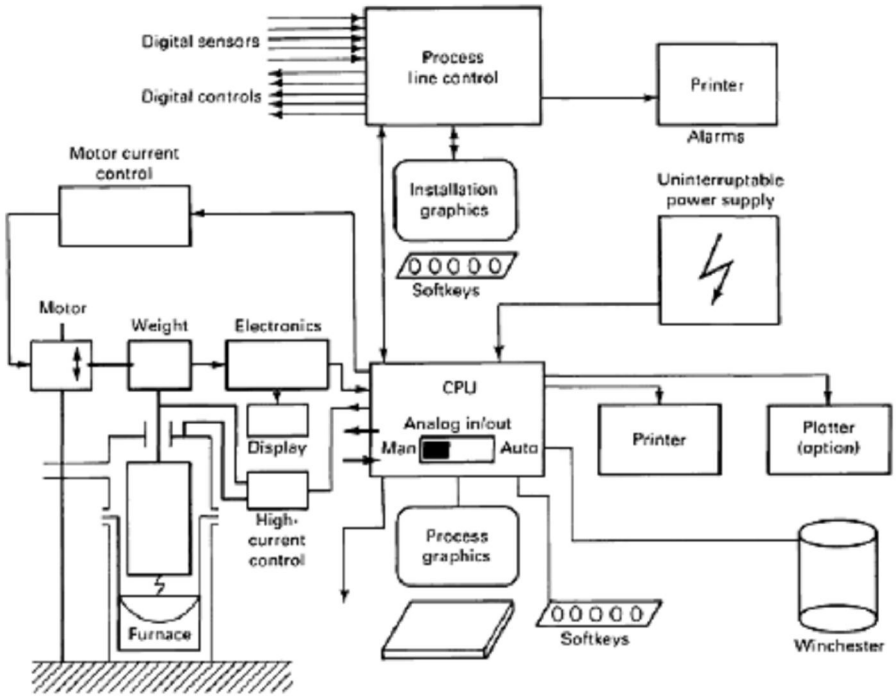

Fig. 5.7 Schematic of automatic melt control system.

5.3.8 Vacuum arc remelting pool details

Figure 5.8 schematically illustrates the features of a molten pool in a VAR ingot. The relative sizes of annulus and arc gap are not to scale. The most important feature shown is the depth of the molten pool. It generally is assumed that the depth of the liquid zone is representative of the depth of the liquid + solid zone.

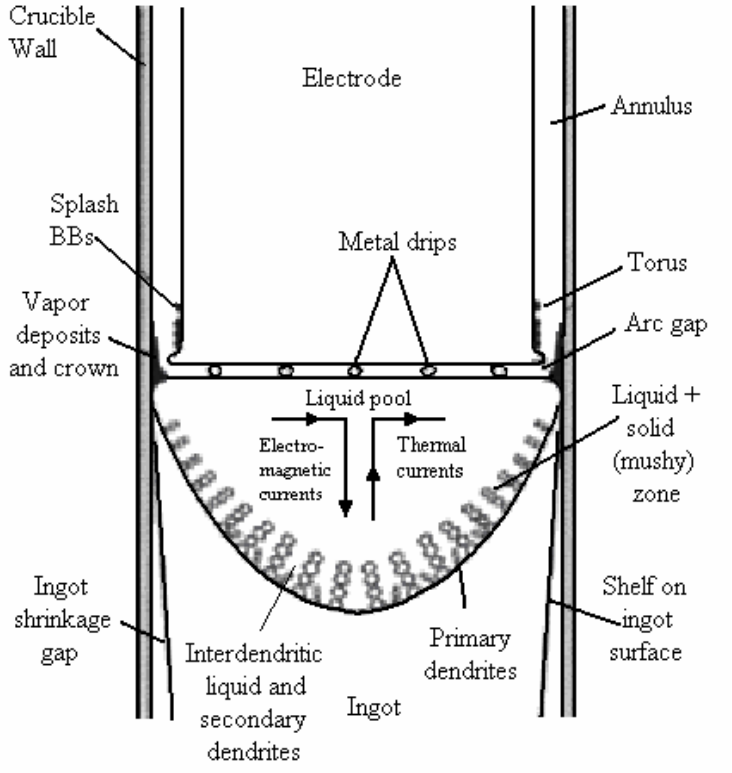

Fig. 5.8 Longitudinal schematic of the structure developed in a VAR ingot during melting

(It will be recalled that the depth and angle of the liquid + solid zone controls freckle formation for any given alloy). The size (depth) and shape of that zone might be thought, for a given crucible diameter, to have a direct relationship with heat input (melt rate) and heat extraction (water cooling). As is shown in Fig. 5.9 (a composite graph from several independent sources), the melt rate is directly proportional to the applied melt current.

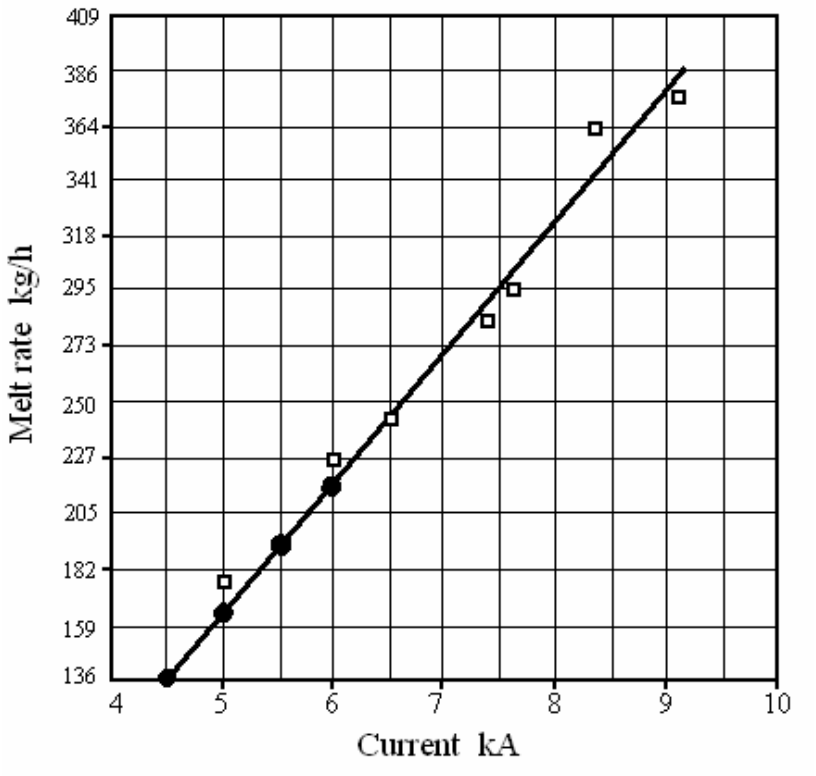

Fig. 5.9 Melt rate vs. VAR melt current (50 cm. ingot)

However, as seen in Fig. 5.10, the relationship between pool depth and melt current is direct but is divided into two separate regions. The reason for this is indicated by the two lines in Fig. 5.10, which indicate the direction of liquid metal flow in the VAR pool.

Competing currents are generated by the tendency of lower-density hot metal to rise along the ingot centerline (thermal buoyancy stirring) versus the tendency of electromagnetic fields (Lorentz stirring) to drive liquid metal from the edge of the crucible to the center of the crucible and down the centerline. Figure 4.16 is divided into two

regimes, because the inflection point (nominally 6600 amperes for 5l cm) marks where Lorentz stirring becomes stronger than thermal buoyancy stirring.

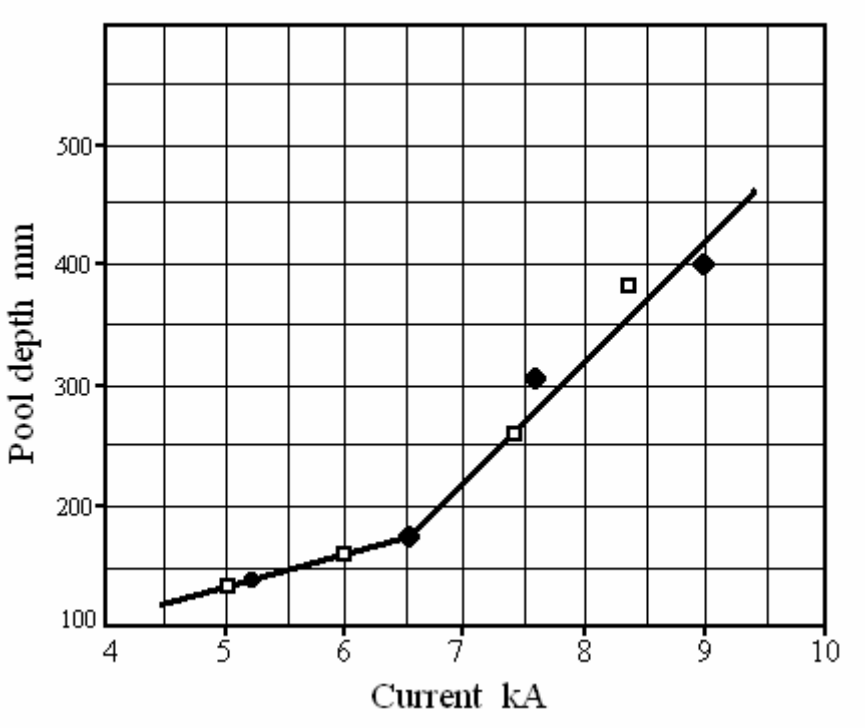

Fig. 5.10 Vacuum arc remelting pool depth vs. melt current

The apparent depth of the molten pool is altered not because there is a change in the volume of molten metal. but because the centreline stirring at higher amperages causes the pool to depart from a nominal U-shape and become deeper in the center. Thus, high VAR amperages not only produce deeper pools, but also alter the angle of the liquid + solid zone, with respect to the ingot axis. In addition to deepening the molten pool and increasing the angle of the liquid + solid zone, melting at a current where Lorentz stirring is dominant has an additional ramification. At low currents, oxides and nitrides in the electrode are melted out, drop onto the molten pool surface. and are swept to the sides of the electrode. When melting at high currents, these particles may not migrate to the edge of the ingot but may be incorporated to some extent in the general structure of the ingot, perhaps with a concentration along the centerline. It is thus considered inadvisable to melt steels at VAR currents in the Lorentz-dominated region.

The edge of a VAR ingot is the first metal to solidify. It is thus, as dictated by the phase rule. alloy-lean. It is present as a skin around VAR ingots and is known as "shelf." The shelf, in addition to being alloy-lean, contains both the oxides and nitrides collected from the melt pool surface as well as portions of the vapour deposits and splash BBs that have been deposited on the crucible wall above the advancing molten pool. This material can sometimes be carried through onto the surfaces of finished forging billet if material removal in peeling the forged billet is insufficient. Figure 5.11 illustrates a forged 15-5PH steel ingot prior to peeling the billet surface. The extent of penetration of the shelf into the forged billet is evident from the extent of the white etching edge regions.

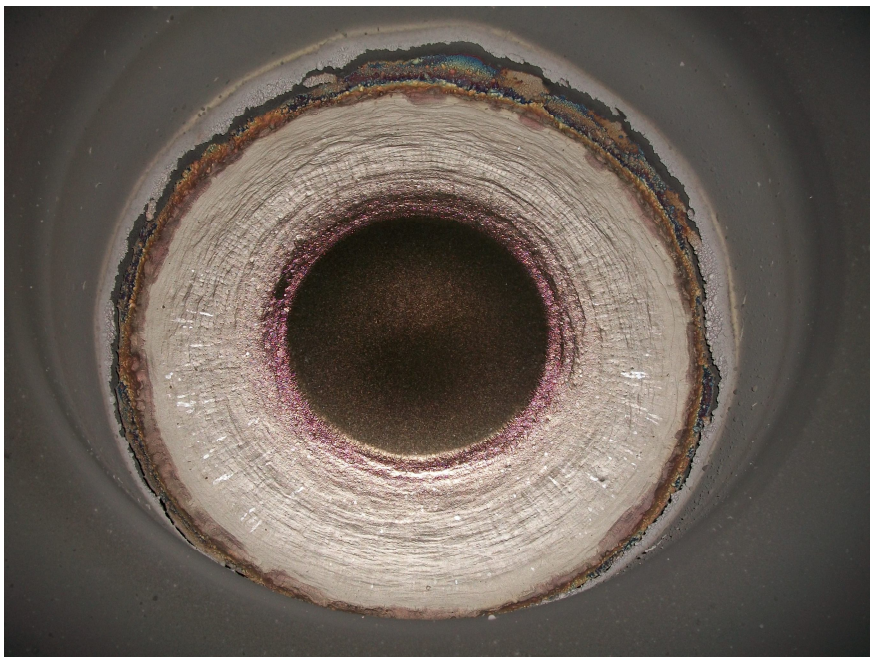

Fig. 5.11 Transverse billet section of 15-5PH steel macro etched to show VAR shelf location and depth at billet surface

5.3.9 Melt-related defects in VAR

In spite of directional dendritic solidification, such defects as tree ring patterns, freckles, and white spots can occur in a remelted ingot. This can lead to rejection of the ingot, particularly in the case of superalloys.

5.3.9.1 Tree ring patterns

Tree ring patterns can be identified in a macroetched transverse section as light-etching rings. They usually represent a negative crystal segregation. Tree ring patterns seem to have little effect on steel material properties.

Tree ring patterns are the result of a wide fluctuation in the remelting rate. In modern remelting plants, however, the remelting rate is maintained at the desired value by means of an exact control of the melting rate during operation, so that the melting rate exhibits no significant fluctuations.

5.3.9.2 Freckles and white spots

Freckles and white spots have a much greater effect on material properties than tree ring patterns, especially in the case of steels. Both defects represent an important cause of the premature failure of turbine blades in aircraft engines.

Freckles are dark-etching circular or nearly circular spots that are generally rich in carbides or carbide forming elements. The formation of freckles is usually a result of a high pool depth or movement of the rotating liquid pool. The liquid pool can be set into motion (rotation) by stray magnetic fields during remelting. Freckles can be avoided by maintaining a low pool depth and by avoiding disturbing magnetic fields through the use of a coaxial current supply.

5.3.9.3 Discrete white spots

Under ideal conditions, the arc is distributed uniformly across the surface of the molten pool. (This is called a diffuse arc.) However. the introduction of conductive ionic species into the melt or increases in the resistance (arc gap) in the system may cause the arc to become locally concentrated (constricted arc). Constricted arcs do not dwell in one place on the molten pool surface, but move about the surface. When constricted arcs undercut the crown/shelf (Fig. 4.l4), small pieces of the shelf may fall into the molten pool.

These pieces move by gravity down the pool profile. They do not readily remelt into the pool, because they have a higher melting point than the pool in general. Ultimately, they are not dissolved and are incorporated into the ingot as regions of low solute content,

containing stringers of oxide and nitride. When detected in the final product, they are seen as light etching defects containing stringers of oxide and nitride and are known as "dirty white spots." More correctly, these regions are called discrete white spots, in keeping with their nature as a distinct but isolated structure within the ingot matrix. Theoretically, a piece of shelf, free of oxides and nitrides, might be undercut and form a discrete white spot that is not dirty. Figure 5.12 shows macro- and micrographs of a discrete white spot containing "dirt" stringers.

Often, because of the lack of solute, the grain size in discrete white spots will be larger than that of the matrix. When present, dirt stringers act as stress raisers. Thus, discrete white spots, which have a high probability of being large-grain and dirty, are acknowledged to be detrimental to properties in steels.

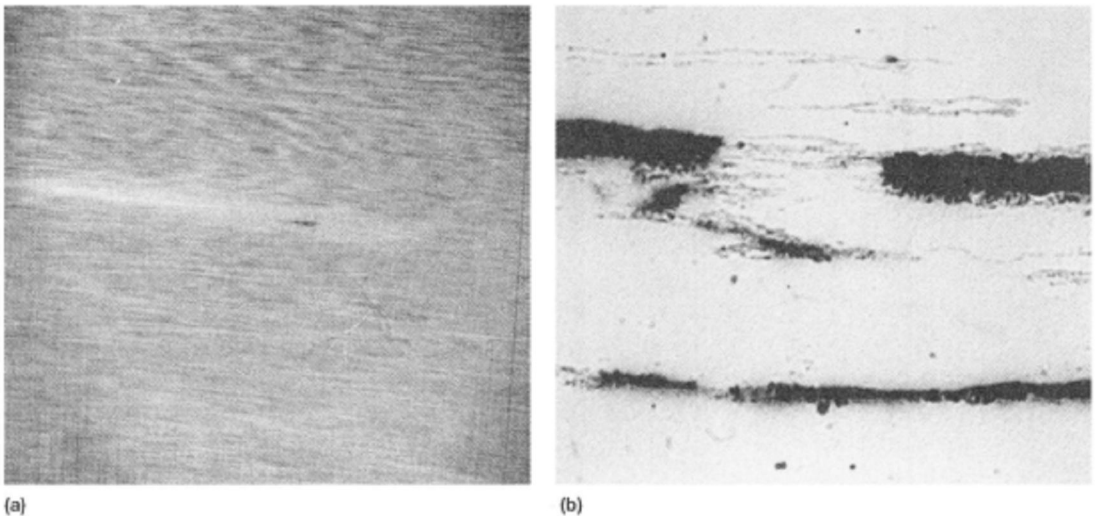

Fig. 5.12 Longitudinal section taken from sonic defect in stainless steel (a) macro etched to show white spot and crack associated with defect and (b) micrograph of same location showing oxide and nitride stringers associated with the discrete white spot.

Unfortunately although best practice for electrode preparation and for VAR melting may minimize the frequency of occurrence of discrete white spots, there is no way to guarantee their elimination in VAR products. The probability of their occurrence in the final component must be considered in the design of the component.

5.3.9.4 Solidification white spots

Because discrete white spots cannot be prevented from forming in VAR products, it is prudent to inspect critical components for the presence of these defects. Currently, there is no method of detecting a subsurface defect except to the extent that, combined with forging deformation, a crack may be generated that will be detectable by ultrasonic inspection. Macroetching of the surface of critical components is a common method for detection of discrete white spots and any other melt-related structure. In considering the results of macroetching, the method by which contrast is obtained between the white spot and the matrix must be considered. However, the fabrication temperatures for most components are such that solute-lean regions will show as light (white) etching features. A problem in inspecting macroetched steel components for harmful light etching features is that steel ingots are not completely homogenous. As an example, Fig. 5.13 shows the same slice of forged VAR IN-718 in two different heat treated conditions. In the first condition, delta precipitation is very high, a high degree of attack by the etchant is obtained, and no contrast is evident. When heat treated at 996 °C, close to the delta solvus temperature, much of the delta in the niobium-lean regions is dissolved and contrast is enhanced. The structure then is shown to consist of concentric rings of alloy (niobium)-lean and alloy rich material. These concentric rings are the inherent solidification structure of a VAR ingot.

Fortunately, most fabrication of IN-718 is conducted in the temperature region close to the delta solvus, and light etching features may be detected on the component structure.

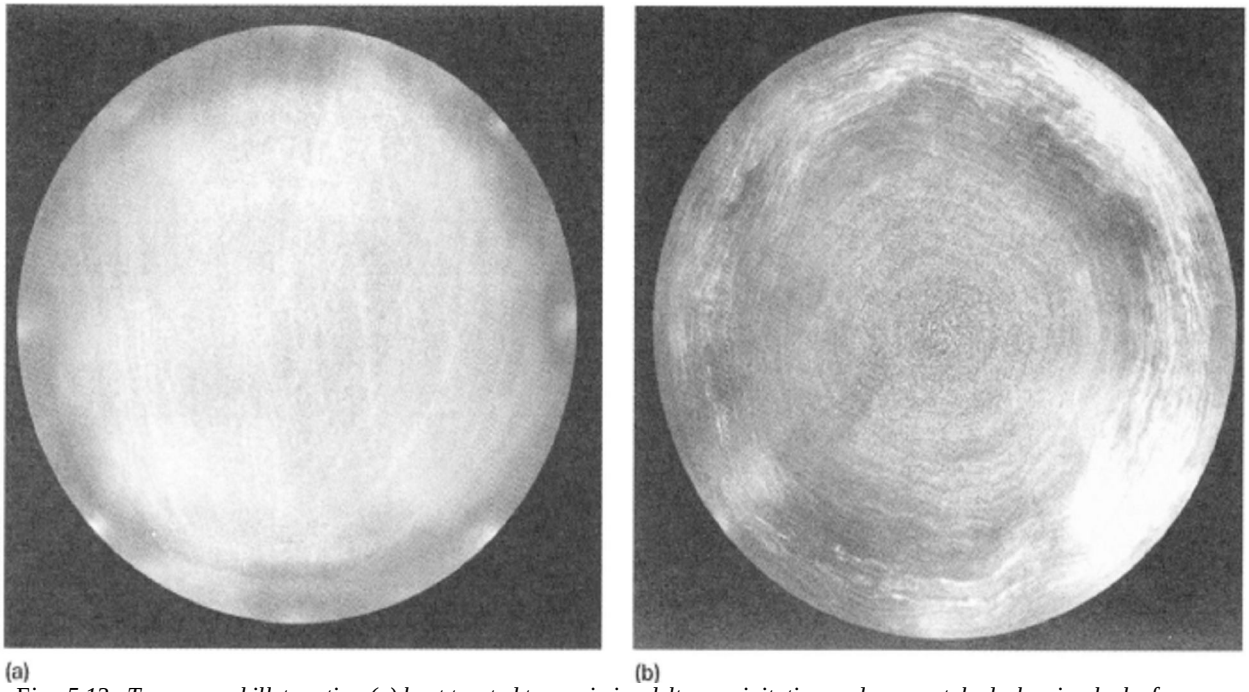

Fig. 5.13 Transverse billet section (a) heat treated to maximize delta precipitation and macroetched, showing lack of contrast in section, and (b) same section heat treated to exceed the local minimum delta solvus and macroetched

A continuing problem in macroetch inspection is that many of the features detected are related to the inherent ring solidification structure of VAR ingots. These regions may simply be wider-than-normal spots in the ring structure or may be reactions to events such as local supercooling caused by the melt-in of splash BBs. Discontinuities in the ring and reaction with splash BBs become more prevalent as the molten pool becomes shallower.

Thus, in the start-up regions of VAR ingots, where equilibrium pool depth has not been achieved and stool cooling is still very strong, there may be a very high frequency of these light etching features. Figure 5.14 shows a macroslice of forged VAR IN-718 taken from the start-up region. The light etching features have been named "solidification white spots." Generally. the only effect of one of these features will be to allow localized grain growth if the forging temperature exceeds the localized decrease in the precipitate solvus temperature. Oxide-nitride stringers are not present in solidification white spots.

Unfortunately, the detection of any light etching defect on the surface of a critical component will be cause for the removal of that component from the production line and critical examination of the features to determine the suitability of the component for its

application. While the presence of oxide-nitride stringers is an obvious cause for rejection of the component, most manufacturers have also developed standards for acceptance or rejection of localized grain-size variation. Thus, while solidification white spots are not immediately rejected as are discrete white spots, efforts are necessary to minimize their formation and inclusion in the VAR product to reduce inspection costs. Generally, these measures include taking crops from the bottom of the ingot to ensure that the start-up region material is not included in the final product. Using high melt rate in the initial start-up reduces the size of the start-up region. Higher melt rates also increase the molten pool depth and thus decrease the occurrence of localized reductions in solidification rate in the ring structure. Other factors related to VAR control, such as the annulus, are also known to affect the frequency of formation of solidification white spots.

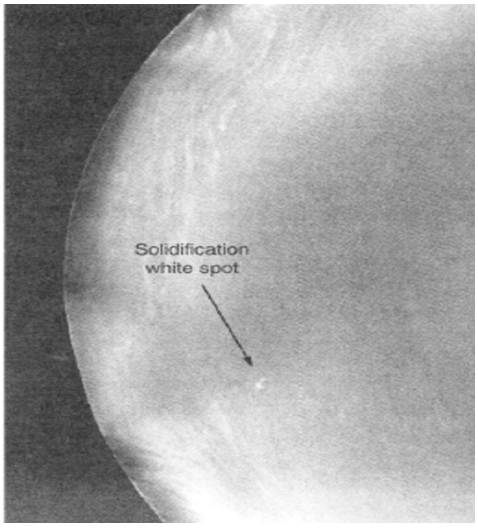

Fig. 5.14 Transverse billet section, macroetched to show solidification white spots resulting from too low a VAR melt rate

5.4 Electroslag remelting (ESR)

The rapid development of modern technology places ever greater demands on engineering alloys. These increasing demands can scarcely be met by classical steelmaking processes. Metallurgists were required to develop new steel refining processes that guarantee uniformly high quality. One of the refining processes used is electroslag remelting with consumable electrodes in a water-cooled copper crucible, usually under normal atmosphere.

The theory behind this process was known in the 1930s and was the subject of a U.S. patent, but a general breakthrough for this process took more than 30 years. Intensive studies carried out in the Soviet Union, Germany, United Kingdom, Austria, and Japan after World War II made the use of electroslag remelting possible on a production scale. In contrast to vacuum arc remelting (VAR), the remelting in the ESR process (Fig. 5.15) does not occur by striking an arc under vacuum. In electroslag remelting the ingot is built up in a water-cooled mold by melting a consumable electrode immersed in a superheated slag.

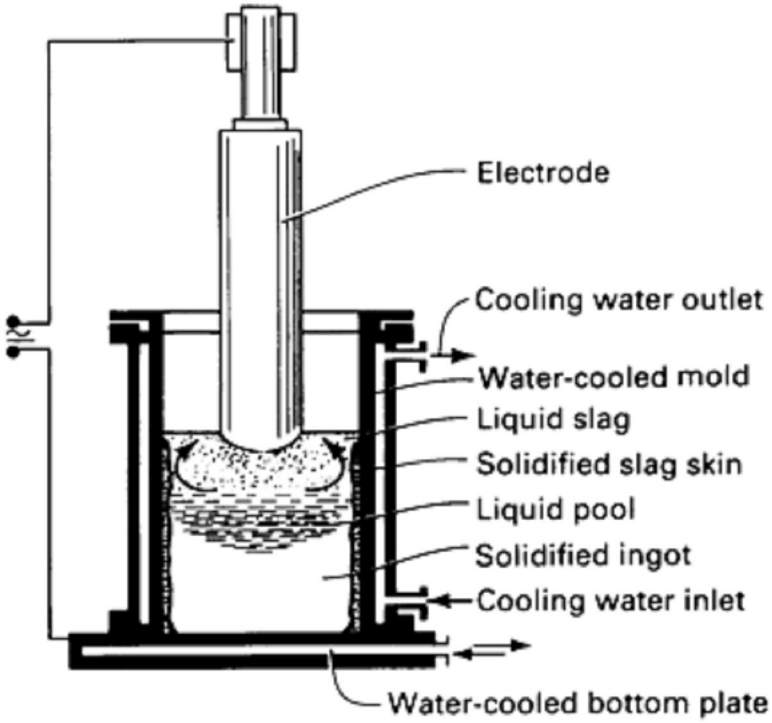

Fig. 5.15 Schematic of the electroslag remelting process.

The heat required is generated by an electrical current (usually ac) flowing through the liquid slag, which provides the electrical resistance. As the slag temperature rises above the liquidus temperature of the metal, the tip of the electrode melts. The molten metal droplets fall through the liquid slag and are collected in the water-cooled mold. During the formation of the liquid film, the metal is refined and cleaned of contaminants, such as oxide particles. The high degree of superheat of the slag and of the metal favours the metal/slag reaction. Melting in the form of metal droplets greatly increases the metal/slag interface surface area. The intensive reactions between metal and slag result in a significant reduction in sulphur and nonmetallic inclusions. The remaining inclusions are very small and are evenly distributed in the remelted ingot.

Another special feature of the ESR process, as in vacuum arc remelting, is the directional solidification of the ingot from bottom to top. The macrostructure is marked by an extraordinarily high density and homogeneity as well as by the absence of segregations and shrinkage cavities.

The homogeneity of the ingot also results in uniform mechanical properties in the longitudinal and transverse directions after hot working. Because of the absence of macrosegregations or a heterogeneity in the distribution of non-metallic inclusions, the yield of good ingot material is increased; the additional cost of the remelting process is therefore justified. In addition, the very clean and smooth surface of the ESR ingot, which is specific to this process, helps to reduce production costs because surface conditioning before hot working is not necessary.

5.4.1 Electroslag remelting process description

Electroslag remelting is not performed in vacuum. The heat source that causes melting from the working face of the electrode is a molten slag composed of CaF_2 plus oxide additions. The process is an alternating current (ac) process, and the current is passed through the electrode. then a slag cover, through the solidifying ingot, and through the stool. The molten slag provides the heart source for melting the electrode face. However, while the VAR molten drops pass through vacuum, the drops from ESR pass through slag.

The exposure of the molten metal. both while it is gathering into droplets on the electrode face and as it is passing through the slag. allows reaction with the slag to occur.

The reaction reduces oxides incorporated in the cast electrode while also greatly reducing the sulphur content through reaction with the CaF_2. Beneficial high-vapour-pressure elements such as magnesium are not reduced to the extent that they are in VAR.

Electroslag remelting produces a cleaner. lower-sulphur ingot than does VAR. The depth of immersion of the electrode into the slag. which is very shallow, is the analogous control to arc gap in VAR. Similarly, the choice of electrode diameter and crucible diameter determine the annulus. which is also in important control factor. Like VAR. melt rate is determined by power input. with melt current being the parameter varied to control the melt rate. Unlike VAR. ESR has incorporated a high volume of molten material (the slag) into the process. Thus, where VAR is a process with low thermal inertia. the ESR process has a high thermal inertia and does not respond as rapidly to changes in power input. Because of the presence of the slag as a heat source in the solidification of an ingot.

The fundamental relationship between mushy-zone thickness and distance from the side of the water-cooled crucible is changed. To a first approximation. it is generally stated that ESR pools are both deeper and steeper than VAR pools at corresponding melt rates and crucible diameters. This means that ESR is inherently more sensitive to the formation of positive segregation than is VAR. An alternative statement of the same phenomenon is that the maximum size of ESR ingot that can be produced free of positive segregation is smaller than the size that would be produced by VAR. An additional benefit for ESR is the ability to melt simple shapes. Much of the volume of steel that is used in sheet or plate form is from electrodes that are cast as rectangular cross-section slabs and melted into larger slab molds in ESR. VAR product is always round.

5.4.2 Electroslag remelting operation: the ESR furnace

Figure 5.16 illustrates, schematically, the construction of an ESR furnace. The ESR crucible is normally selfcontained, unlike the VAR crucible, in that the inside and outside hells through which the cooling water runs are assembled as a single piece. A water-cooled stool is assembled to the shell to form the bottom of the crucible. A starter or striker plate

is usually enclosed in the junction between the crucible shell and the crucible stool. For crucibles to be used with hot slag starts. the crucible may contain an opening at the bottom (a "mouse hole") through which the molten flux will be introduced. Unlike the VAR furnace, the top of the crucible does not mate to the rest of the furnace but operates exposed to air. The top of the ESR furnace contains the ram drive and load cells. It is connected electrically to the crucible stool through, most commonly, four vertical bus bars located at 90° intervals around the crucible. The ESR head commonly is able to be translated in the horizontal direction by an X-Y drive which allows centering of the electrode in the crucible prior to the start of the melt. (Note that X-Y capability is inherently different in ESR compared to VAR.) The power supply is most often AC. Most ESR furnaces have two melting stations (crucible setups). While un electrode is melting in one station, the next station is prepared for melting. When one melt is finished, the ESR head is rotated in the horizontal plane to be located over second crucible/electrode stinger setup (the electrode is attached to the ram through a stinger, which is welded to the electrode). Melting is then ready to begin.

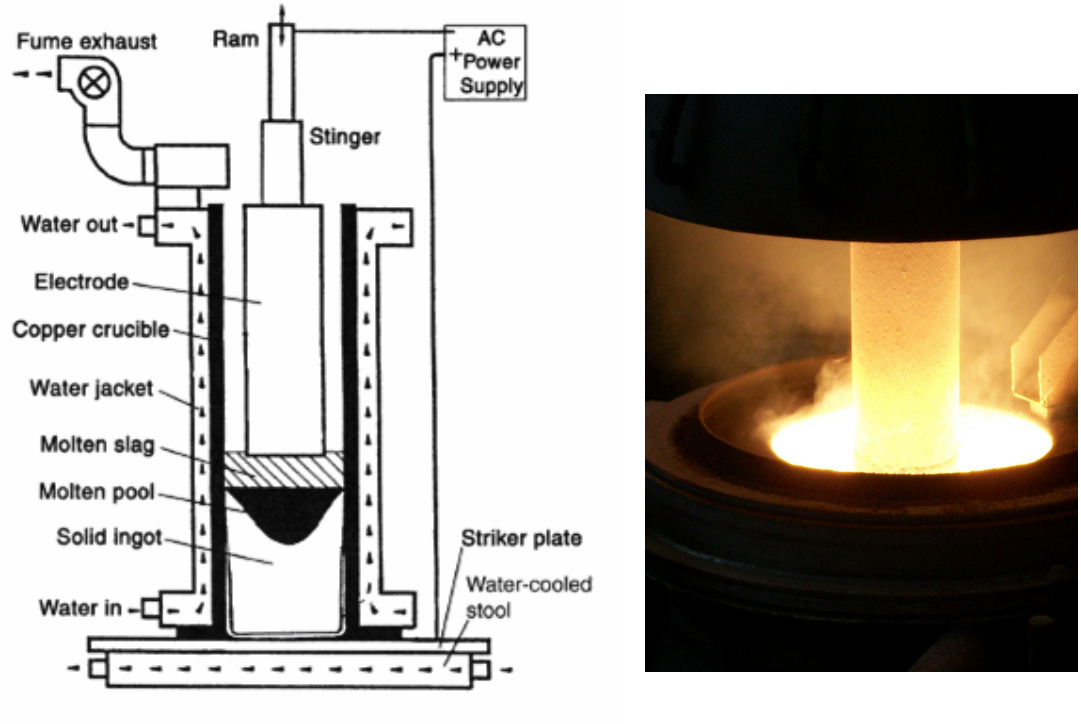

Fig. 5.16 Schematic of electroslag remelting, and the insertion of the electrode into the slag.

Significant advances have been made in the past few years in plant design in the area of process control and coaxial current supply. Figure 5.17 shows the basic design of a modern ESR furnace with a fixed mold for an ingot weight of 20 Mg (22 tons) and an ingot diameter of 1000 mm.

A fully coaxial furnace design is required for the remelting of segregation-sensitive alloys in order to prevent melt stirring by stray magnetic fields. In the case of the retractable bottom plate furnace, current feedback does not take place through a closed copper pipe; instead, it is accomplished with four symmetrically arranged current feedback tubes.

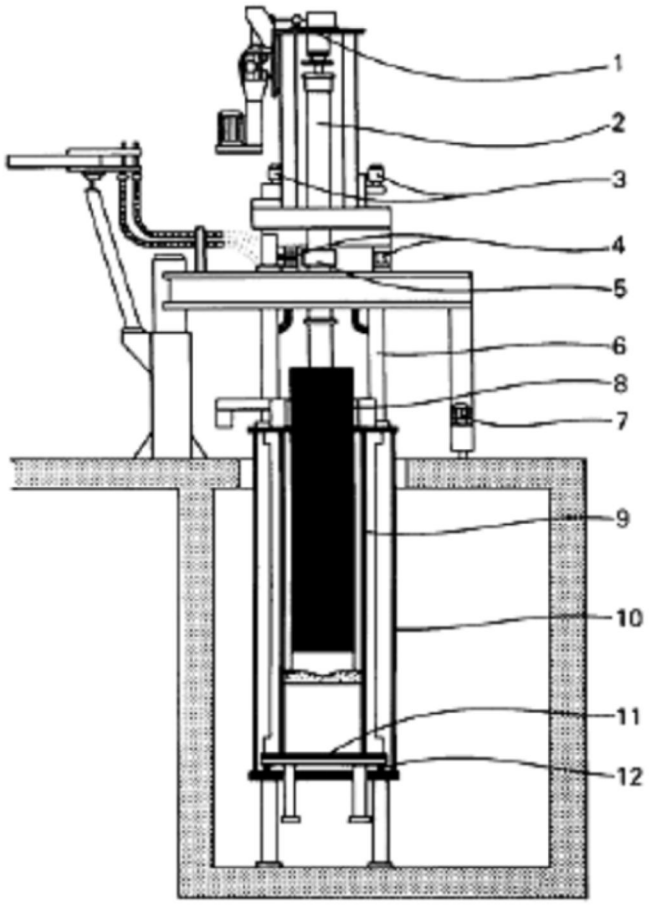

Fig. 5.17 Schematic of an ESR furnace with a stationary mold. 1, RAM drive system; 2, electrode RAM; 3, XY adjustment; 4, load cell system; 5, sliding contact; 6, four bus tubes; 7, pivoting drive; 8, electrode; 9, mold assembly; 10, coaxial bus tube; 11, base plate; 12, multicontacts.

5.4.2.1 Automation of process control

The ESR process, like vacuum arc remelting, is fully automatic. Melting was accomplished in a fully automatic operational mode. Figure 21 shows a modern ESR control desk.

5.4.2.2 Electroslag remelting of heavy ingots

At the end of the 1960s, the concept of using ESR plants to manufacture large ingots weighing UP to 350 Mg (385 tons) gained acceptance. Increasing demands for energy and the trend toward larger electrical power generating units required cast ingots weighing 100 Mg (110 tons) and more for the manufacture of generator and turbine shafts. With ESR, it is possible to achieve higher yields and to avoid such internal defects as porosity, macrosegregation, and the accumulation of nonmetallic inclusions.

Figure 5.18 shows a schematic of a large ESR furnace, which was brought on line in West Germany in 1971 to manufacture ingots 2300 mm in diameter and 5000 mm in length.

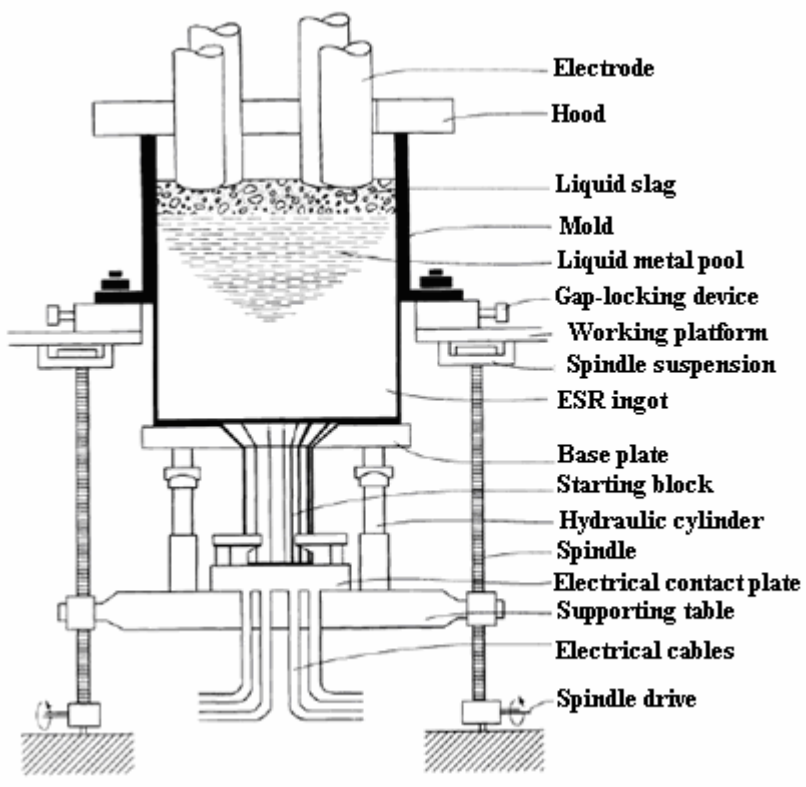

Fig. 5.18 *Schematic of an ESR furnace for the manufacture of large (160 Mg, or 176 ton) ingots.*

Ingots weighing up to 160 Mg (176 tons) can be manufactured using a retractable bottom plate. Several electrode changes are necessary to produce such large ingots.

Remelting of large ingots of this type in retractable bottom plate furnaces demands the solution of specific technical and metallurgical problems, such as:

- Ensuring consistent remelting over a period of several days without interruption
- Prevention of steel and slag breakout when remelting with a retractable bottom plate
- Achieving a good ingot surface
- Ensuring directional solidification to avoid macrosegregation and shrinkage cavities
- Controlling the steel and slag compositions over the entire ingot height
- Adjusting for low hydrogen content
- Adjusting for a low aluminum content (<0.010%) for rotor steels, this has a decisive influence on the creep rupture properties of the rotors

After these problems had been solved, heavy rotors for electrical generators could be manufactured from ESR ingots.

Interior defects such as macrosegregation, shrinkage cavities, and nonuniform distribution of inclusions can be avoided in large ingots only if directional solidification is ensured over the entire ingot section.

By maintaining the correct melting rate and temperature of the slag, directional solidification can be achieved for ingot diameters of 2300 mm. Accordingly, the ESR ingot is free of macrosegregation in spite of the large diameter (Fig. 5.19).

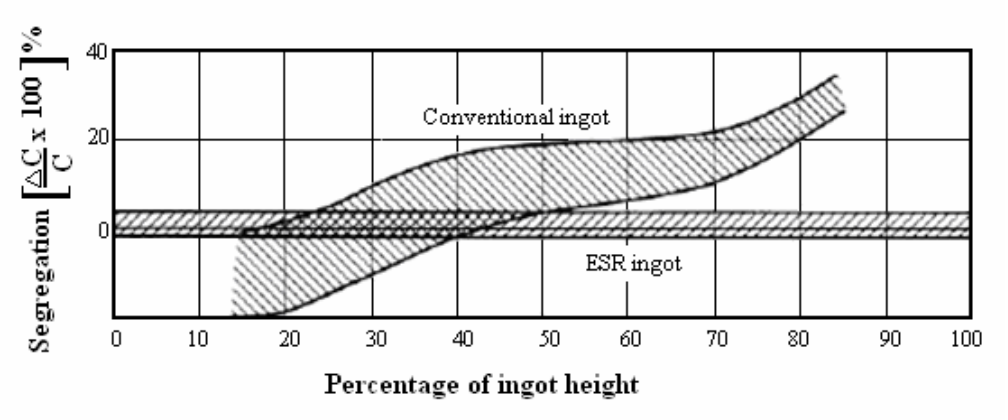

Fig. 5.19 Comparison of carbon segregation in conventional and ESR alloy steel ingots. Specimens were taken from the ingot axis along the entire ingot height.

The cleanliness and homogeneity of ESR ingots result in excellent mechanical properties. Figure 5.20 shows the superior toughness of ESR steel compared to conventionally manufactured steel.

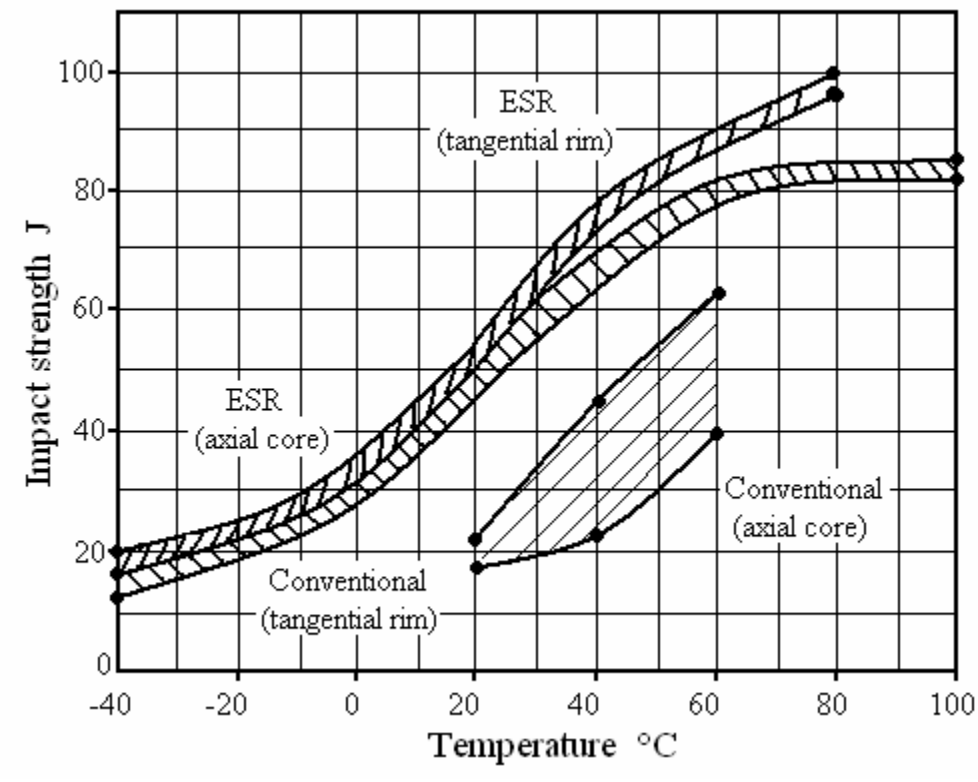

- a

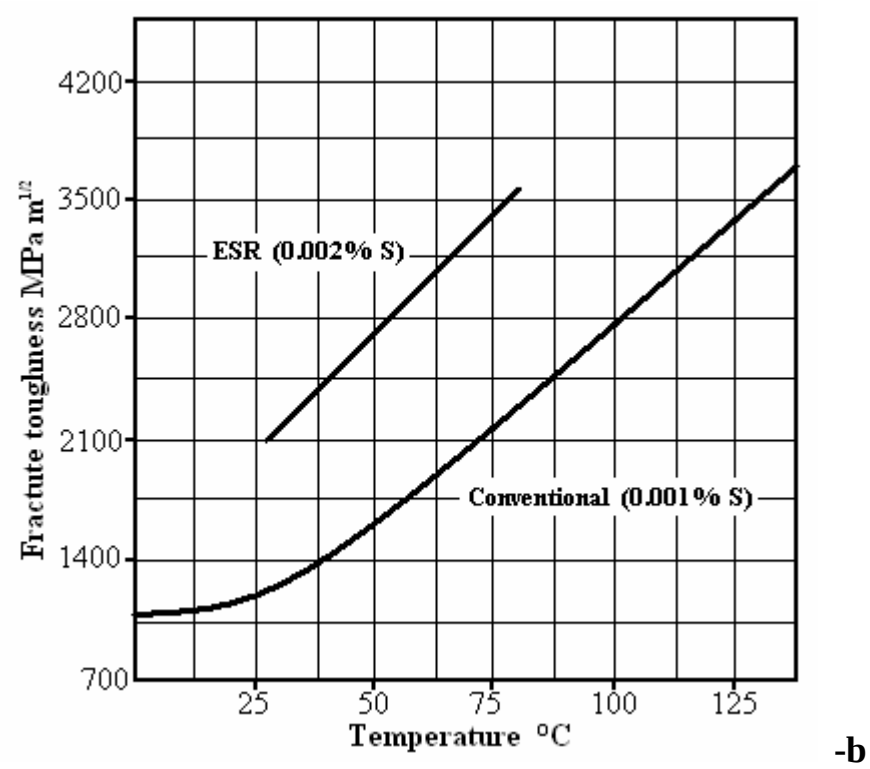

Fig. 5.20 Comparison of properties of steel rotor forgings made from ESR and conventionally melted ingots. (a) Impact strength of grade X22CrMoV121. (b) Fracture toughness of grade 30CrMoNiV511. Specimen orientation and location are indicated next to curves.

5.4.3 Electroslag remelting furnace operation

Unlike VAR, electrode preparation is not it critical part of quality ESR operation. Oxides on an electrode surface are incorporated into the slag. Thus, electrodes for ESR are generally not ground. An exception to this is for production of premium-quality material where the end-user specifications require grinding to ensure the removal of potential iron-mold pullout on the electrode surface. Also, the shrinkage cavity at the top of the electrode is not a problem. if the electrode is melted top down. Thus, electrodes for ESR are not commonly hot topped in VIM or cropped prior to melting. The ESR stinger is welded to the electrode externally from the furnace. The stinger is often tubular. because only the periphery of the electrode is involved in the welding process. The electrode is placed into the crucible and connected to the head. The X-Y drive is used to center the electrode in the

crucible. (Note that the X-Y drive may compensate for welding of the stinger off-center but not compensate for an angle between the stinger axis and the electrode axis).

There are two possible start-up scenarios, cold start and hot start. In cold start, the slag and small particles of the alloy to be melted (usually machining chips) are placed on the starter plate. The electrode is touched into the slag-alloy mix and backed out to establish an arc. High melt power is used in this start-up phase. The arc melts clown both the slag and the metal particles, at which point the electrode becomes immersed in the slag and the melt process shifts to melting of the electrode surface by the slag. It is necessary that the start-up power be sufficiently high that actual welding (melt-in) occurs between the embryonic ingot and the starter plate. This is required so that the electrical conduction path will be predominantly through the electrode, then the slag to the ingot, from the ingot through the starter plate, and then to the stool. In hot slag starts, the slag is melted externally by electric arc in graphite crucibles. The molten slag is introduced, generally through a bottom mouse hole, into the crucible. The electrode is lowered into the slag, and melting commences. Although high initial melt power is not required to melt slag and metal starter material, a high-power profile start-up is generally used to ensure the melt-in of the ingot to the starter plate (to ensure good electrical conduction paths). High-power start-ups also compensate, as they do in VAR, for the extra cooling effect of the proximity of the ingot to the stool and help develop steady-state melt conditions at an earlier time in the melt.

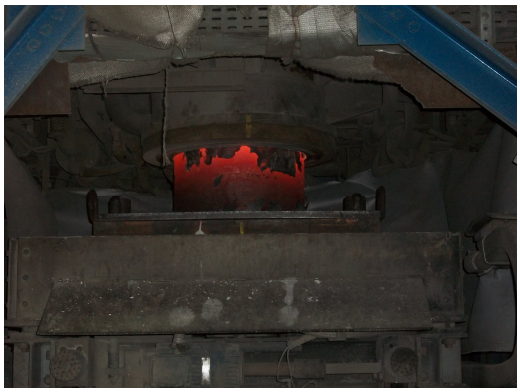

Fig. 5.21 Preheating of the electrode, and the remelted ingot in output.

5.4.4 Electroslag remelting control

The three major parameters defining a melt process are:

- Ingot and electrode diameter (as in VAR)
- Electrode immersion depth in the slag (analogous to arc gap in VAR)
- Melt rate

The choice of ingot and electrode diameter defines the clearance (annulus) between the crucible and the electrode. Insufficient clearance is generally regarded as a problem in processes using cold slag starts. in that the slag-chip mix may get hung up in the annulus. However, a tight annulus may result in more uniform heat distribution across the molten pool. There is no published information to support either viewpoint. Thus, annulus becomes, much more than in VAR, a parameter dictated by the individual producer's philosophy. Electrode immersion is generally thought of as a depth of penetration of the electrode into the slag. There is no definitive method for measuring the immersion, but observation of interrupted melts suggests that the meniscus of slag reaching up the side of the electrode will generally not exceed 6.4 mm. Thus, schematics of the ESR process are misleading when they imply significant immersion into the molten slag. However, the degree of immersion, as affected by the ram drive, can produce drastically different electrical signals. The quality of the melt has been found to be responsive to these signals.

Thus, while there is no realistic understanding of what depth of immersion means physically, the parameter that controls it can be demonstrated to have a significant effect on melt quality. ESR is an AC process, and the electrode immersion plus the thickness of the slag cap may be considered as the resistance (impedance) in this circuit. Changing the weight of slag in the system or the slag composition changes the impedance of the circuit and thus changes the amperage and voltage required to maintain a given power input (for constant melt rate). The slag cap thickness is the primary driver, while electrode immersion may account for 10%-20% of the total impedance. Measurement of the changes in this resistance or of the corresponding changes in voltage may be used to control the immersion of the electrode in the slag. This suggests that the voltage and impedance changes associated with electrode immersion are actually the impedance of the circuit associated

with the interfacial resistance between the electrode melt surface and the slag surface. It thus should be realized that, in ESR of steels, the electrode immersion is always extremely shallow, and, in fact, the most common electrode positioning is that of "skittering" on the top of the molten slag cap. The degree of this skittering is commonly controlled by the repetitive change in voltage in the process (volt swing). The electrode melt rate is the other important parameter to be controlled The melt rate is dependent on the melt current.

Although some VAR processes are run in constant current rather than in melt rate control. ESR processes are exclusively melt rate control. Melt rates are generally calculated using rolling averages. A common averaging time is 20 minutes. Load cells are subject to the generation of false signals and to errors in the absolute value. Thus, load cell design and maintenance are important factors in maintaining the quality of ESR. In ESR, the melt current responds to changes in the melt rate and attempts to hold the melt rate constant at the set point. Because of the presence of the slag, which must be heated or cooled, in the system, the response time of ESR to the melt current change is much slower than that of VAR.

A fourth factor controlling melt quality and unique to ESR is the choice of slag and the volume of slag used. The resistance of the slag cap depends on both the resistivity of the slag and the thickness of the slag cap through which the melt current must travel. An additional consideration is the degree of chemical reactivity of the slag with elemental components of the electrode.

Figure 5.22 shows a nominal representation, for a hypothetical melt. of some of the major control parameters measured during ESR. The melt begins with a high-amp start-up in amperage control and, at the completion of the start-up, is placed into melt rate control. Note that the change in voltage is the result of the deliberate change in amperage. As in VAR, at the end of the melt, if the electrode were completely consumed or the power was just abruptly shut off, the large molten pool would solidify, with the formation of a shrinkage cavity several hundred pounds deep into the ingot. This cavity would have to be removed during subsequent processing.

To minimize the amount of material that must be cropped because of the end of melt shrinkage, it is common to step down the melt current as the end of melt approaches and

leave a small amount of electrode (a nominal 25.4 mm, of electrode length) unmelted. Unlike VAR, this biscuit is generally not used to put electrical power into the melt. Rather, it simply prevents radiation loss from the slag. Because of the presence of the slag as a heat source at the top of the ingot, ESR hot topping practices are not as extended as are those for VAR.

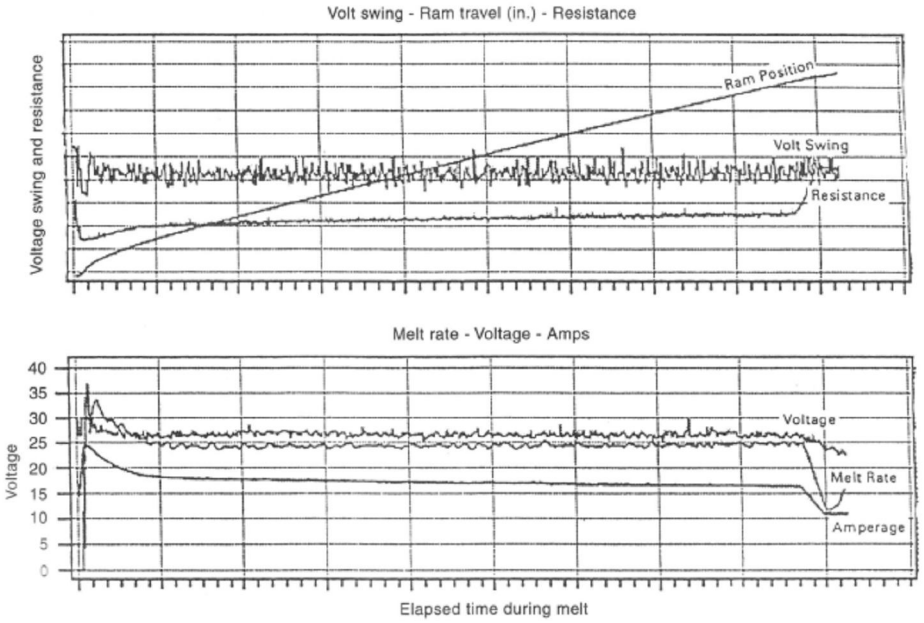

Fig. 5.22 Melt trace for ESR showing variation of melt current, melt rate, ram travel, slag resistance, voltage, and volt swing.

5.4.5 Remelting of steels

There are a number of publications that deal primarily with improvements in the physical properties of remelted steel. However, they discuss not only the directional solidification of the metal but also the influence of liquid, superheated, and therefore reactive slags. The extent and direction of the metallurgical reactions in the ESR process are determined by the steel composition, the slag used, and the atmosphere used (inert gas, air, etc.).

The principal feature of the ESR process is the slag bath. A continuous transport of liquid metal through the slag takes place. During this transport, the slag and the metal

compositions change, according to the kinetic and thermodynamic conditions. To perform its intended function, the slag must have some well-defined properties, for example:

- Its melting point must be lower than that of the metal
- It must be electrically efficient
- Its composition should be such that the desired reactions, such as removal of sulphur and oxides, are ensured
- It must have suitable viscosity at remelting temperature

5.4.5.1 Sulphur

One of the primary advantages of the ESR process for steel is the good desulphurization of the metal. The final desulphurization is determined by two reactions. The first is the metal/slag reaction, in which sulphur is
transferred from the metal to the slag:

$$FeS + CaO \rightarrow CaS + FeO \qquad \textbf{(Eq 1)}$$

The second reaction is the slag/gas phase reaction. In this case, the sulphur absorbed by the slag is removed by the oxygen of the gas phase in the form of gaseous sulphur dioxide:

$$CaS + \frac{2}{3}O_{2(gas)} \rightarrow CaO + SO_{2(gas)} \qquad \textbf{(Eq 2)}$$

It is evident that a saturation of the slag with sulphur does not take place; therefore, the desulphurization capacity of the slag remains intact throughout the entire remelting process. With a highly basic slag ($CaO/SiO_2 > 3$), more than 80% of the sulphur can be removed.

5.4.5.2 Oxygen

As mentioned previously, the ESR process is usually carried out under a normal air atmosphere. Oxidation of the metal is unavoidable. Oxygen can be transferred into the metal in several ways:

- Oxidation of the electrode surface above the slag bath

- Oxidation on the slag surface of elements with variable valences, such as iron and manganese
- Oxides attached to the electrode surface

Transfer of oxygen into the slag also takes place, and oxygen is transferred into the metal according to Eq 1. This results in losses of easily oxydizable elements, such as aluminum and silicon, during remelting. To counteract this oxidation, the slag should be continuously deoxidized, preferably with aluminum. With proper slag composition and remelting techniques, oxygen contents of less than 20 ppm in unalloyed steel are possible. Figure 5.23 shows the influence of slag composition on the final oxygen content of remelted ingots.

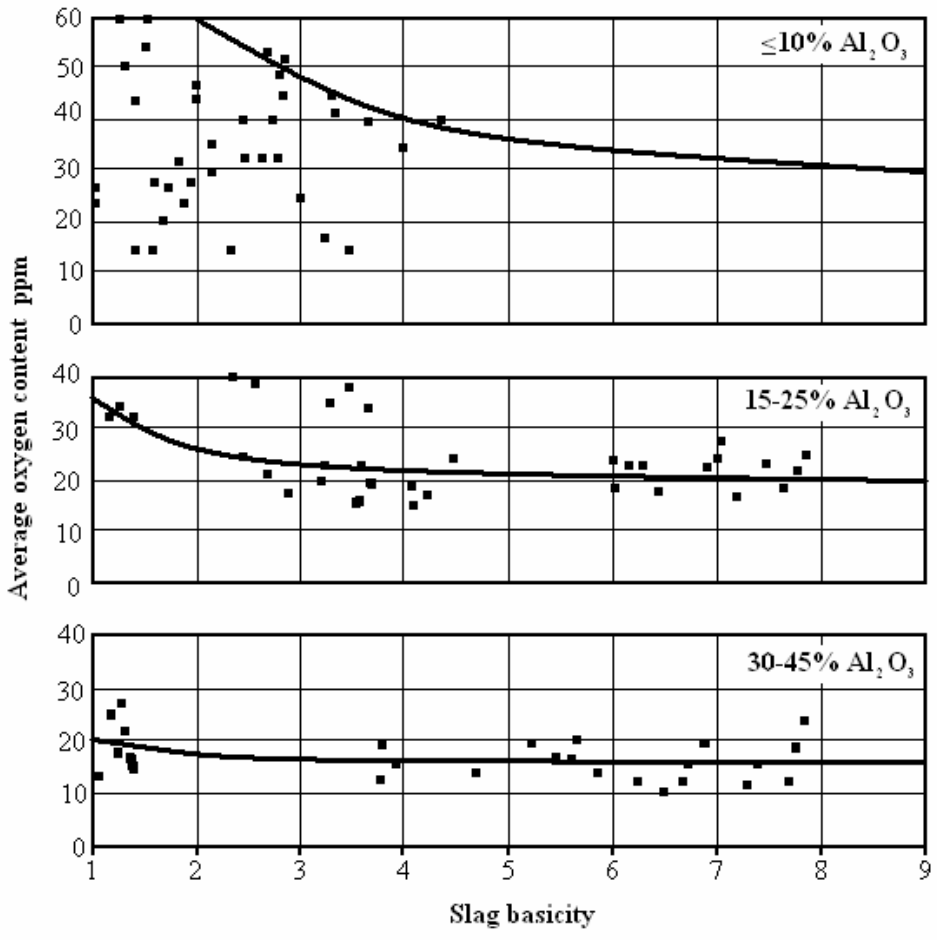

Fig. 5.23 Effect of slag composition on the oxygen content of the remelted ingot. Slag basicity is the ratio of CaO to SiO_2.

5.4.5.3 Slag choices

All ESR slags contain CaF_2 as the primary constituent. Oxides may be added to the slag to raise the resistivity (so as to make melting more efficient electrically) or to modify the slag chemistry with regard to its reactivity with the metal being melted. There is a universal designation system for slags in which the percentage of constituents is listed in the order $CaF_2/MgF_2/CaO/MgO/Al_2O_3$. Thus a common base slag such as 60% CaF_2, 20% CaO, 20% Al_2O_3, should be referred to as 60/0/20/0/20. Unfortunately, the system is seldom adhered to in the industrial world. and 0s are often omitted. Thus, the previously mentioned slag is generally referred to as 60/20/20. Many proprietary slags contain additions of TiO_2 and/or ZrO_2 to prevent excessive loss of these elements into the slag during melting. The loss is due to exchange with any oxide in the slag that is less stable than the element in the electrode. A common problem with titanium-bearing superalloys is that commercially available CaF_2 contains SiO_2.

During ESR, the SiO_2 is converted to silicon. which is picked up by the metal. Thus, the slag is enriched in TiO_2. which reduces the titanium content of the metal. This reaction generally results in a titanium gradient in the ingot, because the SiO_2 content is consumed early in the melt and no longer plays a part in the reaction after the first few hours of melting. When ESR slag is recycled, it is already depleted in SiO_2, and this reaction no longer occurs. The slag always tries to move to chemical equilibrium with the molten metal at the operating temperature of the slag. Thus, repetitive recycle of slag with a given alloy composition produces a slag that is naturally buffered against causing elemental loss from the electrode during ESR. Unfortunately, slag loss (left as a skin on the electrode during the process) generally keeps recovery levels of the slag below 100%, so some fresh slag is always needed in the ESR process.

Slags for electroslag remelting are usually based on calcium fluoride (CaF_2), lime (CaO), and alumina (Al_2O_3). Magnesia (MgO), titania (TiO_2), and silica (SiO_2) are also added, depending on the alloy to be remelted. Table 5.1 shows the compositions of some common ESR slags.

Slag designation	Composition, , %					Comments
	CaF_2	CaO	MgO	Al_2O_3	SiO_2	
100F	100	-	-	-	-	Electrically inefficient; use when oxides are not permissible.
70F/30	70	30	-	-	-	Difficult starting; high conductivity; use when aluminum is not allowed; risk of hydrogen pickup
70F/20/0/10	70	20	-	10	-	Good general-purpose slags; medium resistivity
70F/15/0/15	70	15	-	15	-	
50F/20/0/30	50	20	-	30	-	
70F/0/0/30	70	-	-	30	-	Some risk of aluminum pickup; good for avoiding hydrogen pickup; higher resistivity
40F/30/0/30	40	30	-	30	-	Good general-purpose slags
60F/20/0/20	60	20	-	20	-	
80F/0/10/10	80	10	-	10	-	Moderate resistivity; relatively inert
60F/10/10/10/10	60	10	10	10	10	Low-melting, "long" slag
0F/50/0/50	-	50	-	50	-	Difficult starting; electrically efficient

Tab. 5.1 Compositions of slags commonly used in ESR

5.4.6 Electroslag remelting pool details

Figure 5.24 schematically illustrates the features of a molten pool in an ESR ingot. As in the VAR pool schematic, the relative sizes of annulus and immersion are not to scale. The most important feature shown is the depth of the molten pool. (It will be recalled that the depth and angle of the liquid + solid zone controls freckle formation for any given alloy.) Compared to VAR, very few studies have been done on the nature of the molten pool in ESR. The pool differs fundamentally from a VAR pool in that the molten slag cap provides a source of heat to the system. and the slag skin on the solidifying ingot provides insulation, reducing heat extraction.

Consequently, for comparable melt rates and crucible diameters, an ESR ingot will have a deeper, steeper-sided pool. Thus, compared to VAR, ESR ingots have traditionally been regarded as being more prone to the formation of positive segregation effects. It must be supposed that thermal gradients, similar to those in a VAR pool, are also present in the

ESR pool. However, the nature of the electromagnetic currents has not been identified, to date, in any publications.

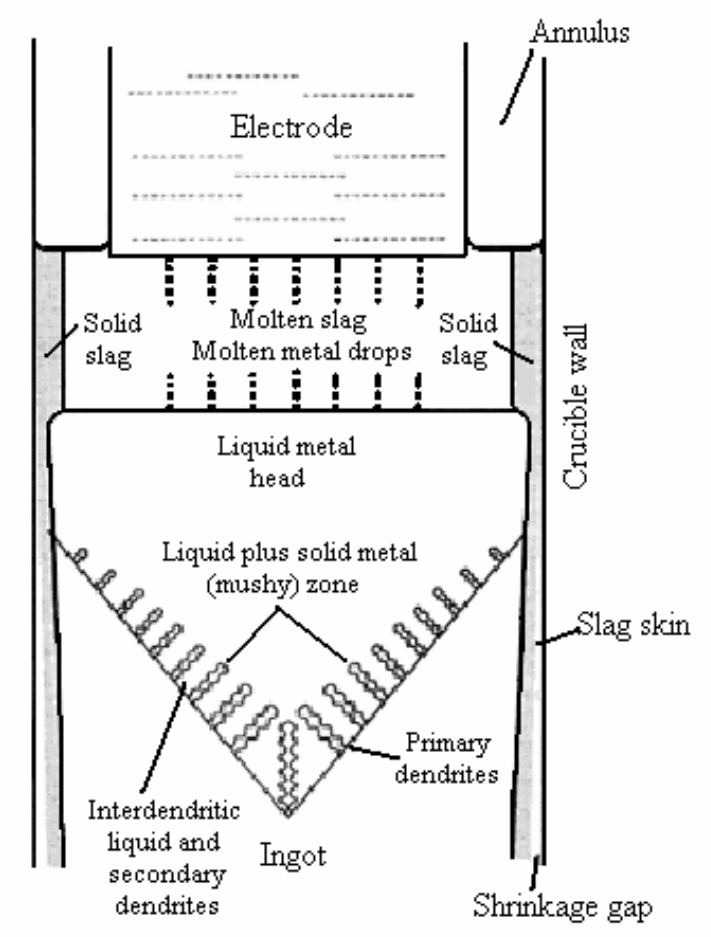

Fig. 5.24 Longitudinal schematic of the structure developed in an ESR ingot during melting

While the shape of an ESR pool may inherently be more prone to positive segregation, that shape may be altered by judicious choice of melting parameters. It is possible to produce a U-shaped pool in ESR that is very similar to that in VAR. For alloy systems that are highly alloyed but have only moderate freckle-forming tendencies, ESR processes can be made sufficiently robust that they can be used for critical rotating components without undue concern for the presence of positive segregation effects.

The thermodynamics of solidification of an ESR ingot are the same as in the VAR process (see the section "Vacuum Arc Remelting (VAR)" in this article). The solidification

structure of an ingot of a given composition is a function of the solidification rate and temperature gradient at the solid/liquid interface. For example, when remelting with a consumable electrode in a water-cooled copper mold, the solidification rate is constant because of the constant heat transfer through the cooling water; therefore, a relatively high temperature gradient at the solidification front must be maintained during the entire remelting period to achieve a directional dendritic structure.

Even in the case of directional dendritic solidification, the microsegregations increase with increasing dendrite arm spacing. For optimum results, the objective should be a solidification structure with dendrites oriented as close to parallel to the ingot axis as possible. However, this is not always possible. To achieve a good ingot surface, there is a minimum energy requirement, and therefore a minimum melting rate, which is a function of ingot diameter. This means that the melting rate for large diameter ingots cannot be maintained for axis-parallel dendrite growth. Figure 5.17 in the section "Vacuum Arc Remelting (VAR)" in this article shows the melting rates for different steels and alloys as a function of ingot diameter. The data are empirical values obtained from experience in operation. These melting rates resulted in low microsegregation while achieving reasonably good surface quality.

5.4.7 Melt-related defects in ESR

5.4.7.1 Introduction

In Fig. 5.24, the schematic for the edge of a solidifying ingot indicates a processing advantage for ESR that has made it desirable to develop this process for use in critical components. The insulating nature of the slag creates conditions at the edge of the ingot that do not produce shelf.

Thus, with no arc instabilities of concern and no shelf to be undercut, the formation of discrete white spots in ESR product could only occur by some infrequent occurrence, such as drop in of pieces from an unsound electrode.

5.4.7.2 Positive segregation

Alloys that have high-density interdendritic liquids may form unique structures in ESR. The high-density liquid tends to flow downhill toward the center of the ingot.

Although channel defects may not be formed, large pools of high-solute alloy may be formed. These regions may form in widely separated parts of an ingot and be separated by "normal" material. Because of the greater number of variables inherent in ESR, the underlying causes for such segregation have not been determined. The nature of these areas and their effect on properties have not been reported.

5.4.7.3 Electroslag remelting ingot surface

The interaction of the molten metal with the slag cap should be understood. with regard to obtaining good surface on ESR ingots. As shown in Fig. 5.24, the molten slag solidifies against the water-cooled crucible side just as the molten metal would. The molten metal pool, in addition to being V-shaped (containing the mushy zone), also contains a fully molten straight-sided component or metal head. The metal head remelts some of the solidifed slag on the crucible wall, so a thinner layer is then contained between the ingot the crucible wall. Should this slag skin be locally penetrated by the metal head, a thin stream of metal will be driven through the hole. Such a metal fin or bleedout is illustrated in Fig. 5.25. Note that the penetration of the slag is through a circular region that is essentially the size of a dime. The molten metal not only moves down the ingot surface in response to gravity, but is forced upward from the penetration due to the combined hydrostatic pressure of the molten metal head and the molten slag cap. Bleedout formation is sensitive to melting conditions and slag composition. While there is no published association of bleedouts with detrimental structure, there is an economic factor involved, in that an ingot with bleedouts will require grinding prior to forging or other hot working.

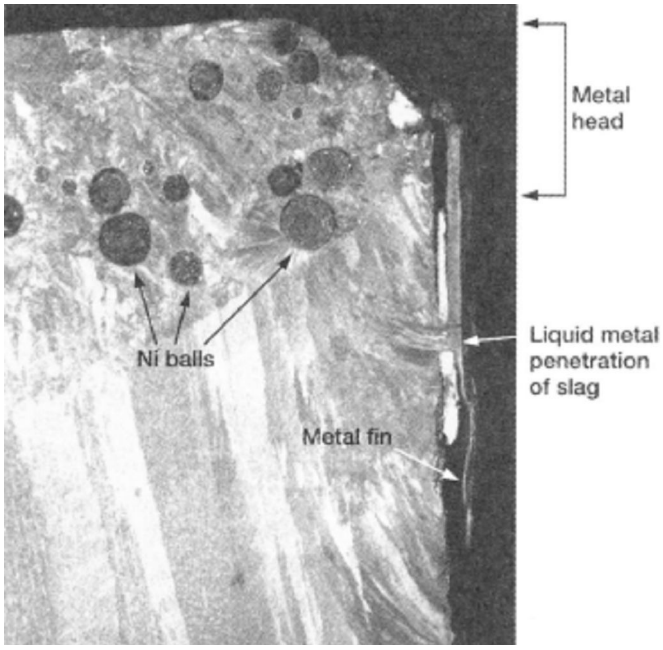

Fig, 5.25 Longitudinal section through a metal fin formed by a bleedout on the surface of an ESR ingot.

Chapter 6

Hot rolling

6.1 History of rolling

Although the basic concepts associated with hot rolling have not, in general, changed appreciably since the last century, mills have become considerably larger, faster, more powerful and capable of rolling products of larger sizes to closer dimensional tolerances and improved surface finishes. Contributing to this situation are improved mill components, including rolls, housing, drive motors, instrumentation and control systems, which have resulted from the impressive advances made in the engineering sciences during the twentieth century. Paralleling these advances has been a better theoretical understanding of rolling technology developed in various industrial and governmental research laboratories throughout the world. In addition, it should be noted that hot rolling is not only used for shaping purposes but is now used to obtain the desired metallurgical properties in the rolled product (controlled rolling), for the cladding of various metals to steel and to impart desired surface finishes, particularly in the case of flat-rolled materials.

With respect to flat-rolling equipment, the conventional four-high mill stand with its d-c motor drive has continued to demonstrate the soundness of its basic design in spite of the advent of mills of unconventional design, such as planetary and six-high mills. Though the arrangement of the rolls in a four-high mill has remained unchanged, such mills have increased in physical size and drive power. For example, plate mill widths have increased to 5.5m, work-roll diameters up to 1.2m, backup-roll diameters up to 239cm and drive powers up to 17.89MW (24000hp) with the electrical power supplied nowadays by silicon-controlled rectifiers instead. of motor-generator sets. In addition, modern tandem rolling-miI1 trains utilize an increased number of mill stands.

The conventional mill housing is, however, slowly being changed. Screws are being gradually replaced by hydraulic roll-positioning systems which respond much more rapidly than screws to automatic-gage-control (AGC) signals and provide adjustable mill stiffness.

Moreover, roll-balance and roll-bending jacks are now being incorporated in the mill housing rather than in the individual roll chocks.

With the availability of electronic computers, the control of rolling mills has become more and more sophisticated. Programmed with mathematical models of the rolling process, computers are now being used to control the pacing and set-up of hot mills and the cross-sectional profile and shape of hot-roll-ed strip.

In recent years the direct rolling of hot workpieces, such as slabs, has been practiced as a method of conserving energy and increasing yield.

A further development along these lines has been the in-line rolling of continuously cast billet and slab strands. Nucor Corporation has built a system linking a billet casting machine to a bar mill in which the rolling speed is varied to match the throughput of the caster and a similar system connecting a rotary caster to a billet mill has been developed in Japan.

Around mid-century, the typical hot-strip mill then being built utilized two or three reheat furnaces, a scale-breaker, four or five roughing stands, a second scale-breaker, a six-stand finishing train and two coilers at the end of a run-out table. Such mills could produce from about 1.5 to 2.5 million tons of hot-rolled strip per year. To meet increased production requirements, the "Generation II" hot strip mill of the 1960rs, as exemplified by U.S. Steel's 2.15m facility at its.

Gary Works, features four slab-reheat furnaces of the five-zone type, a vertical edger, a horizontal scale-breaker, three individual roughers, a two-stand tandem-roughing mill, a finish scale-breaker, seven finishing stands and three coilers. The main drives associated with the mill are rated at 92MW (123,500hp) and the auxiliary drives and other equipment are rated at an additional 55.56MW (74,500hp). This facility has a capacity in excess of 3.5 million tons per year.

Not only is the hot-strip mill of today more productive, it is virtually under complete computer control. Slabs may be charged. And discharged from the reheat furnaces as dictated by the computer and the finishing train, the cooling system on the run-out table and the coilers are all automatically controlled to provide the desired finishing and coiling temperatures.

In the operation of such mills, a number of distinct advances have been made. The cast-iron and steel work rolls originally used are giving way to rolls of improved resistance to wear and firecracking, such as high chromium and centrifugally cast rolls. Moreover, rolling lubricants are becoming more extensively used on the finishing trains of hot-strip mills to minimize rolling force and power requirements, to extend the life of the mill rolls and to enhance the surface quality of the rolled strip. In addition, many mills feature either work- or backup-roll-bending systems to control the flatness of the rolled strip. Furthermore, during the last decade, cooling of the rolled strip on the run-out table has been accomplished more efficiently by the so-called "laminar-flow" low-pressure technique rather than by conventional high-pressure water sprays.

An interesting innovation incorporated in a new hot-strip mill recently commissioned by John Lysaght (Australia) Ltd. is a coil box located after the last rougher for temporarily storing the partially rolled bar in coiled form prior to finishing. This feature enables the length of the holding table ahead of the finishing train to be decreased in length, thereby reducing the overall length of the mill and the capital cost associated with its installation.

Controlled rolling on plate mills involves rolling at lower than normal temperatures so that a smaller grain size at ambient temperature is achieved in the rolled microstructure. As a consequence of the smaller grain size, the yield strength and toughness of the rolled product are usually significantly improved. However, these qualities are generally attained only with higher rolling forces, delays in processing so as to achieve lower temperatures for the final pass, and greater difficulties in obtaining flatness and proper cross-sectional profiles in the rolled workpieces .

In the rolling of structural steel there has been a trend towards increased lengths of workpieces through the use of continuous and semi- continuous mills and the use of subsequent cold sawing. Cooling beds have been built to accept beams 76.2m long and highly automated warehousing is practiced.

Bar mills have generally resisted attempts at sophisticated control and precise measuring devices were found to be unreliable due to the harsh environment. However, there have been considerable mechanical improvements to bar mills with better-controlled, higher-

speed drives. A completely new concept in bar rolling has been developed by Schloemann-Siemag. This is the three-roll planetary mill designed to make large reductions (up to 92 per cent) in a single pass as discussed in Section 7-8. Another recent innovation in bar mill design has been the use of two 3-high roughing stands in tandem with individual gear drives coupled to non-reversing a-c motors.

Rolling of metals is perhaps the most important metalworking process. More than 90% of all the steel, aluminum, and copper produced in 1985, some 800 million tons of material worldwide go through the rolling process at least one time. Thus, rolled products represent a significant portion of the manufacturing economy and can be found in many sectors. Beams and columns used in buildings are rolled from steel. Railroad tracks and cars are made from rolled steel, and airplane bodies are made from rolled aluminum and titanium alloys. The wire used in fences, elevator ropes, electrical conductors, and cables are drawn from rolled rods. Many consumer items, including automobiles, home appliances, kitchen utensils, and beverage cans, use rolled sheet materials.

In rolling, a squeezing type of deformation is accomplished by using two work rolls (*fig. 6.1*) rotating in opposite directions. The principal advantage of rolling lies in its ability to produce desired shapes from relatively large pieces of metals at very high speeds in a somewhat continuous manner. Because other methods of metalworking, such as forging, are relatively slow, most ingots and large blooms are rolled into billets, bars, structural shapes, rods (for drawing into wire), and rounds for making seamless tubing. Steel slabs are rolled into plate and sheet.

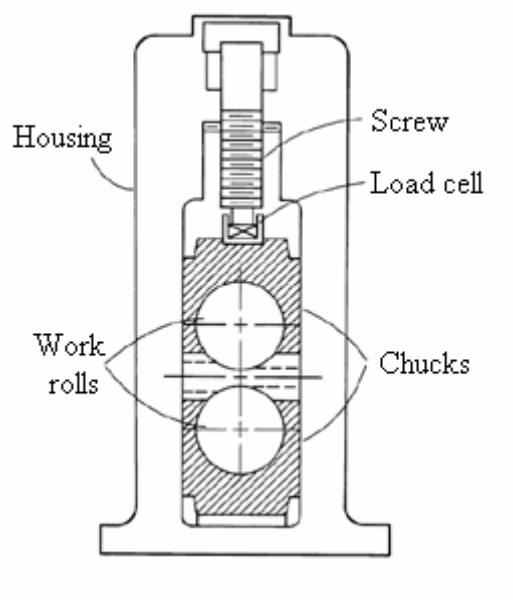

Fig. 6.1 Typical rolling mill stand

Although the rolling of metals has been done for some time and has been a very productive means of working large quantities of metals to a variety of shapes and sizes, the state of the technology had been somewhat stagnant until recently, when major innovations started to appear. With the advent of computer-assisted controls, highly automated, very high-speed rolling mills were installed beginning in the 1970s. One rod mill commissioned in 1980, for example, is reported to roll steel wire rod at the rate of 335 km/h. This mill has a rated output of 545,000 Mg (600,000 tons) per year, and the entire mill is operated from three climate-controlled pulpits equipped with computerized controls and closed-circuit video monitors. Another modern mill came on stream in the early 1980s. It is a 200 cm hot strip mill capable of producing steel coils up to 1,88m wide and weighing up to 33.6 Mg (37 tons). The mill features computer controls that automatically adjust water flow rates, roll speeds, and strip temperatures to meet metallurgical requirements. In addition to these developments, computer-aided modeling of the rolling process is now routinely used at several locations for design of rolls and optimization of the process parameters (see the section "Mechanics of Plate Rolling" in this article). Understanding of the materials also has improved considerably, thereby permitting development of new products such as high-

strength low-alloy (HSLA) steels, which require controlled rolling. In short, significant developments are happening in this field, which was largely neglected for decades.

6.2 Basic rolling processes

Many engineering metals, such as aluminum alloys, copper alloys, and steels, are often cast into ingots and are then further processed by hot rolling into blooms, slabs, and billets, which are subsequently rolled into other products such as plate, sheet, tube, rod, bar, and structural shapes (*fig.6.2*). The definitions of these terms are rather loose and are based on the traditional terminology used in the primary metal industry. For example, a bloom has a nearly square cross section with an area larger than 205 cm^2; the minimum cross section of a billet is about 38 × 38 mm, and a slab is a hot-rolled ingot with a cross-sectional area greater than 103 cm^2 and a section width of at least twice the section thickness. Plates are generally thicker than 6.4 mm, whereas sheets are thinner-gage materials with very large width-to-thickness ratios. Sheet material with a thickness of a few thousandths of an inch is referred to as foil.

Rolling of blooms, slabs, billets, plates, and structural shapes is usually done at temperatures above the recrystallization temperature, that is, in the hot-forming range, where large reductions in height or thickness are possible with moderate forming pressures. Sheet and strip often are rolled cold in order to maintain close thickness tolerances.

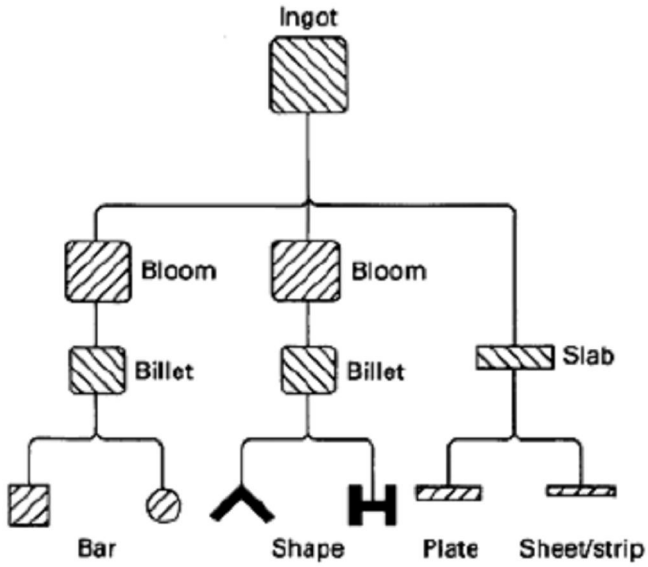

Fig. 6.2 Rolling sequence for fabrication of bars, shapes, and flat products from blooms, billets, and slabs

The primary objectives of the rolling process are to reduce the

cross section of the incoming material while improving its properties and to obtain the desired section at the exit from the rolls. The process can be carried out hot, warm, or cold, depending on the application and the material involved. The technical literature on rolling technology, equipment, and theory is extensive because of the significance of the process. Many industrial investigators prefer to divide rolling into cold and hot rolling processes. From a fundamental point of view, however, it is more appropriate to classify rolling processes on the bases of the complexity of metal flow during the process and the geometry of the rolled product. Thus, the rolling of solid sections can be divided into the categories below.

- *Uniform Reduction in Thickness with No Change in Width.* This is the case with strip, sheet, or foil rolling where the deformation is in plane strain, that is, in the directions of rolling and sheet thickness. This type of metal flow exists when the width of the deformation zone is at least 20 times the length of that zone.
- *Uniform Reduction in Thickness with an Increase in Width.* This type of deformation occurs in the rolling of blooms, slabs, and thick plates. The material is elongated in the rolling (longitudinal) direction, is spread in the width (transverse) direction, and is compressed uniformly in the thickness direction.
- *Moderately Nonuniform Reduction in Cross Section.* In this case, the reduction in the thickness direction is not uniform. The metal is elongated in the rolling direction, is spread in the width direction, and is reduced nonuniformly in the thickness direction. Along the width, metal flow occurs only toward the edges of the section. The rolling of an oval section in rod rolling or of an airfoil section would be considered to be in this category.
- *Highly Nonuniform Reduction in Cross Section.* In this type of deformation, the reduction in the thickness direction is highly nonuniform. A portion of the rolled section is reduced in thickness while other portions may be extruded or increased in thickness. As a result, in the width (lateral) direction metal flow may be toward the center. Of course, in addition, the metal flows in the thickness direction as well as in the rolling (longitudinal) direction. The above discussion illustrates that, except

in strip rolling, metal flow in rolling is in three dimensions (in the thickness, width and rolling directions). Determinations of metal flow and rolling stresses in shape rolling are very important in designing rolling mills and in setting up efficient production operations. However, the theoretical prediction of metal flow in such complex cases is nearly impossible at this time. Numerical techniques are being developed in an attempt to simulate metal flow in such complex rolling operations.

6.3 The basic principles of rolling and pass design introduction

In order to better understand the various types of hot mills described in the following chapters, it is desirable to first consider some of the basic principles involved in the rolling of all types of products, both flat and nonflat. Although plastic flow should be stated at the outset that, although considerable study has been made of the hot-rolling process, there is not yet a universally accepted understanding of it. For example, the older rolling theorists considered sticking friction to occur at the roll and workpiece interfaces with an effective coefficient of friction close to 0.57. However, the presence of scale on workpiece surfaces make such an assumption unrealistic as has been confirmed by recent investigations. Moreover, the behavior of hot steel as it undergoes deformation and its subsequent recrystallization have not yet been adequately researched.

As in so many other fields of technology, the practice of ho trolling has outstripped our theoretical understanding of it. This is particularly so in the case of pass designs which have been in use for the best part of two centuries. Computer programs have been developed for optimizing passes but such programs are largely based on empirical data and practical experience. Accordingly, roll-pass design has been treated as an art rather than a science. The roll-pass designs presented in this chapter, though satisfactory for the circumstances under which they were used may have to be modified if used for different steel grades and different rolling temperatures.

6.3.1 The plastic deformation of a workpiece between two platens

Before examining the process of rolling, it is first pertinent to consider a cube of plastic material, such as steel at a hot-rolling temperature, compressed between two platens as illustrated in figure 6.3.

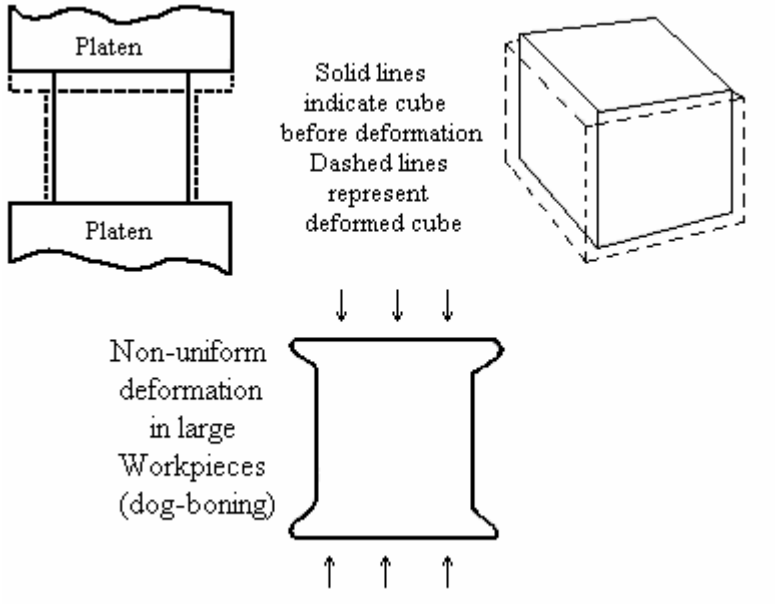

Fig. 6.3 Sketches illustrating the deformation of a plastic workpiece

If the platens are such that there is no friction at the interface between the cubical workpiece and the platens, and the workpiece is small, then when a pressure in excess of the flow stress of the workpiece is reached, the workpiece will decrease in thickness and increase equally in the other two directions maintaining, to all intents and purposes, the same total volume. If the cube is relatively large, however, the top and bottom surfaces of the workpiece will tend to flow more than the center, as illustrated in figure 6.3. This effect is seen in the rounding of the heads of tools, such as chisels, under repeated hammer blows and is of importance with respect to the distortion introduced in such processes as edge rolling, when the cross-section of a slab or bar tends to assume a "dog-bone" shape.

The pressure exerted by each frictionless platen throughout the area of contact is constant, as illustrated by figure 6.4, this pressure being equal to the flow stress. The energy of deformation per unit volume may be shown to be

$$s \cdot \ln\left(\frac{1}{1-r}\right)$$

where *s* is the flow stress and *r* is the reduction given to the workpiece in terms of the ratio of the change in its height to its original height. In the case where friction exists between the platens and the workpiece, two important effects are to be observed.

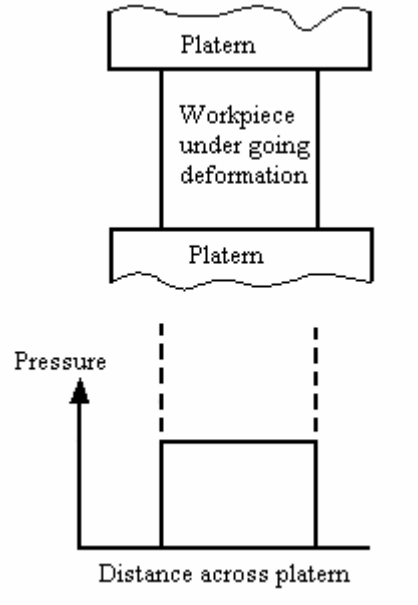

Fig. 6.4 Pressure distribution across face of cube under frictionless conditions.

First, the pressure across the region of contact with each platen is not constant but increases towards the center of the contact area in an exponential manner, as indicated in figure 6.5, this type of pressure distribution often being referred to as a "friction hill".

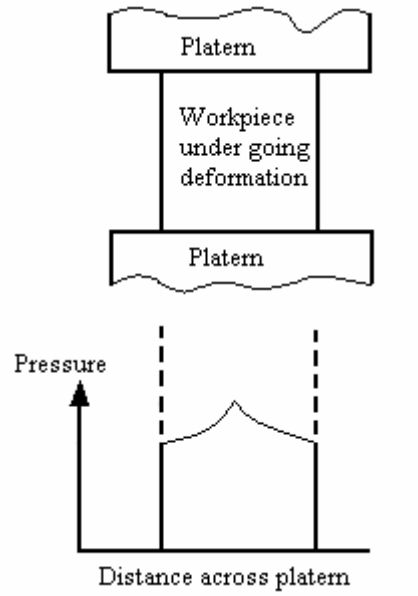

Fig. 6.5 Pressure distribution across face of workpiece in the presence of friction

The greater the coefficient of friction, the higher is the "hill". Thus the total deforming force, which corresponds to the volume under the pressure surface, increases with increasing friction. Second, the deformation of a small workpiece is no longer uniform throughout its thickness. Instead, the workpiece develops rounded edges as shown in figure 6.6; the greater the friction' the more extensive the bowing or "barrelling" becomes. In addition, the energy of deformation per unit volume now exceeds

$$s \cdot \ln\left(\frac{1}{1-r}\right)$$

to an extent depending on the geometry of the workpiece, the extent of its deformation and the magnitude of the coefficient of friction. In effect, therefore, friction appears to increase the flow stress of the piece.

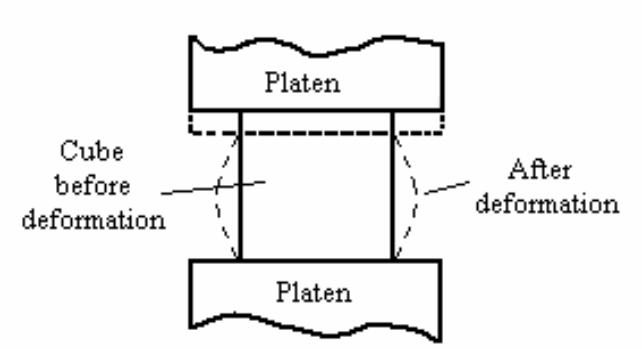

Fig. 6.6 Barrelling of a workpiece as a result of deformation under frictional conditions

It is now of interest to consider the case where the workpiece is restrained from flowing in one direction but can flow under frictionless conditions at right angles, as illustrated in figure 6.7. The pressure is again uniform across the area of contact but assumes a value close to 15.5 per cent higher than the unrestrained flow stress of the piece.

This value is known as the constrained compressive yield stress and the energy of deformation per unit volume therefore assumes the value of :

$$1.155 \cdot s \cdot \ln\left(\frac{1}{1-r}\right)$$

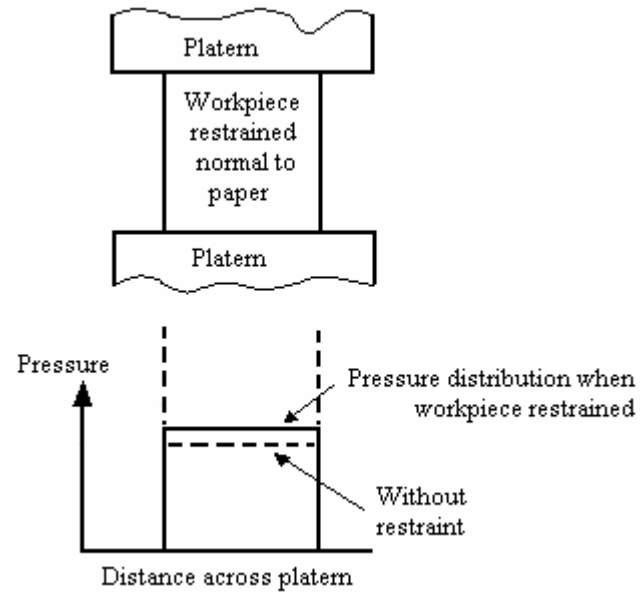

Fig. 6.7 Pressure distribution when workpiece is restrained in one direction but in the absence of friction

When the expanding flow of the workpiece is restricted to one dimension, as discussed above, and friction occurs to impede this f1ow, the pressure distribution again assumes the

form of a friction hill, as indicated in figure 6.8, with the height of the hill being influenced by the magnitude of the coefficient of friction and the geometry of the workpiece.

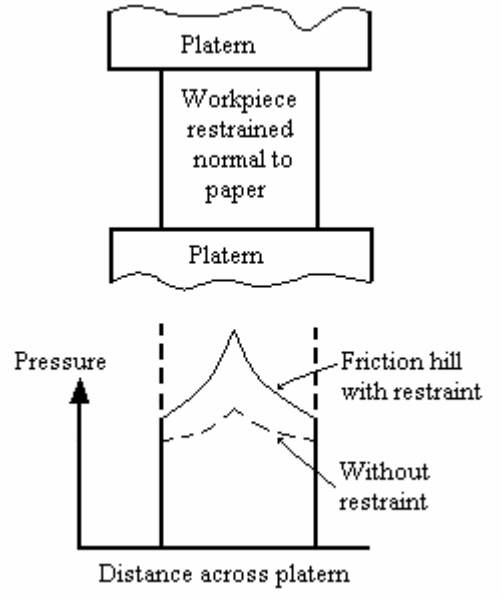

Fig. 6.8 Pressure distribution with friction and restraint

6.3.2 The effect of tensile stresses on the deformation process

If the workpiece, as it is being deformed by compressive stress under frictionless conditions, is subject to tensile stresses in the other two directions, as illustrated in figure 6.9 , the compressive stress required to deform the workpiece becomes less than its flow stress.

If the tensile stresses are s_1 and s_2 where $s_1 > s_2$ then the compressive stress s_p required for deformation is, on the basis of the maximum shear theory of Tresca, given by

$$s_p = s - s_1$$

Where s is the normal flow stress. This pressure s_p is exerted uniformly across the area of contact as illustrated in figure 6.9. However, the total energy of deformation per unit volume is unaffected by the magnitude of the tensile stresses.

If friction exists, then a friction hill again occurs. However, the bottom of each slope corresponds to the frictionless flow stress s_p so that the total deforming force is now determined not only by the coefficient of friction and the workpiece geometry but also by

the tensile stress exerted on the workpiece. The total energy of deformation is, however, virtually unaffected by the tensile stress.

In the case where lateral flow of the workpiece is prevented., the minimum compressive stress at the bottom of each slope of the friction hill is now equal to $1.155 \cdot s - s_1$

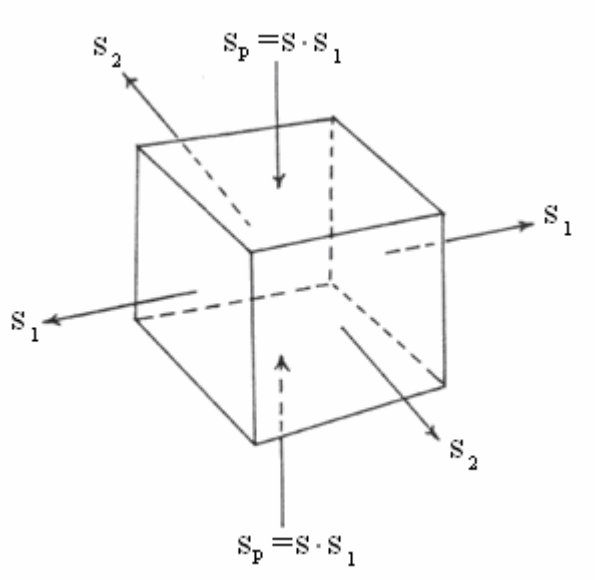

Fig. 6.9 Sketch showing application of tensile stress to workplace

6.3.3 The deformation of a workpiece of rectangular cross section in a roll bite

Some of the basic principles involved in the plastic deformation of a workpiece between two platens may be applied to the rolling process. However, it is important to remember that rolling more closely resembles extrusion than forging since, in rolling, frictional effects drag the workpiece into the roll bite and force it out through the narrower end of the bite. In the absence of any tensile stresses in the workpiece and friction between the rolls and the workpiece, rolling would not be possible since deformation energy could not be transferred from the rotating rolls to the workpiece. On the other hand, forging could theoretically be carried out with frictionless platens because energy could be imparted by the translational movement of the platens relative to each other.

When a relatively wide workpiece is deformed between two plain work rolls, its flow is mainly restricted to the direction of rolling. Thus there is a lateral constraint applied to the workpiece (except near its edges) so that, in the absence of any tensile stresses, the minimum deformation pressure exerted by the rolls at the entry end of the bite is equal to 1.155 times the flow stress. In the presence of friction (and generally in nonlubricated. hot rolling the coefficient of friction lies in the range 0.2 to 0.5), the rolling force is increased by the friction hill as indicated in figure 6.10. In primary mills, the friction must often be increased by ragging or knurling the roll surfaces.

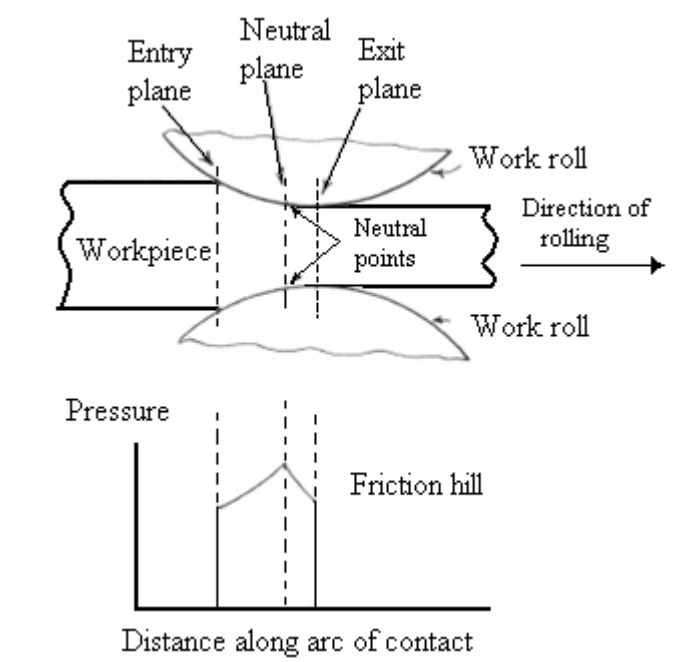

Fig. 6.10 Sketch of roll bite showing neutral plane and pressure distribution along the arc of contact.

The presence of horizontal tensile stresses in the workpiece decreases the rolling force in that it decreases the minimum deformation pressure exerted by the rolls (corresponding to the lower ends of the friction hill). In hot rolling, however, tensile stresses are usually created by adjacent roll stands acting on the same workpiece as it is processed in a continuous mill. Such stresses must not be very large or they will cause necking or a reduction in the cross-sectional area of the workpiece.

In the case of a narrow workpiece, sideways spread may be significant. The greater the friction or the greater the work-roll diameter, the greater the sideways spread. However, it must be remembered that the mass flow of the workpiece entering a roll bite is equal to that leaving it. Thus a fractional increase in the speed of the workpiece created by a rolling process corresponds to the fractional decrease in the cross-sectional area of the piece. Thus if v_1 and v_2 denote the workpiece speed entering and leaving a mill stand and r is the reduction in the cross-sectional area (expressed as a decimal fraction), then

$$v_2 = \frac{v_1}{1-r}$$

While the peripheral speed of a work roll in a mill stand remains constant, the surface speed of a point on the surface of the workpiece increases as it passes through the bite until usually on exit from the bite, it exceeds the speed of the rolls. The workpiece is then said to exhibit forward slip.

Along the arc of contact r or the common interface between each roll and the workpiece, there is a position where the roll and workpiece surface speeds are equal. This position is known as the neutral point. In the case of a rolling operation symmetrical with respect to the passline, the neutral points on each arc of contact lie in a vertical neutral planer ds indicated in figure 6.10. The position of a neutral point is dependent on a number of factors including the coefficient of friction along the arc of contact, the entry and exit tensile stresses in the workpiece and the work-roll diameter. Decreasing the coefficient of friction, reducing the work-roll diameter, increasing the entry tension and decreasing the exit tension all tend to move the neutral point towards the exit plane and thereby decrease the forward slip.

6.4 Strip rolling theory

The most rigorous analysis was performed by Orowan and has been applied and computerized by various investigators. More recent studies consider elastic flattening of the rolls and temperature conditions that exist in rolling. The roll-separating force and the roll torque can be estimated with various levels of approximations by such mathematical

techniques as the slab method, the upper bound method, or the slip line method of analysis. Most recently, computerized numerical techniques are being used to estimate metal flow, stresses, roll-separating force, temperatures, and elastic deflection of the rolls.

6.4.1 Simplified method for estimating roll-separating force

The strip-rolling process is illustrated in figure 6.11. Because of volume constancy, the following relations hold:

$W \cdot H_0 \cdot V_0 = W \cdot H \cdot V = W \cdot H_1 \cdot V_1$ **(Eq 1)**

where W is the width of the strip; H_0, H, and H_1 are the thicknesses at the entrance, in the deformation zone, and at the exit, respectively; and V_0, V, and V_1 are the velocities at the entrance, in the deformation zone, and at the exit, respectively. In order to satisfy *Eq 1*. the exit velocity V_1 must be larger than the entrance velocity V_0. Therefore, the velocity of the deforming material in the x or rolling direction must steadily increase from entrance to exit. At only one point along the roll-strip interface is the surface velocity of the roll, V_R, equal to the velocity of the strip. This point is called the neutral point, or neutral plane, indicated by N in figure 6.11.

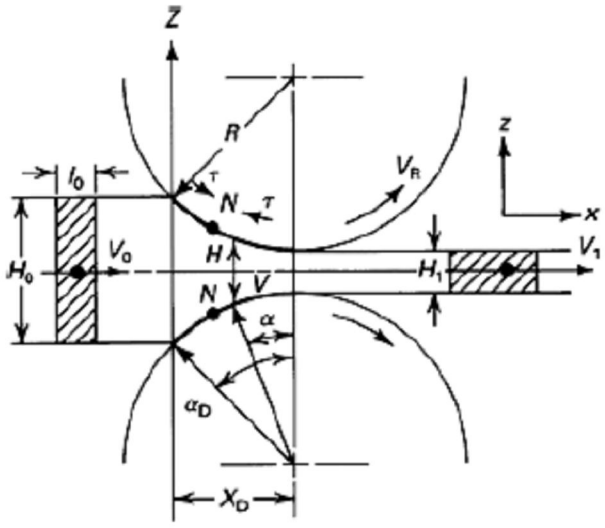

Fig. 6.11 Representation of strip rolling. The strip width w is constant in the y (width) direction.

The interface frictional stresses are directed from the entrance and exit planes toward the neutral plane because the relative velocity between the roll surface and the strip changes its

direction at the neutral plane. This will be considered later in estimating rolling stresses. An approximate value for the roll-separating force can be obtained by approximating the deformation zone, shown in figure 6.11, with the homogeneous plane-strain upsetting process. With this assumption, *Eq 2* is valid, that is, the load per unit width of the strip is given by:

$$L = \frac{2\sigma}{\sqrt{3}} \cdot \left(1 + \frac{m \cdot l}{4h}\right) \cdot l \qquad \textbf{(Eq 2)}$$

However, in this case the following approximations must be made:

- Average strip height $h = 0.5(H_0 + H_1)$
- Average length of the deforming strip $l = R \cdot \alpha_D$, with $\cos\alpha_D = 1-(H_0 - H_1) \cdot 2R$ *i*n the literature, it is often recommended that the value of the projection of strip length X_D (figure 6.11) be used for *l;* however, considering the effect of friction on the roll-strip interface length, $R \cdot \alpha_D$, it is more appropriate to use $l = R \cdot \alpha_D$

To estimate average flow stress $\sigma(\varepsilon, \dot{\varepsilon}, \theta)$ at a given rolling temperature θ, the average strain ε is obtained from the thickness reduction, that is, $\varepsilon = \ln\left(\frac{H_0}{H_1}\right)$

The strain rate is given by:

$$\dot{\varepsilon} \cdot \alpha = \frac{V_z}{H} = 2V_R \cdot \sin\left(\frac{\alpha}{H}\right) = \frac{2V_R \cdot \sin\alpha}{H_1 + 2R \cdot (1 - \cos\alpha)} \qquad \textbf{(Eq 3)}$$

where *Vz* is the velocity at a given plane in the *z* direction (see figure 6.11), *H* is the thickness at a given plane (roll angle) in the deformation zone, and V_R is the roll surface velocity. At the entrance plane:

$V_z = 2V_R \cdot \sin\alpha_D$ e $H = H_0$

At the exit plane:

$H = H_1$ e $V_z = 0$

A more accurate value can be obtained by calculating an integrated average of (*Eq 3*) throughout the deformation zone. Then, an average approximate value is:

$$\dot{\varepsilon} = \frac{V_R}{H_0} \cdot \sqrt{\frac{2 \cdot (H_0 - H_1)}{R}} \qquad \textbf{(Eq 4)}$$

6.4.2 The stress distribution

The stress (roll pressure) distribution in strip rolling is illustrated in figure 6.12. The maximum stress is at the neutral plane *N*. These stresses increase with increasing friction and length of the deformation zone X_D. Tensile stresses applied to the strip at entrance or exit have the effect of reducing the maximum stress (by an amount approximately equal to *z* in figure 6.12b) and shifting the position of the neutral plane. The analogy to plane-strain upsetting is illustrated in figure. 6.12(a).

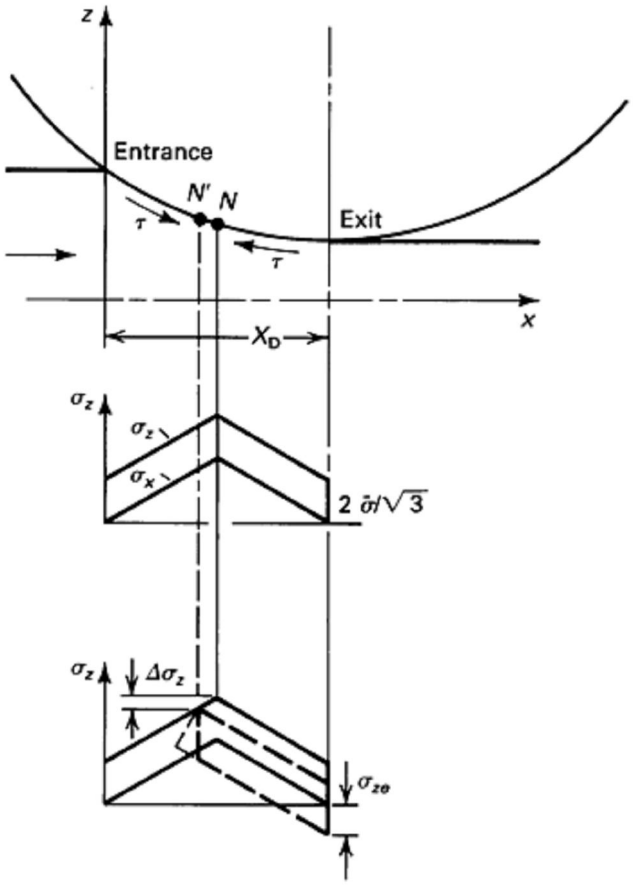

Fig. 6.12 Stress distribution in rolling. (a) With no tensile stresses at entry or exit. (b) With tensile stress σ_{ze} at exit.

The stress distribution can be calculated by using the equations derived in most textbooks or by following the theory presented by Orowan. However, these calculations are quite complex and require numerical techniques in order to avoid an excessive number of simplifying assumptions.

For a numerical/computerized calculation of rolling stresses, the deformation zone can be divided into an arbitrary number of elements with flat, inclined surfaces (figure 6.13). The element, illustrated in this figure, is located between the neutral and exit planes because the frictional stress τ is acting against the direction of metal flow. When this element is located between the entrance and neutral planes, τ acts in the direction of metal flow. The stress distribution within this element can be obtained by use of the slab method, as applied to plane-strain upsetting:

$$\sigma_z = \frac{K_2}{K_1} \cdot \ln\left(\frac{h_1}{h_o + K_1 \cdot X}\right) + \sigma_{Z1} \qquad \textbf{(Eq 5)}$$

where

$$K_1 = -2 \cdot \tan\alpha \qquad \textbf{(Eq 6)}$$

$$K_2 = \frac{-2\sigma K_1}{\sqrt{3}} + 2\tau \cdot \left(1 + \tan^2\alpha\right) \qquad \textbf{(Eq 7)}$$

$$\tau = \frac{m \cdot \sigma}{\sqrt{3}} \qquad \textbf{(Eq 8)}$$

Following figure 6.13, for $x = \Delta x$, $h_0 + K_1 x = h_1$, and therefore *Eq 5* gives $\sigma_z = \sigma_{z1}$, the boundary condition at $x = \Delta x$, which is known. For $x = 0$:

$$\sigma_z = \sigma_{z0} = \frac{K_2}{K_1} \cdot \ln\left(\frac{h_1}{h_o}\right) + \sigma_{Z1}$$

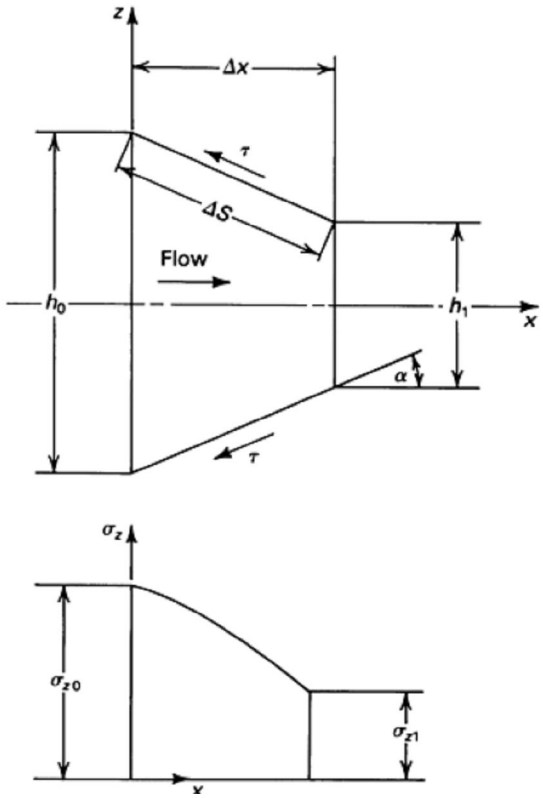

Fig. 6.13 Stresses in a deformation element used in computerized calculation of rolling stresses

If the element shown in figure 6.13 is located between the entrance and neutral planes, then the sign for the frictional shear stress must be reversed. Thus, *Eq 5* and *6* are still valid, but:

$$K_2 = \frac{-2\sigma}{\sqrt{3}} \cdot K_1 - 2\tau \cdot \left(1 + \tan^2 \alpha\right) \qquad \textbf{(Eq 9)}$$

In this case, the value of the boundary condition at $x = 0$, that is, z_0, is known, and z_1, can be determined from *Eq 6*:

$$\sigma_{z1} = \sigma_{z0} - \frac{K_2}{K_1} \cdot \ln\left(\frac{h_1}{h_o + K_1 \cdot \Delta x}\right) \qquad \textbf{(Eq 10)}$$

The stress boundary conditions at exit and entrance are known. Thus, to calculate the complete stress (roll pressure) distribution and to determine the location of the neutral plane, the length of the deformation zone X_D (see figure 6.11 and 6.12) is divided into *n*

deformation elements (figure 6.14). Each element is approximated by flat top and bottom surfaces (figure 6.13).

Starting from both ends of the deformation zone, that is, entrance and exit planes, the stresses are calculated for each element successively from one element to the next. The calculations are carried out simultaneously for both sides of the neutral plane. The location of the neutral plane is the location at which the stresses, calculated progressively from both exit and entrance sides, are equal. This procedure has been computerized and extensively used in cold and hot rolling of sheet, plane-strain forging of turbine blades and in rolling of plates and airfoil shapes.

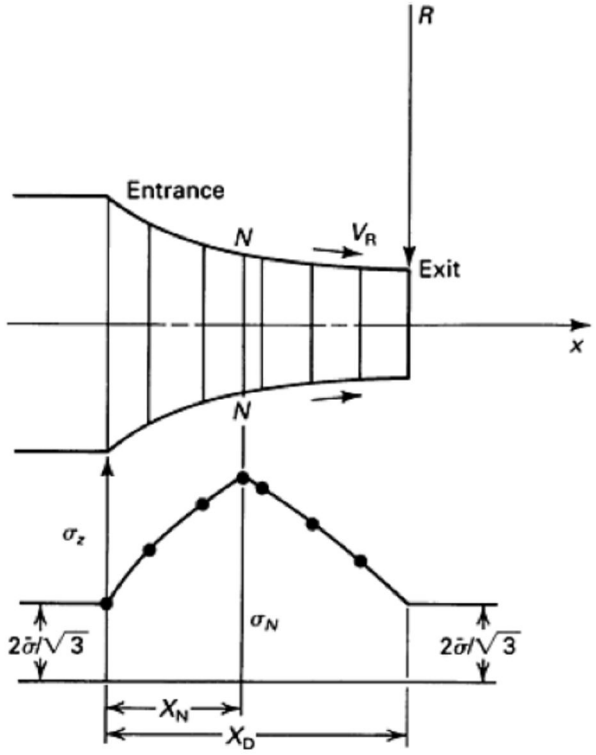

Fig. 6.14 Calculation of stress distribution by dividing the deformation zone into a number of tapered elements.

In this case, tensile stresses in the strip are zero at both entrance and exit.

6.4.3 Roll-separating force and torque

The integration of the stress distribution over the length of the deformation zone gives the total roll-separating force per unit width in strip rolling. In addition, the total torque is given by:

$$T = \int_0^{x_D} RdF \qquad \textbf{(Eq 11)}$$

where X_D is the length of the deformation zone (Fig. 6.14), R is roll radius, and F is the tangential force acting on the roll. Assuming that all energy is transmitted from the roll to the workpiece by frictional force:

$$dF = \tau dS \qquad \textbf{(Eq 12)}$$

In figure 6.13, it can be seen that:

$$dS = \frac{dx}{\cos\alpha} = \sqrt{1+\tan^2\alpha}\cdot dx \qquad \textbf{(Eq 13)}$$

In the deformation zone, the frictional force is in the rolling direction between entry and neutral planes. It changes direction between the neutral and exit planes. Thus, the total roll torque per unit width is:

$$T = R\cdot\tau\cdot\left[\int_0^{X_N}\left(1+\tan^2\alpha\right)dx - \int_{X_N}^{X_D}\left(1+\tan^2\alpha\right)dx\right] \qquad \textbf{(Eq 14)}$$

Where τ equals $m\sigma/\sqrt{3}$; R is roll radius; α is roll angle (figure 6.11); X_N is the x distance of the neutral plane from the entrance (figure 6.14); and X_D is the length of the deformation zone (figure 6.14).

6.4.4 Elastic deflection of rolls

During rolling of strip, especially at room temperature, a considerable amount of roll deflection and flattening may take place. In the width direction, the rolls are bent between the roll bearings, and a certain amount of crowning, or thickening of the strip, occurs at the center. This can be corrected by either grinding the rolls to a larger diameter at the center or by using backup rolls.

In the thickness direction, roll flattening causes the roll radius to "enlarge," increasing the contact length. There are several numerical methods for calculating the elastic deformation of the rolls. A method for approximate correction of the force and torque calculations for roll flattening entails replacement of the original roll radius *R* with a larger value *R*'. A value of *R*' is suggested by Hitchcock and is referred to extensively in the literature.

This is given as:

$$R' = R \cdot \left[1 + \frac{16 \cdot \left(1 - \nu^2\right) \cdot p}{\pi \cdot E \cdot \left(H_0 - H_1\right)} \right] \qquad \textbf{(Eq 15)}$$

Where ν is Poisson's ratio of the roll material, *p* is the average roll pressure, and *E* is the elastic modulus of the roll material.

It is obvious that *R*' and *p* influence each other. Therefore, a computerized iteration procedure is necessary for consideration of roll flattening in calculating rolling force or pressure. Thus, the value of *p* is calculated for the nominal roll radius *R*. Then *R*' is calculated from *Eq 15*. If $R'/R \neq 1$, the calculation of *p* is repeated with the new *R*' value, and so on, until *R*'/*R* has approximately the value of 1.

6.5 Various types of roll passes

In flat rolling, as in the case of plate and hot-strip mills, the work rolls are basically cylindrical. However, in nonflat rolling, the cross sectional geometry of the workpiece is established by the use of grooves cut into the pair of work rolls in each stand, these grooves being denoted as passes. Matching grooves made in both rolls of a set constitute an open pass, whereas a pass made by a projection on one roll fitting into a groove on the mating roll is called a closed or tongue-and-groove pass. Passes of various designs are illustrated in figure 6.15, the dotted lines showing the cross-section of the entering workpiece.

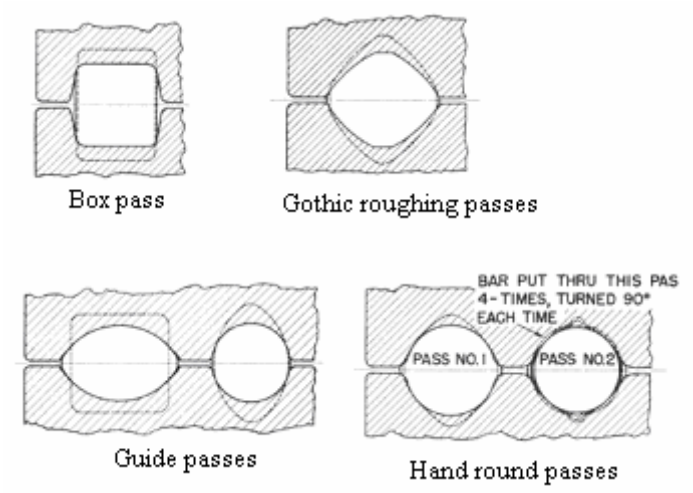

Fig. 6.15 Some common types of roll grooves or passes (dotted lines indicate cross-sections of entering pieces)

Where both sides of the material in a roll groove are in contact with a different roll, the groove is designated a "live" hole. On the other hand, where a deep groove is cut into one roll so that material entering the hole is influenced little by the other roll, such a groove is known as a "dead" hole.

Whereas in flat rolling the tangential speed is the same for each roll and very close to being constant across the roll face, in rolling with passes such cannot be the case. The bottom of a groove will exhibit a tangential speed less than a tongue so that forward slip will be different for different locations on the same cross-section. In non symmetrical passes, this can lead to a tendency for the workpiece to curl upwards or downwards, hence necessitating the use of stripper guides. Several other facts should be noted about the design of various passes. In a box pass, perfectly parallel sides would lead to their excessive wear and difficulty in extracting the workpiece from the pass.

In the case of the former, the cross-section of the workpiece will be less than desired and surface irregularities will result. On the other hand, overfilling will create fins or projections on the sides of the piece which, if excessive, may result in damaged rolls and/or bearings. However, it should be noted that, in the U.S.S.R., experiments have been conducted with lightly grooved or undulated rolls for the rolling of semi-finished tubes in an attempt to lessen the frequency of surface cracks.

6.6 Basic designs of primary mills

The two-high reversing mill, the operation of which is illustrated in figure 6.17, is the most commonly used type of primary mill. It exhibits maximum flexibility in size range of ingot and product as well as a wide range in the reduction and rolling speed to be executed for any given pass. However, it has a lower productivity than other mills of comparable size due to the necessary reversals of the mill.

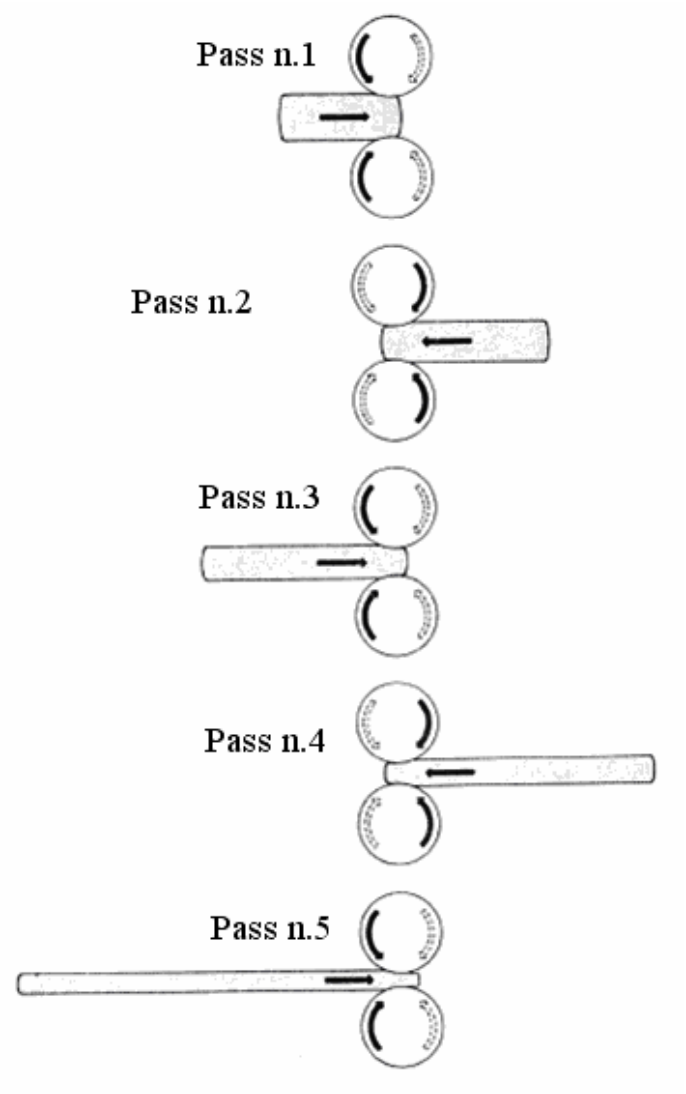

Fig. 6.18 Sequence of rolling operations involved in reducing an ingot to a slab on a reversing mill

The size of primary mills, such as blooming mills, is based on the center-to-center spacing of the pinions and therefore only approximately to the center-to-center spacing or the diameter of the work rolls.

The maximum length of the workpiece to be rolled on a primary mill is determined by economic considerations and appears to be about 27.5m. Increased lengths would involve undesirable heat losses from the pieces and an increased size of the building housing the mill.

Basically, there are three types of two-high reversing mills in common use, these being

- so-called blooming mills with grooved rolls,
- high-lift blooming mills (sometimes called blooming-and-slabbing mills)
- universal slabbing mills.

Blooming mills exist in a wide range of sizes and are designed to roll-ingots of square or nearly square cross-section with a maximum thickness of about 865mm. They can edge vertically, in a grooved pass, a workpiece with a maximum width of about 1020mm.

The high-lift blooming mill is designed to edge workpieces with widths up to about 1980mm by rolling them when standing on their narrower faces. It is provided with tall mill housings to permit greater elevation of the top work roll for the edging passes on wide workpieces, as illustrated in figure 6.19.

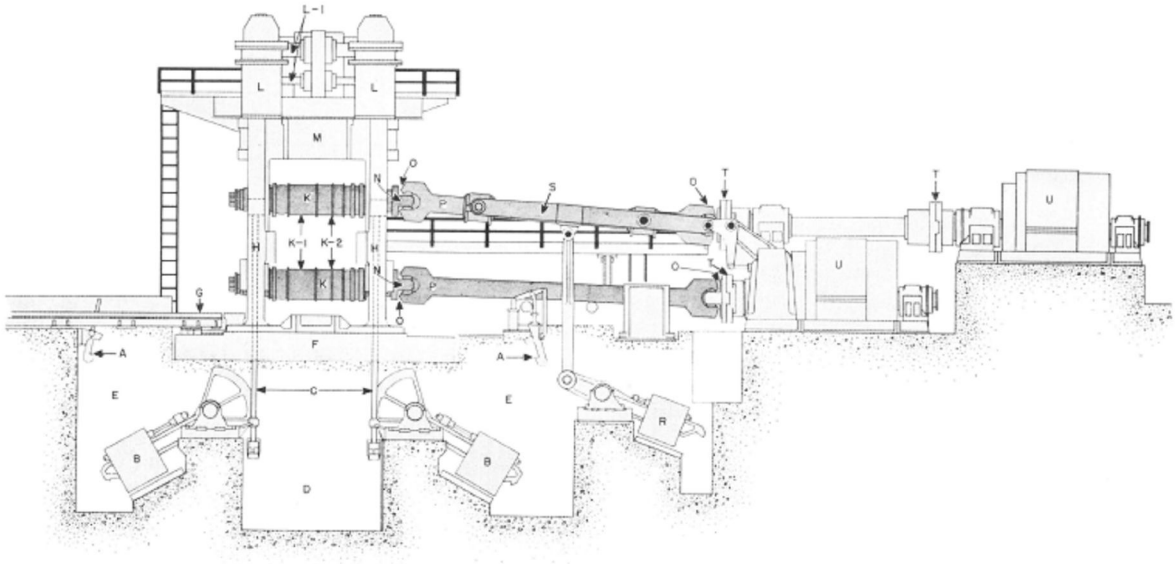

Fig. 6.19a High-lift, two-high reversing blooming mill

Fig. 6.19b High-lift blooming mill in Valbruna SPA plants

It is to be noted that the roll body is usually larger and has fewer grooved passes than the normal blooming mill and the motors which operate the mill screws are usually larger in order to provide f aster raising and lowering of the top work roll. Moreover, this form of mill can be provided with interchangeable sets of work rolls so that it can produce wide slabs as well as blooms.

Of the three types of reversing mills, the high-lift mill can produce the greatest range of product sizes.

The universal slabbing mills limited to the production of slabs up to about 198mm width. It is designed to increase the production rate for wide slabs by avoiding the expenditure of time required for vertical edging passes in a blooming mill through the use of vertical edging rolls. No grooves are used in either pair of rolls and the corners of the rolled product are generally sharper than those of product rolled in grooves.

Higher production rates are attained by the use of tandem mills which consist of two or more two-high mill stands through which the workpiece is passed in one direction only (figure 6.20).

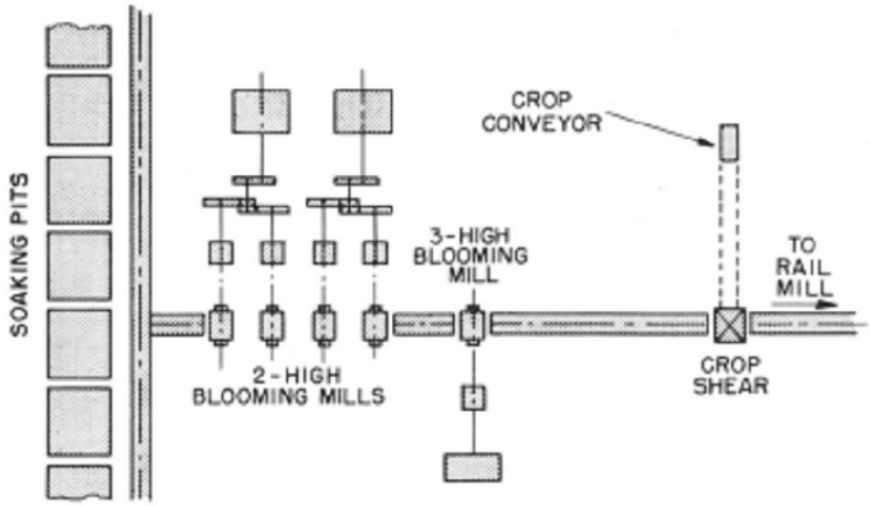

Fig. 6.20 Arrangement of blooming mills in tandem, supplying blooms to a rail mill

The spacing of the stands is such that the workpiece is only in one stand at any given time, however. Generally, tandem mills are used as roughing mills to supply hot steel to billet or narrow slabbing mills. Though capable of rolling any size bloom or slab for which they are designed, tandem mills have been applied chiefly to medium and small-sized semi-finished products since these have been the only sizes in which sufficient orders could be obtained to appropriately match the capacity of the mill.

Circled numbers indicate pass sequence *B* represents bullhead pass.

Three-high mill stands, utilize a vertical stack of three horizontal rolls, each of which has grooved passes, together with an elevating table on each side of the mill. These tables permit the workpiece to be passed alternately between the bottom and middle rolls and the top and middle rolls. Thus the direction of rolling of the workpiece may be reversed between successive passes without reversing the direction of rotation of the rolls. So that the roll dimensions and the mill and roller -table dimensions are not excessively large, a compromise pass design is used wherein the grooves in the middle roll are used for rolling with both other rolls. This method limits the reduction possible in the second pass through each groove in the middle roll to less than that possible in single passes. Moreover, the rotating speed of the mill is a compromise since each pass should be progressively faster than the preceding one. Yet, with all passes in one set of rolls, this is not possible.

Accordingly, the speed selected is usually too fast for the early passes and too slow for the last ones.

Often, it is necessary to employ heavy ragging in at least the first two passes to provide adequate friction in the roll bite.

To drive a three-high mill in one direction and at constant speed, a relatively simple drive system coupled to a flywheel may be used. Accordingly, a three-high mill is less expensive to build than a comparable two-high reversing mill and has a higher output rate than the latter in rolling the same-sized ingot to the same-sized product.

The three-high mill is most conveniently used as an intermediate stand in a primary hot-mill train where it can roll bloomed-down (partially rolled) ingots or large blooms into smaller blooms for a succeeding mill. Also, it may be used to roll small ingots (with cross-sectional dimensions of 35.5mm or less) to billets or as a roughing stand for a directly connected bill-et mill.

It should be mentioned that, during the operation of a blooming or slabbing mill, cooling water should be copiously and uniformly applied to the roll surfaces. The rolls should be warm, never chilled, otherwise firecracking of the roll surfaces will develop. The water should be turned off when the mill is not rolling but, if the coolant flow is continuous, the rolls should be kept turning so as to provide uniform cooling. In some mills, the rolls are preheated prior to use to prevent firecracking and breakage.

6.6.1 Two-high reversing blooming mills

One of the more recent installations of conventional blooming mills was made by British Steel Corporation at Scunthorpe, England, to produce an output of blooms and billets (ranging from 75 to 280 mm^2) and slabs (ranging from 175 to 430 mm wide and from 50 to l00 mm thick) totalling 2,680,000 tonnes per year. The facility, was designed for single and tandem rolling using two stands designated as the primary and secondary blooming mills. When tandem rolling, the workpieces are separated after the penultimate pass and rolled individually for the last pass. Partially rolled blooms from the primary mill are rolled individually on the secondary mill. Therefore, when tandem rolling, the second bloom produced on the primary mill is held and reciprocated between the two mills. To

eliminate extra manipulation time, the two mills are offset so that the last pass out of the primary mill is in line with the first pass on the secondary mill.

The primary mill utilizes cast-steel ro1ls 1400 mm in diameter by 2600 mm in length to roll three sizes of ingots (7, l0 and 14 tons) to blooms 460 by 400 mm for the production of smaller blooms and 480 by 355 mm for the production of slabs. The mill is powered by a twin-drive system comprising 4 motors each 0/4375/4375 hp at 0/50/100 rpm. The rolls are driven through universal-type spindles fitted with bronze slippers, each suspended in two pivoted bearings mounted in carriers, hydraulically balanced at the mill end and spring-balanced at the motor end. The motor-end slippers are oil-lubricated in an enclosed casing whereas those at the opposite end are automatically greased through a lubricator attached to the spindles.

The primary mill is designed for a maximum rolling force of 1300 tonnes utilizing hydraulic roll balancing and conventional screws for roll positioning. The rolls are carried in four tapered roller bearings fitted in each chock. Loadmeters are located between the screws and the upper roll chocks and are supported so that they remain in position during roll changes.

At each side of the mill and driven independently are two feed rollers supported in roller-bearing-equipped cartridges. The first is situated in circular bores in the roll housings and the second keyed into a pocket on the outside of the housings. Fire bars at each side of the bottom roll are mounted on a deep frame supported from the mill bedplates. The screwdown has a speed of 5/10 meters per minute and each screw is driven through a worm and wheel by a 0/275/550 hp and 0/390/780 rpm motor, this arrangement providing a low-inertia drive for maximum acceleration. Each motor has twin disc brakes to lock the screws during rolling. A disengaging coupling is provided for roll levelling and, in addition, a mechanical dial with position reset tachometers is associated with each screwdown motor so that the screwdowns may be operated automatically and a digital display of their settings is presented in the control pulpit of the mill. To minimize friction of the screws, all threads of the screw nuts are individually lubricated with oil.

When roll changing, the two rolls and their chocks are withdrawn from the mill stand on an articulated sled by a rack-and-pinion driven crab. A duplex rig is provided for

quick roll changing with the new rolls being positioned on the rig before the worn rolls are withdrawn from the stand. Hydraulic cylinders are provided for the axial alignment of the bottom roll and for the latch plates associated with the chocks.

The manipulators on each side of the primary mill are independently driven and controlled. The manipulator heads are driven by low ratio gear drives using motors running at reduced voltage and speed.

This low-inertia arrangement gives a rapid response and also the lowest slamming loads when the heads come together on an ingot. The rack beams carrying the heads are supported on pivoted pads located outside the working area to protect them from scale and the drive-side rack beams are cranked so that the drives are at a common level. The heads are each fitted with renewable wear plates (which also act as heat shields and minimize distortion) as well as twin-guide stalks (to resist end thrusts which occur in the direction of rolling as well as to eliminate the trapping of scale and ingot tops in the guideways).

The manipulator heads on the drive side of the mil1 are equipped with six tilting fingers, arranged to work in unison through a magnetic clutch or to operate as two sections of three fingers. This provision allows the individual operation of one set of fingers during tandem rolling, in cases when only one ingot has been tilted, allowing the other ingot to be tilted and avoiding the need to run one ingot out of the manipulator heads.

The main mill tables are designed to withstand heavy loads as well as the thrust developed by the mill. The rollers are individually driven and are supported in self-aligning, roller-bearing equipped cartridges. The first three rollers on each side of the mill are mounted in a separate frame and, if damaged, may be conveniently replaced by spare unit.

The secondary blooming mill is very similar to the mill stand discussed above. It utilizes rolls 1060 mm in diameter by 2200 mm in length twin-driven by two motors 0/4500/4500 hp at 0/70/140 rpm. The mill stand is designed for a maximum rolling force of 700 tonnes and utilizes a single feed roller each side of the mill. As the duty of the mill is the single rolling of blooms from the primary mill, only four tilting fingers are located on each drive-side head of the manipulators and these are operated by a single drive.

After conditioning, the workpieces are cut by a bloom shear, which is an up-and-down unit capable of cutting up to about 93000 mm^2 with a maximum blade force of 700 tons. After cropping, the blooms are transferred either to the billet mill or to bloom storage.

6.6.2 High-lift blooming and slabbing mills

As an example of a post-Wor1d War II high-lift slabbing mill, the 42-inch facility installed at the Shotton Works of British Steel Corporation may be cited which, dt the time of commissioning, was driven by a three-cylinder horizontal steam engine operating with a nominal output of 3 MW (4000 hp) at 55 rpm and a maximum power of 4 MW (5300 hp) at 105 rpm .

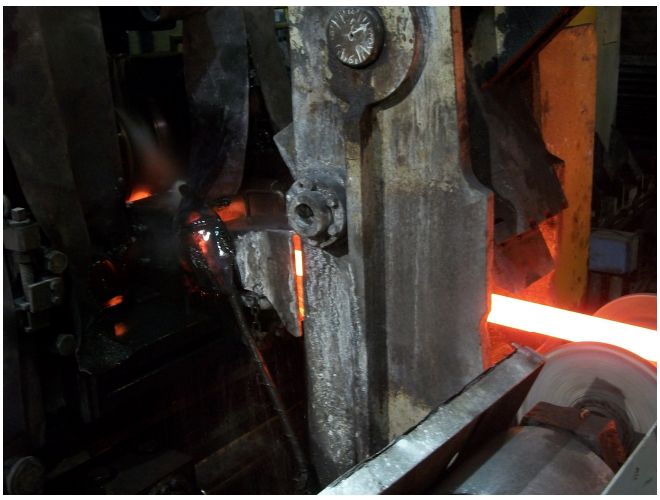

Fig. 6.22 Slabbing mill at Valbruna

The mill was operated by a three-man crew housed in a control pulpit positioned above and athwart the mill-approach table.

The mill featured roll housings of the closed-top type with minimum cross-sectional post areas of 0.32 m^2 which were specially designed to accomodate a lift of 1550 mm for the top roll. The housings were lined on the insides of the windows with steel wear plates. Cast-steel roll chocks were used, these being fitted with rollneck bearings of the flood-oil lubricated type. The two bottom chocks were mounted on a heavy cast-steel sled by which both rolls could be withdrawn simultaneously for ro11 changing.

Two 112kW (150 hp) motors powering the screws provided a mill-lift speed of 6350 mm per minute. The 400 mm diameter screws were driven through totally enclosed spur-gear and worm gearing. The worms, constantly lubricated, were connected together by a center shaft having a flexible coupling at one end and a clutch at the other, thereby enabling the rolls to be levelled.

The top roll balance was powered by two hydraulic cylinders carried in the housing tops and featured 300 mm diameter cast-iron rams used in conjunction with a hydraulic pressure of 4.87 to 5.17 MPa The ram of each cylinder was connected by a crosshead, levers and links to two balance beams running across between the housings which, in turn, were mechanically connected by special bolts (which had to be removed for roll changing) to the top roll chocks.

The steam engine was coupled to the pinion gears via a 3:1 reduction gear box. Couplings between the pinion stand and the mill were made with hydraulically balanced spindles of the universal jaw-end type equipped for centralized lubrication at the pinion-housing end and for lubrication by grease gun at the mill end.

The manipulators were 8 m long and were fitted with separate cast-steel-wearing faces. Each manipulator was driven by a pair of slab rams with racks operated by electrically driven pinions via double reduction gear units. The side-guard travel was 2.5 m while provision was made for 700 mm over-travel on the drive-side heads to allow for the removal of rollers from the main mill tables.

The heads of the manipulators on the ingoing side had a vertical dimension of 1.2 m to enable them to handle the largest slabs processed.

Both manipulator heads on the ingoing side were connected through pinion shafts to the corresponding heads on the outgoing side of the mill thus ensuring that, when the slab entered at either side of the mill, the opposing heads were always positioned in the exactly corresponding position on the other side of the mill. This ensured that the slab left the mill normal to the axes of the rolls. Equipment for tilting the workpiece, which was driven by a 74.5 kW (100 hp) motor via reduction gears, was utilized only on the entry side of the mill stand.

The first and breast rollers on both sides of the mill were driven by independent motors through flexible couplings and independent gear boxes. The breast rollers proper were loose on their shafts. The rolls used in the roller tables had stepped diameters to match the mill rolls, this feature lessening the noise and shock occurring when a workpiece entered or left the roll bite.

Roll cooling was effected by sprays from a water box carried between the two balance beams for the top roll. Scale disposal was carried out by hydraulic sluicing under the mill tables and by scrap conveyors under the mill, the material being deposited in boxes at suitable collection points.

After rolling, the slabs travelled down the continuous roller table to an open-sided up-cutting hydraulic slab shear capable of cutting slabs 1.5 m wide by 127 mm thick or an equivalent section up to a maximum thickness of 205 mm. The shear could withstand a maximum blade load of 999 tons with a maximum stroke of 305 mm and was capable of making 3 cuts per minute continuously. The blades were 1.52 m long and were powered by a main ram with a diameter of 25 inches working under a hydraulic pressure of 31 MPa.

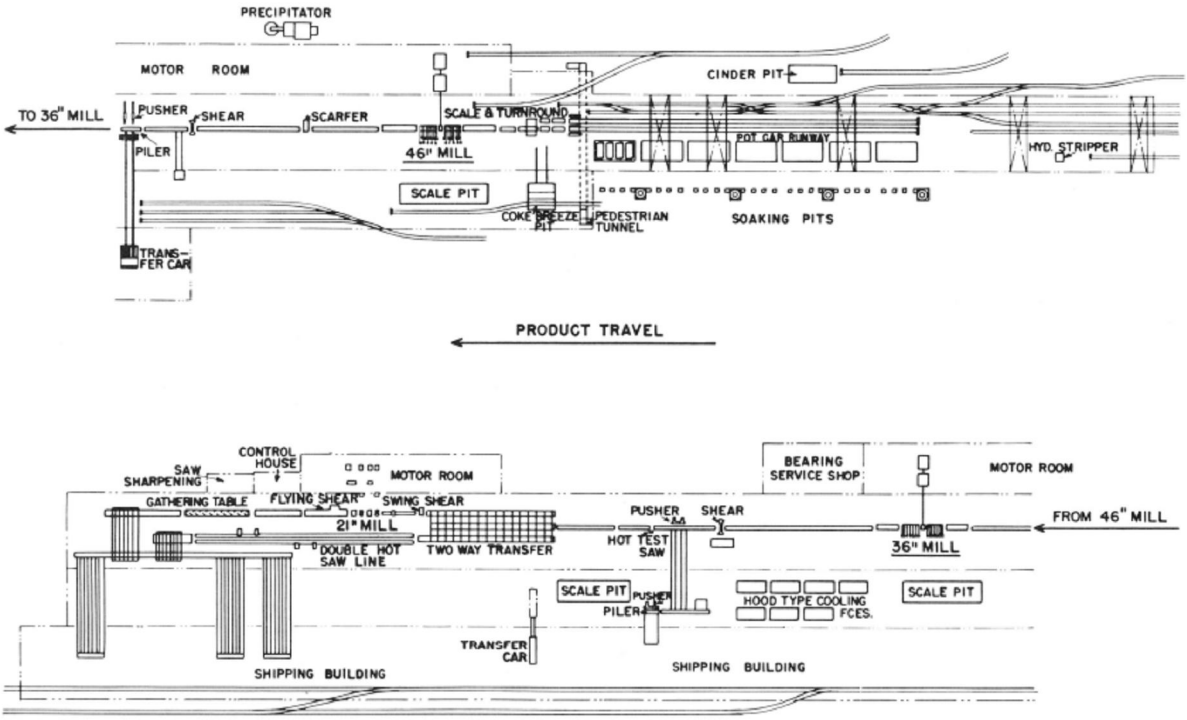

Fig. 6.23 Schematic arrangement of primary mill

This facility is capable of rolling product ranging in size from 1130mm^2 billets up to and including 1.3 m wide slabs and it consists of stripping cranes, soaking pits, a 1.17 m blooming and slabbing mill, a 0.92 m blooming mill and a four-stand continuous 0.5 m billet mill, all in tandem and enclosed in one building.

The 1.17 m by 2.8 m blooming and slabbing mill is a high-lift reversing mill with individual roll drives. Each roll is powered by a 5000 hp motor capable of speeds up to 100 rpm and reversals in 1½, seconds.

The 0.92 m by 2 m two-high reversing blooming mill rolls products ranging from 20 cm^2 billets to 98 cm^2 blooms.

The stand is powered by two 3000 hp motors with a speed range of 60 to 150 rpm individually driving the two rolls. It is to be noted that this mill is equipped with 4-row roller bearings and hydraulic roll-balancing equipment.

Chapter 7

Precipitation-hardening

7.1 Precipitation-Hardening stainless steels

Crucible 15-5 is a Premium Quality precipitation-hardening stainless steel which is capable of high strength and hardness levels after a relatively simple heat-treatment procedure. This grade is a Vacuum Arc remelted for improved cleanliness. The 15-5 PH stainless steel is martensitic and magnetic in both the solution-treated and precipitation hardened conditions. It has a high resistance to crack propagation, good transverse properties, and corrosion resistance is normally superior to the regular martensitic chromium-type stainless steels.

Because of the single low-temperature (482-621°C) precipitation-hardening heat treatment of this grade, scaling and distortion are virtually eliminated. This enables material to be finish machined to close tolerances prior to heat treatment.

7.1.1 Interactions between dislocations and precipitate particles

A dislocation moving on its slip plane containing a distribution of precipitate particles may cut through the particles or avoid them by moving out of its slip plane or by bending between the particles, leaving a dislocation ring around each precipitate (Frank-Read source). For all of these process energy must be expended. Which takes place, however, depends on the applied stress and the nature of the precipitate. For a dislocation to shear a particle, sufficient energy must be supplied to break favourable bonds within the particle thus increasing its surface area. Interstitial carbon in a-iron will always be in excess of its solubility limit at room temperature. It will precipitate as carbide along dislocations and in the volume of the matrix especially if grain boundaries are absent. This gives rise to a pronounced yield point as well as an increase in the flow stress both of which depend on heat treatment. As an alternative process carbon atoms can form a more o less condensed solute atmosphere around dislocations, as considered by Cottrell and coworkers. This would also explain a sharp yield point which in details differs from the

precipitate yield point. The Cottrell yield stress should be strongly temperature dependent, as has been calculated using the assumption that the dislocation-line energy is not increased significantly in the yield process. On the other hand thermal fluctuations would not help much to free a dislocation from a row of precipitates. A precipitate yield point can be overaged but not the Cottrell maximum. The magnitude of the precipitate yield depends on the curvature the dislocation has attained by ageing under load on the line tension, contrary to the behavior of a Cottrell-locked dislocation.

7.2 Martensitic precipitation-hardening stainless steel

During the heat treatment of precipitation-hardening stainless steels, regardless of their type, austenitization in the single-phase austenite region is always the first step. Austenitization is then followed by a relatively rapid cooling (quenching).

The martensite finish temperature (Mf) of the martensitic precipitation-hardening stainless steels - such as 15-5 PH, and 17-4 PH (AISI 630). Thus, upon quenching from the solution-treatment temperature they transform completely into martensite. Precipitation hardening is achieved by a single aging treatment at 482 °C to 621 °C for 1 to 4 hours.

The martensite start temperature (Ms) of the martensitic precipitation-hardening stainless steels is required to be above room temperature in order to ensure a full martensite-to-austenite transformation upon quenching.

One of the empirical equations that is often used to predict the martensite start temperature (in °F) is as follows:

Ms = 2160 - 66·(% Cr) - 102·(% Ni) - 2620·(% C + % N)

Where: Cr = 10-18 %, Ni = 5-12.5 %, and C + N = 0.035-0.17 %.

Precipitation hardening in the martensitic steels is achieved by reheating to temperatures at which very fine intermetallic phases - such as Ni_3Al, Ni_3Ti, $Ni_3(Al,Ti)$, NiAl, Ni_3Nb, Ni_3Cu, carbides, and Laves phase - precipitate.

A lath martensite structure provides an abundance of nucleation sites for the precipitation of intermetallic phases.

7.3 Surface treatment in precipitation-hardening stainless steel

In the heat treating of precipitation-hardening (PH) stainless steels, areas of primary interest include:

- Cleaning prior to heat treatment
- Furnace atmospheres
- Time-temperature cycles
- Effect of variations in cycles
- Scale removal after heat treatment

All parts must be cleaned thoroughly prior to heat treating. Because the chemical composition of these steels is delicately balanced, failure to remove drawing lubricants, cutting oils, and grease can lead to surface carburization and improper response to heat treatment. As a secondary benefit, thorough cleaning promotes the formation of a uniform surface scale that is readily removable.

The recommended cleaning procedure comprises vapour decreasing or solvent cleaning, followed by mechanical scrubbing with a mild abrasive alkaline cleaner to remove insoluble soils. All traces of cleaners should be removed by thoroughly rinsing with warm water.

Wet or dry abrasive blasting may be substituted for the above procedures. Recommended grits and operating details for blasting are given in Table 7.1. After blasting, all traces of abrasive must be removed from the work by scrubbing thoroughly.

Abrasive		**Nozzle**		**Air Pressure**	**Cleaning speed**
		Size	**Angle °**		
Material	*Grint n°*	*mm*	-	*kPa*	*mm^2/s*
Alumina (dry)	30	6,4	45 ÷ 60	170 ÷ 655[(a)]	130 ÷ 215
Garnet or Alumina (dry)	36	9,5	60	240	645

(a) Depending on metal thickness

Tab. 7.1 Recommended conditions for abrasive blast cleaning of precipitation-hardening stainless steels prior to heat treatment. All abrasives must be removed by thorough scrubbing.

In some applications, cleaning prior to heat treating may be accomplished by closely controlled pickling in a 10% HNO_3 - 2% HF aqueous solution at 45 to 60 °C. Time should be limited to 2 or 3 min. This method is not recommended for cleaning severely formed or previously heat-treated parts. Proprietary inhibited scale-removal preparations are available.

Furnaces fired with oil or natural gas are not entirely satisfactory for the heat treatment of these steels where finished surfaces are not to be subsequently machined. In such units, it is difficult to control combustion contaminants and to eliminate flame impingement on the parts being treated. Electric furnaces or gas-fired radiant-tube furnaces are generally used for heat treating precipitation-hardening stainless steels.

7.4 Furnace atmospheres

Air is a satisfactory furnace atmosphere for austenite-conditioning and annealing operations. Controlled reducing atmospheres, such as dissociated ammonia or bright-annealing gas, introduce the potential hazard of nitriding or carburizing, either of which has a deleterious effect on mechanical properties.

Bright annealing may be done in hydrogen, argon, or helium atmospheres, provided a dew point of -55 °C or lower is maintained. The cooling rate from the annealing temperature must be approximately equal to that of cooling in still air. Austenite-conditioning treatments at temperatures as high as 925 to 955 °C may also be performed in dry hydrogen, argon, or helium, maintaining the same low dew point. A scale-free surface will be obtained.

The lower austenite-conditioning temperatures, such as 760 °C, present difficulties in achieving scale-free surfaces in dry hydrogen, argon, or helium. An air atmosphere is generally used at these temperatures. For complete freedom from scale or discoloration at the lower temperatures, a vacuum furnace is required.

Final hardening of these steels is performed at relatively low temperatures, and an air atmosphere is acceptable for these treatments.

7.5 Scale removal after heat treating

The amount and nature of scale vary with the degree of cleanness of the work being treated, the furnace atmosphere, and the temperature and duration of heat treatment. In the following discussion, it will be assumed that all heat-treating operations are performed in an air atmosphere. A variety of descaling methods may be employed; the choice depends on the type of steel and the facilities available.

In removing scale formed during homogenization or full annealing, the use of a 10% HNO_3-2% HF aqueous solution at 45 to 60 °C has been effective. Exposure to the acid solution should be limited to a period of 3 min.

Removal of loosened scale may be facilitated by the use of high-pressure water or steam. A uniform surface is evidence of a well-cleaned part. The use of molten salts to condition the scale is limited because the temperature involved (about 450 °C) can age harden any martensite in the microstructure.

The austenite-conditioning treatments produce a scale that is best removed by mechanical means. Acids should be avoided because they are a possible source of intergranular attack. Wet grit-blasting processes have been widely used to remove these scales and have been found to be highly satisfactory.

The final step in heat treating (precipitation hardening) produces a discoloration of heat tint. It is desirable to use mechanical means to remove this oxide from the steel. The HNO_3-HF solution has been used on these steels, but extreme care is required to prevent intergranular attack. The acid solution may be used satisfactorily with 17-4 PH. To a lesser extent, electro-polishing has also been used to remove the final heat tint resulting from precipitation hardening. Also available are proprietary cleaners that have been successful in removing the heat tint discoloration.

7.6 Precipitation-hardening heat treatments

In designing alloys for strength, an approach often taken is to develop an alloy in which the structure consists of particles which impede dislocation motion dispersed in a ductile matrix. The finer the dispersion, for the same amount of particles, the stronger the material.

Such a dispersion can be obtained by choosing an alloy which, at elevated temperature, is single phase, but which on cooling will precipitate another phase in the matrix. A heat treatment is then developed to give the desired distribution of the precipitate in the matrix. If hardening occurs from this structure, then the process is called precipitation hardening or age hardening. It is to be noted that not all alloys in which such a dispersion can be developed will harden.

The mechanism of strengthening by precipitation hardening involves the formation of coherent clusters of solute atoms (that is, the solute atoms have collected into a cluster but still have the same crystal structure as the solvent phase). This causes a great deal of strain because of mismatch in size between the solvent and solute atoms. The cluster stabilizes dislocations, because dislocations tend to reduce the strain, similar to the reduction in strain energy of a single solute atom by a dislocation. When dislocations are anchored or trapped by coherent solute clusters, the alloy is considerably strengthened and hardened.

However, if the precipitates are semicoherent (sharing a dislocation-containing interface with the matrix), incoherent (sharing a disordered interface, akin to a large-angle grain boundary, with the matrix), or are incapable of reducing strain behavior because they are too strong, a dislocation can circumvent the particles only by bowing into a roughly semicircular shape between them under the action of an applied shear stress. Consequently, the presence of the precipitate particles, and even more importantly the strain fields in the matrix surrounding the coherent particles, provide higher strength by obstructing and retarding the movement of dislocations. The characteristic that determines whether a precipitate phase is coherent or noncoherent is the closeness of match or degree of disregistry between the atomic spacings on the lattice of the matrix and on that of the precipitate.

7.7 Solution heat treatment

A prerequisite to precipitation hardening is the ability to heat the alloy to a temperature range wherein all of the solute is dissolved, so that a single-phase structure is attained. This is shown schematically in figure 7.1 for a 10% B alloy in a hypothetical

system A-B. Heating above the solvus temperature *T*2 for this alloy, and holding in the α range for sufficient time, will form the single phase α. This is the required solution heat treatment. This structure is then retained at ambient temperatures by cooling rapidly (for example, water quenching) from the α range to prevent the precipitate from forming. The structure is supersaturated with respect to the solute, and hence is unstable.

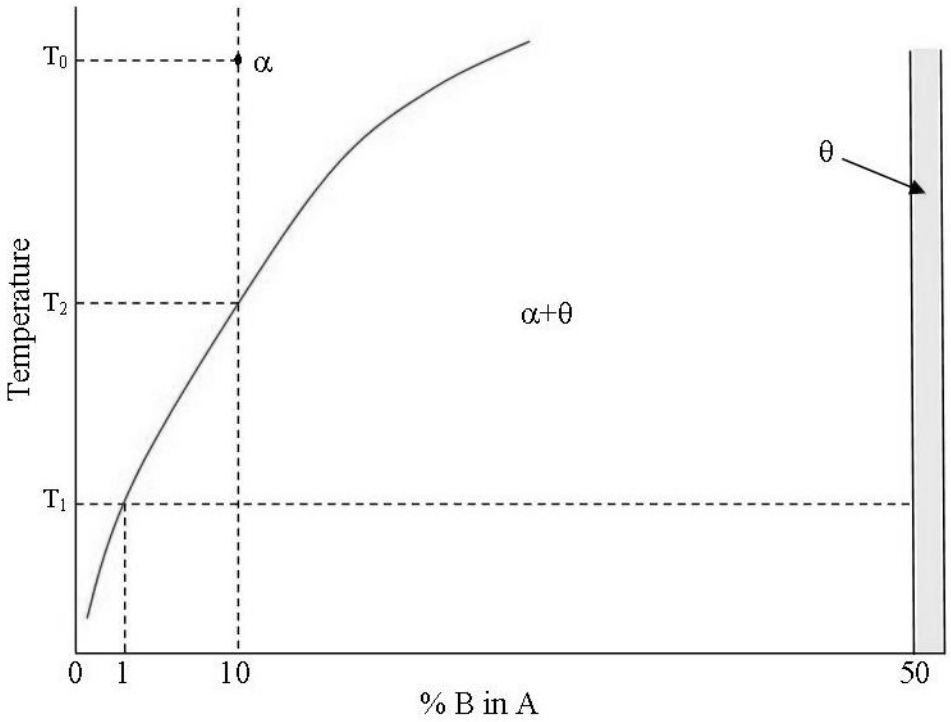

Fig. 7.1 Hypothetical phase diagram of system A-B. The decreasing solubility of B in α with decreasing temperature allows an alloy containing 10% B to be single-phase at high temperature (that is, above T_2) but two-phase at low temperature (T_1).

7.8 The process of precipitation

After quenching from the α region (Fig. 7.1), precipitation is achieved by reheating the alloy below the solvus (*T*2 in Fig. 7.1) at a suitable temperature for a suitable time. During this time, at localized regions (for example, grain boundaries), the precipitates nucleate. Because these precipitates have a higher solute content than the matrix, the region in the matrix surrounding them is reduced in solute content. This forms a concentration gradient such that the solute atoms diffuse from the adjacent matrix toward the particles, allowing the precipitates to continue to grow. The rate of growth is diffusion-

controlled and is given by an appropriate solution to Fick's law. The precipitation process is depicted schematically in figure 7.2. Here the precipitate contains 50% B (see Fig. 7.1).

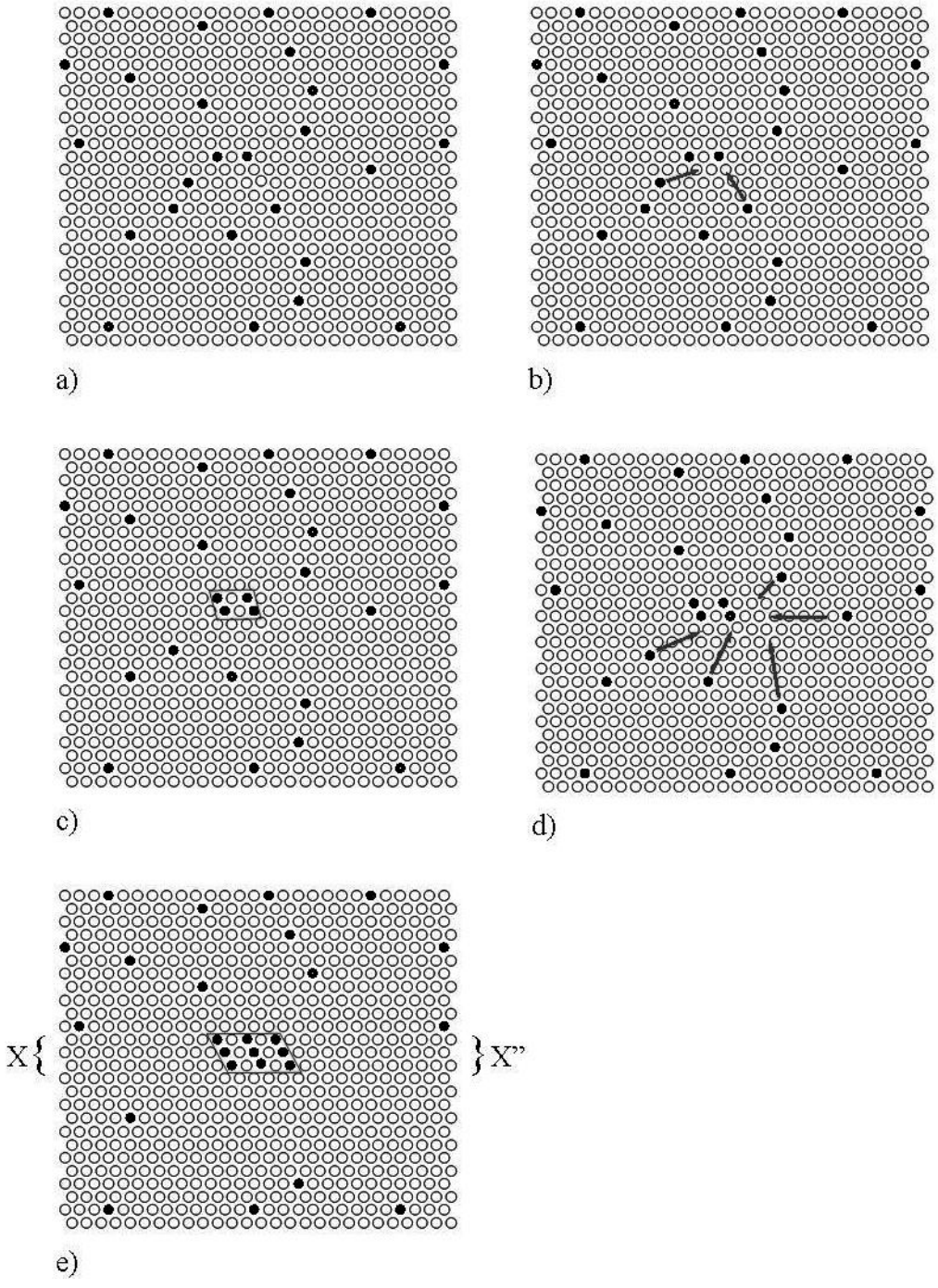

(a) Random array of B (black) and A (white) atoms containing 10%B

(b) The three atoms shown shift to the new position indicated by arrows

(c) Small precipitate of θ now formed

(d) Atoms indicated by arrows move to new positions

(e) Crystal of θ now increased in size

Fig. 7.2 Schematic illustration of formation of a precipitate in a supersaturated matrix. Time is increasing from (a) to (e), but at (e) equilibrium is not yet attained. Concentration profile through the precipitate in (e).

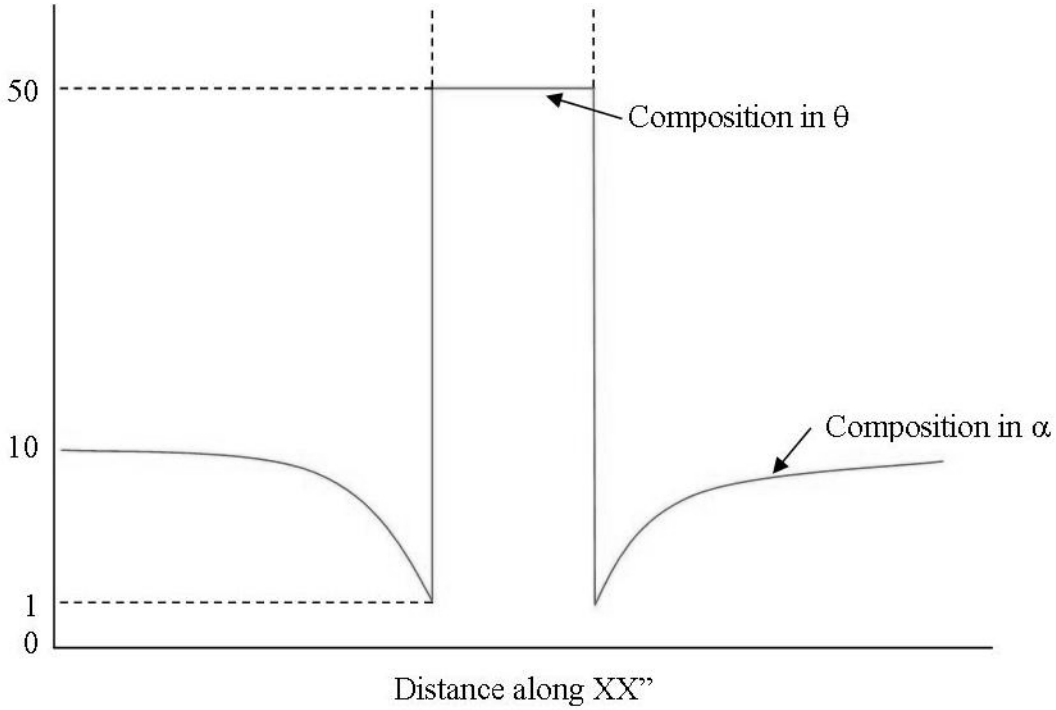

Fig. 7.3 Concentration profile through the precipitate in (e).

The precipitation hardening process for a steel containing a solution of 10% B atoms in an array of atoms A, is the motion of solute atoms through the matrix to new locations so close together, forming the core particle pellet θ. The difference of the concentration gradient leads to the diffusion of solute atoms in new positions in the matrix, thus the crystal θ increases its size.

The maximum amount of precipitate which can form is given by the equilibrium amount, which can be calculated from a mass balance (lever rule). Once this equilibrium amount of precipitate has been attained, then further change in the precipitates is caused by

the tendency for the system to reduce the precipitate/matrix interfacial area. Thus, with time at a given aging temperature, the smaller precipitates dissolve, with the solute diffusing through the matrix to contribute to the growth of the larger particles. This results in a microstructure containing larger, but fewer, particles. An equivalent effect is obtained by using a high aging temperature for a given time. These changes are depicted schematically in figure 7.4.

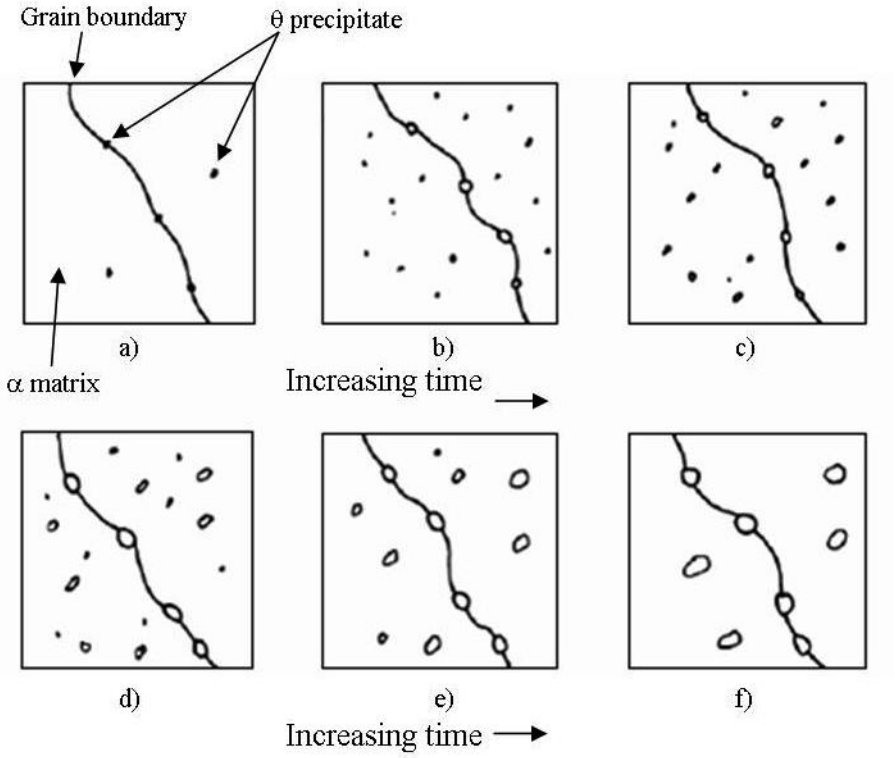

Fig. 7.4 Schematic illustration of formation of θ precipitates in the α matrix (a and b) and their coarsening (c to f)

7.9 Heat-treating procedures: control of precipitation through heat treatment

15-5PH Precipitation Hardening Stainless Steel Alloy (S15500) is a variant of the older 17-4 PH (S17400) chromium-nickel-copper precipitation hardening stainless steel.

Both alloys exhibit high strength and moderate corrosion resistance. High strength is maintained to approximately 316°C. The 15-5 PH alloy was designed to have greater toughness than 17-4 PH, especially in the through-thickness (short transverse) direction.

This improved toughness is achieved by reduced delta ferrite content and control of inclusion size and shape. The composition and processing of 15-5 PH alloy is carefully

controlled to minimize its content of delta ferrite, which is present in the 17-4 PH stainless steel material. Inclusion control is done by consumable electrode remelting using the electro-slag remelting (ESR) process. The 15-5 PH alloy is martensitic in structure in the annealed condition and is further strengthened by a relatively low temperature heat treatment which precipitates a copper containing phase in the alloy. Like the 17-4PH alloy, the 15-5 PH stainless steel alloy requires only a simple heat treatment; a one step process conducted at a temperature in the range 482°C to 621°C depending on the combination of strength and toughness desired. A wide range of properties can be produced by this one step heat treatment. Heat treatment in the 482°C range produces highest strength, although slightly less than those of semi-austenitic alloys. The latter precipitation hardening alloys generally require more steps to complete heat treatment. The15-5 PH alloy is generally better-suited for plate applications than are the semi austenitic alloys.

The precipitation heat treatment for the desired properties is determined empirically. Higher precipitation temperatures usually are associated with a lower nucleation rate and thus a coarser precipitate distribution. Also, as the precipitation temperature used approaches the solvus, the amount of precipitate decreases (vanishing at the solvus).

The microstructural effects by referring to the aging an 15-5PH alloy, this alloy is heated, then aged at a temperature in the range of 480 to 620 °C for 1 to 4 h, depending on the temperature, and then air cooling. The precipitates are fine and evenly distributed, and are about 1 μm in size.

Recommended procedures for full annealing at 1040 ± 15 °C for 1 h (the time at heat is dependent upon section size, normally, a 1h hold at temperature is suggested) in water quench, austenite conditioning, transformation cooling, and age tempering (precipitation hardening) are given in Table 7.2.

Typical 15-5 PH (UNS S15500) tensile strengths shown may be obtained by the following treatments:

Heat Treating Parameters for AL 15-5™ alloy		
Condition	Temperature	Time
H 900	482 °C ± 5	60 min. ± 5 min.
H 925	496 °C ± 5	4 hrs. ± 0.25 hr.
H 1025	552 °C ± 5	4 hrs. ± 0.25 hr.
H 1075	579 °C ± 5	4 hrs. ± 0.25 hr.
H 1100	593 °C ± 5	4 hrs. ± 0.25 hr.
H 1150	621 °C ± 5	4 hrs. ± 0.25 hr.

Tab. 7.2 Recommended heat-treating procedures for martensitic precipitation-hardenable stainless steels.

15-5 PH alloys (UNS S15500) are normally supplied in the solution-treated condition. As with 17-4 PH, care should be used in applying the material in the solution-treated condition. The alloy can be hardened by heating to a temperature in the range of 480 to 620 °C for 1 to 4 h, depending on the temperature, and then air cooling. For example the H1150M treatment condition (after annealing) at 760 ± 8 °C for 2 h, and cooling in air cool from 620 ± 5 °C for 4 h, produced a typical tensile strength of 860 MPa. Table 7.3 illustrates typical strength levels versus hardening procedures.

15-5 PH		**Condition**			
		A	**H900**	**H1075**	**H1150**
Yield strength	MPa	760	1200	930	860
UTS	MPa	1030	1340	1070	1000
Elongation	%	8	15	15	15
Hardness Rockwell	HRc	33	43	31	28

Tab. 7.3 Typical 15-5PH stainless steel mechanical properties versus precipitation-hardening procedures.

Chapter 8

Test methods

8.1 ASTM E 8M: Standard test methods for tension testing of metallic material [metric]

8.1.1 Scope

This test method cover the tension testing of metallic material in any heat treatment form at room temperature, specifically, the methods of determination of yield strength, yield point elongation, tensile strength, elongation, and reduction of area.

These metric test methods are essentially the same as those in Test Methods E 8, and are compatible in technical content except that gage lengths are required to be 5D for most round specimens rather than 4D as specified in Test Methods E8.

Exceptions to the provisions of these test methods may need to be made in individual specifications or test methods for a particular material.

The room temperature shall be considered to be l0 to 38°C unless otherwise specified.

8.1.2 Terminology

The definitions of terms relating to tension testing appearing in Terminology E 6 shall be considered as applying to the terms used in these test methods of tension testing. Additional terms being defined are as follows:

- *Discontinuous yielding*: a hesitation or fluctuation of force observed at the onset of plastic deformation, due to localized yielding. (The stress-strain curve need not appear to be discontinuous.)
- *Lower yield strength, LYS [FL^{-2}]:* the minimum stress recorded during discontinuous yielding, ignoring transient effects.
- *Upper yield strength, UYS [FL^{-2}]:* the first stress maximum (stress at hrst zero slope) associated with discontinuous yielding.
- *Yield point elongation, YPE:* the strain (expressed in percent) separating the stress-

strain curve's first point of zero slope from the point of transition from discontinuous yielding to uniform strain hardening. If the transition occurs over a range of strain, the YPE end point is the intersection between (a) a horizontal line drawn tangent to the curve at the last zero slope and (b) a line drawn tangent to the strain hardening portion of the stress-strain curve at the point of inflection. If there is no point at or near the onset of yielding at which the slope reaches zero) the material has 0 % YPE.

8.1.3 Significance and use

Tension tests provide information on the strength and ductility of materials under uniaxial tensile stresses. This information may be useful in comparisons of materials, alloy development, quality control, and design under certain circumstances.

The results of tension tests of specimens machined to standardized dimensions from selected portions of a part or material may not totally represent the strength and ductility properties of the entire end product or its in-service behavior in different environments.

These test methods are considered satisfactory for acceptance testing of commercial shipments. The test methods have been used extensively in the trade for this purpose.

8.1.4 Apparatus

8.1.4.1 Testing machines

Machines used for tension testing shall conform to the requirements of Practices E 4. The forces used in determining tensile strength and yield strength shall be within the verified force application range of the testing machine as defined in Practices E 4.

8.1.4.2 Gripping devices

Various types of gripping devices may be used to transmit the measured force applied by the testing machine to the test specimens. To ensure axial tensile stress within the gage length, the axis of the test specimen should coincide with the center line of the heads of the testing machine. Any departure from this requirement may introduce bending stresses that are not included in the usual stress computation (force divided by cross-sectional area).

The effect of this eccentric force application may be illustrated by calculating the bending moment and stress thus added. For a standard 12.5-mm diameter specimen, the stress increase is 1.5 % for each 0.025 mm of eccentricity. This error increases to about 2.5 %/0.025 mm for a 9-mm diameter specimen and to about 3.2 %10.025 mm for a 6-mm diameter specimen. Alignment methods are given in Practice E 1012.

Testing machines usually are equipped with wedge grips. If, however, for any reason, one grip of a pair advances farther than the other as the grips tighten, an undesirable bending stress may be introduced. For best results, the wedges should be supported over their entire lengths by the heads of the testing machine. This requires that liners of several thicknesses be available to cover the range of specimen thickness. For proper gripping, it is desirable that the entire length of the serrated face of each wedge be in contact with the specimen. For short specimens and for specimens of many materials, it is generally necessary to use machined test specimens and to use a special means of gripping to ensure that the specimens, when under load, shall be as nearly as possible in uniformly distributed pure axial tension.

8.1.4.3 Dimension-measuring devices

Micrometers and other devices used for measuring linear dimensions shall be accurate and precise to at least one half the smallest unit to which the individual dimension is required to be measured.

8.1.5 Test specimens

8.1.5.1 General

Test specimens shall be either substantially full size or machined, as prescribed in the product specifications for the material being tested.

Improperly prepared test specimens often are the reason for unsatisfactory and incorrect test results. It is important, therefore, that care be exercised in the preparation of specimens, particularly in the machining, to ensure the desired precision and bias in test results.

It is desirable to have the cross-sectional area of the specimen smallest at the center of the reduced section to ensure fracture within the gage length. For this reason, a small taper is permitted in the reduced section of each of the specimens described in the following sections.

8.1.5.2 Round specimens

The standard 12.5 mm diameter round test specimen shown in figure 8.1.1 is used quite generally for testing metallic materials, both cast and wrought.

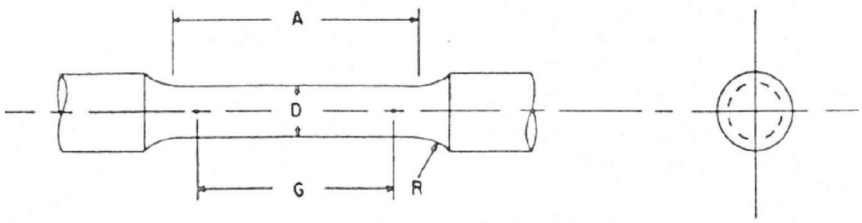

Fig. 8.1.1 Standard 12.5 mm round tension test specimen with gage lengths five times the diameters (5D).

The figure 8.1.1 also shows small-size specimens proportional to the standard specimen. These may be used when it is necessary to test material from which the standard specimen cannot be prepared. Other sizes of small, round specimens may be used. In any such small-size specimen, it is important that the gage length for measurement of elongation be five times the diameter of the specimen.

The shape of the ends of the specimen outside of the gage length shall be suitable to the material and of a shape to fit the holders or grips of the testing machine so that the forces may be applied axially.

For round bar, test specimens having the full cross-sectional area of the bar shall be used wherever practicable. In testing bar that has a 4 mm or larger diameter, unless otherwise specified, a gage length equal to five times. The diameter shall be used. The total length of the specimens shall be at least equal to the gage length plus the length of material required for the full use of the grips employed.

For rod and bar, the largest practical size of round specimen as described, may be used in place of a test specimen of full cross section. Unless otherwise specified in the product specification, specimens shall be parallel to the direction of rolling or extrusion.

For specimens with reduced sections, gripping of the specimen shall be restricted to the grip section, because gripping in the reduced section or in the filet can significantly affect test results.

8.1.6 Gage length of test specimens

The gage length for the determination of elongation shall be in accordance with the product specifications for the material being tested. Gage marks shall be stamped lightly with a punch, scribed lightly with dividers or drawn with ink as preferred. For material that is sensitive to the effect of slight notches and for small specimens, the use of layout ink will aid in locating the original gage marks after fracture.

Extensometers with gage lengths equal to or shorter than the nominal gage length (dimension shown as "G-Gage Length" in the accompanying figures) of the specimen may be used to determine the yield phenomenon.

8.1.7 Location of test specimens

Unless otherwise specified, the axis of the test specimen shall be located as follows: Midway from the center to the surface for products over 40 mm in thickness, diameter.

For forgings, specimens shall be taken as provided in the applicable product specifications, either from the predominant or thickest part of the forging from which a coupon can be obtained, or from a prolongation of the forging, or from separately forged coupons representative of the forging. When not otherwise specified, the axis of the specimen shall be parallel to the direction of the grain flow.

Surface Finish or Specimens, when materials are tested with surface condition other than as manufactured, the surface finish of the test specimens shall be as provided in the applicable product specifications. Particular attention should be given to the uniformity and quality of surface finishes of specimen for high strength and very low ductility materials since this as been show to be a factor in the variability of test results.

8.1.8 Procedures

To determine the cross-sectional area of a test specimen, measure the dimensions of the cross section at the center of the reduced section. For referee testing of specimens under 5 mm in their least dimension, measure the dimensions where the least cross-sectional area is found. Measure and record the cross-sectional dimensions of tension test specimens 5 mm and over to the nearest 0.02 mm, the cross-sectional dimensions less than 5 mm and not less than 2.5 mm to the nearest 0.01 mm, the cross-sectional dimensions less than 2.5 mm and not less than 0.50 mm to the nearest 0.002 mm, and when practical, the cross sectional dimensions less than 0.50 mm to at least the nearest 1 % but in all cases to at least the nearest 0.002 mm.

Rough surfaces due to the manufacturing process such as hot rolling, metallic coating, etc., may lead to inaccuracy of the computed areas greater than the measured dimensions would indicate. Therefore, cross-sectional dimensions of tension test specimens with rough surfaces due to processing may be measured and recorded to the nearest 0.02 mm.

Determine cross-sectional areas of full-size test specimens of non symmetrical cross sections by weighing a length not less than 20 times the largest cross-sectional dimension and using the value of density of the material. Determine the weight to the nearest 0.5 % or less.

8.1.9 Zeroing of the testing machine

The testing machine shall be set up in such a manner that zero force indication signifier a state of zero force on the specimen. Any force (or preload) imparted by the gripping of the specimen must be indicated by the force measuring system unless the preload is physically removed prior testing. Artificial methods of re moving the preload on the specimen, such as taring it out by a zero adjust pot or removing it mathematically by software, are prohibited because these would affect the accuracy of the test results.

Preloads generated by gripping of specimens may be either tensile or compressive in nature and may be the result of such things as:

- grip design
- malfunction of gripping apparatus (sticking, binding, etc.)
- excessive gripping force
- sensitivity of the control loop

It is the operator's responsibility to verify that an observed preload is acceptable and to ensure that grips operate in a smooth manner. Unless otherwise specified, it is recommended that momentary (dynamic) forces due to gripping not exceed 20% of the material's nominal yield strength and that static preloads not exceed l0% of the material's nominal yield strength.

8.1.10 Speed of testing

Speed of testing may be defined in terms of

a) rate of straining of the specimen
b) rate of stressing of the specimen
c) rate of separation of the two heads of the testing machine during a test
d) the elapsed time for completing part or all of the test
e) free-running crosshead speed (rate of movement of the crosshead of the testing machine when not under load) or free-running rate of grip separation.

Specifying suitable numerical limits for speed and selection of the method are the responsibilities of the product committees. Suitable limits for speed of testing should be specified for materials for which the differences resulting from the use of different speeds are of such magnitude that the test results are unsatisfactory for determining the acceptability of the material. In such instances, depending upon the material and the use for which the test results are intended, one or more of the methods described in the following paragraphs is recommended for specifying speed of testing.

Speed of testing can affect test values because of the rate sensitivity of materials and the temperature-time effects.

Rate of straining: the allowable limits for rate of straining shall be specified in metres per metre per second. Some testing machines are equipped with pacing or indicating devices for the measurement and control of rate of straining, but in the absence of such a device the average rate of straining can be determined with a timing device by observing the time required to effect a known increment of strain.

Rate of stressing: the allowable limits for rate of stressing shall be specified in megapascals per second. Many testing machines are equipped with pacing or indicating devices for the measurement and control of the rate of stressing, but in the absence of such a device the average rate of stressing can be determined with a timing device by observing the time required to apply a known increment of stress.

Rate of separation of heads during tests: the allowable limits for rate of separation of the heads of the testing machine, during a test, shall be specified in metres per metre of length of reduced section (or distance between grips for specimens not having reduced sections) per second. The limits for the rate of separation may be further qualified by specifying different limits for various types and sizes of specimens. Many testing machines are equipped with pacing or indicating devices for the measurement and control of the rate of separation of the heads of the machine during a test, but in the absence of such a device the average rate of separation of the heads can be experimentally determined by using suitable length-measuring and timing devices.

Elapsed time: the allowable limits for the elapsed time from the beginning of force application (or from some specified stress) to the instant of fracture, to the maximum force, or to some other stated stress, shall be specified in minutes or seconds. The elapsed time can be determined with a timing device.

Free-running crosshead speed: the allowable limits for the rate of movement of the crosshead of the testing machine (or free-running rate of grip separation), with no force applied by the testing machine, shall be specified in metres per metre of length of reduced section (or distance between grips for specimens not having reduced sections) per second.

The limits for the crosshead speed may be further qualified by specifying different limits for various types and sizes of specimens. The average crosshead speed can be experimentally determined by using suitable length-measuring and timing devices.

8.1.10.1 Speed of testing when determining yield properties

Unless otherwise specified, any convenient speed of testing may be used up to one half the specified yield strength or up to one quarter the specified tensile strength, whichever is smaller. The speed above this point shall be within the limits specified. If different speed limitations are required for use in determining yield strength, yield point elongation, tensile strength, elongation, and reduction of area, they should be stated in the product specifications. The yield properties referred to include yield strength and yield point elongation. In the absence of any specified limitations on speed of testing, the following general rules shall apply.

The speed of testing shall be such that the forces and strains used in obtaining the test results are accurately indicated.

When performing a test to determine yield properties, the rate of stress application shall be between 1.15 and 11.5 MPa/s.

When a specimen being tested begins to yield, the stressing rate decreases and may even become negative in the case of a specimen with discontinuous yielding. To maintain a constant stressing rate in this case would require the testing machine to operate at extremely high speeds and, in many cases, this is not practical. The speed of the testing machine shall not be increased in order to maintain a stressing rate when the specimen begins to yield. In practice, it is simpler to use either a strain rate, a rate of separation of the heads, or1 free-running crosshead speed which approximates the desired stressing rate. As an example, use a strain rate that is less than 11.5 MPa/s divided by the nominal Young's Modulus of the material being tested. Arate of separation of the heads through experimentation which would approximate the desired stressing rats prior to the onset of yielding, and maintain that rate of separation of the heads through the region that yield properties are determined. While both of these methods will provide similar rates of stressing and straining prior to the onset of yielding, the rates of stressing and straining may be different in the region where yield properties are determined. This difference is due to the change in the rate of elastic deformation of the testing machine, before and after the onset of yielding. In addition, the use of any of the methods other than rate of straining

may result in different stressing and straining rates when using different testing machines, due to differences in the stiffness of the testing machines used.

8.1.10.2 Speed of testing when determining tensile strength

In the absence of any specified limitations on speed of testing, the following general rules shall apply. When determining only the tensile strength, or after the yield properties have been determined, the speed of the testing machine may be increased to correspond to a strain rate between 0.05 and 0.5 m/m/min. An extensometer and strain rate indicator may be used to set the strain rate. If an extensometer and strain rate indicator are not used to set this strain rate, the speed of the testing machine shall be set between 0.05 and 0.5 m/m of the length of the reduced section (or distance between the grips for specimens not having reduced sections) per minute.

8.1.10.3 Determination of yield strength

Offset Method: to determine the yield strength by the offset method, it is necessary to secure data (autographic or numerical) from which a stress-strain diagram may be drawn. Then on the stress-strain diagram (Fig. 8.1.2) lay off *Om* equal to the specified value of the offset, draw *mn* parallel to *OA*, and thus locate *r*, the intersection of *mn* with the stress-strain diagram.

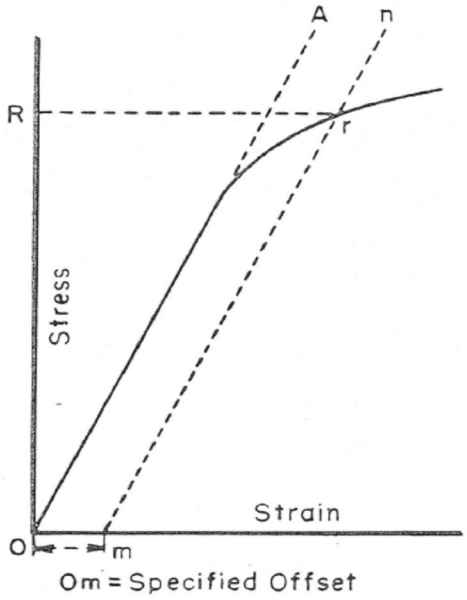

Fig. 8.1.2 Stress-strain diagram for determination of yield strength by the Offset method

In reporting values of yield strength obtained by this method, the specified value of offset used should be stated in parentheses after the term yield strength, as follows:

yield strength (offset = 0.2 %) = 360 MPa

In using this method, a Class B2 or better extensometer shall be used.
There are two general types of extensometers, averaging and non-averaging, the use of which is dependent on the product tested. For most machined specimens, there are minimal differences. However, for some forgings and tube sections, significant differences in measured yield strength can occur. For these cases, it is recommended that the averaging type be used.
When there is a disagreement over yield properties, the offset method for determining yield strength is recommended as the referee method.

Extension-Under-Load Method: yield strength by the extension-under-load method may be determined by: using autographic or numerical devices to secure stress-strain data, and then analyzing this data (graphically or using automated methods) to determine the stress value at the specified value of extension, or using devices that indicate when the specified extension occurs, so that the stress then occurring may be ascertained. Any of these devices may be automatic. This method is illustrated in Fig.8.1.3.

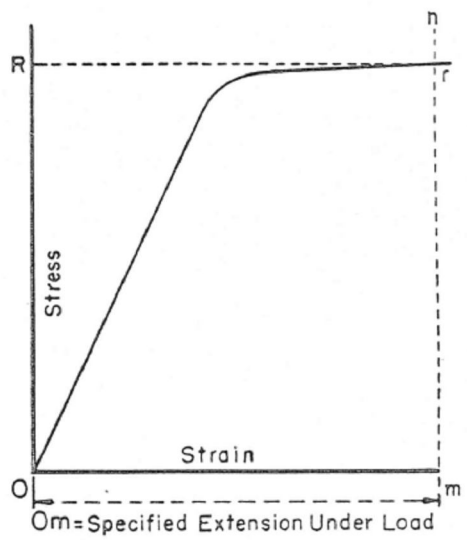

Fig. 8.1.3 Stress-Strain diagram for determination of yield strength by the Extension-Under-Load Method

The stress at the specified extension shall be reported as follows:

yield strength (EUL = 0.5 %) = 360 MPa

Extensometers and other devices used in determination of the extension shall meet Class 82 requirements at the strain of interest, except where use of low magnification Class C devices is helpful, such as in facilitating measurement of YPE if observed. If Class C devices are used, this must be reported along with the results. The appropriate value of the total extension must be specified. For steels with nominal yield strengths of less than 550 MPa, an appropriate value is 0.005 mm/mm (0.5 %) of the gage length. For higher strength steels, a greater extension or the offset method should be used. When no other means of measuring elongation are available, a pair of dividers or similar device can be used to determine a point of detectable elongation between two gage marks on the specimen. The gage length shall be 50 mm. The stress corresponding to the load at the instant of detectable elongation may be recorded as the approximate extension-under-load yield strength.

Autographic Diagram Method (for materials exhibiting discontinuous yielding): Obtain stress-strain (or force elongation) data or construct a stress-strain (or load-elongation) diagram using an autographic device. Determine the upper or lower yield strength as follows:

Record the stress corresponding to the maximum force at the onset of discontinuous yielding as the upper yield strength. This is illustrated in Fig. 8.1.4.

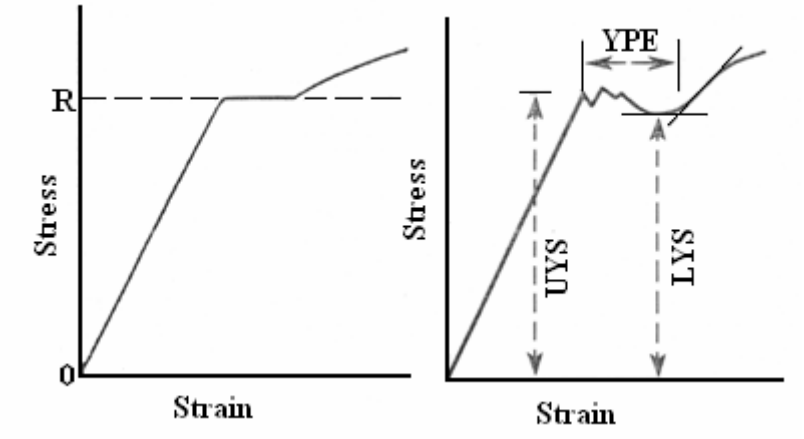

Fig. 8.1.4 Stress-Strain Diagram Showing Upper Yield strength corresponding with top of knee. The diagram showing yield point elongation and upper and lower yield strengths

If multiple peaks are observed at the onset of discontinuous yielding, the first is considered the upper yield strength.

Yield properties of materials exhibiting yield point elongation are often less repeatable and less reproducible than those of similar materials having no YPE. Offset and EUL yield strengths may be significantly affected by force fluctuations occurring in the region where the offset or extension intersects the stress-strain curve. Determination of upper or lower yield strengths (or both) may therefore be preferable for such materials, although these properties are dependent on variables such as test machine stiffness and alignment. Speed of testing may also have a significant effect, regardless of the method employed.

Where low-magnification autographic recordings are needed to facilitate measurement of yield point elongation for materials which may have discontinuous yielding, Class C extensometers may be employed.

Halt-of-the-Force Method (for materials exhibiting discontinuous yielding): Apply an increasing force to the specimen at a uniform deformation rate. When the force hesitates, record the corresponding stress as the upper yield strength.

The Halt-of-the-Force Method was formerly known as the Halt-of-the-Pointer Method, the Drop-of-the-Beam Method, and the Halt-of-the-Load Method.

Strain Rate Method (for materials that do not exhibit well-define discontinuous yielding): Attach a Class B2, or better, extensometer to the specimen at the gage marks. Increase the force at a reasonably uniform rate and watch the elongation of the specimen as indicated by the extensometer. Note the force at which the rate of elongation shows a sudden increase.

8.1.10.4 Yield point elongation

Calculate the yield point elongation from the stress-strain diagram or data by determining the difference in strain between the upper yield strength (first zero slope) and the onset of uniform strain hardening.

The stress-strain curve of a material exhibiting only a hint of the behavior causing YPE may have an inflection at the onset of yielding with no point where the slope reaches zero. Such a material has no YPE, but may be characterized as exhibiting an inflection. Materials exhibiting inflections, like those with measurable YPE, may, in certain applications, acquire an unacceptable surface appearance during forming.

8.1.10.5 Tensile strength

Calculate the tensile strength by dividing the maximum force carried by the specimen during the tension test by the original cross-sectional area of the specimen.

If the upper yield strength is the maximum stress recorded, and if the stress-strain curve resembles, it is recommended that the maximum stress after discontinuous yielding be reported as the tensile strength. Where this may occur, determination of the tensile strength should be in accordance with the agreement between the parties involved.

8.1.10.6 Elongation

In reporting values of elongation, give both the original gage length and the percentage increase. If any device other than an extensometer is placed in contact with the specimen's reduced section during the test, this shall also be noted.

Example: elongation =30 % increase (50mm gage length)

Elongation results are very sensitive to variables such as:

- speed of testing
- specimen geometry (gage length, diameter, width, and thickness)
- heat dissipation (through grips, extensometers, or other devices in contact with the reduced section),
- surface finish in reduced section (especially burrs or notches)
- alignment
- fillets and tapers

Parties involved in comparison or conformance testing should standardize the above items, and it is recommended that use of ancillary devices (such as extensometer supports) which may remove heat from specimens be avoided.

When the specified elongation is greater than 3 %, fit ends of the fractured specimen together carefully and measure the distance between the gage marks to the nearest 0.25 mm for gage lengths of 50 mm and under, and to at least the nearest 0.5 % of the gage length for gage lengths over 50 mm. A percentage scale reading to 0.5 % of the gage length may be used.

When the specified elongation is 3 % or less, determine the elongation of standard round specimens using the following procedure, except that the procedure given in 7.8.2 may be used instead when the measured elongation is greater than 3 %.

The measure of the original gage length of the specimen can be made to the nearest 0.05 mm, and so remove partly torn fragments that will interfere with fitting together the ends of the fractured specimen or with making the final measurement.

Fit the fractured ends together with matched surfaces and apply a force along the axis of the specimen sufficient to close the fractured ends together. If desired, this force may then be removed carefully, provided the specimen remains intact.

Measure the final gage length to the nearest 0.05 mm and report the elongation to the nearest 0.2 %.

If any part of the fracture takes place outside of the middle half of the gage length or in a punched or scribed mark within the reduced section, the elongation value obtained may not be representative of the material. In acceptance testing, if the elongation so measured meets the minimum requirements specified, no further testing is required, but if the elongation is less than the minimum requirements, discard the test and retest.

Elongation at fracture is defined as the elongation measured just prior to the sudden decrease in force associated with fracture. For many ductile materials not exhibiting a sudden decrease in force, the elongation at fracture can be taken as the strain measured just prior to when the force falls below l0 % of the maximum force encountered during the test.

Elongation at fracture shall include elastic and plastic elongation and may be determined with autographic or automated methods using extensometers. Use a class 82 or

better extensometer for materials having less than 5 % elongation, a class C or better extensometer for materials having elongation greater than or equal to 5 % but less than 50 %, and a class D or better extensometer for materials having 50 % or greater elongation. In all cases, the extensometer gage length shall be the nominal gage length required for the specimen being tested. Due to the lack of precision in fitting fractured ends together, the elongation after fracture using the manual methods of the preceding paragraphs may differ from the elongation at fracture determined with extensometers.

Percent elongation at fracture may be calculated directly from elongation at fracture data and be reported instead of percent elongation. However, these two parameters are not interchangeable. Use of the elongation at fracture method generally provides more repeatable results.

8.1.10.7 Reduction of area

The reduced area used to calculate reduction of area shall be the minimum cross section at the location of fracture.

Specimens with originally circular cross sections, must be fit the ends of the fractured specimen together and measure the reduced diameter to the same accuracy as the original measurement.

Because of anisotropy, circular cross sections often do not remain circular during straining in tension. The shape is usually elliptical, thus, the area may be calculated by $\pi * d_1 * d_2/4$, where d_1, and d_2 are the major and minor diameters, respectively.
The difference between the area thus found and the area of the original cross section expressed as a percentage of the original area is the reduction of area.

If any part of the fracture takes place outside the middle half of the reduced section or in a punched or scribed gage mark within the reduced section, the reduction of area value obtained may not be representative of the material. In acceptance testing, if the reduction of area so calculated meets the minimum requirements specified, no further testing is required, but if the reduction of area is less than the minimum requirements, discard the test results and retest.

Results of measurements of reduction of area shall be rounded. In the absence of a specified procedure, it is recommended that reduction of area test values in the range from 0 to 10 % be rounded to the nearest 0.5 % and test values of 10 % and greater to the nearest 1 %.

Rounding reported test data for yield strength and tensile strength, test data should be rounded. In the absence of a specified procedure for rounding the test data, one of the procedures described in the following paragraphs is recommended. For test values up to 500 MPa, round to the nearest 1 MPa; for test values of 500 MPa and up to 1000 Mpa, round to the nearest 5 MPa; for test values of 1000 MPa and greater, round to the nearest 10 MPa.

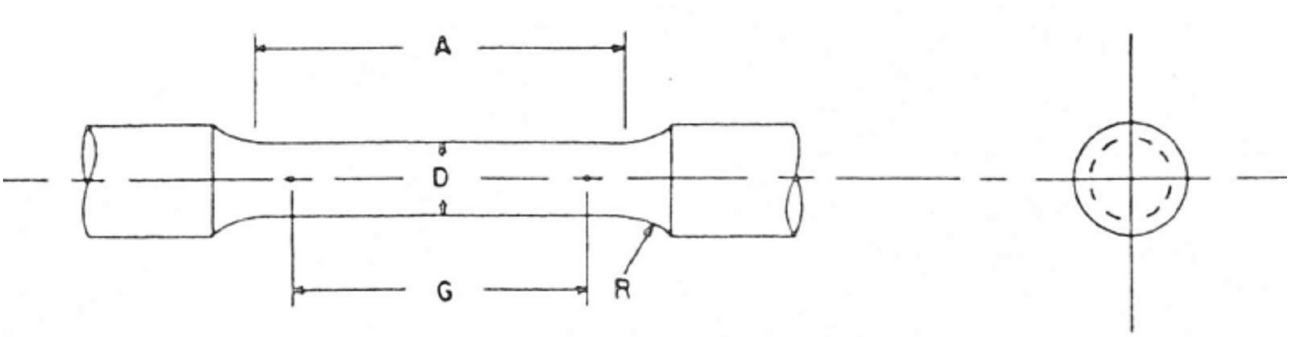

Dimension, mm					
	Standard Specimen	**Small-Size Specimens Proportional to Standard**			
	12,5	9	6	4	2,5
G – Gage length	62,5 ± 0,1	45,0 ± 0,1	30,0 ± 0,1	20,0 ± 0,1	12,5 ± 0,1
D – Diameter (Note1)	12,5 ± 0,2	9,0 ± 0,1	6,0 ± 0,1	4,0 ± 0,1	2,5 ± 0,1
R – Radius of fillet, min	10	8	6	4	2
A - Length of reduced section, min (Note 2)	75	54	36	24	20

Fig. 8.1.5 Standard 12.5-mm Round Tension Test Specimen with Gage Lengths Five Times the Diameters (5D), and Examples of Small-Size Specimens Proportional to the Standard Specimen

Note 1 - The reduced section may have a gradual taper from the ends toward the center, with the ends not more than 1 % larger in diameter than the center (controlling dimension).

Note 2 - If desired, the length of the reduced section may be increased to accommodate an extensometer of any convenient gage length. Reference marks for the measurement of elongation should, nevertheless, be spaced at the indicated gage length.

8.2 ASTM E10: Standard test method for Brinell Hardness of metallic material

8.2.1 Scope

This test method covers the determination of the Brinell hardness of metallic material.

In Brinell hardness test an indenter is forced into the surface of a test piece and the diameter of the indentation d left in the surface after removal of the test force, F is measured. The Brinell hardness number is proportional to the test force and the curved surface area of the indentation.

The Brinell hardness test is an empirical indentation hardness test. Brinell hardness tests provide useful information about metallic materials. This information may correlate to tensile strength, wear resistance, ductility, or other physical characteristics of metallic materials, and may be useful in quality control and selection of materials. Brinell hardness testing at the specific location on a part may not represent the physical characteristics of the whole part or end product. Brinell hardness tests are considered satisfactory for acceptance testing of commercial shipments, and they have been used extensively in industry for this purpose.

8.2.2 Principle

In Brinell hardness test an indenter (hardened steel ball or tungsten carbide ball with diameter D) is forced into the surface of a test piece and the diameter of the indentation d left in the surface after removal of the test force, F is measured.

The steel or tungsten carbide ball may be used for materials with a Brinell hardness not exceeding 450. The tungsten carbide ball shall be used for materials with a Brinell hardness greater than 450 and less than or equal to 650.

For Brinell hardnesses above 450, a significant difference is observed between results obtained using steel balls and those obtained using tungsten carbide balls.

A number, defined Brinell hardness number, which is proportional to the quotient obtained by dividing the test force by the curved surface area of the indentation which is assumed to be spherical and of the diameter of the ball.

$$\text{HBS or HBW} = Constant \cdot \frac{Testforce}{Surface\ \ area\ \ of\ \ indentation} = 0.102 \cdot \frac{2F}{\pi \cdot D \cdot \left(D - \sqrt{D^2 - d^2}\right)}$$

where:

D : diameter of the ball, mm

F : test force, N

d : mean diameter of the indentation, mm

h : depth of the indentation $h = \frac{D - \sqrt{D^2 - d^2}}{2}$

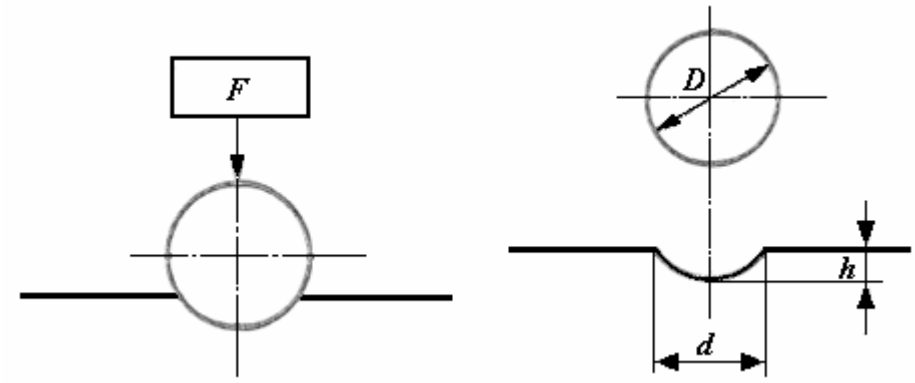

Fig 8.2.1 Principle of test

The Brinell hardness is denoted by the following symbols:

HBS in cases where a steel ball is used.

HBW in cases where a tungsten carbide ball is used.

In former standards, in cases when a steel ball was used, the Brinell hardness was denoted by HB.

The symbol HBS or HBW is preceded by the hardness value. When conditions other than those are used, the hardness value is supplemented by an index indicating the test conditions in the order:

- Diameter of the ball, in millimetres
- A value representing the test force in kilogram-force
- Duration of loading, in seconds

Brinell hardness numbers vary with the test force used; however, test results will generally be in agreement when the ratio of the test force to the square of the ball diameter is held constant.

The Brinell hardness number corresponding to various diameters of indentations for 29.4 kN (3000 kgf), 14.7 kN (1500 kgf), and 4.90 kN (500 kgf) test forces making it unnecessary to calculate for each test the value of the Brinell hardness number are tabulated, by the above equation when these forces are used with a 10 mm diameter ball.

8.2.3 Apparatus

Testing Machine-Equipment for Brinell hardness testing usually consists of a testing machine which supports the test specimen and applies an indenting force to a ball in contact with the specimen. The design of the testing machines shall be such that no rocking or lateral movement of the indenter or specimen occurs while the force is being applied.

The design of the testing machine shall ensure that the force to the indenter shall be applied smoothly and without impact forces. Precautions shall be taken to prevent a momentary high test force caused by the inertia of the system, hydraulic system overshoot, etc. See equipment manufacturer's instruction manual for a description of the machine's characteristics, limitations, and respective operating procedure.

8.2.3.1 Brinell balls

The standard ball for Brinell hardness testing shall be 10mm in diameter with a deviation from this value of not more than 0.005 mm in any diameter. The ball shall be polished and free of surface defects. Smaller balls having the diameters and tolerances indicated in table 8.2.1

Ball Diameter	Tolerance
mm	mm
10	± 0.005
5	± 0.004
2.5	± 0.003
2	± 0.003
1	± 0.003

Tab. 8.2.1 Tolerances for Brinell hardness ball

A hardened steel ball having a hardness of at least 850 HV10 using a 98.07 N (10 kgf) test force may be used on material having a Brinell hardness value not over 450, or a tungsten carbide ball having a hardness of 1500 HV10 on material over 450.
The Brinell test is not recommended for material having hardness over 650 HBW.
The chemical composition of tungsten carbide balls shall be:

Tungsten Carbide (WC)	Balance
Cobalt (Co)	5.0 to 7.0 %
Total other Carbides	2.0 % max

If a ball is used in a test of a specimen which shows a Brinell hardness number greater than the limit for the ball as detailed before, the results of the test shall be considered invalid and the ball shall be discarded.

8.2.3.2 Measuring device

The divisions of the micrometer scale of the microscope or other measuring devices used for the measurement of the diameter of the indentations shall be such as to permit the direct measuring of the diameter to 0.1 mm and the estimation of the diameter to 0.05 mm. This requirement applies to the construction of the device only and is not a requirement for measurement of the indentation.
When direct verification is used, the Brinell hardness testing machine is acceptable for use over a test force range within which the error in test force does not exceed +l %. When indirect verification is used, the Brinell hardness machine is acceptable for use over a test

force range within which the mean hardness value obtained is within +3 % of the Brinell hardness of the standardized test blocks used.

8.2.4 Test specimen

There is no standard shape or size for a Brinell test specimen. The specimen upon which the indentation is made shall conform to the following:

The thickness of the specimen tested shall be such that no bulge or other marking showing the effect of the test force appears on the side of the piece opposite the indentation. As a general rule, the thickness of the specimen shall be at least ten times the depth of the indentation (Table 8.2.2).

Minimum thickness of specimen	**Minimum hardness for which the Brinell test may safely be made vs Load**		
mm	*29.4 kN (3000 kg)*	*14.7kN (1500 kg)*	*4.9 kN (500 kg)*
1.6	602	301	100
3.2	301	150	50
4.8	201	100	33
6.4	150	75	25
8.0	120	60	20
9.6	100	50	17

Tab. 8.2.2 Minimum thickness requirements for Brinell hardness test

When necessary, the surface on which the indentation is to be made shall be filed, ground, machined or polished with abrasive material so that the edge of the indentation shall be clearly defined to permit the measurement of the diameter to the specified accuracy. Care should be taken to avoid overheating or cold working the surface.

8.2.5 Procedure

Typically, the force in the standard Brinell test shall be 29.42 kN (3000 kgf), 14.7 kN (1500 kgf), or 4.90 kN (500 kgf). It is recommended that the diameter of the indentation be between 24 and 60% of the ball diameter. A lower limit in indentation diameter is necessary because of the risk in damaging the ball and difficulty measuring the indentation. The upper limit is necessary because of a reduction in sensitivity as the

diameter of the indentation approaches the ball diameter. The thickness and spacing requirements may determine the maximum permissible diameter of indentation for a specific test. Table 8.2.3 gives standard test forces and approximate Brinell hardness numbers for the above range of indentation diameters. It is not mandatory that the Brinell test conform to these hardness ranges, but it should be realized that different Brinell hardness numbers may be obtained for a given material by using different forces on a 10 mm diameter ball.

Ball Diameter	**Force**	**Recommended Range**
mm	*kN*	*HB*
10	29.42	96 to 600
10	14.7	48 to 300
10	4.9	16 to 100

Tab. 8.2.3 Standard test forces for hardness recommended range

For the purpose of obtaining a continuous scale of values it may be desirable, however, to use a single force to cover the complete range of hardness for a given class of materials. For softer metals, forces of 2.45 kN (250 kgf), 1.23 kN (125 kgf), or 0.981 kN (100 kgf) are sometimes used.

For testing thin or small specimens, a ball less than l0 mm in diameter is sometimes used. Such tests (which are not to be regarded as standard tests) will approximate the standard tests more closely if the relation between the applied force,F, measured in Newtons, and the diameter of the ball, D, measured in millimetres is the same as in the standard tests, where:

$0.l02F/D^2 = 30$ for 29.42 kN force and 10 mm ball

$0.102F/D^2 = 15$ for 14.72 kN force and 10 mm ball

$0.102F/D^2 = 5$ for 4.90 kN force and 10 mm ball

When indentations are made on a curved surface, the minimum radius of curvature of the surface shall be not less than 2½ times the diameter of the ball. Indentations made on curved surfaces may be slightly elliptical rather than circular in shape. The measurements of the indentation shall be taken as the mean of the major and minor axes.

The distance of the center of the indentation from the edge of the specimen or edge of another indentation shall be at least two and one half times the diameter of the indentation. Application of test force to the specimen must be uniformly taking precautions to prevent a momentary overload of the system. Apply the full test force for 10 to 15 s.

If a duration of test force application other than l0 to 15 s is used, results of the test shall be reported using the nomenclature outlined.

A correct alignment is made if the angle between the indentor force line and the surface of the specimen shall be 90 + 2°.

8.2.6 Measurement of indentation

In the Brinell hardness test, two diameters of the indentation at right angles to each other shall be measured and their mean value used as a basis for calculation of the Brinell hardness number for flat specimens. If the largest and smallest diameters for two readings of the same indentation differ by 0.1 mm or more, refer to the material specifications for further guidance. For routine tests and for tests to determine compliance with a material or product specification, the diameter of the indentation shall be estimated to 0.05 mm.

These measurements are usually made with a low-magnification portable measuring device (approximately 20x) having a fixed scale in the eyepiece. If a more accurate determination is needed, as in referee or standardization tests, a laboratory comparator such as a micrometer measuring device is required.

8.3 ASTM E23: Standard test methods for notched bar impact testing of metallic materials

8.3.1 Scope

This test method describe notched-bar impact testing of metallic material by the Charpy (simple-beam) apparatus.

The essential features of an impact test are: a suitable specimen-(specimens of several different types are recognized), an anvil or support on which the test specimen is placed to receive the blow of the moving mass, a moving mass that has been released from

a sufficient height to cause the mass to break the specimen placed in its path, and a device for measuring the energy absorbed by the broken specimen.

These test methods of impact testing relate specifically to the behavior of metal when subjected to a single application of a load resulting in multiaxial stresses associated with a notch, coupled with high rates of loading and in some cases with high or low temperatures. For some materials and temperatures, impact tests on notched specimens have been found to predict the likelihood of brittle fracture better than tension tests or other tests used in material specifications.

8.3.2 Apparatus

The testing machine shall be a pendulum type of rigid construction and of capacity more than sufficient to break the specimen in one blow.

The machine frame shall be equipped with a bubble level or a machined surface suitable for establishing levelness of the axis of pendulum bearings or, alternatively, the levelness of the axis of rotation of the pendulum may be measured directly. The machine shall be level to within 3:1000 and securely bolted to a concrete floor not less than 150 mm thick or, when this is not practical, the machine shall be bolted to a foundation having a mass not less than 40 times that of the pendulum. The bolts shall be tightened as specified by the machine manufacturer.

The machine shall be furnished with scales graduated either in degrees or directly in energy on which readings can be estimated in increments of 0.25 % of the energy range or less. The scales may be compensated for windage and pendulum friction. The error in the scale reading at any point shall not exceed 0.2 % of the range or 0.4 % of the reading, whichever is larger.

The total friction and windage losses of the machine during the swing in the striking direction shall not exceed 0.75 % of the scale range capacity, and pendulum energy loss from friction in the indicating mechanism shall not exceed 0.25 % of scale range capacity. When hanging free, the pendulum shall hang so that the striking edge is within 2.5 mm of the position where it would just touch the test specimen. When the indicator has been positioned to read zero energy in a free swing, it shall read within 0.2 % of scale range

when the striking edge of the pendulum is held against the test specimen. The plane of swing of the pendulum shall be perpendicular to the transverse axis of the Charpy specimen anvils or Izod vise within 3:1000.

Transverse play of the pendulum at the striker shall not exceed 0.75 mm under a transverse force of 4 % of the effective weight of the pendulum applied at the center of strike. Radial play of the pendulum bearings shall not exceed 0.075 mm. The tangential velocity (the impact velocity) of the pendulum at the center of the strike shall not be less than 3 nor more than 6 m/s.

Before release, the height of the center of strike above its free hanging position shall be within 0.4 % of the range capacity divided by the supporting force. If windage and friction are compensated for by increasing the height of drop, the height of drop may be increased by not more than 1%.

The mechanism for releasing the pendulum from its initial position shall operate freely and permit release of the pendulum without initial impulse, retardation, or side vibration. If the same lever that is used to release the pendulum is also used to engage the brake, means shall be provided for preventing the brake from being accidentally engaged. Means shall be provided to locate and support the test specimen against two anvil blocks in such a position that the center of the notch can be located within 0.25 mm of the midpoint between the anvils. The supports and striking edge shall be of the forms and dimensions shown in figure 8.3.1.

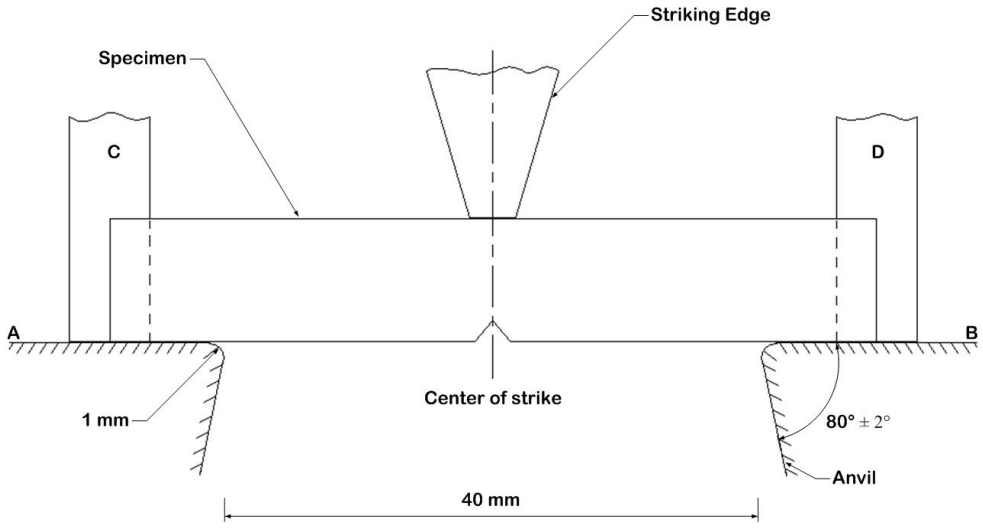

Fig. 8.3.1 Charpy Striking Tup

Other dimensions of the pendulum and supports should be such as to minimize interference between the pendulum and broken specimens. The center line of the striking edge shall advance in the plane that is within 0.40 mm of the midpoint between the supporting edges of the specimen anvils. The striking edge shall be perpendicular to the longitudinal axis of the specimen within 5:1000. The striking edge shall be parallel within 1:1000 to the face of a perfectly square test specimen held against the anvil.

8.3.3 Specimen clearance

To ensure satisfactory results when testing materials of different strengths and compositions, the test specimen shall be free to leave the machine with a minimum of interference and shall not rebound into
the pendulum before the pendulum completes its swing.

The choice of specimen depends to some extent upon the characteristics of the material to be tested. A given specimen may not be equally satisfactory for soft nonferrous metals and hardened steels; therefore, a number of types of specimens are recognized. In general, sharper and deeper notches are required to distinguish differences in the more ductile materials or with lower testing velocities.
Pendulums used on Charpy machines are of three basic designs.

When using a C-type pendulum or a compound pendulum, the broken specimen will not rebound into the pendulum and slow it down if the clearance at the end of the specimen is at least l3 mm or if the specimen is deflected out of the machine.

When using the U-type pendulum, means shall be provided to prevent the broken specimen from rebounding against the pendulum. In most U-type pendulum machines, the shrouds should be designed and installed to the following requirements: have a thickness of approximately 1.5 mm have a minimum hardness of 45 HRC have a radius of less than 1.5 mm at the underside corners, and be so positioned that the clearance between them and the pendulum overhang (both top and sides) does not exceed 1.5 mm.

8.3.3.1 Specimen machining

When heat-treated materials are being evaluated, the specimen shall be finish machined, including notching, after the final heat treatment, unless it can be demonstrated that there is no difference when machined prior to heat treatment.

Notches shall be smoothly machined but polishing has proven generally unnecessary. However, since variations in notch dimensions will seriously affect the results of the tests, it is necessary to adhere to the tolerances given in figure 8.3.2.

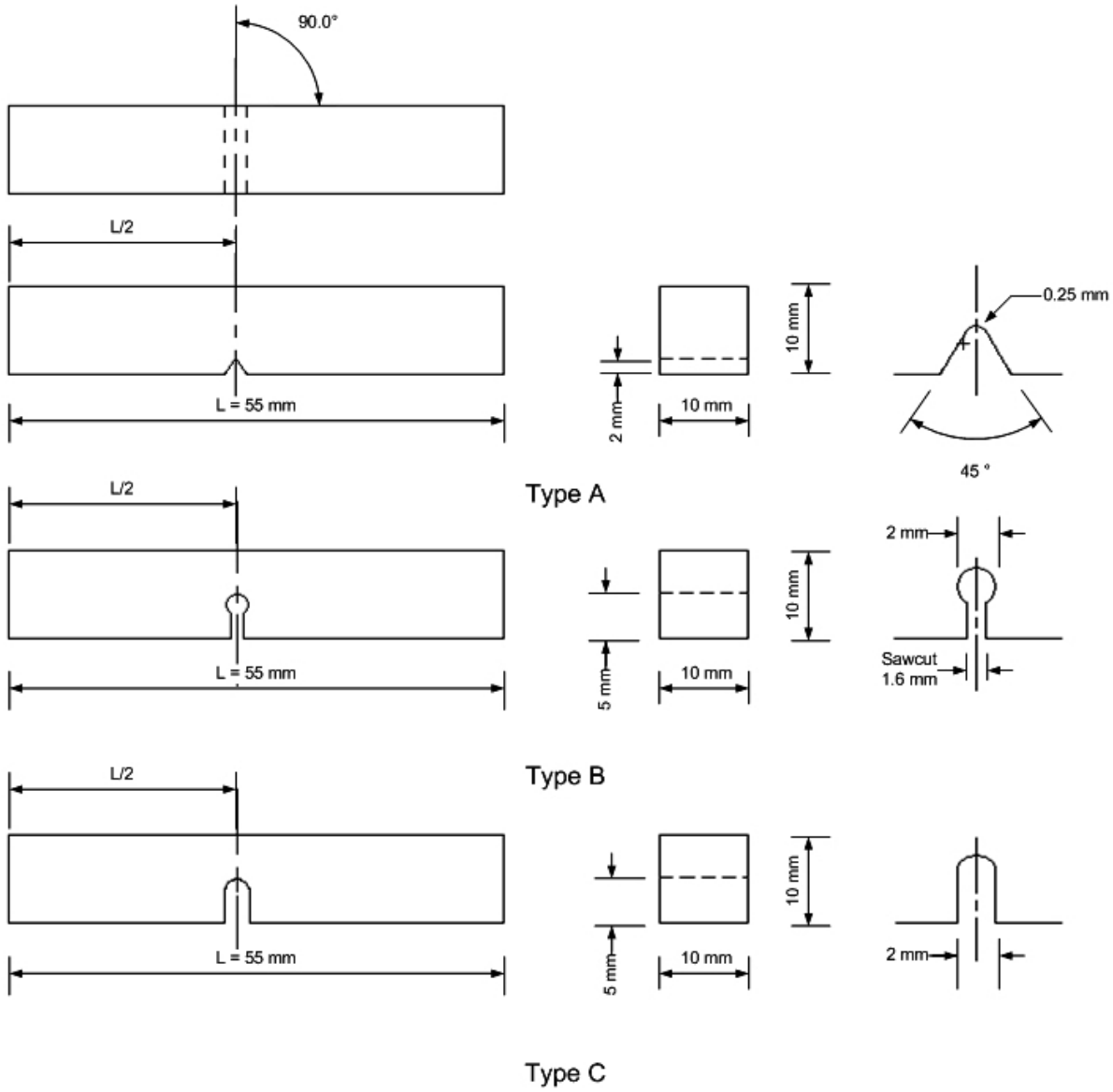

Fig. 8.3.2 Charpy (simple-beam) impact test specimens, types A, B, and C

Specimen dimension are strictly specified in notched bar impact test, the length of specimen (L) is 55mm with to the tolerances of +0, -2,5 mm, the centering of notch (L/2) have tolerance of ±1 mm. Cross-section dimensions are 10 mm ±0,075 mm, and adjacent sides shall be at 90° ±0,1°.

Notch length to edge is produce at 90 ±2°, with angle of notch tolerance of ±1°, and radius of notch ±0,025 mm. Notch depth in type A specimen is 2mm ±0,025 mm, in types B and C specimen are 5 mm ±0,075 mm.

Finish requirements 2 μm on notched surface and opposite face; 4 μm on other two surfaces.

In keyhole specimens, the round hole shall be carefully drilled with a slow feed. The slot may be cut by any feasible method. Care must be exercised in cutting the slot to see that the surface of the drilled hole opposite the slot is not marked.

Identification marks shall only be placed in the following locations on specimens: either of the 10 mm square ends; the side of the specimen which faces up when the specimen is positioned in the anvils, or the portion of the side opposite the notch which is at least l0mm away from the center line of the notch. No marking shall be done on any portion of the specimen that is visibly deformed during fracture. An electrostatic pencil may be used for identification purposes, but caution must be taken to avoid excessive heat.

8.3.4 Procedure

The Charpy test procedure may be summarized as follows: the test specimen is removed from its cooling (or heating) medium, if used, and positioned on the specimen supports; the pendulum is released without vibration, and the specimen is broken within 5s after removal from the medium. Information is obtained from the machine and from the broken specimen.

8.3.4.1 Temperature of testing

In most materials, impact values vary with temperature. Unless otherwise specified, tests shall be made at 15 to 32°C. Accuracy of results when testing at other temperatures

requires the following procedure: For liquid cooling or heating fill a suitable container, which has a grid raised at least 25 mm from the bottom, with liquid so that the specimen when immersed will be covered with at least 25 mm of the liquid. Bring the liquid to the desired temperature by any convenient method. The device used to measure the temperature of the bath should be placed in the center of a group of the specimens. Verify all temperature-measuring equipment at least twice annually. When using a liquid medium, hold the specimens in an agitated bath at the desired temperature within +l°C for at least 5 min. When using a gas medium, position the specimens so that the gas circulates around them and hold the gas at the desired temperature within +l°C for at least 30 min. Leave the mechanism used to remove the specimen from the medium in the medium except when handling the specimens.

8.3.4.2 Placement of test specimen in machine

It is recommended that self-centering tongs be used in placing the specimen in the machine. The tongs are specific for V-notch specimens. If keyhole specimens are used, modification of the tong design may be necessary. If an end-centering device is used, caution must be taken to ensure that low-energy high-strength specimens will not rebound off this device into the pendulum and cause erroneously high recorded values. Many such devices are permanent fixtures of machines, and if the clearance between the end of a specimen in test position and the centering device is not approximately 13 mm, the broken specimens may rebound into the pendulum.

8.3.4.3 Operation of the machine

Set the energy indicator at the maximum scale reading; take the test specimen from its cooling (or heating) medium, if used; place it in proper position on the specimen anvils; and release the pendulum smoothly. This entire sequence shall take less than 5 s if a cooling or heating medium is used.

With the exception described as follows, any specimen, which when struck by a single blow does not separate into two pieces, shall be reported as unbroken. If the specimen can be separated by force applied by bare hands, the specimen may be

considered as having been separated by the blow. Impact values from unbroken specimens with absorbed energy less than 80% of the machine capacity may be averaged with values from broken specimens. If the individual values are not listed, the percent of unbroken specimens shall be reported with the average. If the absorbed energy exceeds 80% of the machine capacity and the specimen passes completely between the anvils, the value shall be reported as approximate and not averaged with others. If an unbroken specimen does not pass between the machine anvils, the result will be reported as exceeding the stated machine capacity. In no case shall the specimen be struck more than once.

If any specimen jams in the machine, disregard the results and check the machine thoroughly for damage or maladjustment, which would affect its calibration.

To prevent recording an erroneous value caused by jarring the indicator when locking the pendulum in its upright position, read the value from the indicator prior to locking the pendulum for the next test.

8.3.5 Information obtainable from the test

Absorbed Energy-The amount of energy required to fracture the specimen is determined from the machine reading.

8.3.5.1 Lateral expansion

The method for measuring lateral expansion must take into account the fact that the fracture path seldom bisects the point of maximum expansion on both sides of a specimen. One half of a broken specimen may include the maximum expansion for both sides, one side only, or neither. The technique used must therefore provide an expansion value equal to the sum of the higher of the two values obtained for each side by measuring the two halves separately. The amount of expansion on each side of each half must be measured relative to the plane defined by the undeformed portion of the side of the specimen. Expansion may be measured by using a gage. Measure the two broken halves individually. First, though, check the sides perpendicular to the notch to ensure that no burrs were formed on these sides during impact testing; if such burrs exist, they must be removed, for example, by rubbing on emery cloth, making sure that the protrusions to be measured are

not rubbed during the removal of the burr. Next, place the halves together so that the compression sides are facing one another. Take one half and press it firmly against the reference supports, with the protrusions against the gage anvil. Note the reading, then repeat this step with the other broken half, ensuring that the same side of the specimen is measured. The larger of the two values is the expansion of that side of the specimen. Next, repeat this procedure to measure the protrusions on the opposite side, then add the larger values obtained for each side. Measure each specimen.

8.3.5.2 Fracture appearance

The percentage of shear fracture may be determined by any of the following methods:

1. measure the length and width of the cleavage portion of the fracture surface, as shown in figure 8.3.3, and determine the percent shear from either Table I or Table 2 depending on the units of measurement

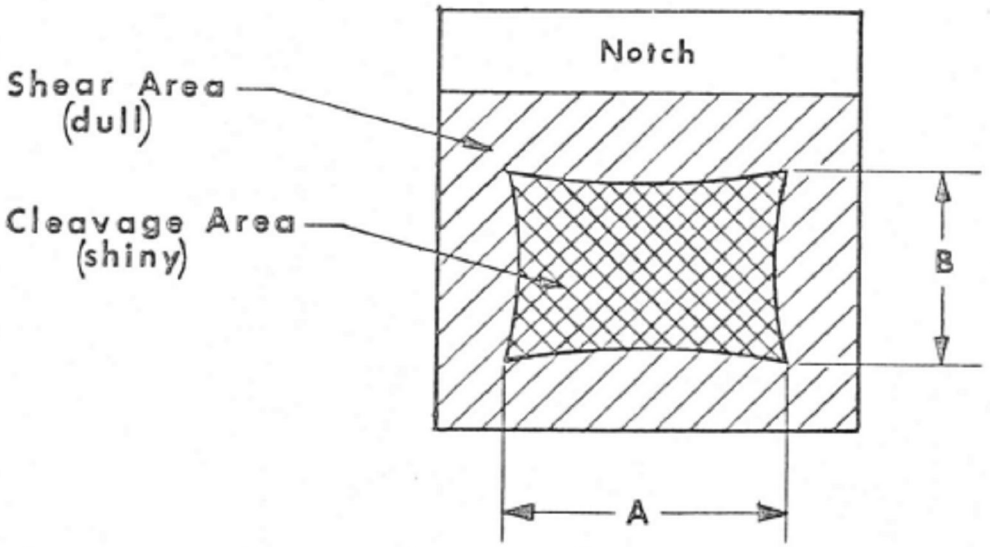

Fig. 8.3.3 Determination of Percent Shear Fracture Measure average dimensions A and B to the nearest 0.5 mm

2. compare the appearance of the fracture of the specimen with a fracture appearance chart such as that shown in figure 8.3.4

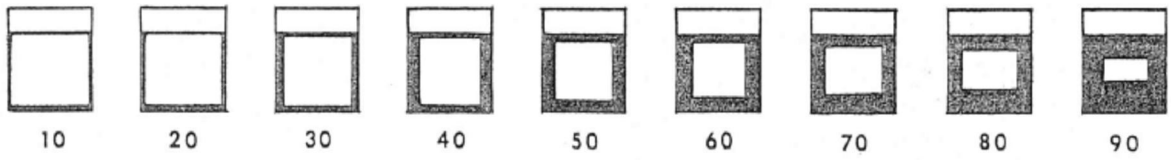

Fig. 8.3.4 Fracture Appearance

3. magnify the fracture surface and compare it to a precalibrated overlay chart or measure the percent shear fracture by means of a planimeter
4. photograph the fracture surface at a suitable magnification and measure the percent shear fracture by means of a planimeter.

8.4 ASTM E45: Standard test methods for determining the inclusion content of steel

8.4.1 Scope

These test methods cover a number of recognized methods for determining the nonmetallic inclusion content of wrought steel. Macroscopical methods include macroetch, fracture, step-down, and magnetic particle tests. Microscopical methods include five generally accepted systems of examination. In these microscopical methods, inclusions are assigned to a category based on similarities in morphology, and not necessarily on their chemical identity. Metallographic techniques that allow simple differentiation between morphologically similar inclusions are briefly discussed. While the methods are primarily intended for rating inclusions, constituents such as carbides, nitrides, carbonitrides, borides, and intermetallic phases may be rated using some of the microscopical methods. In some cases, alloys other than steels may be rated using one or more of these methods; the methods will be described in terms of their use on steels.

These test methods are suitable for manual rating of inclusion content.

Depending on the type of steel and the properties required, either a macroscopical or a microscopical method for determining the inclusion content, or combinations of the two methods, may be found most satisfactory.

These test methods deal only with recommended test methods and nothing in them should be construed as defining or establishing limits of acceptability for any grade of steel.

These test methods cover four macroscopical and five microscopical test methods for describing the inclusion content of steel and procedures for expressing test results.

Inclusions are characterized by size, shape, concentration, and distribution rather than chemical composition. Although compositions are not identified, microscopical methods place inclusions into one of several composition-related categories (sulphides, oxides, and silicates-the last as a type of oxide). Only those inclusions present at the test surface can be detected.

The macroscopical test methods evaluate larger surface areas than microscopical test methods and because examination is visual or at low magnifications, these methods are best suited for detecting larger inclusions. Macroscopical methods are not suitable for detecting inclusions smaller than about 0.40 mm in length and the methods do not discriminate inclusions by type.

The microscopical test methods are employed to characterize inclusions that form as a result of deoxidation or due to limited solubility in solid steel (indigenous inclusions).

These inclusions are characterized by morphological type, that is, by size, shape, concentration, and distribution, but not specifically by composition. The microscopical methods are not intended for assessing the content of exogenous inclusions (those from entrapped slag or refractories) nor for rating the content of carbides, carbonitrides, nitrides, borides, or intermetallic phases, although they are sometimes used for this latter purpose.
Because the inclusion population within a given lot of steel varies with position, the lot must be statistically sampled in order to assess its inclusion content. The degree of sampling must be adequate for the lot size and its specific characteristics. Materials with very low inclusion contents may be more accurately rated by automatic image analysis, which permits more precise microscopical ratings.

8.4.2 Microscopical test methods

Microscopical methods are used to characterize the size, distribution, number, and type of inclusions on a polished specimen surface. This may be done by examining the specimen with a light microscope and reporting the types of inclusions encountered, accompanied by a few representative photomicrographs. This method, however, does not

lend itself to a uniform reporting style. Therefore, standard reference charts depicting a series of typical inclusion configurations (size, type, and number) were created for direct comparison with the microscopical field of view.

No chart can represent all of the various types and forms of inclusions. The use of any chart is thus limited to determining the content of the most common types of inclusions, and it must be kept in mind that such a determination is not a complete metallographic study of inclusions

In addition, photomicrographs may also be taken to characterize the so called background inclusions that were not long enough to measure.

The advantages of the microscopical methods are:

- Inclusions can be characterized as to their size, type, and number.
- Extremely small inclusions can be revealed.

A disadvantage of the microscopical methods is that individual rating fields are very small (0.50 mm^2).This limits the practical size of the specimen as it would simply take a prohibitive number of fields to characterize a large specimen. The result obtained by a microscopical characterization of the inclusions in a large section is governed by chance if local variations in the inclusion distribution are substantial. The end use of the product determines the importance of the microscopical results. Experience in interpreting these results is necessary in order not to exaggerate the importance of small inclusions in some applications.

In determining the inclusion content, it is important to realize that, whatever method is used, the result actually applies only to the areas of the specimens that were examined. For practical reasons, such specimens are relatively small compared with the total amount of steel represented by them. For the inclusion determination to have any value, adequate sampling is just as necessary as a proper method of testing.

Steel often differs in inclusion content not only from heat to heat, but also from ingot to ingot in the same heat and even in different portions of the same ingot. It is essential that the unit lot of steel, the inclusion content of which is to be determined, shall not be larger than one heat. Sufficient samples should be selected to represent the lot adequately. The

exact sampling procedure should be incorporated in the individual product requirements or specifications.

For semifinished products, the specimens should be selected after the material has been sufficiently cropped and suitable discards made. If the locations of the different ingots and portions of ingots in the heat cannot be identified in the lot being tested, random sampling should involve a greater number of test specimens for an equivalent weight of steel. A value for the inclusion content of an isolated piece of steel, even if accurately determined, should not be expected to represent the inclusion content of the whole heat.

The size and shape of the wrought steel product tested has a marked influence on the size and shape of the inclusions. During reduction from the cast shape by rolling or forging, the inclusions are elongated and broken up according to the degree of reduction of the steel cross section Specimens cut lengthwise or parallel to the direction of rolling or forging shall be used.

It may be convenient, in order to obtain more readily comparable results, to forge coupons from larger billets. These forged sections may then be sampled in the same way as rolled sections. Exercise care, however, to crop specimens of sufficient length from the billets for forging; otherwise, there is danger of the shear-dragged ends being incorporated in the specimens. Such distorted material will give a false result in the inclusion determination. To avoid this, it is helpful to saw the ends of the billet length for forging and to take the specimen from the middle of the forged length.

In precipitation hardened steels inclusion may be globular after heat treatment.
Several of the methods described in these test methods require that a specific area of the prepared surface of the specimen be surveyed, and all the significant inclusions observed be recorded and expressed in the results.

8.4.3 Test specimen

The recommended polished surface area of a specimen for the microscopical determination of inclusion content is 160 mm^2. The polished surface must be parallel to the longitudinal axis of the product. In addition, for flat-rolled products, the section shall also

be perpendicular to the rolling plane; for rounds and tubular shapes, the section shall be in the radial direction.

Product section size of the bar greater than 9.5 mm, one-quarter point along the product width is commonly used to provide representative material.

For round sections, the manner of cutting a specimen from a diameter section is shown in Fig. 3. A disk about 9.5 mm thick is cut from the product. The quarter-section indicated in Fig. 3 is cut from the disk and the shaded area is polished. Thus the specimen extends 9.5 mm along the length of the product from the outside to the center.

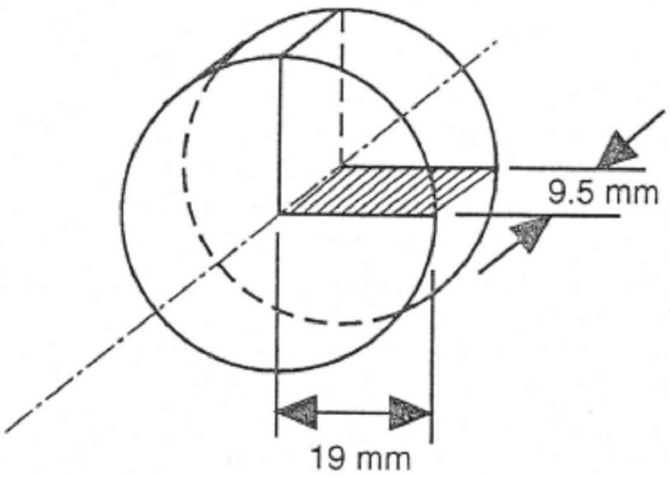

Fig. 8.4.1 Specimen from round section for microscopical test

8.4.3.1 Preparation of specimens

Methods of specimen preparation must be such that a polished, microscopically flat section is achieved in order that the sizes and shapes of inclusions are accurately shown.

To obtain satisfactory and consistent inclusion ratings, the specimen must have a polished surface free of artifacts such as pitting, foreign material (for example, polishing media), and scratches. When polishing the specimen it is very important that the inclusions not be pitted, dragged, or obscured. Specimens must be examined in the as-polished condition, free from the effects of any prior etching (if used).

If the conditions for inclusion evaluation cannot be met in the as-polished condition with the as-received sample, the sample shall be heat-treated to the maximum attainable

hardness before polishing. Necessary precautions shall be taken to eliminate the effects of heat treatment such as scale, decarburization, etc in stainless steels.

8.4.4 Procedure

Either of two techniques may be employed to achieve a 0.50 mm^2 square field of view. One method is to project the 100x microscope image onto a viewing screen that has a square mask with 71.0 mm sides drawn on it. Another option is to use a reticle made for the microscope which will superimpose the required square mask directly onto the field of view.

To begin, outline the required test area on the specimen surface using either an indelible marker or a carbide-tipped scribe. Place the specimen on the microscope stage and start the examination with a field in one of the corners of the marked test area.

Compare this field to the images on Plate I-r. Record the severity level in whole numbers from 0 to 3.0 for each inclusion type (A, B, C, and D) that most resembles the field under observation. It is important to note here that if a field of inclusions falls between two severity levels, its value is rounded down to the lower severity level.

For example, when using Plate I-r, a held that contains fewer inclusions, or less inclusion length than Severity Level Number l, is counted as a 0.

Move the microscope stage to reveal an adjacent held and repeat the comparison procedure.

Continue this process until the required polished surface area of the specimen has been scanned.

A typical scan configuration is shown in figure 8.4.2.

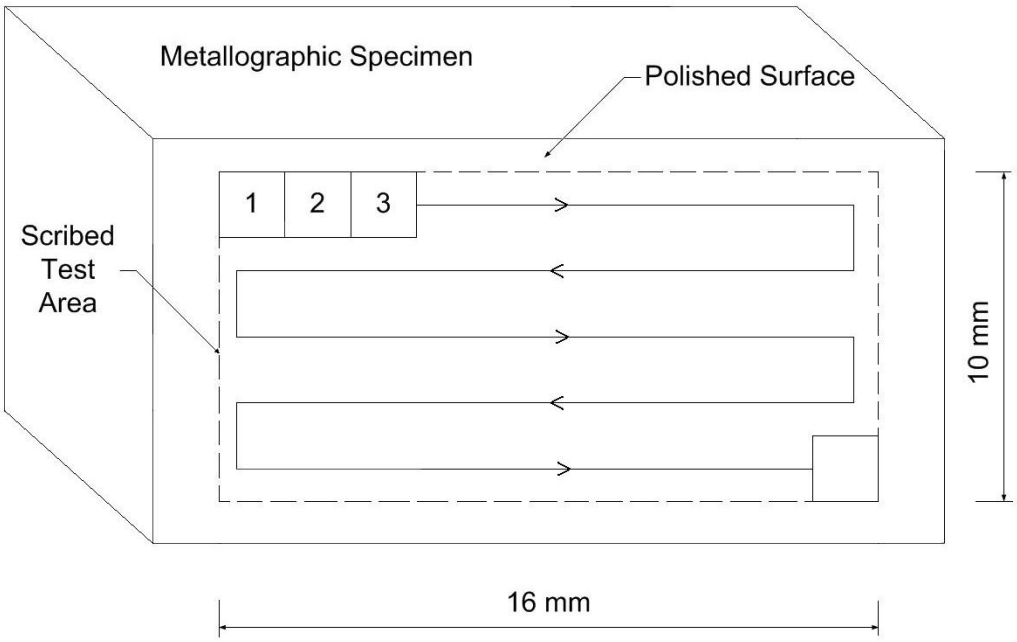

Fig. 8.4.2 Typical scan pattern for microscopical methods

This method requires adjustment of the microscope stage to maximize an inclusion severity level.

That is, the field of view is adjusted using the microscope stage controls, such that inclusions are moved inside the square mask in order to locate the worst field. In practice, the rater is actually scanning the specimen and stopping only when a potential worst field of each type and thickness is in view.

The minimum inclusion lengths that determine the Severity Level Numbers are printed on plate I-r and listed in table 8.4.1.

Severity Level	Total Length in One Field at 100X min, mm			Number of inclusions in One Field, min
	Type A	Type B	Type C	Type D
½	3.7	1.7	1.8	1
1	12.7	7.7	7.6	4
1½	26.1	18.4	17.6	9
2	43.6	34.3	32.0	16
2½	64.9	55.5	51.0	25
3	89.8	82.2	74.6	36
3½	118.1	114.7	102.9	49
4	149.8	153.0	135.9	64
4½	189.8	197.3	173.7	81
5	223.0	247.6	216.3	100

Tab. 8.4.1 Minimum for Severity Level Numbers

Inclusion width parameters for classification into the Thin or Heavy category are listed in tabulated. An inclusion whose width varies from Thin to Heavy along its length shall be placed in the category that best represents its whole. That is to say, if more than half its length falls into the Heavy range, classify it as Heavy. Although Method A was originally designed to rate inclusions in whole numbers, various standards permit rating to t/z severity level numbers.

The typical chemical types of inclusions listed at the top of Plate I-r for Categories A, B, C, and D are not meant to suggest that knowledge of inclusion composition is necessary. In this method, inclusions are assigned to a category based on similarities in morphology and not on their chemical identity. Type A (sulphide) and Type C (silicate) inclusions are very similar in size and shape. Therefore, discrimination between these types should be aided by metallographic techniques, such as viewing the questionable inclusions with darkfield illumination (or cross polarizers) where properly polished sulphide inclusions are dark and silicate inclusions appear luminescent. A second technique is to note the hue of the inclusions; sulphides are generally light grey and silicates are very dark or sometimes glassy in appearance. This test method may be used to rate non-traditional types of inclusions based on their size and shape; that is, sulphides that have been

subjected to shape, control treatments, or encapsulated oxides. In addition, borides, carbides, nitrides, or the like may also be rated. It is required, however, that the results clearly reflect that other than the traditional types of nonmetallic inclusions, as depicted on Plate I-r, have been rated.

Classify discontinuous-type stringer inclusions of Types B or C as two distinct inclusions when they are separated by at least 40 μm (or offset by more than 15 μm) on the specimen surface. If two or more inclusions of the same type (A, B, or C) appear in one microscope field, their summed length determines the severity level number. Usually, direct comparison with Plate I-r will establish the severity levels without the necessity for measurements.

The averages of the worst fields for each inclusion type in all the specimens of the lot shall be calculated in accordance with the Severity Level Numbers given at the sides of Plate I-r or table 8.4.1.

The fields shown in Plate I-r represent the total lengths of the A inclusions, the total stringer lengths of B and C inclusions, the number of D inclusions, and their respective limiting widths or diameters. If any inclusions are present that are longer than the fields shown in Plate I-r, their lengths shall be recorded separately. If their widths or diameters are greater than the limiting values shown in Plate I-r, they shall be recorded separately.

Note that an oversize A, B, or C inclusion or inclusion stringer still contributes to the determination of a field's severity level number. Therefore, if an A, B, or C inclusion is oversized either in length or thickness that portion that is within the held boundaries shall be included in the appropriate Thin or Heavy severity level measurement. Likewise, if an oversize D inclusion is encountered in a field, it is also included in the count that determines the D heavy rating. For reference, illustrations of large, globular oxides appear at the bottom of Plate I-r. A Type D globular oxide may not exceed an aspect ratio of 5: 1.

Chapter 9

Report

9.1 Tension test

This test method is used to determine the tensile strength in metallic material, at room temperature. In particular, the parameters determined are: the yield stress $R_{p0.2\%}$, the tensile strength R_m, the elongation and E 4d, and the section reduction Z%.

The room temperature must be maintained at 25 ° C, as specified in ASTM E8M.

Specimen	**Load**	**R_m**	**Load**	**R_p 0.2%**	**E 4d**	**Z**
-	*kN*	*MPa*	*kN*	*MPa*	-	*%*
H900	167.90	1368	153.86	1254	16	54
H925	160.22	1306	147.56	1202	15	59
H1025	141.54	1153	137.21	1118	17	64
H1075	136.12	1109	133.73	1090	17	66
H1100	134.19	1094	131.43	1071	17	66
H1150	121.82	993	113.51	925	19	70

Tab.9.1.1 Tension test report in 15-5PH VAR remelted specimens, in heat treatment condition.

Specimen	**Load**	**R_m**	**Load**	**R_p 0.2%**	**E 4d**	**Z**
-	*kN*	*MPa*	*kN*	*MPa*	-	*%*
H900	172.8	1408	157.60	1284	15	50
H925	160.80	1310	151.74	1236	16	56
H1025	140.32	1143	137.17	1118	18	60
H1075	135.86	1107	132.99	1084	17	60
H1100	132.19	1077	129.08	1052	17	78
H1150	125.64	1024	116.78	952	18	63

Tab.9.1.2 Tension test report in 15-5PH ESR remelted specimens, in heat treatment condition.

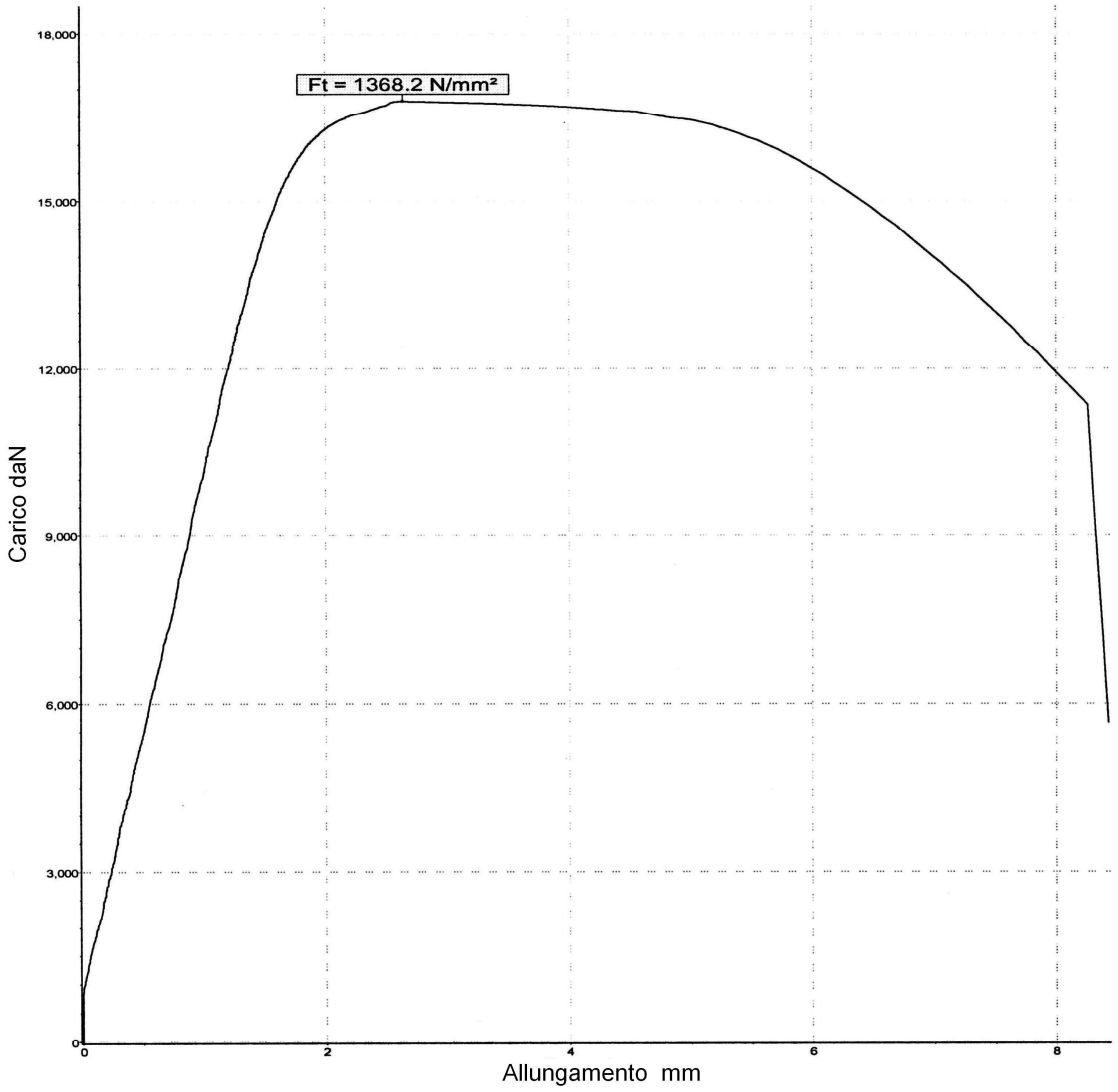

Fig. 9.1.1 Tension test load-elongation in 15-5PH VAR remelted specimens, in H900 heat treatment condition (ageing parameters: T = 482 ° C, t = 60min)

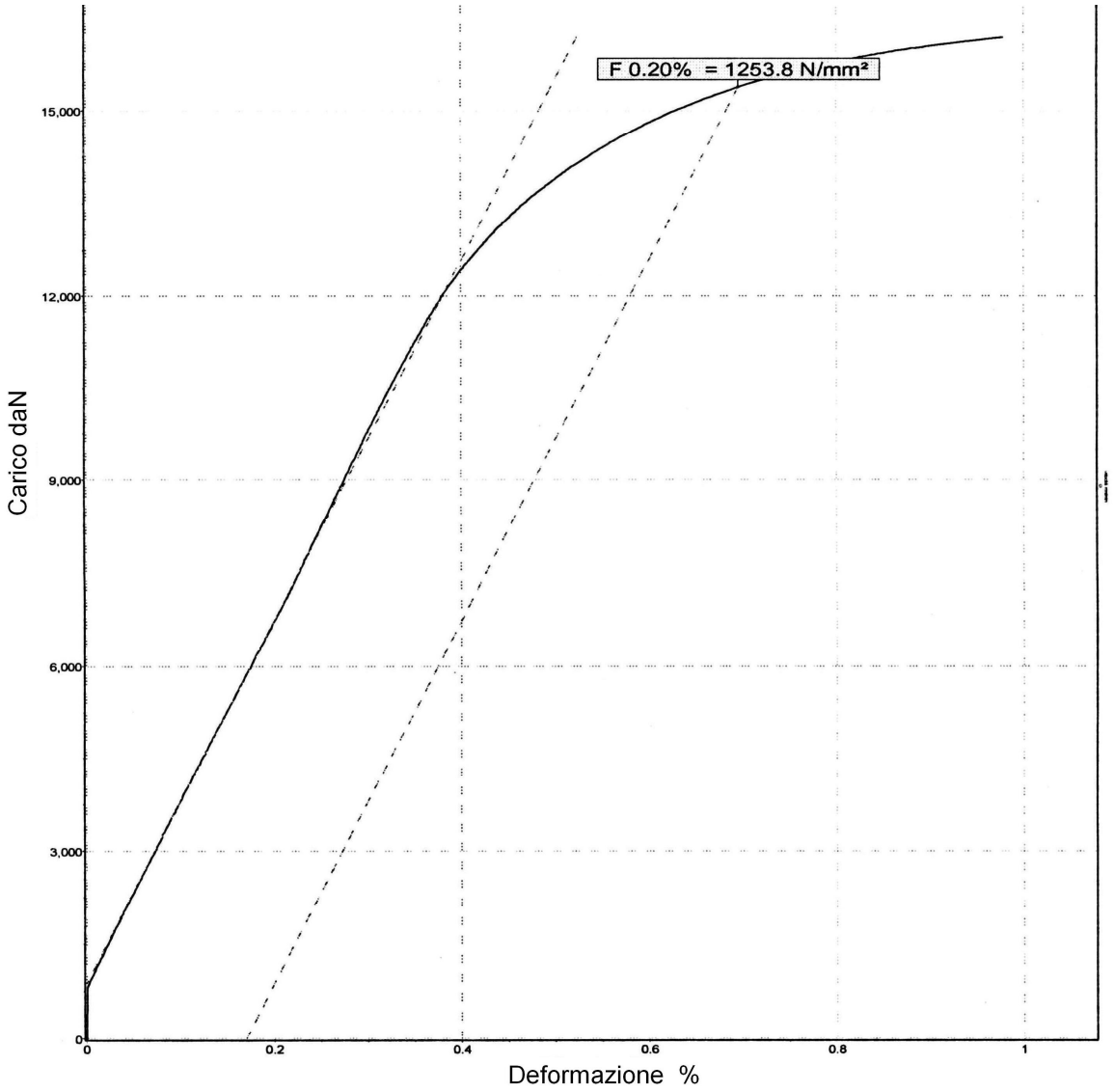

Fig. 9.1.2 Tension test load-deformation in 15-5PH VAR remelted specimens, in H900 heat treatment condition (ageing parameters: T = 482 ° C, t = 60min)

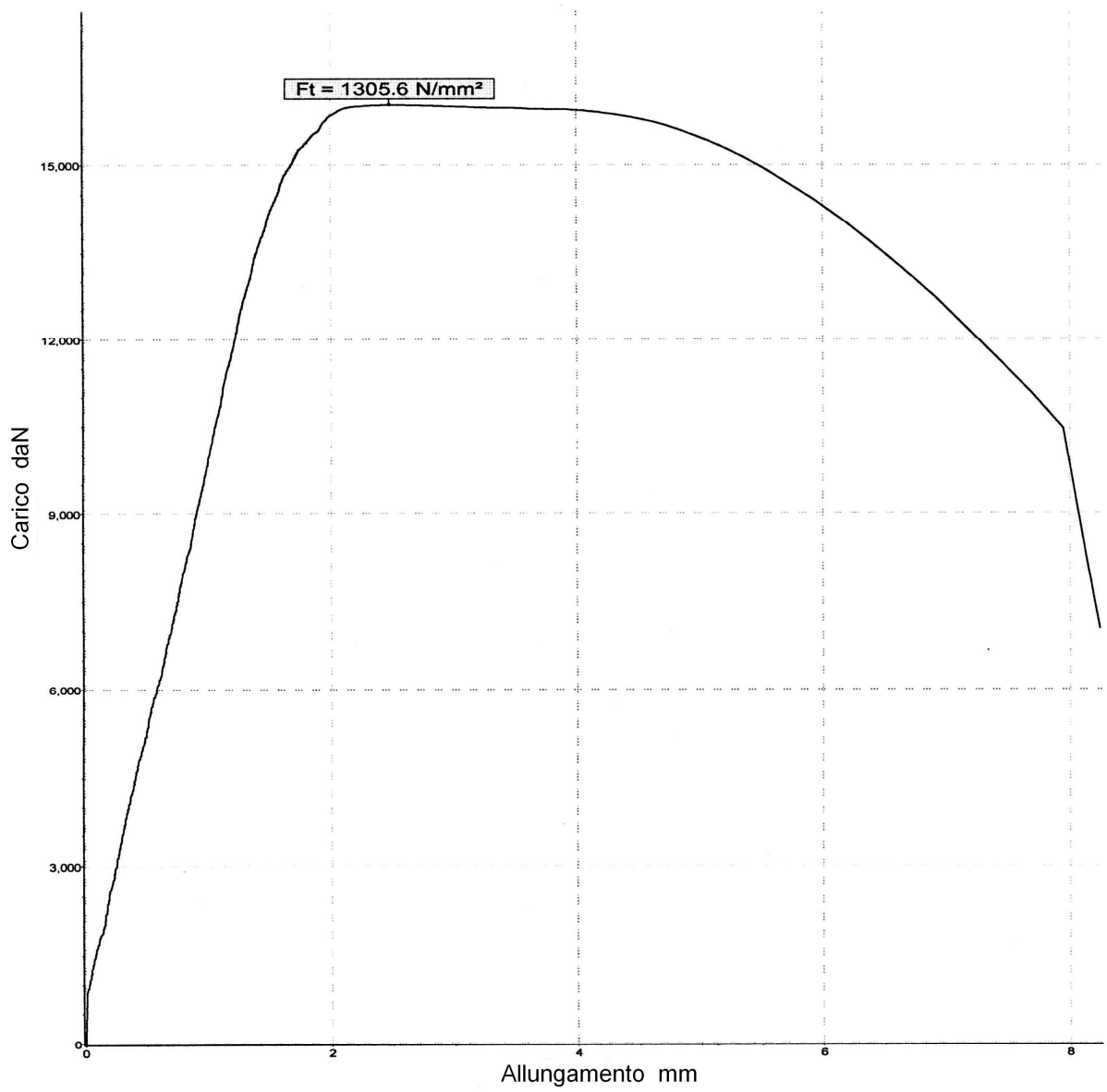

Fig. 9.1.3 Tension test load-elongation in 15-5PH VAR remelted specimens, in H925 heat treatment condition (ageing parameters: T = 496 ° C, t = 4h)

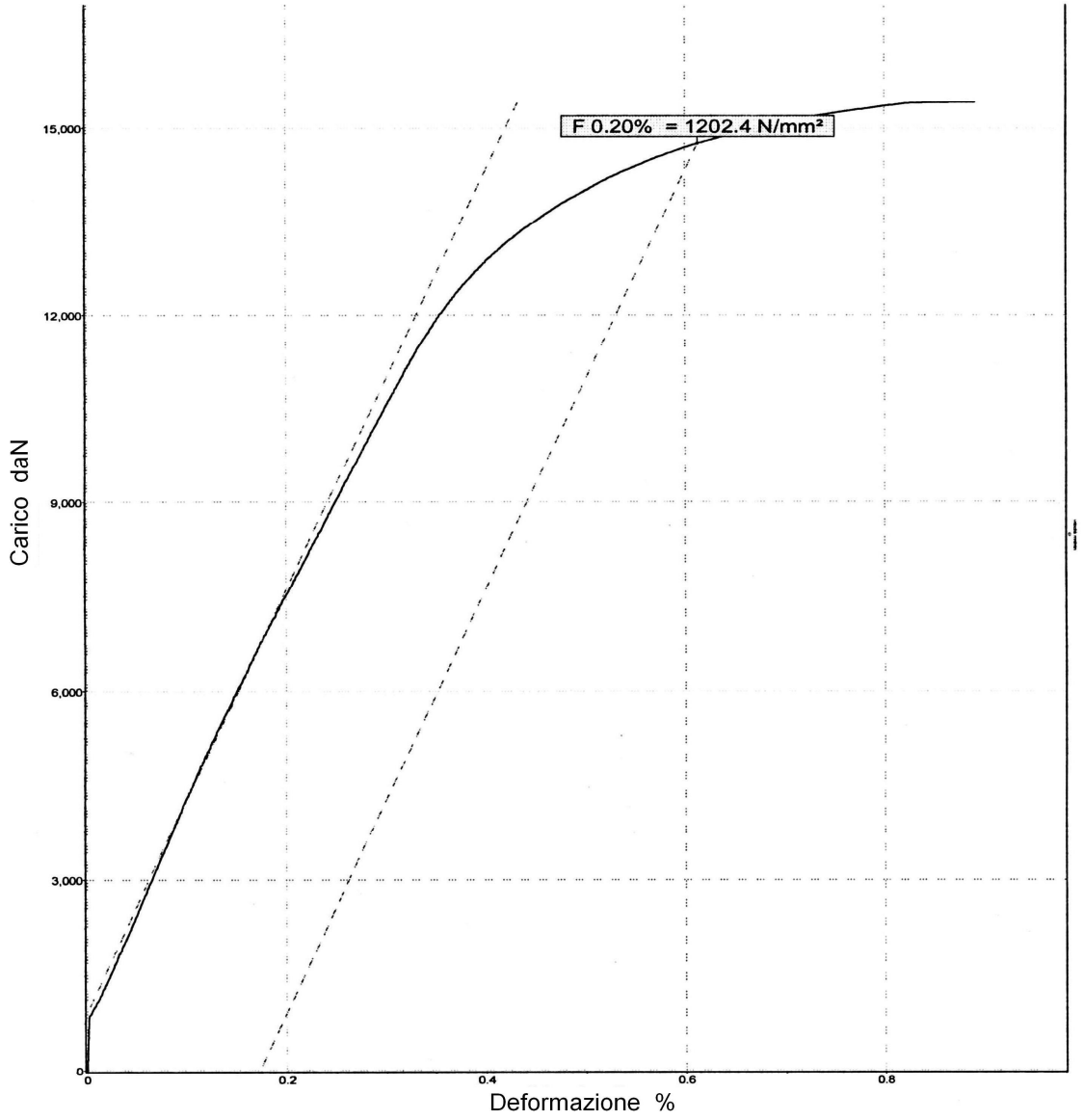

Fig. 9.1.4 Tension test load-deformation in 15-5PH VAR remelted specimens, in H925 heat treatment condition (ageing parameters: T = 496 ° C, t = 4h)

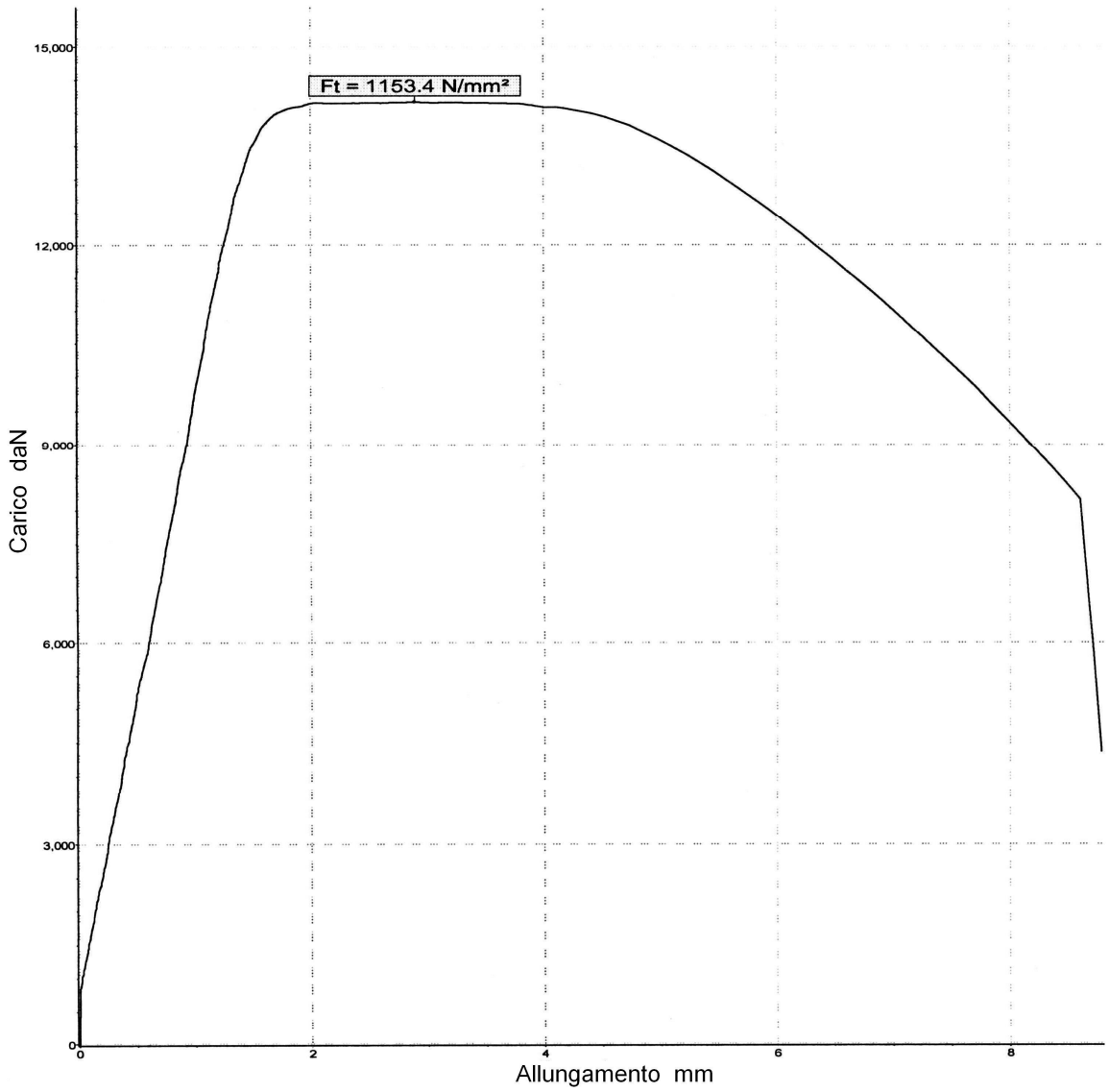

Fig. 9.1.5 Tension test load-elongation in 15-5PH VAR remelted specimens, in H1025 heat treatment condition (ageing parameters: T = 552 ° C, t = 4h)

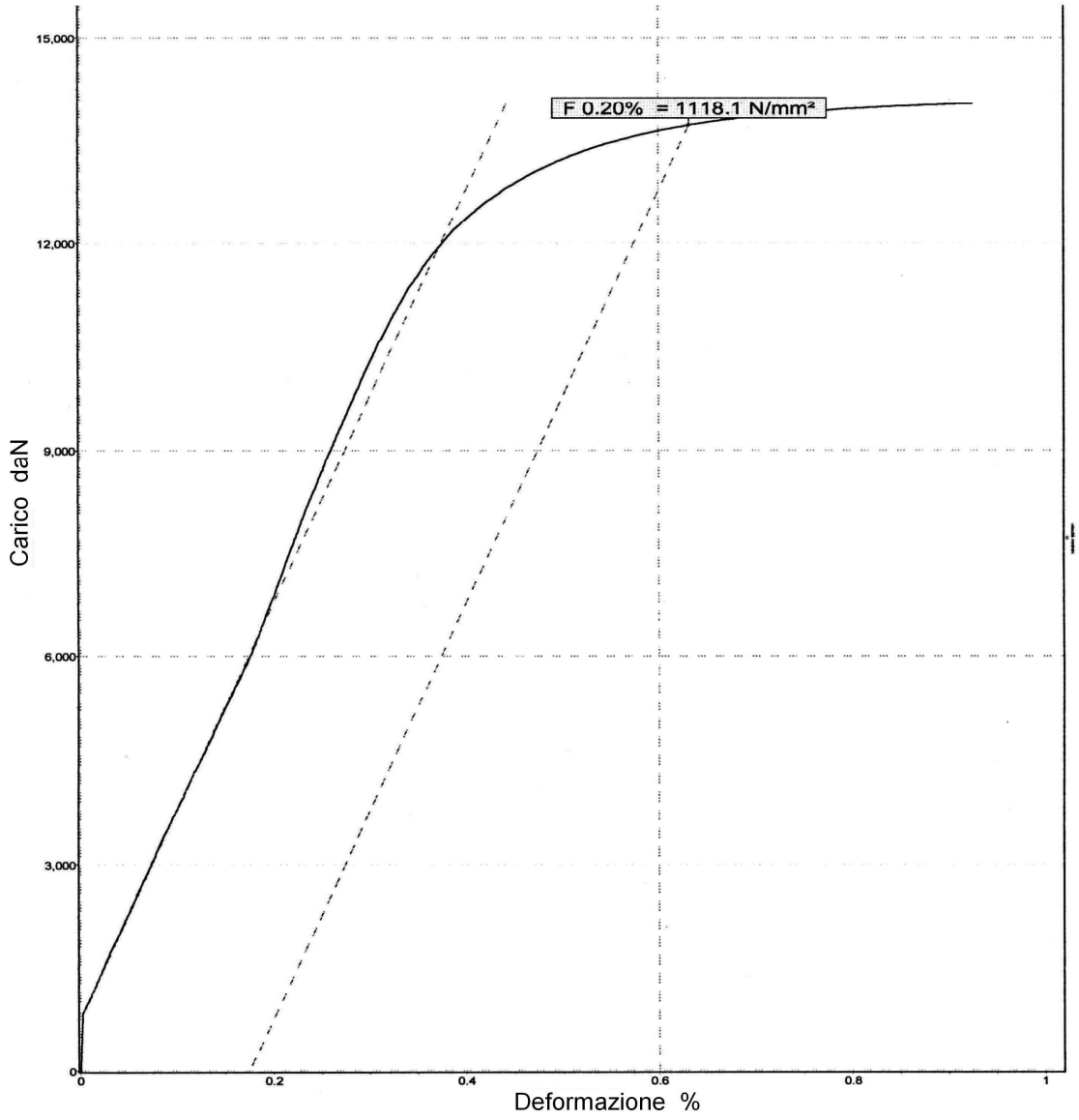

Fig. 9.1.6 Tension test load-deformation in 15-5PH VAR remelted specimens, in H1025 heat treatment condition (ageing parameters: T = 552 ° C, t = 4h)

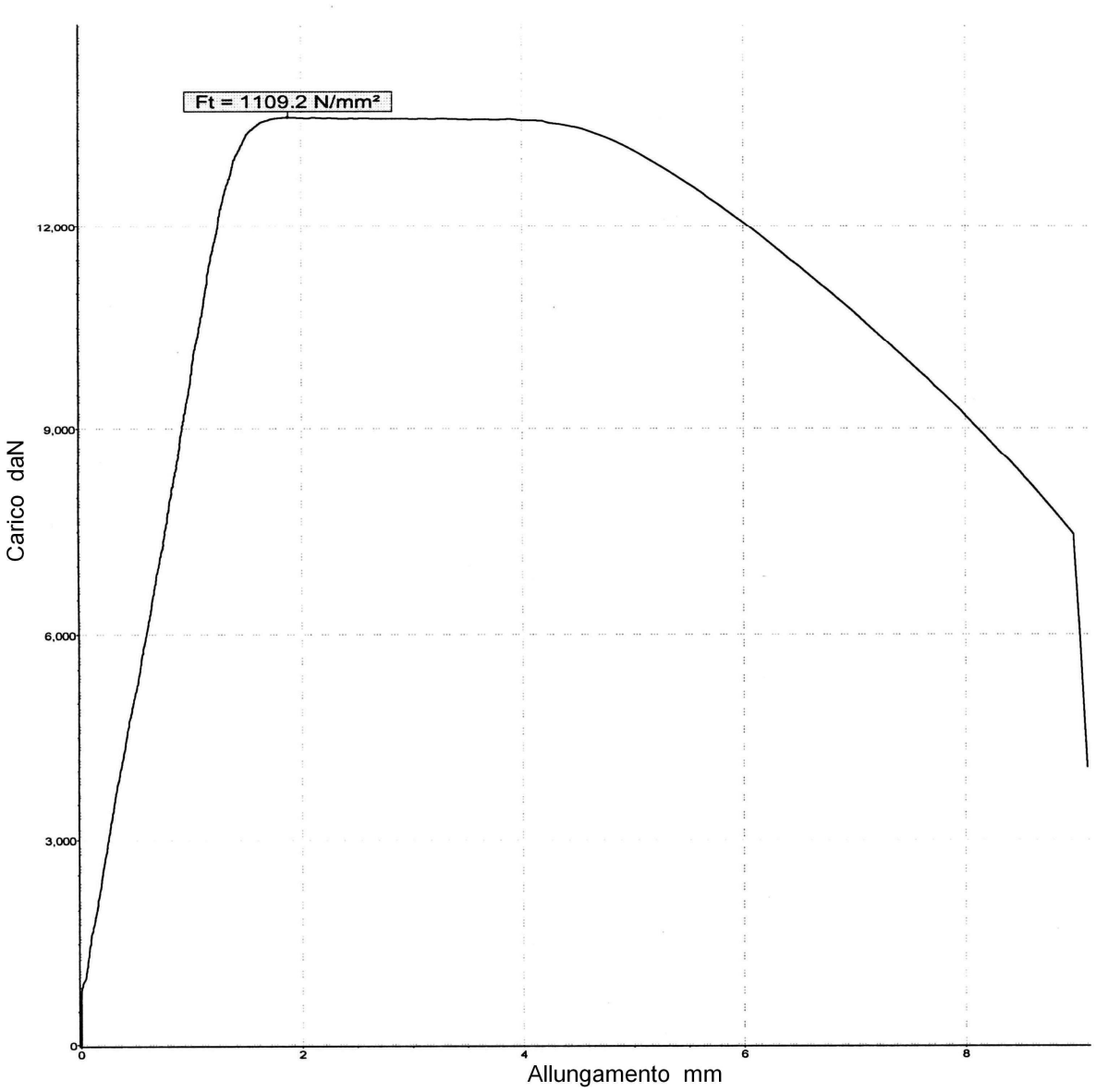

Fig. 9.1.7 Tension test load-elongation in 15-5PH VAR remelted specimens, in H1075 heat treatment condition (ageing parameters: T = 579 ° C, t = 4h)

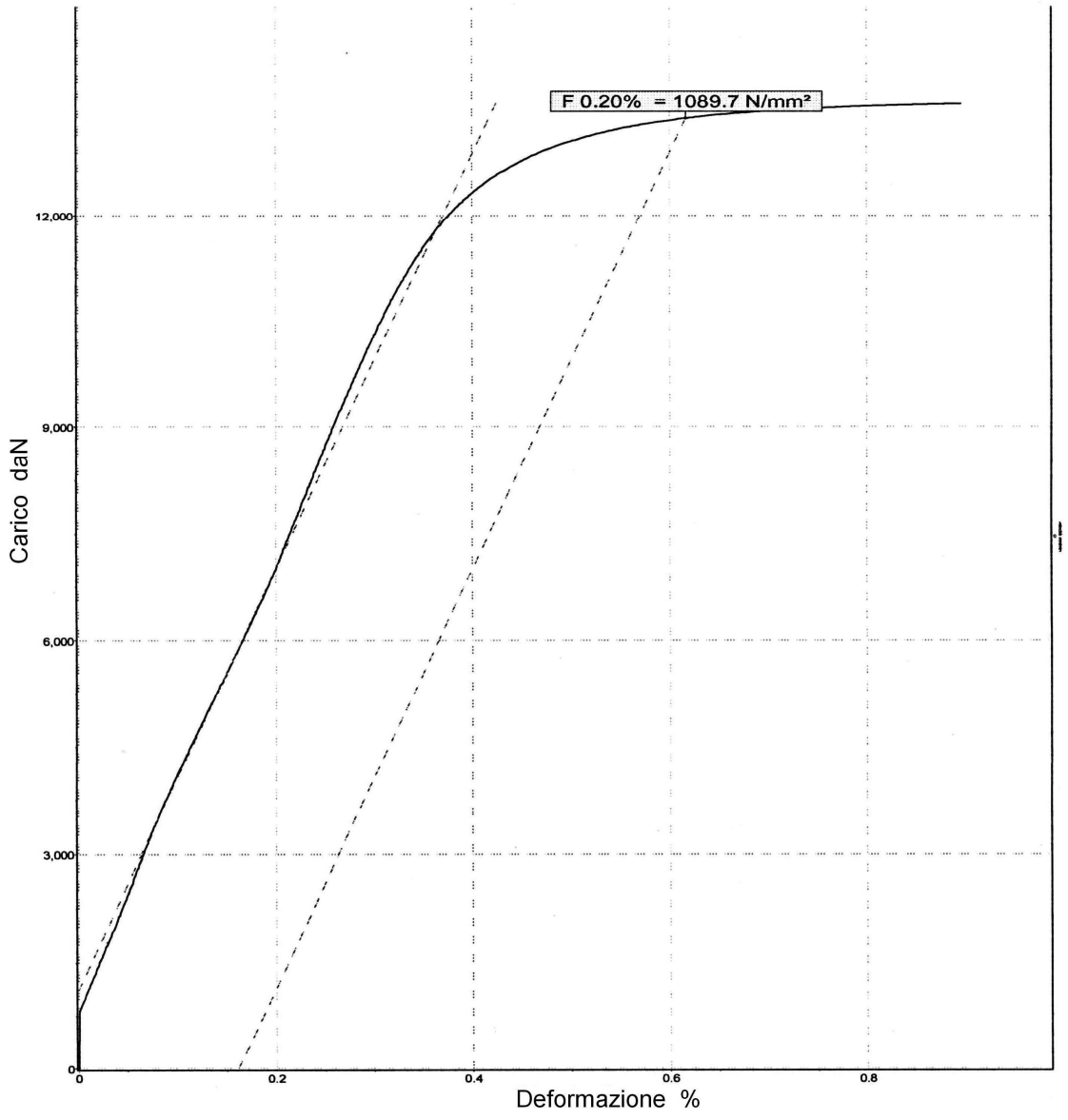

Fig. 9.1.8 Tension test load-deformation in 15-5PH VAR remelted specimens, in H1075 heat treatment condition (ageing parameters: T = 579 ° C, t = 4h)

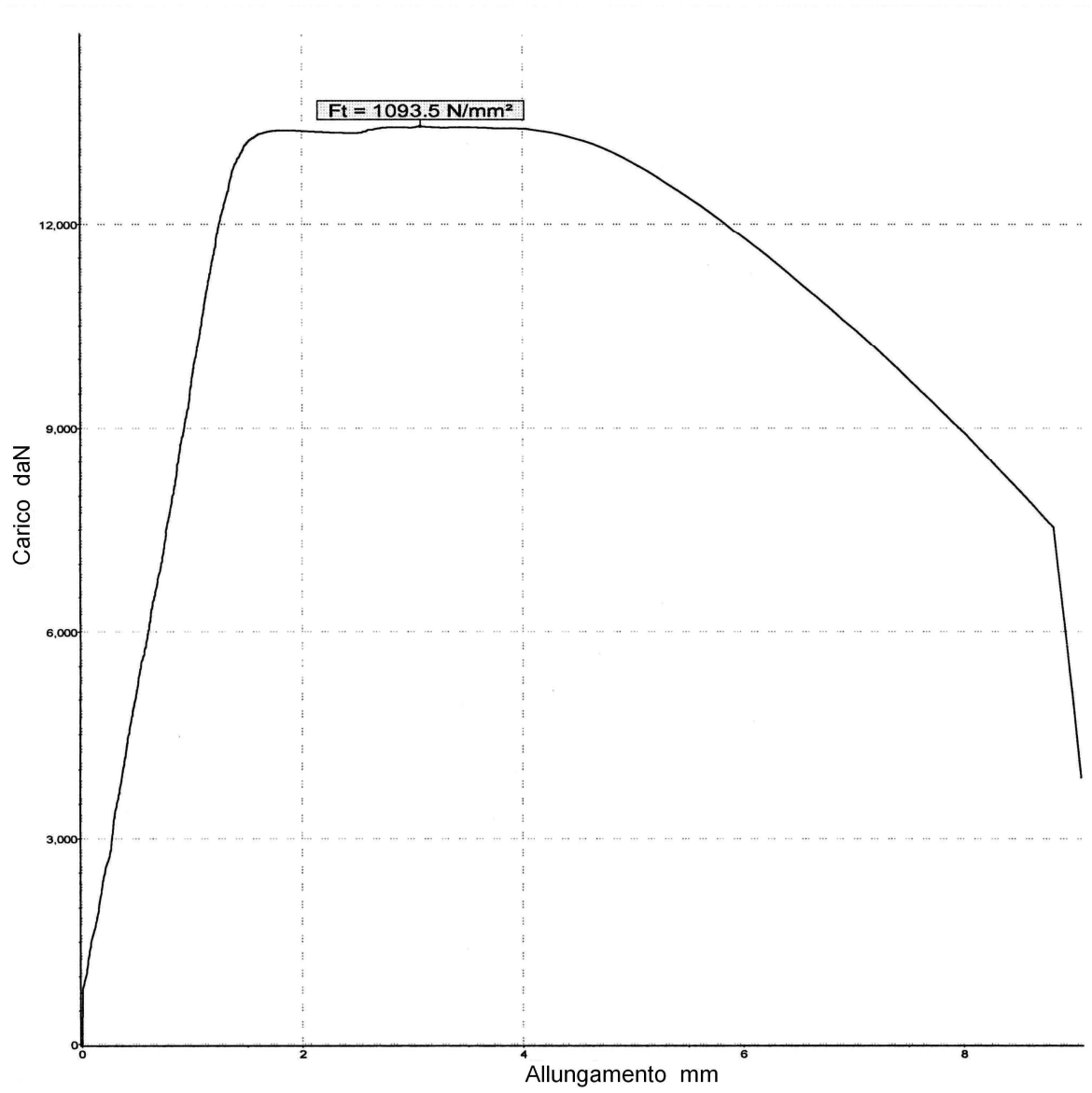

Fig. 9.1.9 Tension test load-elongation in 15-5PH VAR remelted specimens, in H1100 heat treatment condition (ageing parameters: T = 593 ° C, t = 4h)

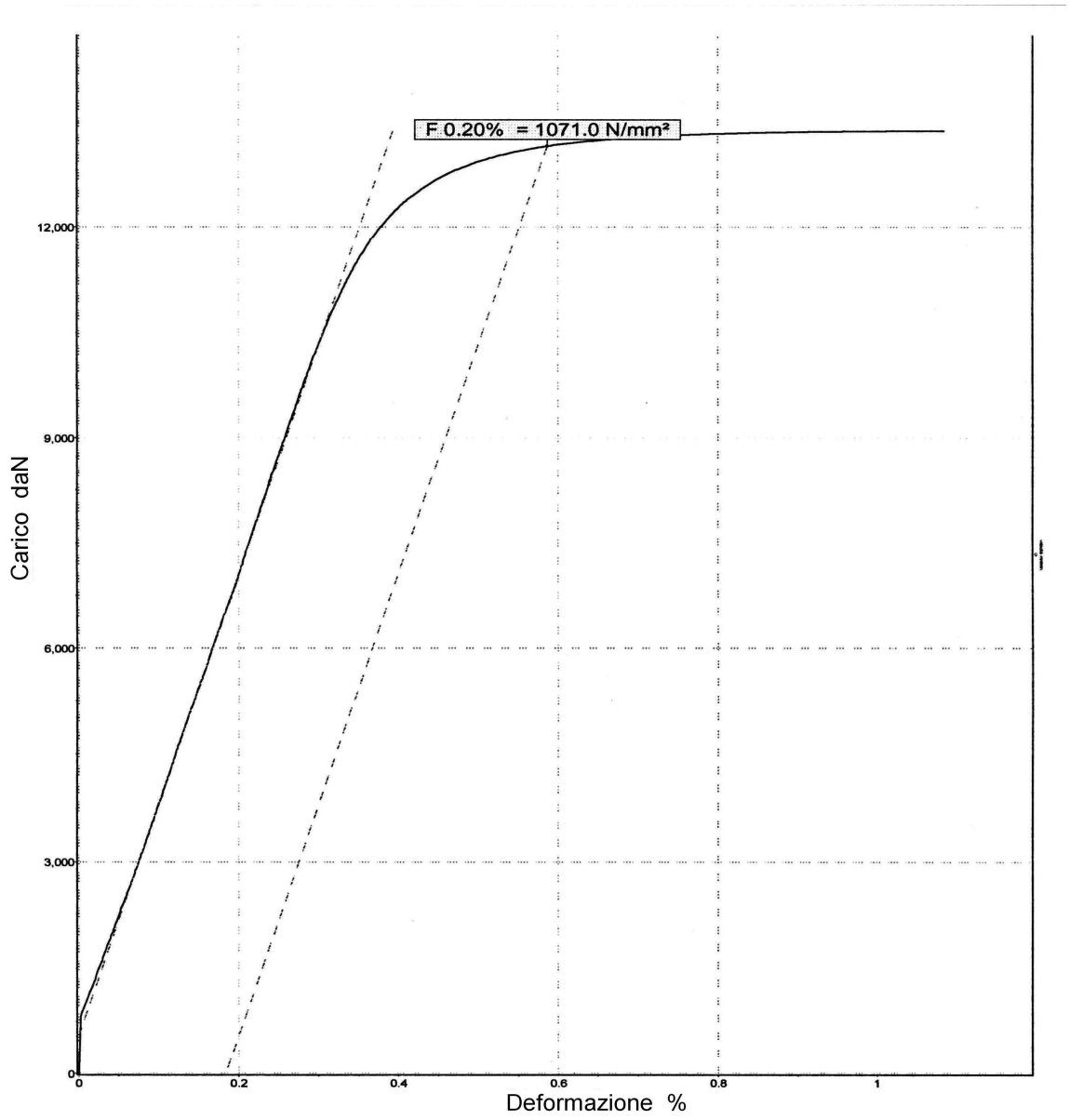

Fig. 9.1.10 Tension test load-deformation in 15-5PH VAR remelted specimens, in H1100 heat treatment condition (ageing parameters: T = 593 ° C, t = 4h)

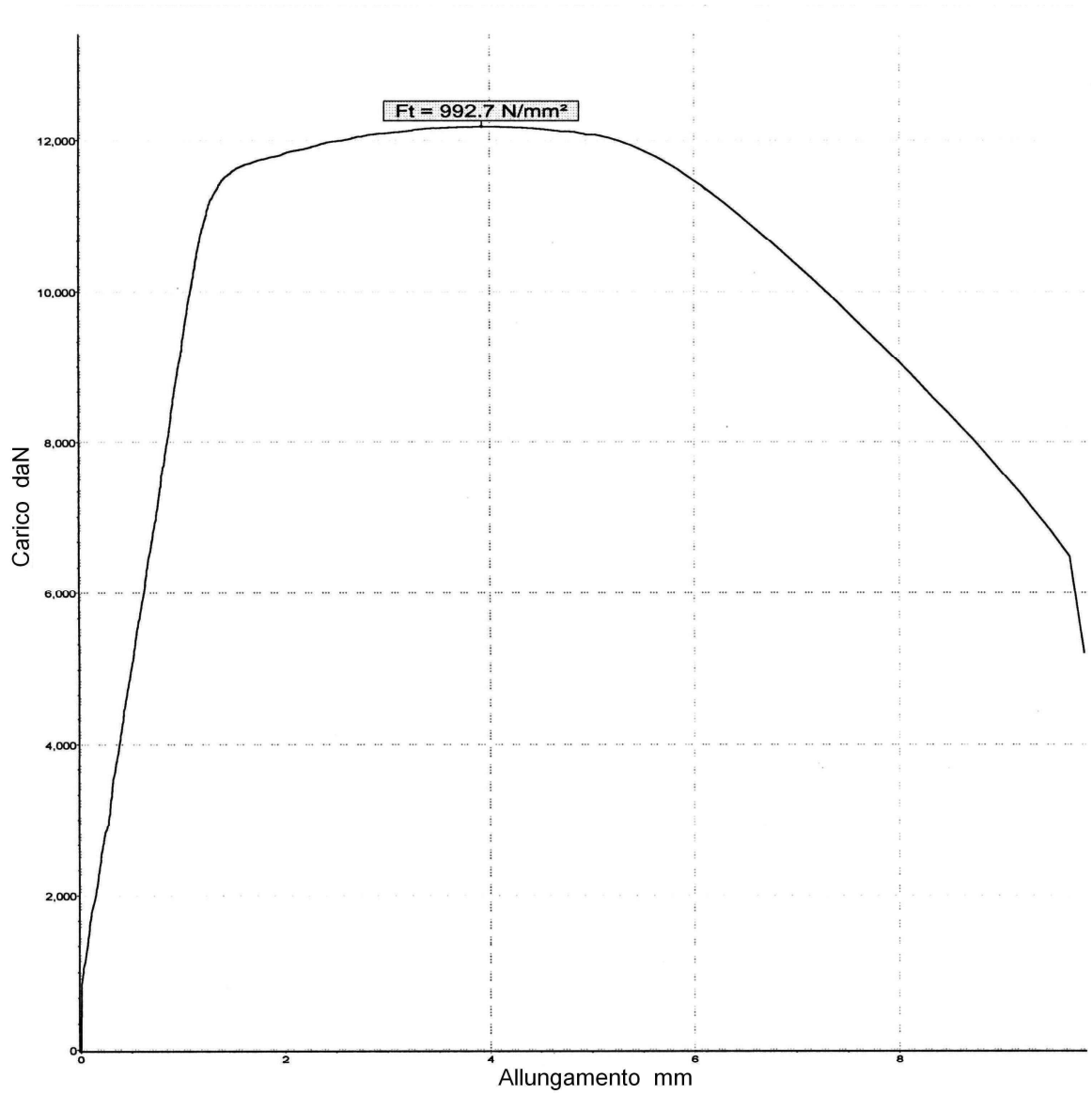

Fig. 9.1.11 Tension test load-elongation in 15-5PH VAR remelted specimens, in H1150 heat treatment condition (ageing parameters: T = 621 ° C, t = 4h)

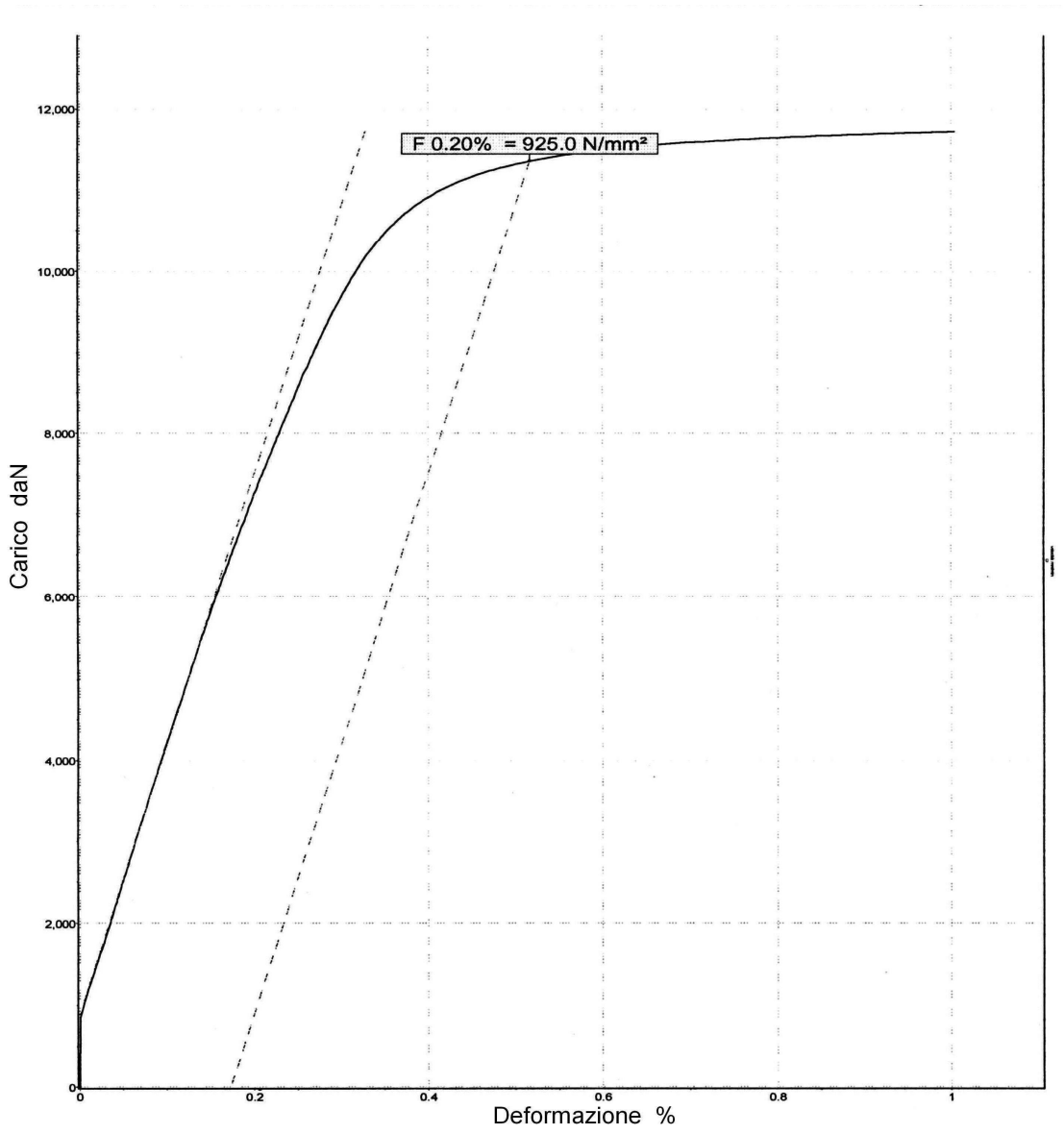

Fig. 9.1.12 Tension test load-deformation in 15-5PH VAR remelted specimens, in H1150 heat treatment condition (ageing parameters: T = 621 ° C, t = 4h)

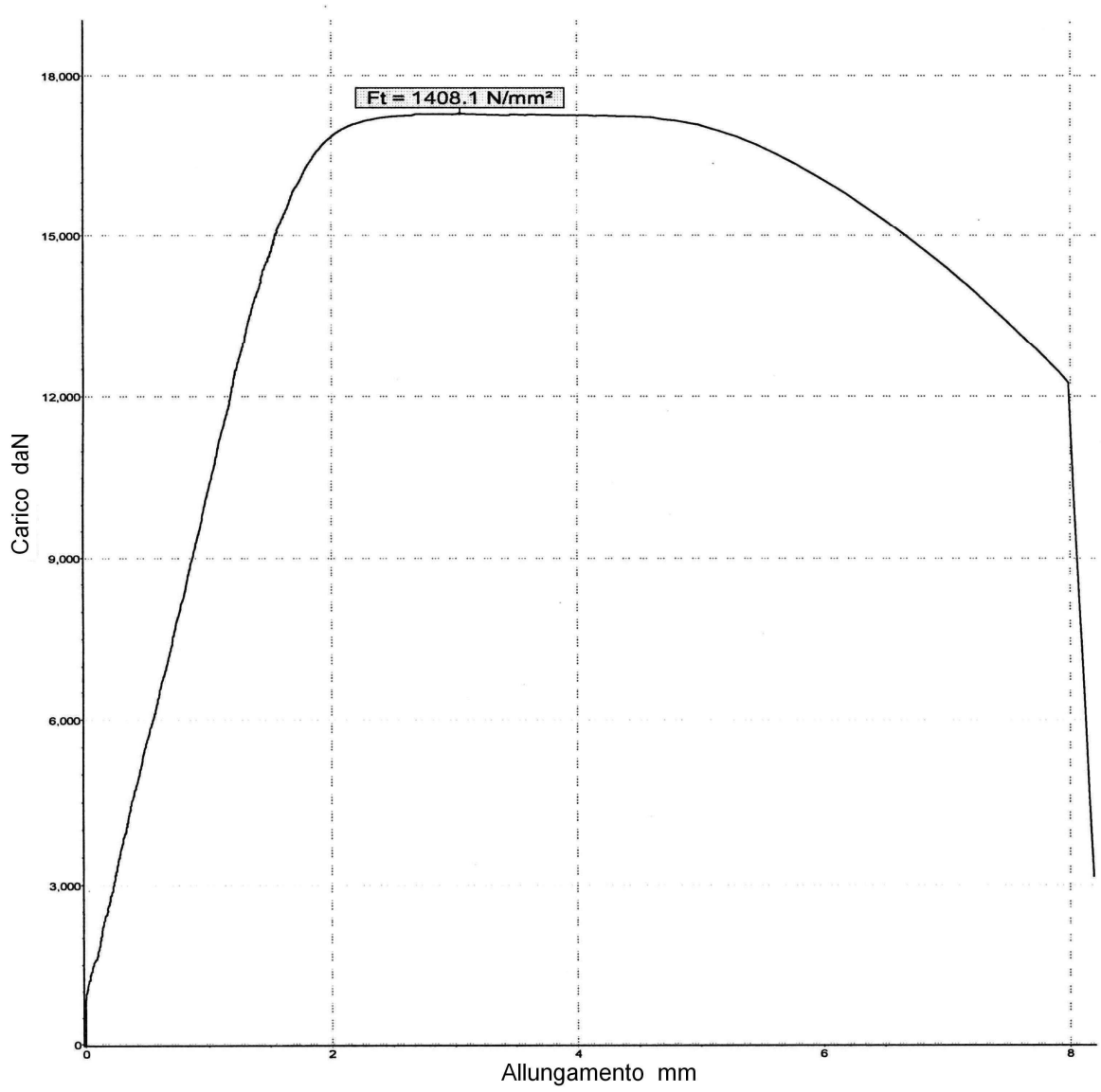

Fig. 9.1.13 Tension test load-elongation in 15-5PH ESR remelted specimens, in H900 heat treatment condition (ageing parameters: T = 482 ° C, t = 60min)

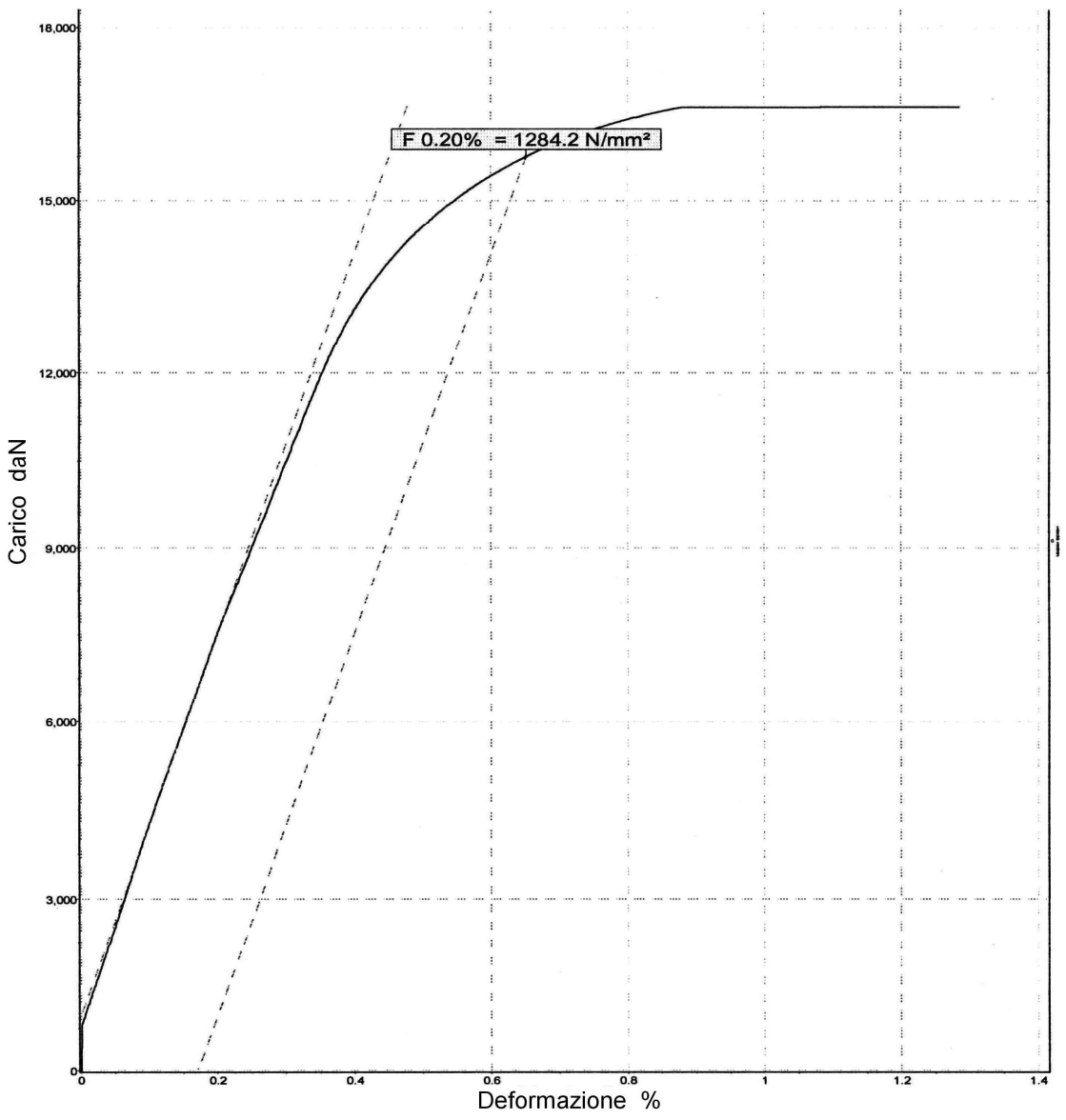

Fig. 9.1.14 Tension test load-deformation in 15-5PH ESR remelted specimens, in H900 heat treatment condition (ageing parameters: T = 482 ° C, t = 60min)

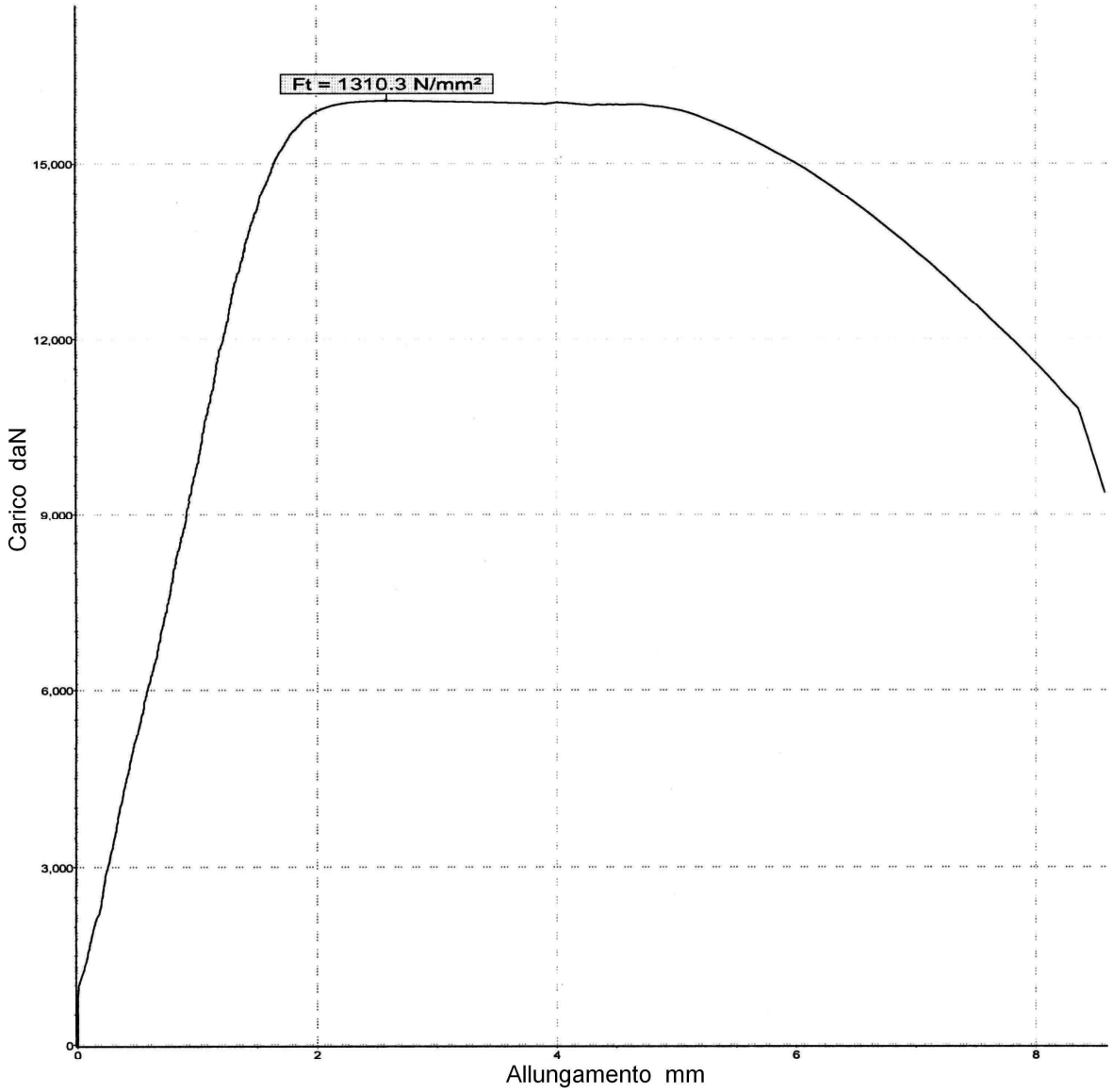

Fig. 9.1.15 Tension test load-elongation in 15-5PH ESR remelted specimens, in H925 heat treatment condition (ageing parameters: T = 496 ° C, t = 4h)

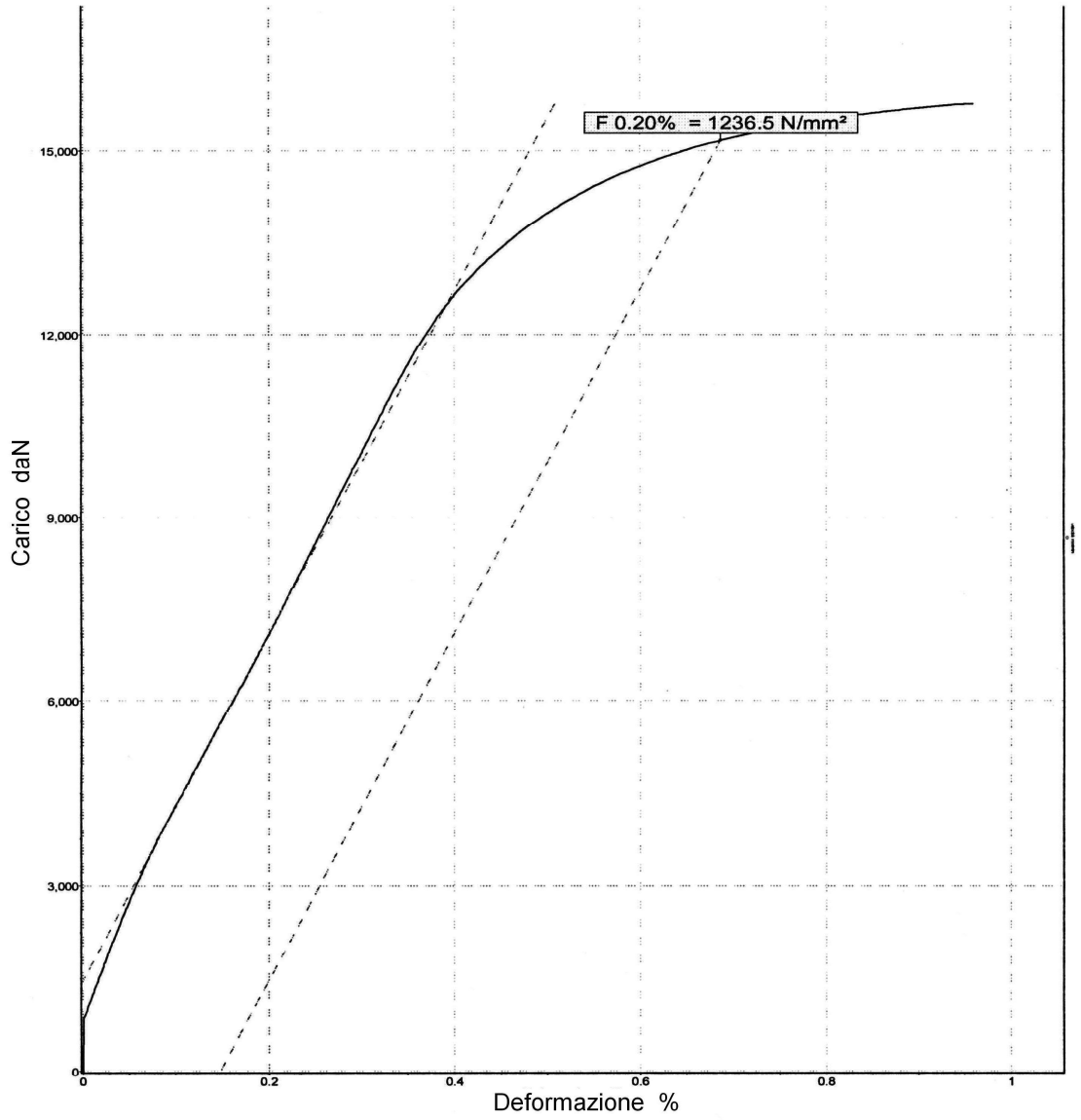

Fig. 9.1.16 Tension test load-deformation in 15-5PH ESR remelted specimens, in H925 heat treatment condition (ageing parameters: T = 496 ° C, t = 4h)

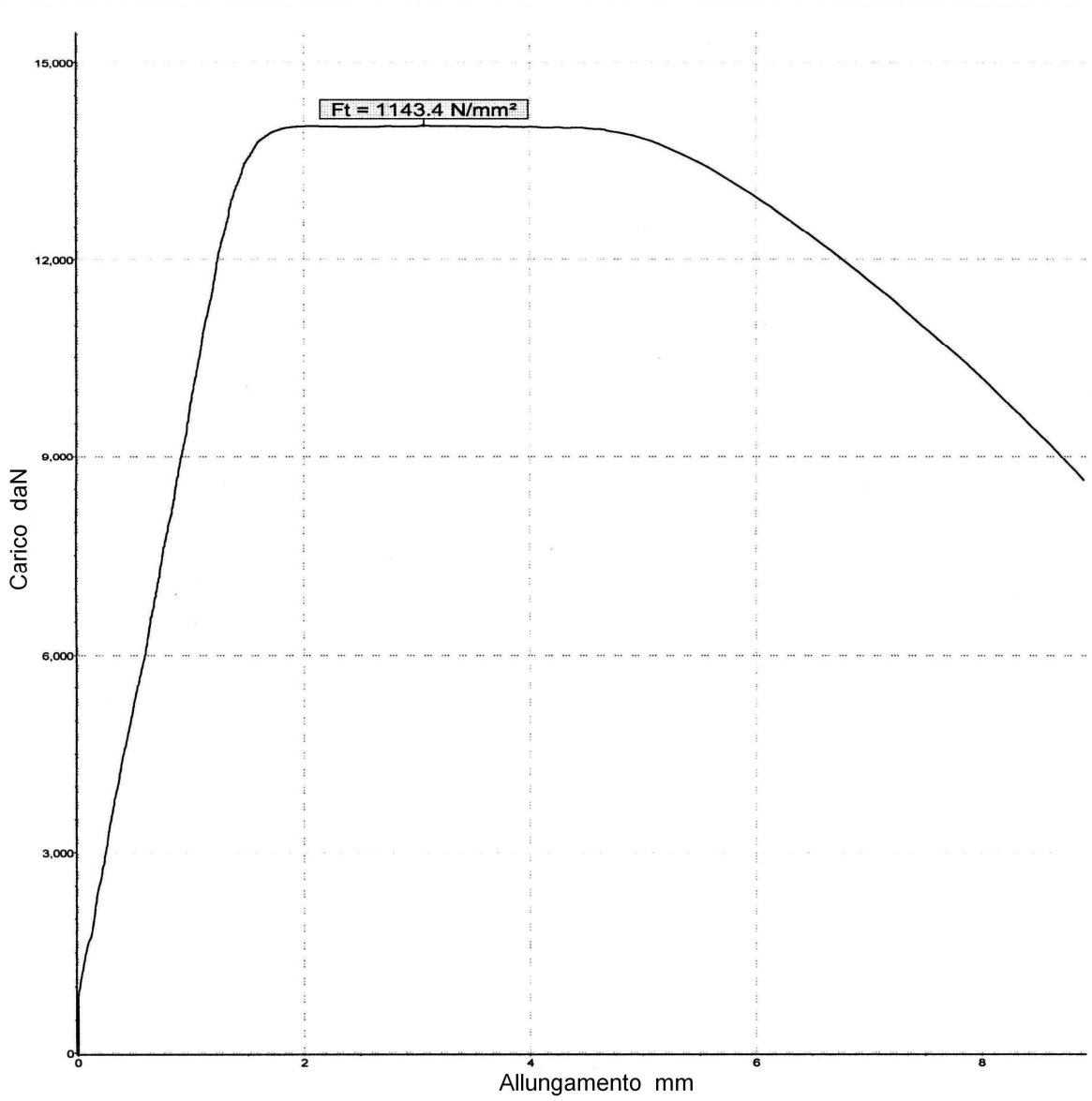

Fig. 9.1.17 Tension test load-elongation in 15-5PH ESR remelted specimens, in H1025 heat treatment condition (ageing parameters: T = 552 ° C, t = 4h)

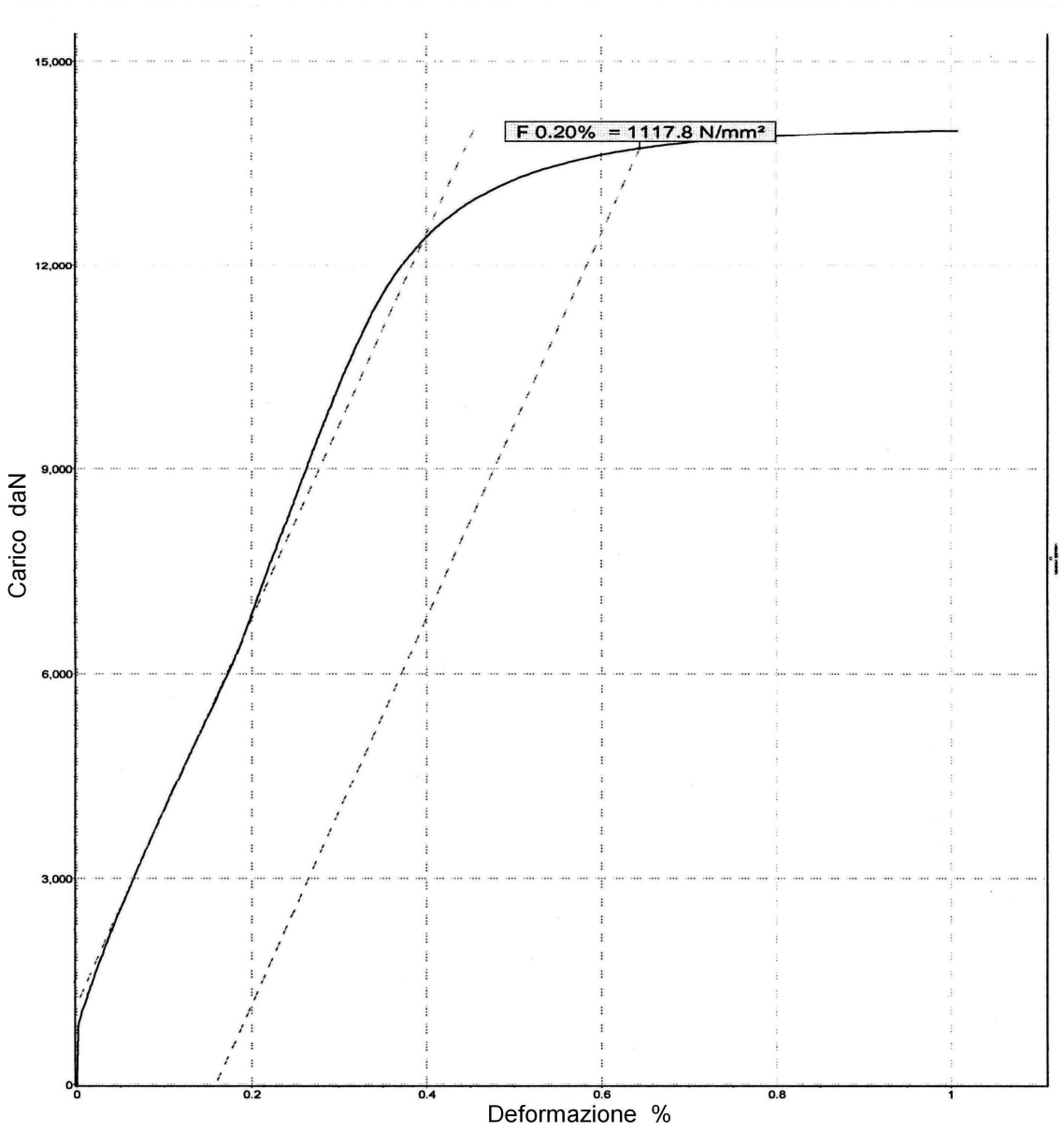

Fig. 9.1.18 Tension test load-deformation in 15-5PH ESR remelted specimens, in H1025 heat treatment condition (ageing parameters: T = 552 ° C, t = 4h)

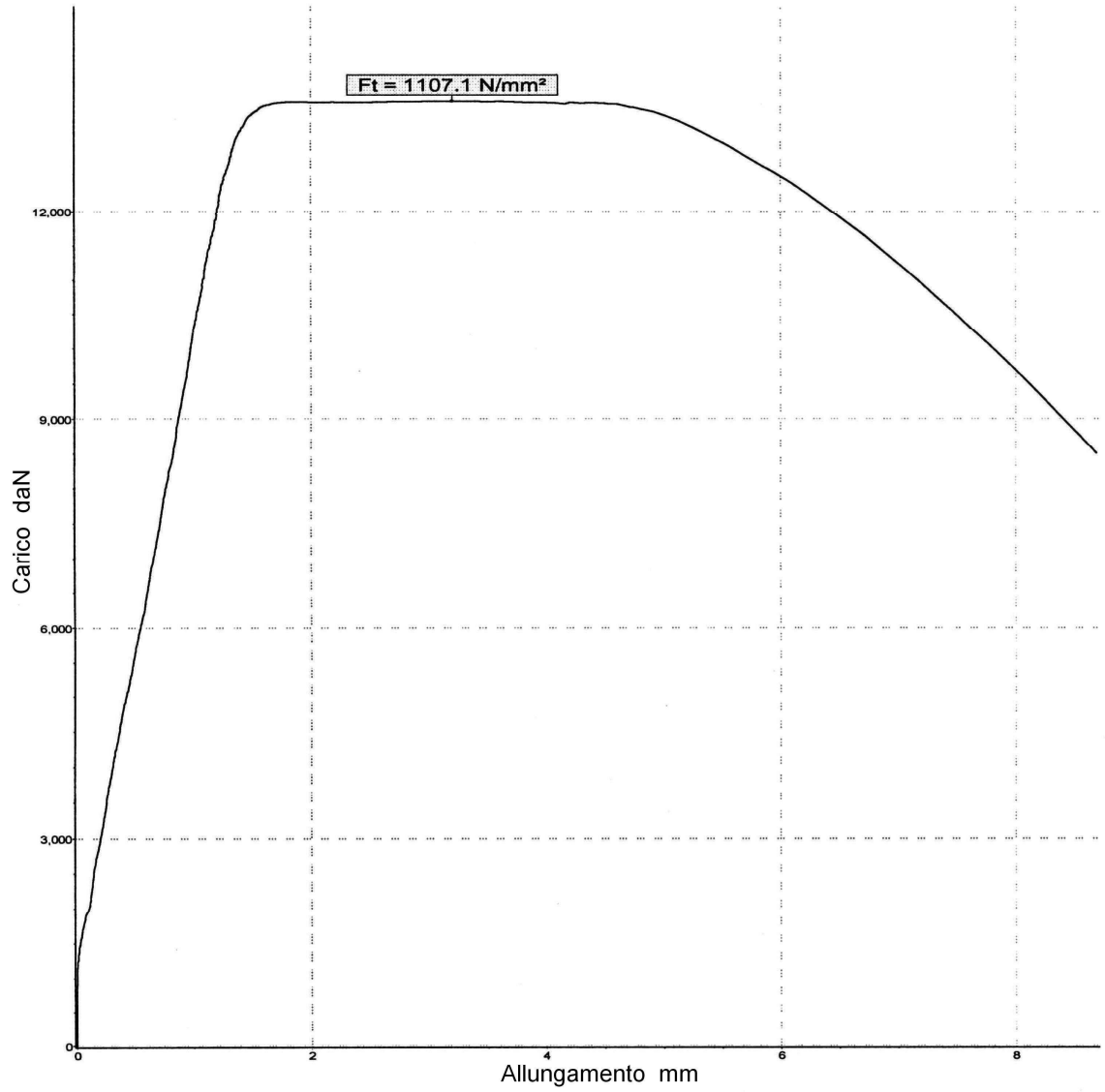

Fig. 9.1.19 Tension test load-elongation in 15-5PH ESR remelted specimens, in H1075 heat treatment condition (ageing parameters: T = 579 ° C, t = 4h)

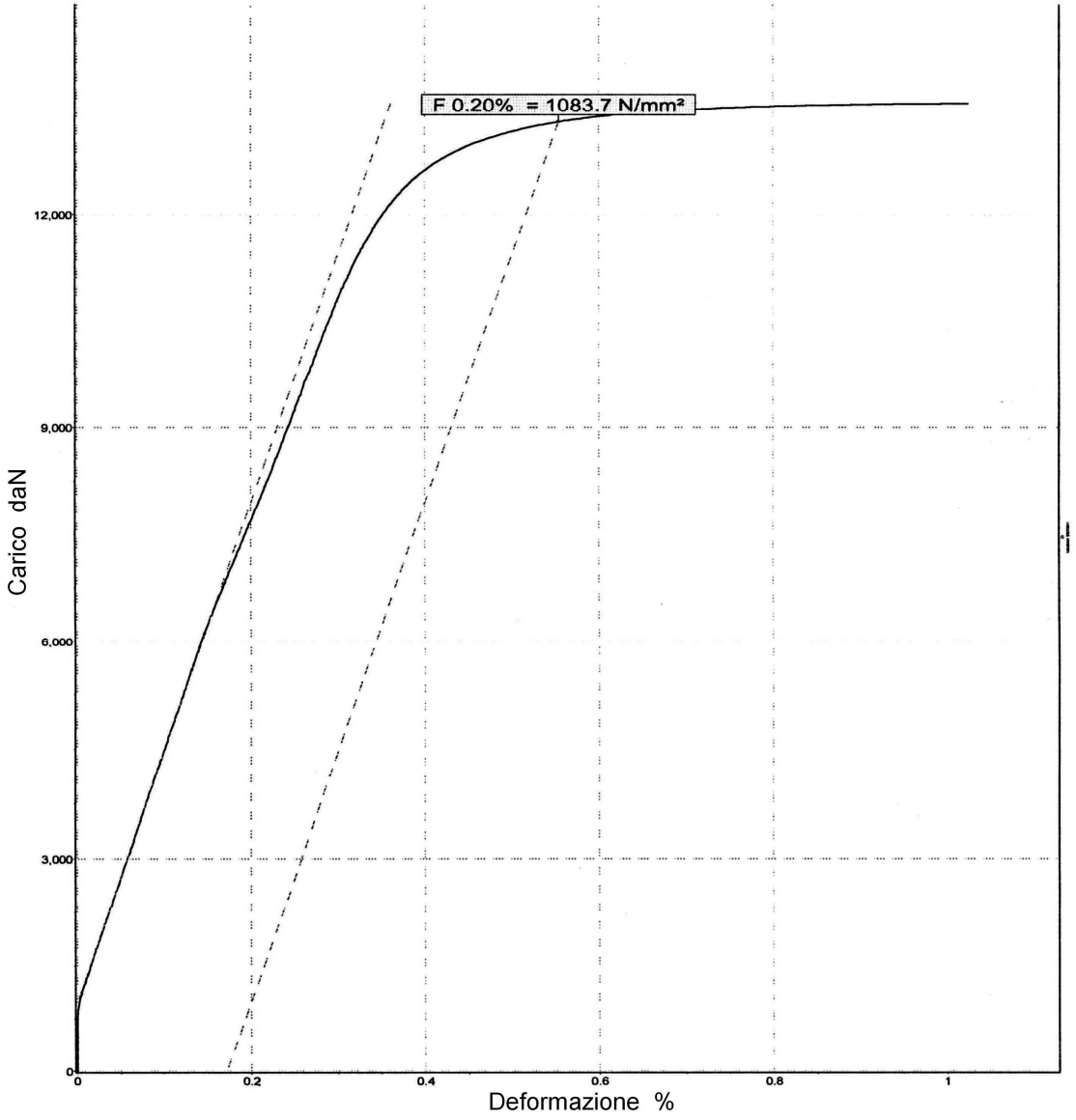

Fig. 9.1.20 Tension test load-deformation in 15-5PH ESR s remelted specimens, in H1075 heat treatment condition (ageing parameters: T = 579 ° C, t = 4h)

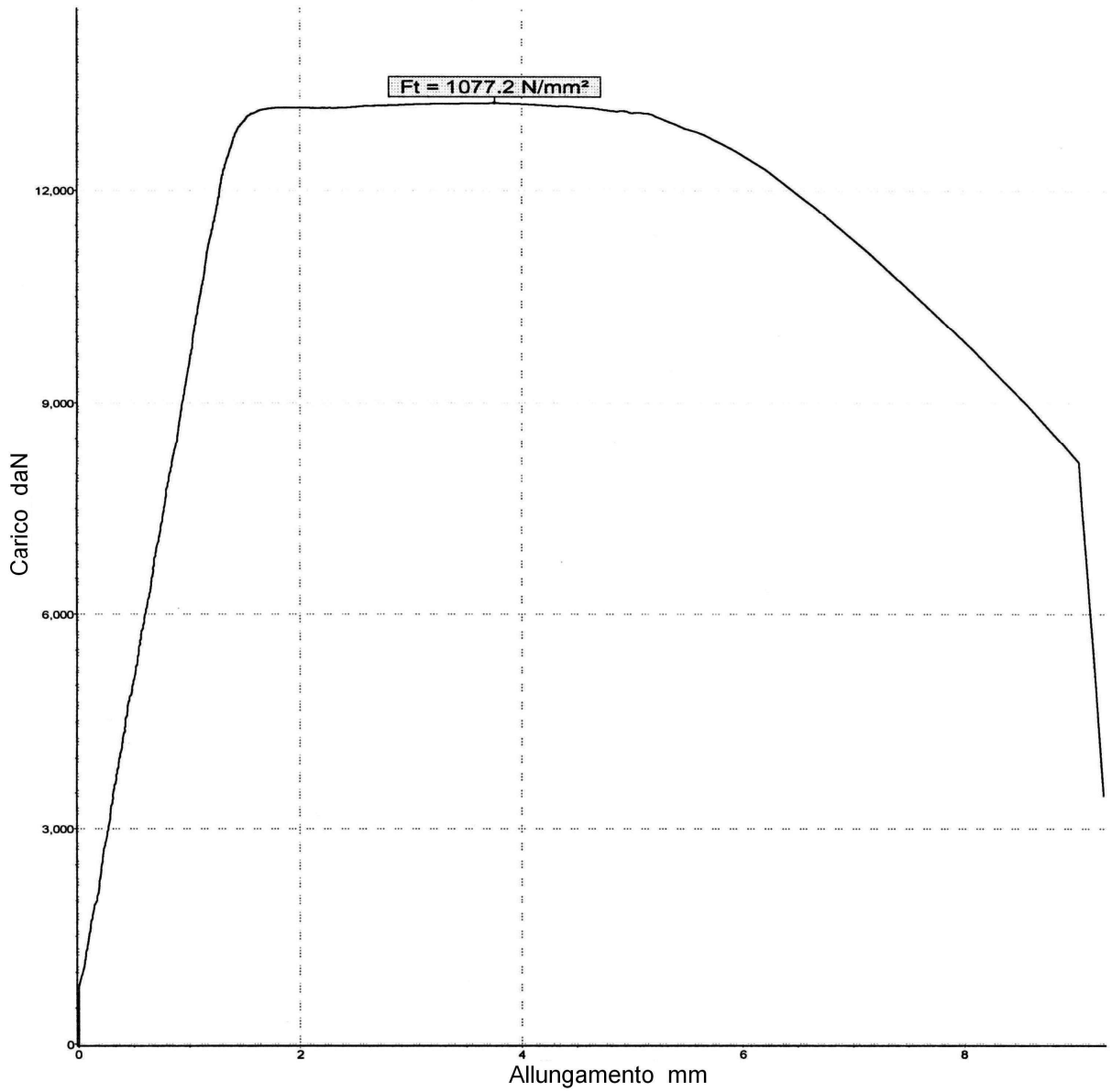

Fig. 9.1.21 Tension test load-elongation in 15-5PH ESR remelted specimens, in H1100 heat treatment condition (ageing parameters: T = 593 ° C, t = 4h)

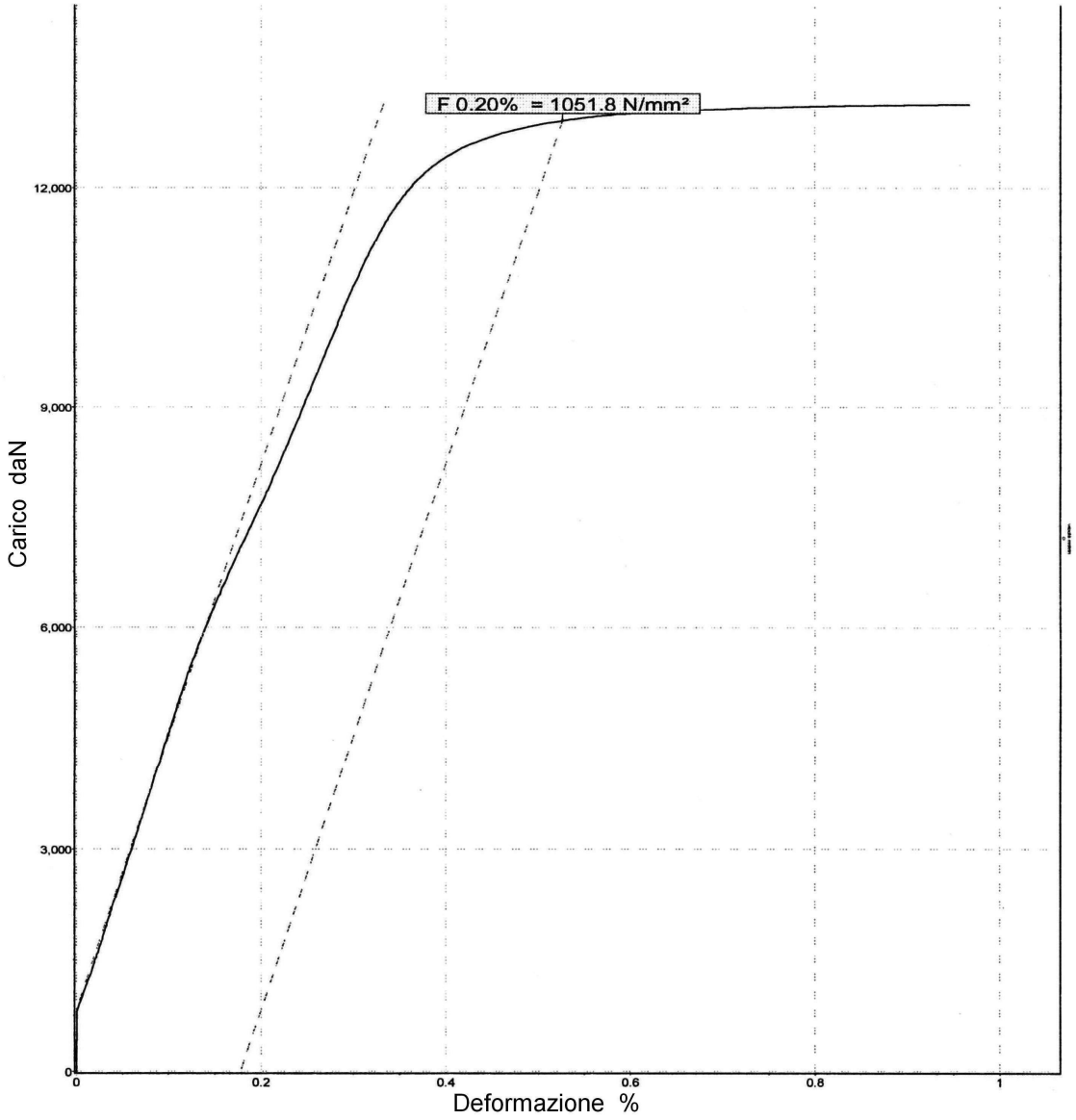

Fig. 9.1.22 Tension test load-deformation in 15-5PH ESR remelted specimens, in H1100 heat treatment condition (ageing parameters: T = 593 ° C, t = 4h)

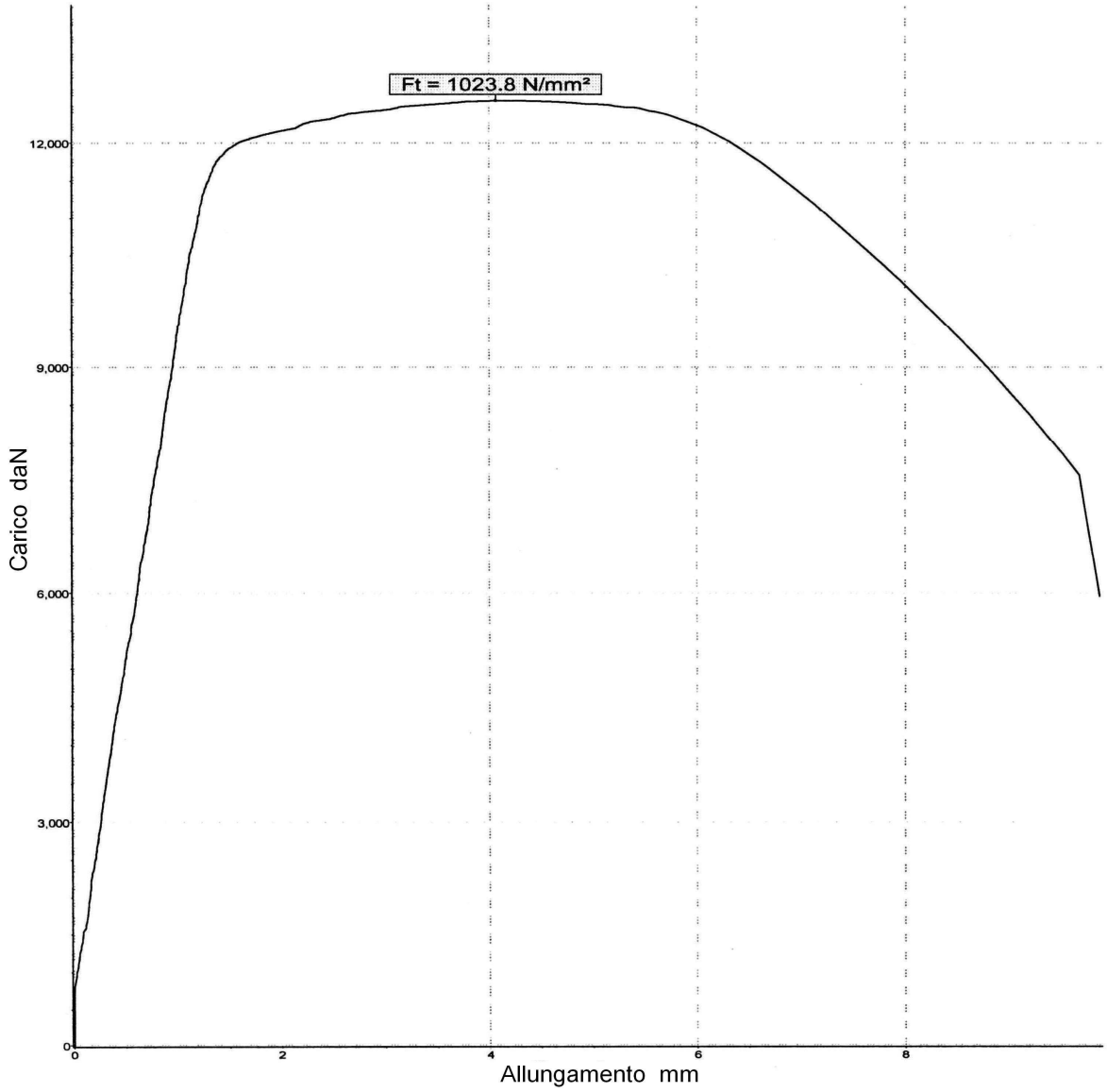

Fig. 9.1.23 Tension test load-elongation in 15-5PH ESR remelted specimens, in H1150 heat treatment condition (ageing parameters: T = 621 ° C, t = 4h)

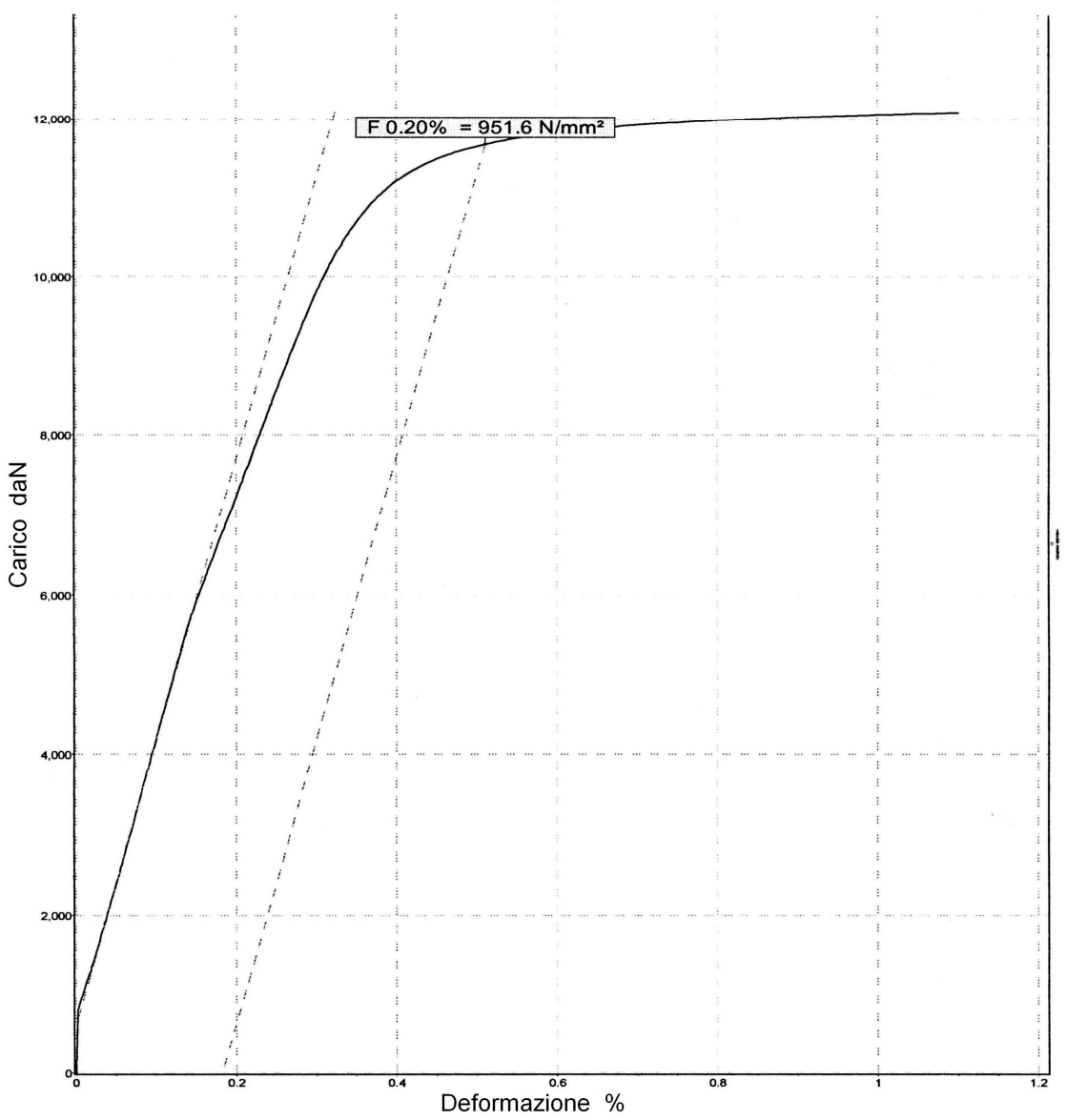

Fig. 9.1.24 Tension test load-deformation in 15-5PH ESR remelted specimens, in H1150 heat treatment condition (ageing parameters: T = 621 ° C, t = 4h)

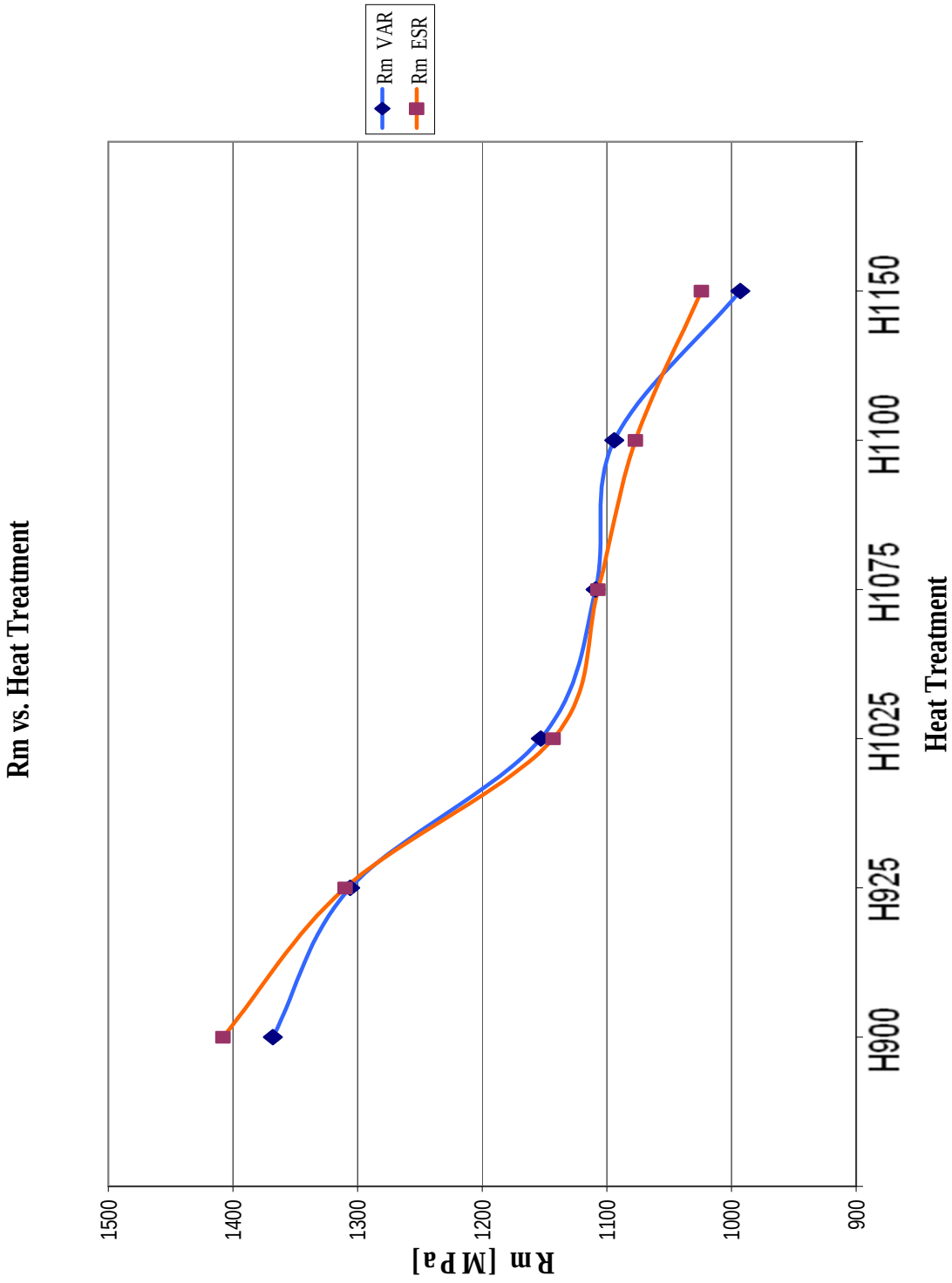

Fig. 9.1.25 Tensile strength R_m, in VAR and ESR remelted specimens, function of the aging period

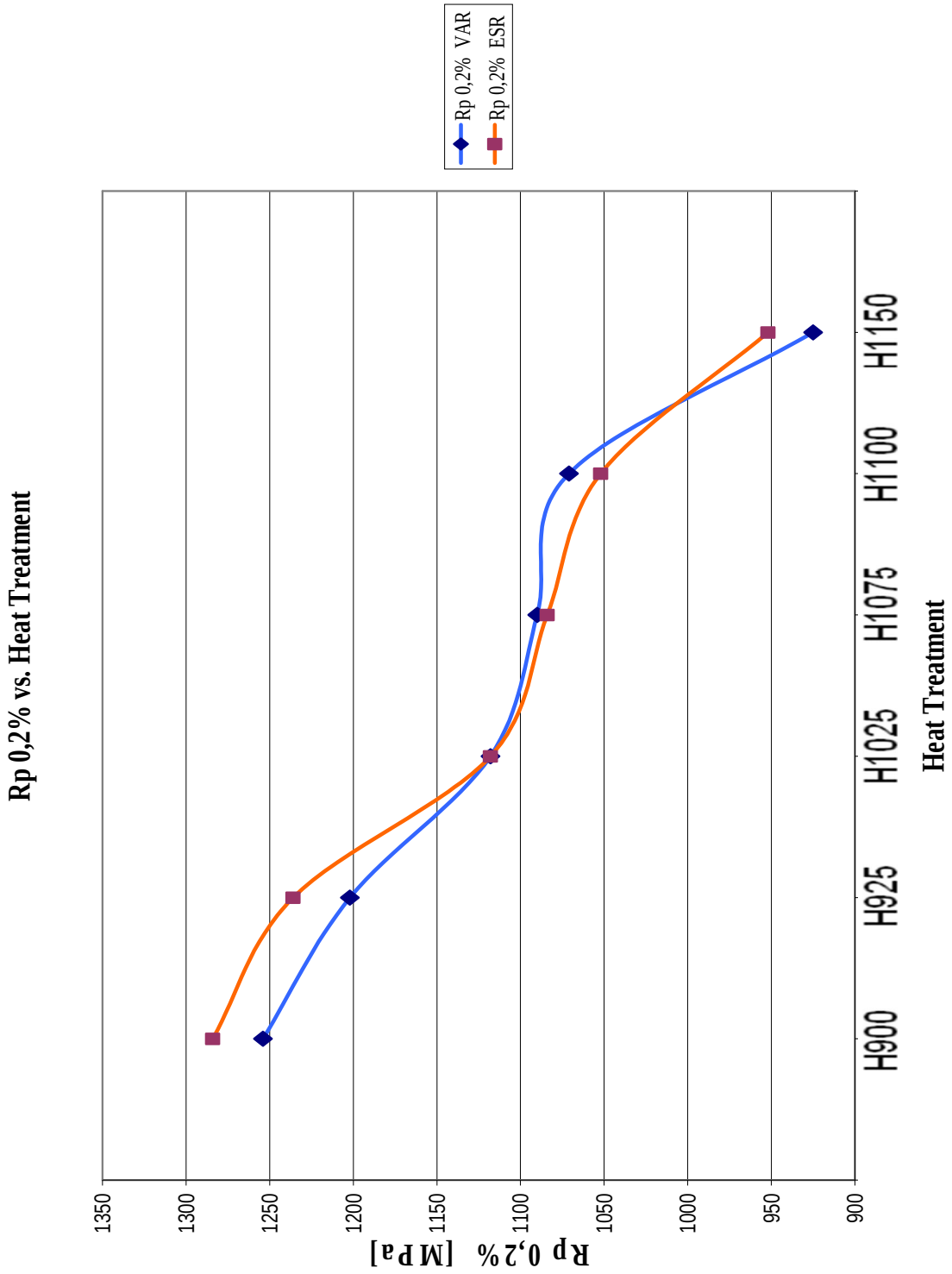

Fig. 9.1.26 Yield stress $R_{p0.2\%}$, in VAR and ESR remelted specimens, function of the aging period

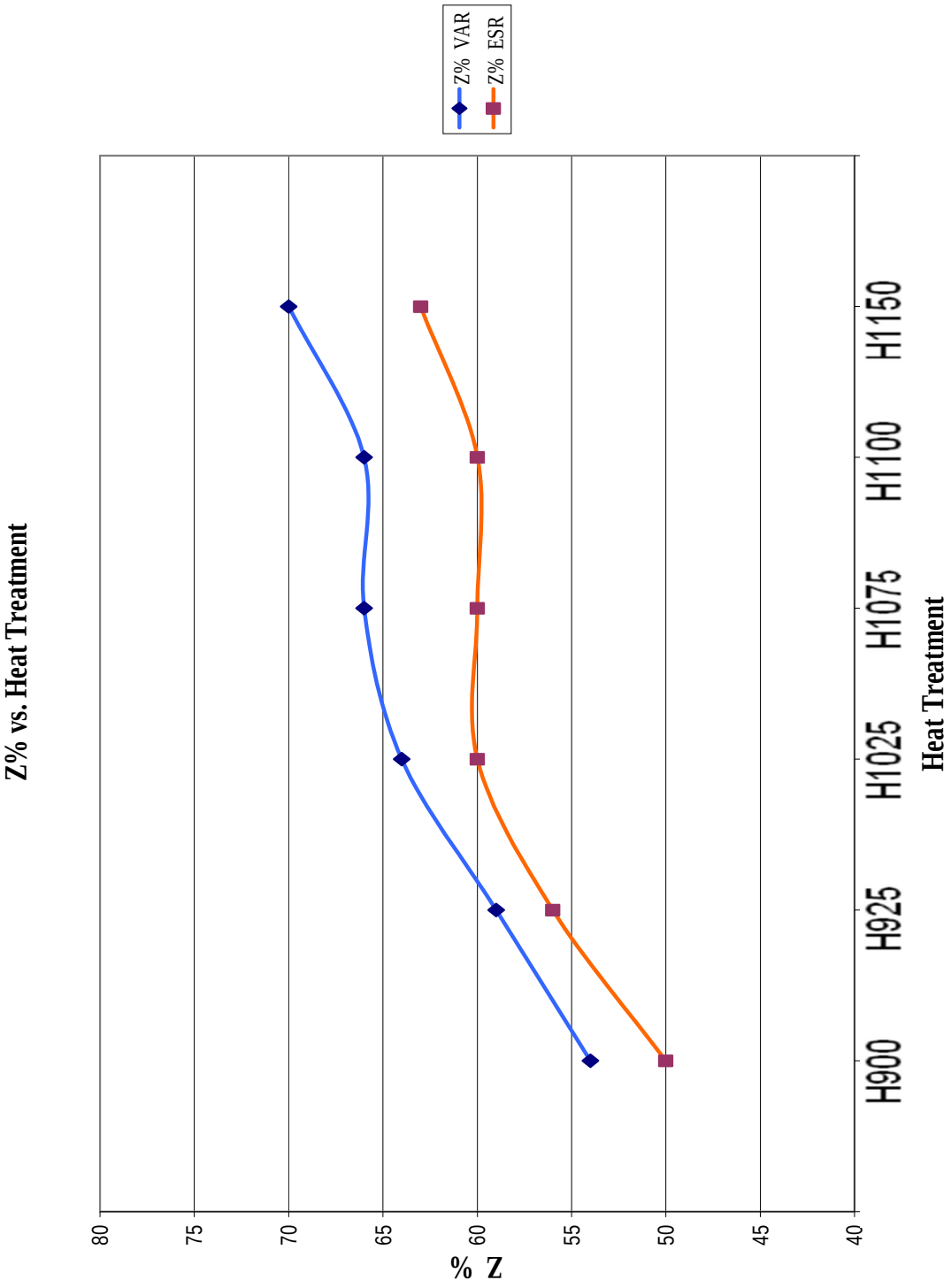

Fig. 9.1.27 Reduction factor Z%, in VAR and ESR remelted specimens, function of the aging period

The tensile tests show that the samples, remelted at the VAR and ESR process, present values of the unit load tensile strength R_m [MPa] and the unit load deviation from proportionality $R_{p\ 0.2\%}$ (0.2) [MPa] very similar all together for the six different degrees of ageing.

The tensile strength values decreases with increasing of aging degree, thus increasing the number and the size of precipitates at boundary grains. This produce a reduction content of carbon in martensite matrix. The specimens occur after rupture, a break to "cup and cone" typical of very tough steels, homogeneous and isotropic; ESR in specimens however, showed a higher frequency of breakage to" shell parts. "

The reduction of area coefficient Z% for the specimens remelted in the VAR process, present values constantly higher than those remelted in ESR process, in all different degrees of ageing. The lower inclusions level produced in VAR remelting process, induces a greater deformability of steel before break. In fact, the greater presence of non-metallic inclusions in ESR remelted steel .

9.2 Brinell hardness test

This test method completes, the characteristics determined by tensile testing of metallic material at room temperature, in particular, the method of determining the hardness is closely related to tensile strength, wear resistance, ductility, or other physical characteristics of metallic materials.

The room temperature must be maintained at 25 ° C, as specified in ASTM E10.

		Heat Treatment						
		A	**H900**	**H925**	**H1025**	**H1075**	**H1100**	**H1150**
VAR	***HB***	313	439	423	382	363	360	322
ESR	***HB***	328	447	431	376	369	357	332

Tab. 9.2.1 Hardness comparison between VAR and ESR specimens The solubilization heat treated condition, is called condition A.

The hardness is not affected by processing. In fact, both samples ESR and VAR have hardness values very similar to each other, since the hardness is related only to the structure and not to the presence of inclusions. The decrease of the values of hardness is related to the fact that during the heat treatment of precipitation, the martensitic structure become poor of carbon that will form at the grain boundary carbides.

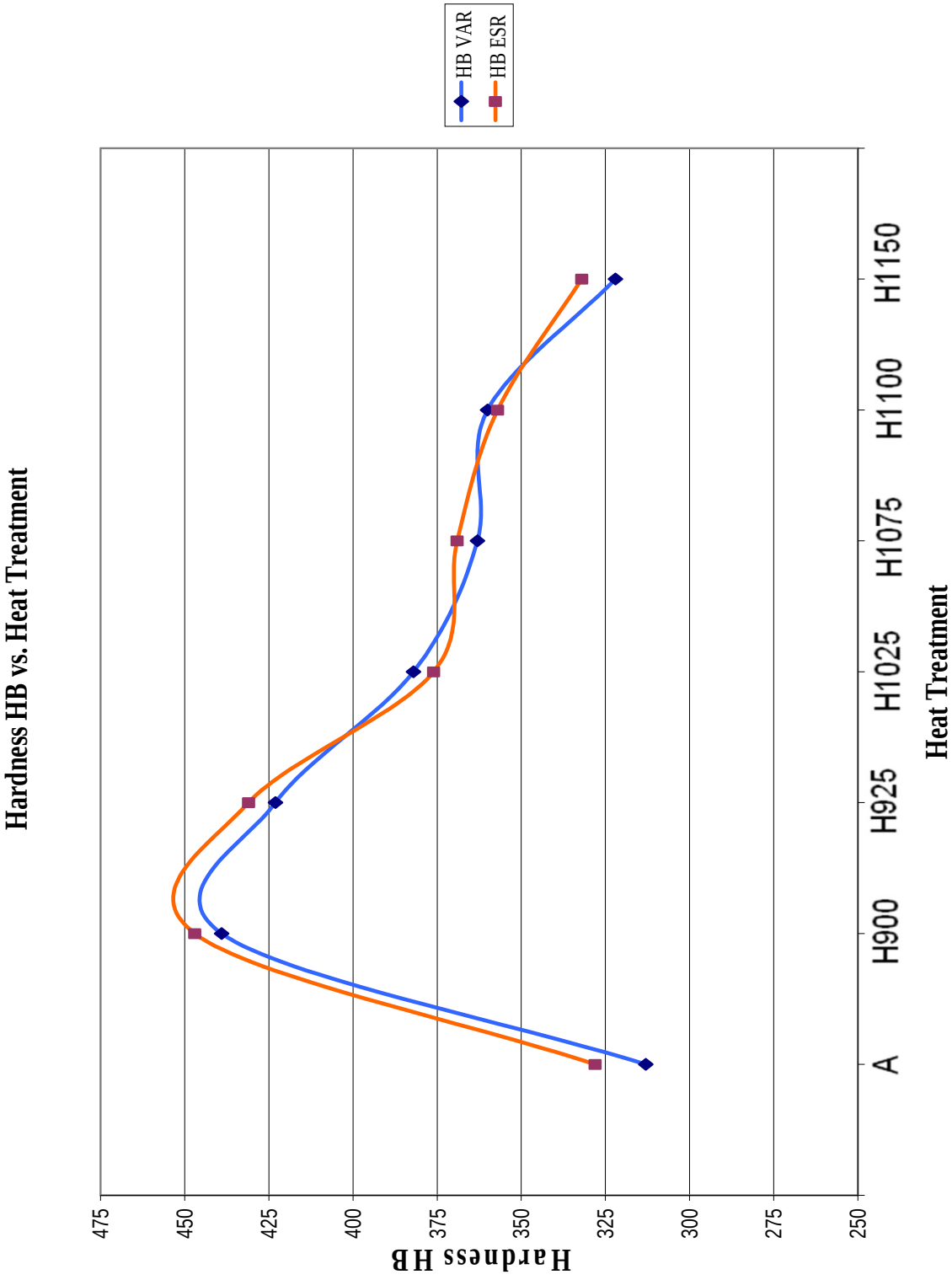

Fig. 9.2.1 Hardness comparison between VAR and ESR remelted specimens.

9.3 Impact test

This impact test method specifically evaluate the behavior of the metal, when subjected to the application of a load that generates multiaxial stress in notch bar that can cause rupture of the standardized specimen. The test is then conducted with high rates of loading, and ambient temperature (T_{amb}) and at a temperature of -40 ° C, to predict the likelihood of brittle fracture.

The room temperature must be maintained at 25 ° C, as specified in ASTM E23.

		Heat Treatment					
		H900	**H925**	**H1025**	**H1075**	**H1100**	**H1150**
KV	*J*	17	45	223	206	180	211
KV	*J*	14	31	195	196	182	195
KV	*J*	10	47	196	195	185	211

Tab. 9.3.1 Notched bar impact test report in 15-5PH VAR remelted specimens, in heat treatment condition at room temperature T_{amb}.

		Heat Treatment					
		H900	**H925**	**H1025**	**H1075**	**H1100**	**H1150**
KV	*J*	6	10	14	44	44	166
KV	*J*	9	10	27	45	53	189
KV	*J*	8	12	29	45	36	193

Tab. 9.3.2 Notched bar impact test report in 15-5PH VAR remelted specimens, in heat treatment condition at -40°C.

		Heat Treatment					
		H900	**H925**	**H1025**	**H1075**	**H1100**	**H1150**
KV	*J*	13	24	115	148	151	161
KV	*J*	11	35	105	148	150	161
KV	*J*	9	18	129	155	152	156

Tab. 9.3.3 Notched bar impact test report in 15-5PH ESR remelted specimens, in heat treatment condition at room temperature T_{amb}.

		Heat Treatment					
		H900	**H925**	**H1025**	**H1075**	**H1100**	**H1150**
KV	*J*	7	10	20	35	41	109
KV	*J*	4	9	22	34	34	75
KV	*J*	5	10	22	35	40	66

Tab. 9.3.1 Notched bar impact test report in 15-5PH ESR remelted specimens, in heat treatment condition at -40°C.

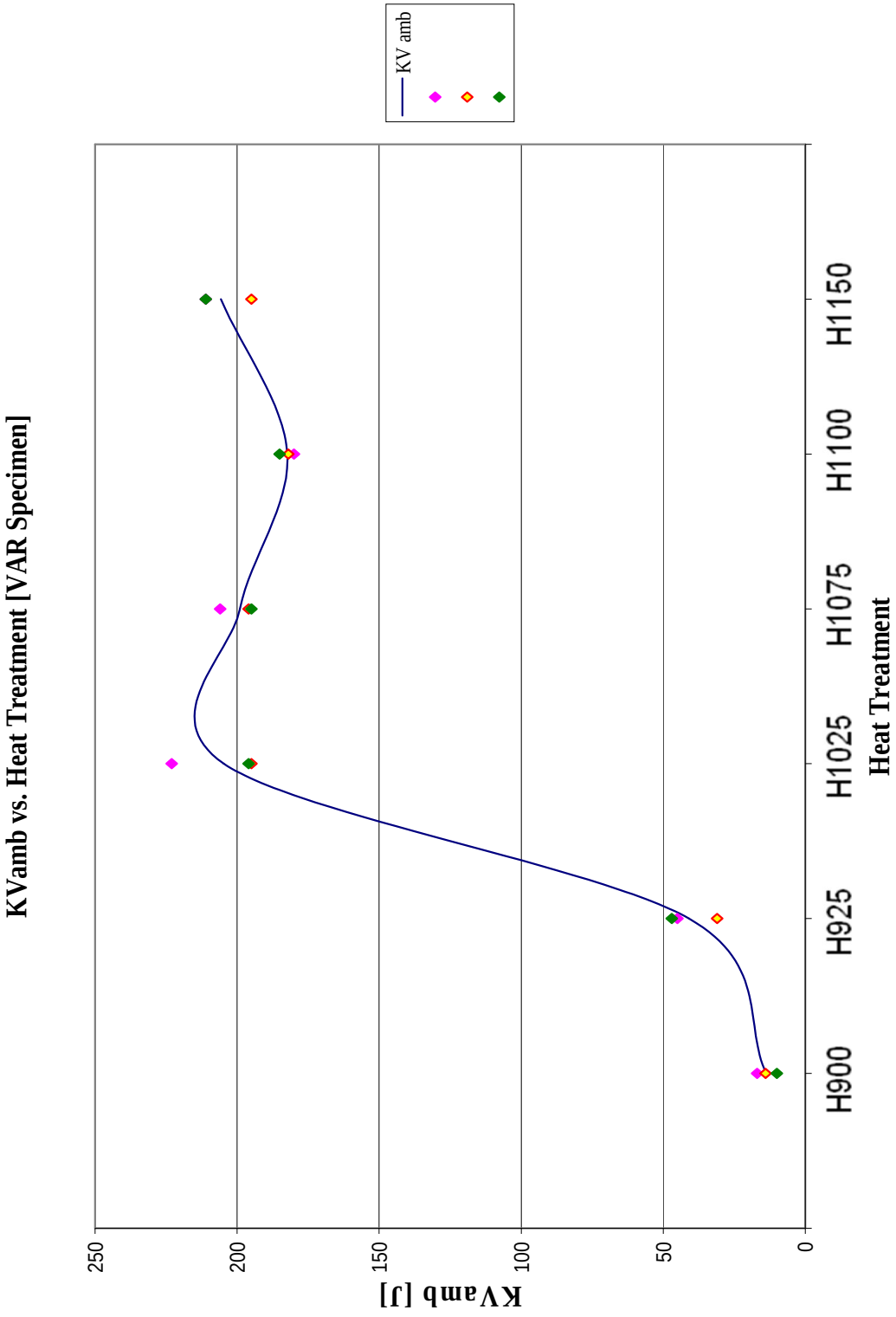

Fig. 9.3.1 Notched bar impact test in VAR remelted specimens, at room temperature.

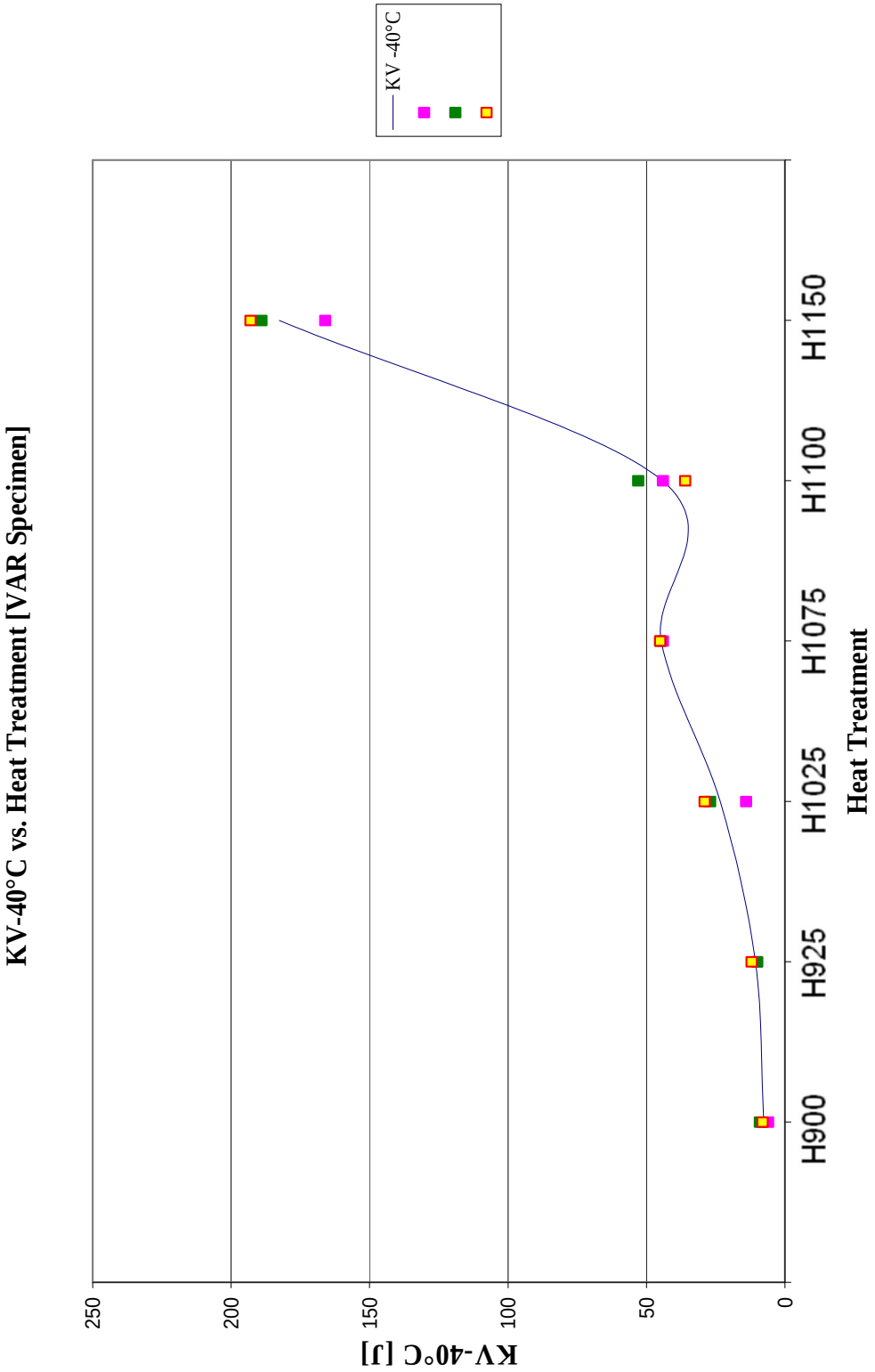

Fig. 9.3.2 Notched bar impact test in VAR remelted specimens, at -40°C.

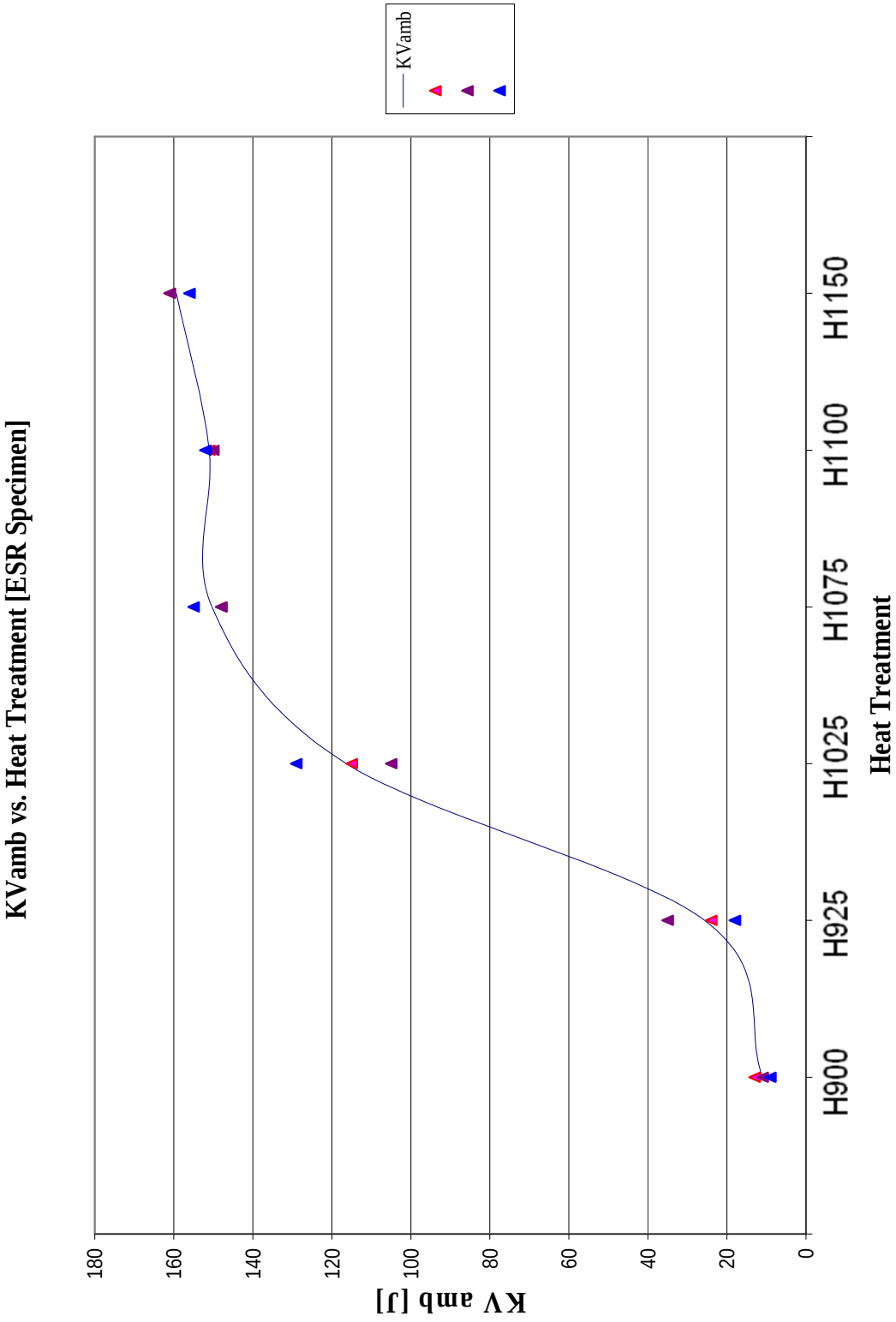

Fig. 9.3.3 Notched bar impact test in ESR remelted specimens, at room temperature

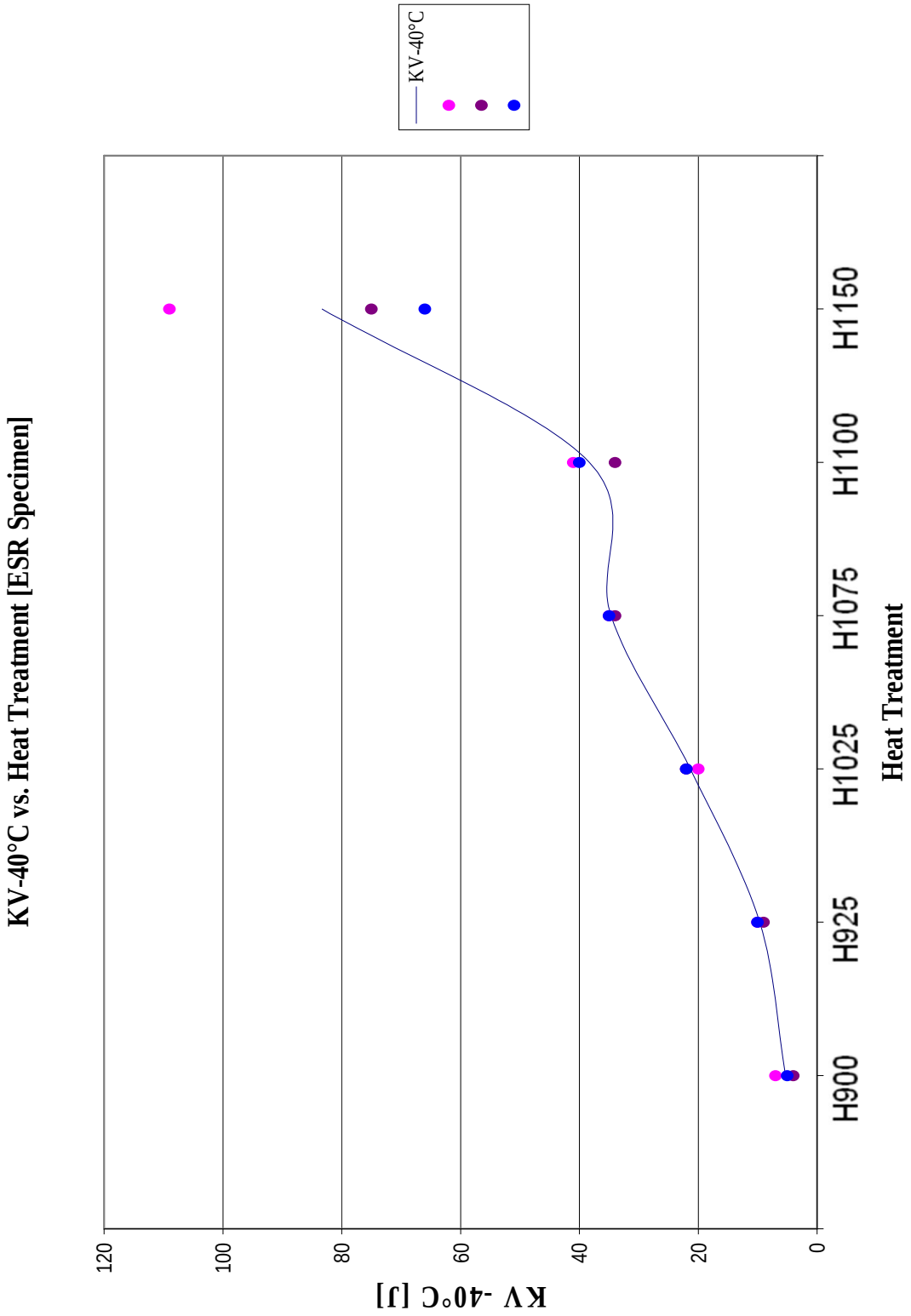

Fig. 9.3.4 Notched bar impact test in ESR remelted specimens, at -40°C.

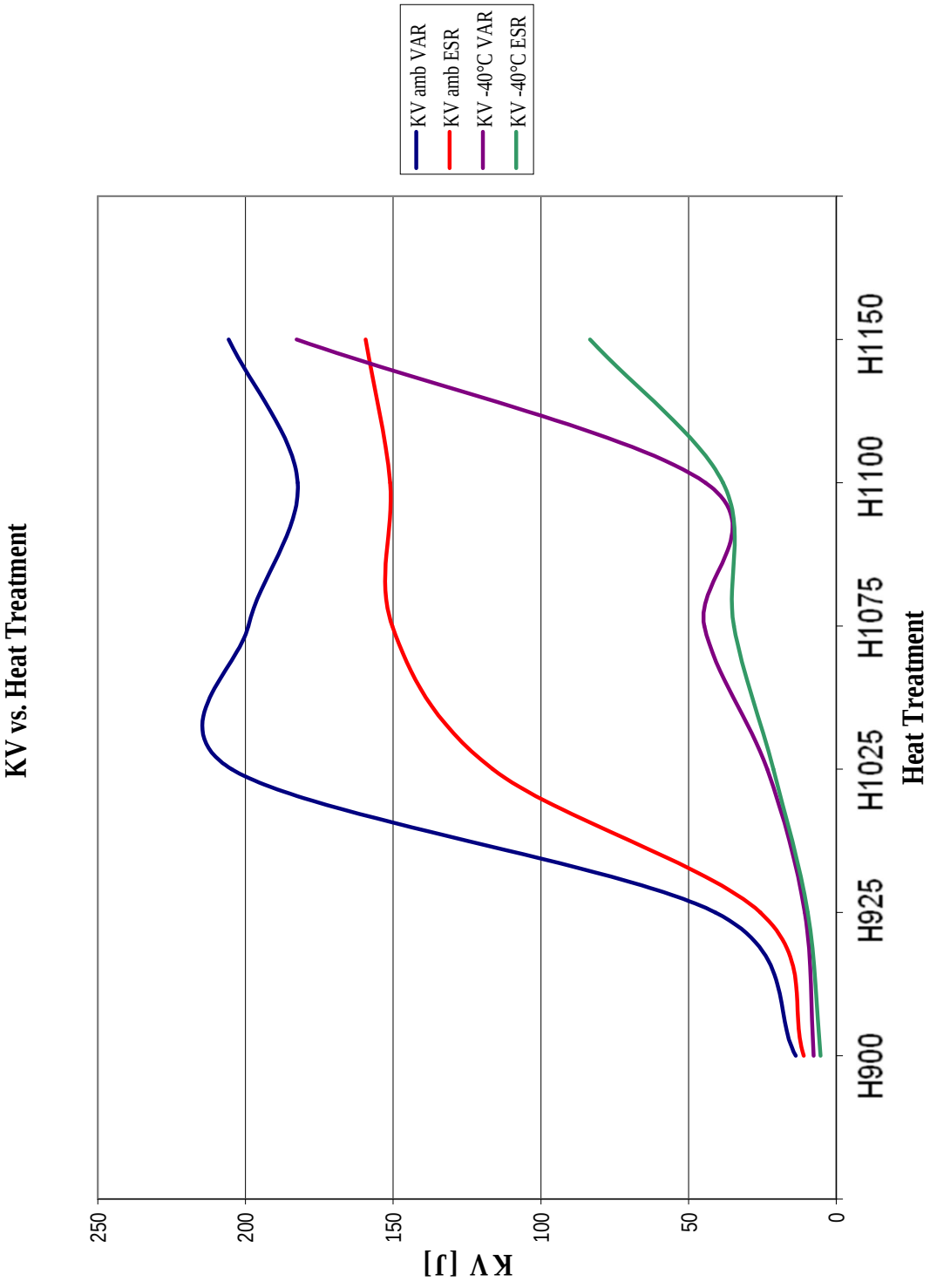

Fig. 9.3.5 Notched bar impact test comparison between VAR and ESR remelted specimens.

The impact tests show that the toughness is influenced by the production cycle. In fact, the samples remelted in ESR and VAR processes, have impact strength values very different, since resilience is linked to both the structure and inclusions presence. At room temperature (T_{amb}) the remelted VAR samples, have toughness values significantly higher than those ESR remelted samples, this is surely due to the sharp inclusions level reduction which occur in VAR remelting process.

The impact tests conducted at -40 ° C, maintaining superior toughness values in VAR remelted specimens, but there's not a clear separation of values between the two types of remelting processes. This is because at this temperature 15-5PH stainless steel presents ductile-brittle transition. The higher ageing degree, you still have an increase in measured values, especially for specimens aged in accordance with requirements H1150 (ageing parameters: T = 621 ° C, t = 4 hours), this is due to the presence of retained austenite in the martensitic matrix after ageing treatment.

9.4 Micrograph

The micrographic analysis was performed on the entire sample test of VAR and ESR specimens, in order to evaluate the structure obtained after solubilization treatment, and aging treatments of precipitation hardening. It was also evaluated the inclusions level and the grain size is as required by the standards methods ASTM E45 and E112.

VAR remelted specimen A (solubilized), 100X

VAR remelted specimen A (solubilized), 500X

VAR remelted specimen H900, 100X

VAR remelted specimen H900, 500X

VAR remelted specimen H925, 100X

VAR remelted specimen H925, 500X

VAR remelted specimen H1025, 100X

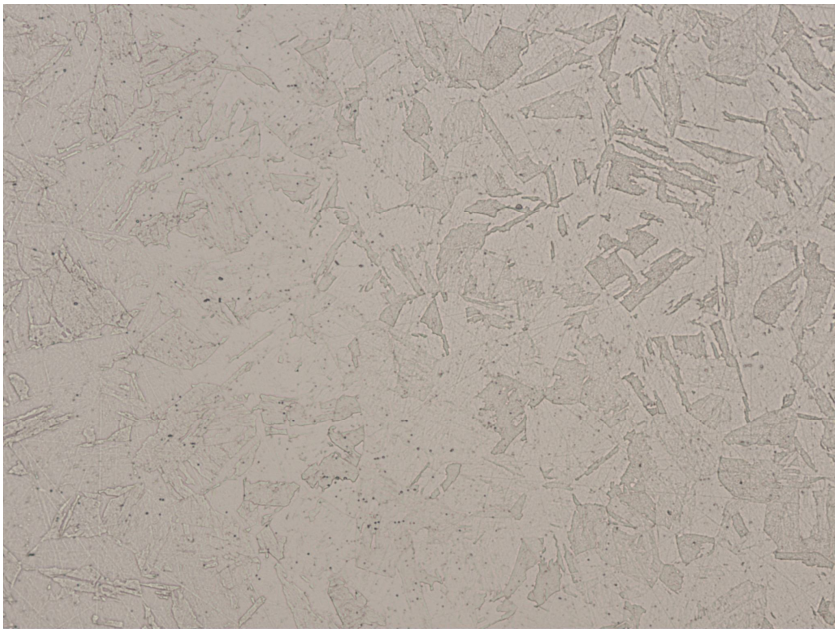

VAR remelted specimen H1025, 500X

VAR remelted specimen H1075, 100X

VAR remelted specimen H1075, 500X

VAR remelted specimen H1100, 100X

VAR remelted specimen H1100, 500X

VAR remelted specimen H1150, 100X

VAR remelted specimen H1150, 500X

Fig. 9.4.1 Micrographs specimens remelted in VAR process, in terms of solubilized (A) and in different degrees of aging (H), at 100X and 500X.

ESR remelted specimen A (solubilized), 100X

ESR remelted specimen A (solubilized), 500X

ESR remelted specimen H900, 100X

ESR remelted specimen H900, 500X

ESR remelted specimen H925, 100X

ESR remelted specimen H925, 500X

ESR remelted specimen H1025, 100X

ESR remelted specimen H1025, 500X

ESR remelted specimen H1075, 100X

ESR remelted specimen H1075, 500X

ESR remelted specimen H1100, 100X

ESR remelted specimen H1100, 500X

ESR remelted specimen H1150, 100X

ESR remelted specimen H1150, 500X

Fig. 9.4.2 Micrographs specimens remelted in ESR process, in terms of solubilized (A) and in different degrees of aging (H), at 100x and 500x.

The detection of inclusions level, in the different samples, was carried out as required by the ASTM E45 method A. Then it was proceeded to scan through an light microscope, with a computer handling in a rectangular surface (18x8mm) of 126.02mm^2. The standard ASTM E45 divide inclusions detected into four categories:

- A: sulphide inclusions
- B: alumina inclusions (Note 1)
- C: silicate inclusions (Note 1)
- D: globular oxide inclusions

Note 1: B and C inclusions type are often not chemically distinguishable, are then classified by the shape. Inclusions of type B can be identified by their elongated and jagged form typical for alumina, inclusions of type C instead are identified by their elongated shape without jagged.

The distinction in Thin and Heavy is defined by the standard ASTM E45 assessing a range of maximum permissible length for inclusion.

Inclusion Type	**"Thin" Inclusion**		**"Heavy" Inclusion**	
	Length, min	Length, max	Length, min	Length, max
	μm	*μm*	*μm*	*μm*
A	2	4	>4	12
B	2	9	>9	15
C	2	5	>5	12
D	2	8	>8	13

Tab. 9.4.1 Classification of inclusions, determined by ASTM E45

Area of polished surface evaluated, in mm²	Type of inclusion and worst field rating							
	A		B		C		D	
	Thin	Heavy	Thin	Heavy	Thin	Heavy	Thin	Heavy
126,02	0	0	0	0	0	0	0,5	0,5
Average Worst field rating:	**0**	**0**	**0**	**0**	**0**	**0**	**0,5**	**0,5**

Tab. 9.4.2 Types of inclusions found in samples remelted with VAR system

Area of polished surface evaluated, in mm²	Type of inclusion and worst field rating							
	A		B		C		D	
	Thin	Heavy	Thin	Heavy	Thin	Heavy	Thin	Heavy
126,02	0	0	0,5	0	0	0	1	0,5
Average Worst field rating:	**0**	**0**	**0,5**	**0**	**0**	**0**	**1**	**0,5**

Tab. 9.4.3 Types of inclusions found in samples remelted with ESR system

Both VAR and ESR materials presents a structure with low content of inclusions, and uniformly distributed in the material. This was possible by a careful refining process in the furnace during the AOD refining. How, easy to imagine, the level of inclusions in samples remelted with the ESR system, is greater than that achieved in the VAR system, this is due to pass through the molten slag that not removes the optimum inclusions from the metal.

The detection of the grain size in different samples, was carried out as required by ASTM E112. The scan was performed using light microscopy with computerized handling and resolution to 100X.

The structure examined is presented with a fine and homogeneous martensitic structure.

The grain size is defined by ASTM E112:

Specimen	Grain Size Number	Grain/ Area	Averasge Grain Area	Average grain diameter
	N°	*No./in^2*	*μm^2*	*μm*
VAR	6.5	45.25	1426	37.8
ESR	6	32.00	2016	44.9

Tab. 9.4.4 Crystalline grain size

Chapter 10

Conclusions

The purpose of this thesis is to assess difference between the ESR and VAR remelting systems of 15-5PH steel, and subsequent heat treatments of ageing (precipitation hardening) can influence the microstructure of stainless steel 15-5PH, the mechanical properties and then see if this has any effect on application capabilities of the material.

Moreover, the study report will help to decide which remelting technique ensure the best stainless steel performances, to ensure the customer a continuous higher quality product.

The different types of steel remelting process, carried out in vacuum with the VAR process, or by passing through a liquid slag as in the ESR process, can lead to a more or less thrust, purification from non-metallic inclusions of the material.
Furthermore, the different time of heat treatment is a further element of diversification. All this may indeed affect the quality of the material.

To assess these aspects we have been carried out light microscopic observations to assess, even from a visual standpoint, as the two different processes and time of heat treatment act on microcrystalline grains and then on the final properties of the material.

Light microscopy was performed to characterize the microstructure of solubilized material after the hot rolling, with degree of reduction of 80%, and in specimens subjected to different treatment times and temperature of aging. This analysis reveals that:

- The solubilized material (state A) present martensitic microstructure with fine grain acicular. In addition, the microstructure is characterized by slightly anisotropy, especially for the longitudinal section, with microstructure characterized by a light presence of micro-bands due to hot rolling.

- The material treated by precipitation hardening (state: H) presents an aged martensitic structure, with fine-grained and homogeneous.

- The specimens which have undergone ageing treatment H1025, H1075, H1100 and H1150, in VAR and ESR remelting process, show a progressive increase in the percentage of retained austenite dispersed in the martensitic matrix.

- The metallographic analysis also, shows how the precipitation of niobium carbides at the grain boundary occurs in a gradual manner, and take place with the formation of very fine carbides, hardly visible after acid attack, but which carries a significant change in mechanical properties. However, their coalesce with ageing treatment H1150 (ageing parameters: T = 621 ° C, t = 4 hours), giving a brown color to the martensitic structure.

The mechanical tests have been carried out to characterize the resistance properties of the material subjected to various times and temperatures of ageing treatment, and if you compare significant changes in mechanical properties between samples remelted in VAR process and those remelted in ESR process.
This analysis reveals that:

- The tensile tests show that the samples, remelted at the VAR and ESR process, present values of the unit load tensile strength R_m [MPa] and the unit load deviation from proportionality $R_{p\ 0.2\%}$ (0.2) [MPa] very similar all together for the six different degrees of ageing.

- The tensile strength values decreases with increasing of aging degree, thus increasing the number and the size of precipitates at boundary grains. This is caused by the reduction content of carbon in martensite matrix, due to formation of niobium carbides at boundary grains. The specimens occur after rupture, a break to

"cup and cone" typical of very tough steels, homogeneous and isotropic; ESR in specimens however, showed a higher frequency of breakage to" shell parts. "

- The reduction of area coefficient Z% for the specimens remelted in the VAR process, present values constantly higher than those remelted in ESR process, in all different degrees of ageing. The lower inclusions level produced in VAR remelting process, induces a greater deformability of steel before break. In fact, the greater presence of non-metallic inclusions in ESR remelted steel means that, beyond yielding, produce faster microvoids nucleation leading the matrix detachment and then the specimen break.

- The hardness is not affected by production cycle. In fact, both samples remelted in ESR and VAR processes, have hardness values very similar, since the hardness is only linked to the structure and the inclusions presence. The decrease in hardness values is related to the fact that, during the heat treatment of precipitation, the martensitic structure becomes increasingly poorer in carbon, which form niobium carbides along boundary grain.

The hardness is a parameter sensitive to the variation of amount of boundary grain's carbides precipitation, so it can be used to make a first qualitative assessment of the precipitation hardening heat treatment results.

- The impact tests show that the toughness is influenced by the production cycle. In fact, the samples remelted in ESR and VAR processes, have impact strength values very different, since resilience is linked to both the structure and inclusions presence. At room temperature (T_{amb}) the remelted VAR samples, have toughness values significantly higher than those ESR remelted samples, this is surely due to the sharp inclusions level reduction which occur in VAR remelting process.

- The impact tests conducted at -40 ° C, maintaining superior toughness values in VAR remelted specimens, but there’s not a clear separation of values between the two types of remelting processes. This is because at this temperature 15-5PH stainless steel presents ductile-brittle transition. The higher ageing degree, you still have an increase in measured values, especially for specimens aged in accordance with requirements H1150 (ageing parameters: T = 621 ° C, t = 4 hours), this is due to the presence of retained austenite in the martensitic matrix after ageing treatment.

Chapter 11

Bibliography

- *ASM Metals HandBook Volume 01: Properties and Selection Irons Steels and High Performance Alloys*, Ed. ASM, 2004
- *ASM Metals HandBook Volume 4: Heat Treating*, Ed. ASM, 2004
- *ASM Metals HandBook Volume 14: Forming and Forging*, Ed. ASM, 2004
- *ASM Metals HandBook Volume 15: Casting*, Ed. ASM, 2004
- *Lezioni di Metallurgia: Struttura, Proprietà e Comportamento dei Materiali Metallici*, G.M. Paolucci, Ed. Progetto, 2002
- *Lezioni di Metallurgia: Analisi, Prove e Controlli sui Materiali Metallici*, G.M. Paolucci, Ed. Progetto, 2002
- *Siderurgia processi e impianti*, Walter Nicodemi, Ed. AIM, 2004
- *Physical metallurgy,* P. Haasen, Ed. Cambridge University Press, 2003
- *Conoscere l'acciaio speciale: la metallurgia speciale*, R. Ebner, P. Hellman, F. Koch, R. Ponti Sgargi, A. Schindler, Ed. Sipiel, 2001
- *Conoscere l'acciaio speciale: nozioni di metallografia e difettologia*, R. Roberti, A. Schindler, Ed. Sipiel, 1995
- *The Eletric Arc Fornace*, Ed. International iron and steel institute, 1990
- *Superalloy: a technical guide*, M. J. Donachie, S. J. Donachie, Ed. ASM, 2002
- *Steel: handbook for materials research and engineering Vol:1*, Ed. Springer-Verlag, 2000

- *Steel: handbook for materials research and engineering Vol:2,* Ed. Springer-Verlag, 2000
- *Electroslag technology,* B. I. Medovar, G.A. Boyko, Ed. Springer- Verlag, 1991
- *Physical metallurgy,* R. W.Cahn P. Haasen, Ed. North-Holland Physics Publishing, 1983
- *Steelmacking,* C. Moore, R.I. Marshall, Ed. The Institute of Metals, 1991
- *Hot rolling of steel,* R. L. William, Ed.Marcel Dekker inc, 1983
- *The technology of metallurgy,* William k. Dalton, Ed. Merrill 1994
- *Steels metallurgy e applications (third edition),* D.T. Llewellyn & R.C. Hudd, Ed. Butterworth Heinemann, 2004
- *Tecnologia meccanica Lavorazioni per deformazione* plastica , Antonio Zompì , Raffaello Levi , Ed. UTET Milano, 2007
- *Recent developments in stainless steels* (Materials Science & Engineering R), K.H. Lo, C.H. Shek e J.K.L. Lai, Ed. Article in Press, 2009
- *Appunti di Tecnologia Meccanica,* Filippo Gabrielli, Ed. Pitagora Editrice Bologna, 2006
- *Modern Physical Metallurgy,* R.E. Smallman, Ed. Butterworths, 1970
- *Manuale dei Materiali per l'Ingegneria,* Ed. AIMAT McGraw-Hill, 1996
- *ASTM E8M- Standard Test Methods for Tension Testing of Metallic Materials [Metric],*Ed. ASTM International, 2002
- *ASTM E10 - Standard Test Method for Brinell Hardness of Metallic Materials,* Ed. ASTM International, 2003

- *ASTM E23 - Standard Test Methods for Notched Bar Impact Testing of Metallic Materials,* Ed. ASTM International, 2003
- *ASTM E1236- Standard Practice for Qualifying Charpy Impact Machines as Reference Machines*, Ed. ASTM International, 2006
- *ASTM E1271- Standard Practice for Qualifying Charpy Verification Specimens of Heat-Treated Steel,* Ed. ASTM International, 2003
- *ASTM E112 - Standard Test Methods for Determining Average Grain Size,* Ed. ASTM International, 2002
- *ASTM E45 - Standard Test Methods for Determining the Inclusion Content of Steel,* Ed. ASTM International, 2002
- *Proceedings of the Materials Engineering Workshop*, Nickel Institute
- *Eurofer: European Confederation of Iron & Steel Industries*, www.eurofer.org > News & Pubblications > Annual Report > 2008 Annual Report.
- *Euro Inox, The European Stainless Steel Development Association*, www.euro-inox.org.

INDEX